# TEMPORAL PATTERNS AND MECHANISMS OF BIODIVERSITY ACROSS SCALES IN EAST ASIA

EDITED BY: Zehao Shen, George P. Malanson, Jinlong Zhang and Meng Yao
PUBLISHED IN: Frontiers in Ecology and Evolution

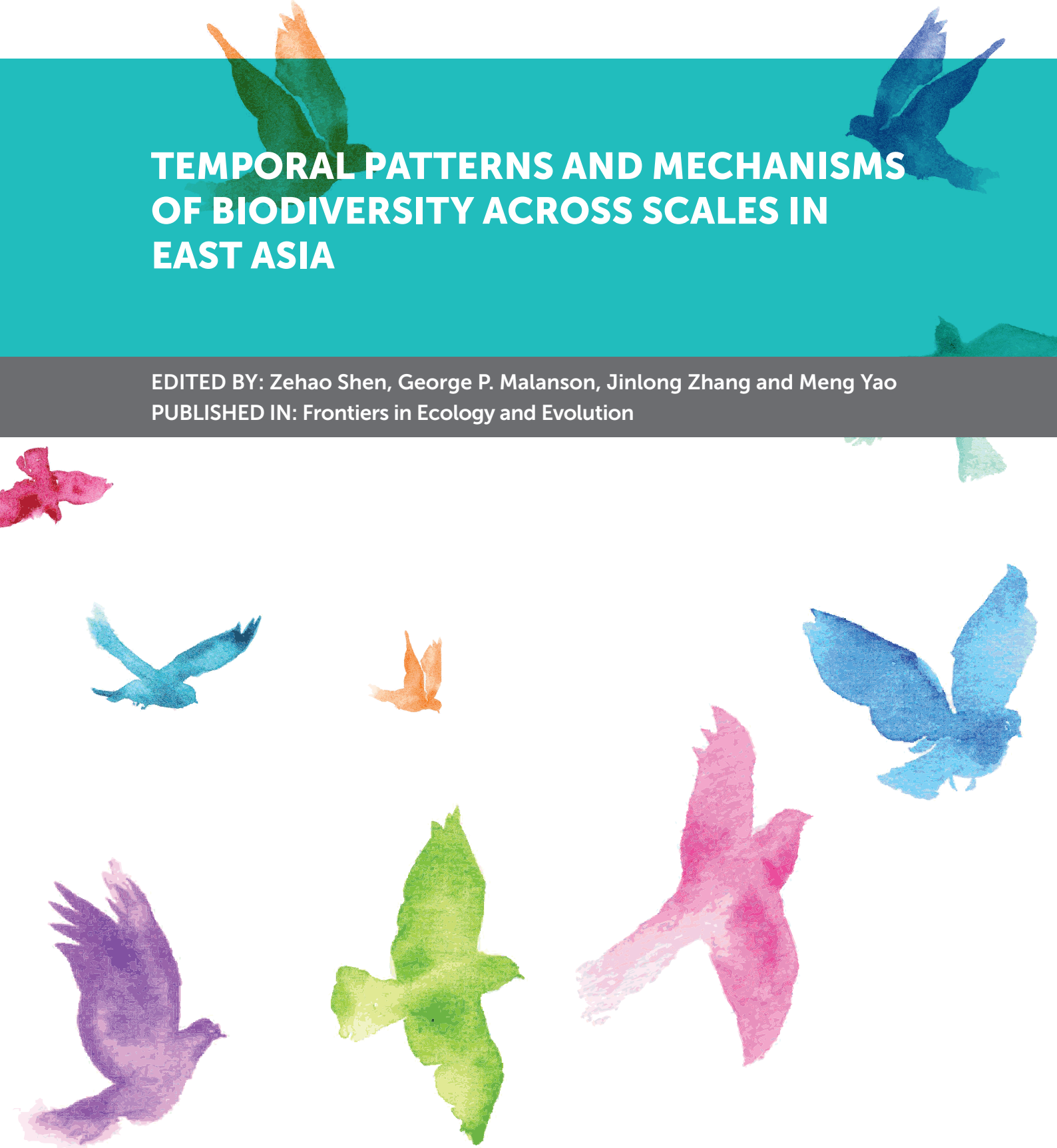

frontiers Research Topics

ISSN 1664-8714
ISBN 978-2-88971-080-5
DOI 10.3389/978-2-88971-080-5

## About Frontiers

Frontiers is more than just an open-access publisher of scholarly articles: it is a pioneering approach to the world of academia, radically improving the way scholarly research is managed. The grand vision of Frontiers is a world where all people have an equal opportunity to seek, share and generate knowledge. Frontiers provides immediate and permanent online open access to all its publications, but this alone is not enough to realize our grand goals.

## Frontiers Journal Series

The Frontiers Journal Series is a multi-tier and interdisciplinary set of open-access, online journals, promising a paradigm shift from the current review, selection and dissemination processes in academic publishing. All Frontiers journals are driven by researchers for researchers; therefore, they constitute a service to the scholarly community. At the same time, the Frontiers Journal Series operates on a revolutionary invention, the tiered publishing system, initially addressing specific communities of scholars, and gradually climbing up to broader public understanding, thus serving the interests of the lay society, too.

## Dedication to Quality

Each Frontiers article is a landmark of the highest quality, thanks to genuinely collaborative interactions between authors and review editors, who include some of the world's best academicians. Research must be certified by peers before entering a stream of knowledge that may eventually reach the public - and shape society; therefore, Frontiers only applies the most rigorous and unbiased reviews.
Frontiers revolutionizes research publishing by freely delivering the most outstanding research, evaluated with no bias from both the academic and social point of view. By applying the most advanced information technologies, Frontiers is catapulting scholarly publishing into a new generation.

## What are Frontiers Research Topics?

Frontiers Research Topics are very popular trademarks of the Frontiers Journals Series: they are collections of at least ten articles, all centered on a particular subject. With their unique mix of varied contributions from Original Research to Review Articles, Frontiers Research Topics unify the most influential researchers, the latest key findings and historical advances in a hot research area! Find out more on how to host your own Frontiers Research Topic or contribute to one as an author by contacting the Frontiers Editorial Office: frontiersin.org/about/contact

# TEMPORAL PATTERNS AND MECHANISMS OF BIODIVERSITY ACROSS SCALES IN EAST ASIA

Topic Editors:
**Zehao Shen,** Peking University, China
**George P. Malanson,** The University of Iowa, United States
**Jinlong Zhang,** Kadoorie Farm and Botanic Garden, SAR China
**Meng Yao,** Peking University, China

**Citation:** Shen, Z., Malanson, G. P., Zhang, J., Yao, M., eds. (2021). Temporal Patterns and Mechanisms of Biodiversity Across Scales in East Asia. Lausanne: Frontiers Media SA. doi: 10.3389/978-2-88971-080-5

# Table of Contents

frontiers in Ecology and Evolution

EDITORIAL
published: 31 May 2021
doi: 10.3389/fevo.2021.662454

# Editorial: Temporal Patterns and Mechanisms of Biodiversity Across Scales in East Asia

*Zehao Shen*[1]*, *George P. Malanson*[2], *Meng Yao*[1] and *Jinlong Zhang*[3]

[1] Ministry of Education Laboratory of Earth Surface Processes, College of Urban and Environmental Sciences, Institute of Ecology, Peking University, Beijing, China, [2] Department of Geography, Iowa University, Iowa City, IA, United States, [3] Flora Conservation Department, Kadoorie Farm and Botanic Garden, Hong Kong, China

**Keywords: biodiversity, process, ecological, environmental, evolutionary, temporal scale**

**Editorial on the Research Topic**

**Temporal Patterns and Mechanisms of Biodiversity Across Scales in East Asia**

With regard to islands—the "type specimen" of biodiversity studies, the island biogeography model predicts species richness based on the spatial attributes, e.g., island area and distance to the mainland, but the theory is recognized as an equilibrium framework of dispersal, competition, and extinction processes (MacArthur and Wilson, 1967; Warren et al., 2015). In the past half-century, the geographical (especially latitudinal and altitudinal) distribution of species diversity and its explanations may be the most intensive area of biodiversity studies (Rohde, 1992; Rahbek, 1995; Willig et al., 2003; Pontarp et al., 2019). Spatially-based explanations, such as climatic gradients and habitat heterogeneity, and temporal hypotheses, for example environmental or speciation rate, are both supported. But the accumulating evidence increasingly demonstrated the importance of exploring temporal variations and process-based mechanisms at multiple scales for a final understanding of biodiversity variations on earth (Ricklefs, 1987). As an instant in hundreds of millions of years, the spatial pattern of biodiversity is just a snapshot of the evolutionary history of the biosphere. This perspective is embedded in either the "cradle—museum—grave" framework of biodiversity at the macro-scale (Chown and Gaston, 2000; Jablonski et al., 2006; Qian et al., 2020), or the "niche—neutral—fitness" theory of community assembly and species coexistence at local scales (Leibold and McPeek, 2006; Adler et al., 2007).

Concurrently, rapid technological progress have enhanced our power and potential for exploring biogeographical evidence in deep time. On the one hand, the historical scenarios of environmental changes have been increasingly reconstructed for paleoclimate dynamics, plate tectonics and orogeny, wildfire regimes, and land-use and land-cover changes. On the other hand, the accumulation of dated fossil evidence and the establishment of molecular evolution models helped to disclose the evolutionary processes of speciation, migration, and extinction of various lineages of organisms. It is not surprising that the differences and combinations of spatiotemporal scales of various environmental changes, unique or similar evolutionary processes of different organism groups, convergence, or differentiation of various biotic functional traits, as well as interspecific and intraspecific interactions, have greatly enriched the character of biodiversity research in the past 50 years (Hembry and Weber, 2020).

Ultimately, the spatial pattern of biodiversity results from the overlay of distributions of taxa, and hence a hierarchical framework integrating processes across temporal, spatial, and trophic scales is critical for understanding biodiversity patterns. On the temporal aspect, a phylogenetic tree not only sets up a historical framework for the biogeography of a focal lineage, but also provides an approach to estimate the evolutionary relationship across taxa within a community, and help



***Edited and reviewed by:***
*Peter Convey,*
*British Antarctic Survey (BAS),*
*United Kingdom*

***Correspondence:**
*Zehao Shen*
*shzh@urban.pku.edu.cn*

***Specialty section:***
*This article was submitted to Biogeography and Macroecology, a section of the journal Frontiers in Ecology and Evolution*

***Received:*** *01 February 2021*
***Accepted:*** *18 February 2021*
***Published:*** *31 May 2021*

***Citation:***
*Shen Z, Malanson GP, Yao M and Zhang J (2021) Editorial: Temporal Patterns and Mechanisms of Biodiversity Across Scales in East Asia. Front. Ecol. Evol. 9:662454. doi: 10.3389/fevo.2021.662454*

to reveal the effects of environmental filtering on the regional species pool (Wiens, 1998; Losos, 2008). On the spatial aspect, species niche modeling predicts species distribution ranges based on their local responses of presence/absence and population abundance to habitat conditions (Howard et al., 2014). Recently, prominent progress in the impact of cross-trophic biotic relationships on biodiversity have stimulated unprecedented attention (Chen L. et al., 2019; Wang et al., 2019). The interactions between microorganisms and higher plants and animals not only affect the species richness and composition at the community or site scale but also regulate the macro-scale pattern of biodiversity (Ellis et al., 2015; Milici et al., 2020). The spread of the COVID-19 pandemic through human migration and its impact on human global behavior may be the latest footnote of the macro-micro interaction mechanism of biodiversity (Feng et al., 2020). Therefore, exploring the effects of eco-evolutionary process in response to environmental processes across scales seems to be one of the most important current tasks in understanding the spatiotemporal patterns of biodiversity.

Due to the individualistic response of species to environmental changes (Gleason, 1926; Whittaker, 1967), it will still be a long journey toward a deep understanding of the adaptive evolution of biological groups and the response of population dynamics (including growth, migration, and extinction) to multi-scale spatial-temporal changes of the environment. For this purpose, East Asia, traditionally composed of China, Japan, Korea, South Korea, and Mongolia, is undoubtedly one of the most valuable study areas in the world. The land in this area is composed of several blocks that were scattered in the southern and northern hemispheres in the Mesozoic, belonging to the Laurasia and Gondwana continents (Suo et al., 2020). In the Cenozoic, it experienced the uplift of the largest and highest plateau, the development of the strongest and largest monsoon in the world, and the largest land area in the northern hemisphere free from glaciers during the Quaternary ice ages (Batchelor et al., 2019). Since the Holocene, ecosystems in East Asia have probably experienced the most persistent and extensive human disturbance, including the largest scale deforestation, urbanization, and reforestation in China in the last 40 years (Cao et al., 2012; Chen C. et al., 2019; Wu et al., 2020). Therefore, the rich and unique biodiversity sources, the complexity of the evolutionary history of the biota, and the spatiotemporal heterogeneity of the environment provide incomparable opportunities to explore the temporal patterns and multi-scale mechanisms of biodiversity.

In this Research Topic, 11 research reports represent an effort with empirical approaches to understanding the temporal patterns and driving processes of biodiversity in East Asia, including the comparison of biodiversity at different times, the biogeographic evolutionary history of different biological assemblages, and the comparison and exploration of the effects of ecological and environmental processes on different temporal scales. The study area of these papers shares a common biogeographic context characterized by regional geological process (dominated by the uplift of Qinghai-Tibet Plateau), monsoon-regulated climates, and long histories of intensive human perturbation on natural ecosystems. Our Research Topic aims to reflect recent progress in studies at population, species, and community levels.

Three papers focused on ecological processes and their effects on biodiversity patterns at different spatial scales, Song et al. studied the effects of grazing exclusion on the composition, structure, and community spatial heterogeneity of the alpine grassland ecosystem on the Qinghai-Tibet Plateau; they found that the effects of grazing were differentiated by the duration of exclusion experiment (3–5 vs. 9–11 year). Zhang et al. addressed the effect of spatial heterogeneity or average supply rates of limiting resources. They reported that resource heterogeneity and local population dispersal, but not resource quantity, played an important role in determining species diversity in these two old-growth forests. In contrast, Li and Shen focused on the dispersal process of alien plants at a broad scale. By reconstructing the history of plant invasion in China and differentiating the geographical patterns of alien invasive plant species, the study found that low temperature and time since introduction were dominant determinants of invasive plant species diversity in China, which indicated that global warming and economic globalization would continue to driving forces of alien plant invasions.

Three papers explored the environmental processes that are particularly important for their influences on biodiversity patterns in China. Using phylogenetic tree construction and ancestral area reconstruction, Yan et al. focused on the role of the uplift of the Qinghai-Tibet Plateau in the phylogeography of a tree frog species *Hyla chinensis*. The paper delineated six clusters of the species and showed their spatial and temporal patterns. Dispersal models with different isolation estimates were compared to explain the spatial patterns of the present six groups within this complex. Xu et al. compared climate seasonality and glacial-interglacial climate variation for their roles on species richness patterns of evergreen broadleaved woody plants in China. They found that short- and long-term climate variability played complementary roles and should relate to distinct mechanisms. In particular, precipitation seasonality played a dominant role as a unique feature of the mid-latitude monsoon climate. Thus, a better understanding of the effects of climate change on species distributions requires exploration at multiple time scales. Urbanization is a spatial process that causes rapid landscape evolution as a product of economic globalization and has caused widespread concerns about regional scale biodiversity. Taking a space-for-time substitution approach, Yu et al. addressed the effect of urbanization on soil mesofauna diversity, and a median disturbance effect was reported for urbanization intensity as indicated by the interaction of landscape features and soil nutrients/heavy metal content.

The role of evolutionary process on contemporary biodiversity patterns was represented by two studies. Using a relaxed-clock method to estimate divergent times for *Holcoglossum* (Orchidaceae), Zhao et al. explored biogeographic patterns of this endemic epiphytic genus in East Asia. They inferred four dispersal events to explain the expansion of this genus to the Sino-Himalayan, Sino-Japanese, and Taiwan regions from the latest Miocene to Quaternary, and linked these events with the intensification of East Asian monsoon around

3.6–2.6 Ma and global cooling since the latest Pliocene. Liu X. et al. addressed the differentiation of Fagaceae in Hainan Island with fossil dating and distribution, and speculated on the dispersal and differentiation of genera of Fagaceae in tropical south China, including southern Yunnan, the Leizhou Peninsula of Guangdong, Hainan Island, and the southern part of Taiwan Island. The fossil evidence suggested the ancestral components of Fagaceae seemed to migrate southward from temperate regions of East Asia and diversified there no later than in the Eocene.

After decades of intensive exploration of patterns of biodiversity and underlying mechanisms, it is recognized that biodiversity has multi-facet and internally-linked information. This understanding is typically represented by measuring and comparing indices of taxonomic, phylogenetic, and functional diversity and relating them to environmental factors at multiple spatial and temporal scales (Liu L. et al.). Meanwhile, new diversity metrics also keep emerging to explore the temporal features of biodiversity. Li L. et al. explored the diversity of reproductive phenology among species of *Poa* and found the diversity of reproductive phenology among subtropical grasses is constrained by evolution and climatic niche, and that photosynthetic pathway and life history have an interactive effect on the timing and the duration of reproduction. Shi et al. compared phylogenetic and functional diversity and explored two aspects of diversity linked with mechanisms of biodiversity at distinct temporal scales: functional structure is better linked with modern and local factors while phylogenetic structure is more associated with historical and regional processes. These results highlighted the importance of the associations between the different biodiversity dimensions and divergent drivers.

With all efforts aiming to explain biodiversity patterns in terms of ecological, environmental, and evolutionary processes, evidence has been accumulating rapidly at various temporal scales and for distinct assemblages of organisms, including a small collection in this thematic issue. The importance of this approach is also indicated by the evolution of the interpretative framework in a process-based direction: from the "colonization-extinction" paradigm of island biogeography (MacArthur and Wilson, 1967) to the "cradle-museum" paradigm created by Chown and Gaston (2000), even to the random dispersal process-based neutral models of biodiversity (Hubbell, 2001; Colwell et al., 2004). In recent decades, genome technologies rapidly uncovered the genetic mechanisms of population dynamics and evolutionary process; remote sensing techniques improved the monitoring capacity for animal dispersal and landscape changes; isotopic techniques and fossil analyses helped with dating the geological processes of deep history. All these signs of technological progress combine to augment our capacity to explore the temporal aspect of biodiversity. The myriad patterns of biodiversity, with unique histories and geographies, manifest the complexity of mechanisms for its generation and maintenance. Disentangling the roles of multiple processes in determining biodiversity patterns seems to be a goal that still requires a long journey to achieve, while exploring biodiversity dynamics and driving processes at multiple temporal scales should prove to be a necessary and promising path.

## AUTHOR CONTRIBUTIONS

ZS wrote the draft. GM, JZ, MY, and ZS revised the manuscript. All authors contributed to the article and approved the submitted version.

## FUNDING

This work was sponsored by the Biodiversity Survey and Assessment Project of the Ministry of Ecology and Environment, China (Grant Number 2019-HJ-061-N-001-B-008).

## ACKNOWLEDGMENTS

We appreciate the constructive review comments and suggestions from all reviewers, editors, and the guest editor team. We are grateful to the editorial office for their patience and great help with the review process. We thank all authors for their valuable contributions to this interesting Research Topic.

## REFERENCES

Adler, P. B., HilleRisLambers, J., and Levine, J. M. (2007). A niche for neutrality. *Ecol. Lett.* 10, 95–104. doi: 10.1111/j.1461-0248.2006.00996.x

Batchelor, C. L., Margold, M., Krapp, M., Murton, D. K., Dalton, A. S., Gibbard, P. L., et al. (2019). The configuration of Northern Hemisphere ice sheets through the quaternary. *Nat. Commun.* 10:3713. doi: 10.1038/s41467-019-11601-2

Cao, G.-Y., Chen, G., Pang, L.-H., Zheng, X.-Y., and Nilsson, S. (2012). Urban growth in China: past, prospect, and its impacts. *Popul. Environ.* 33, 137–160. doi: 10.1007/s11111-011-0140-6

Chen, C., Park, T., Wang, X., Piao, S., Xu, B., Chaturvedi, R.K., et al. (2019). China and India lead in greening of the world through land-use management. *Nat. Sustain.* 2, 122–129. doi: 10.1038/s41893-019-0220-7

Chen, L., Swenson, N. G., Ji, N. N., Mi, X. C., Ren, H. B., Guo, L. D., et al. (2019). Differential soil fungus accumulation and density dependence of trees in a subtropical forest. *Science* 366, 124–128. doi: 10.1126/science.aau1361

Chown, S. L., and Gaston, K. J. (2000). Areas, cradles and museums: the latitudinal gradient in species richness. *Trends Ecol. Evol.* 15, 311–315. doi: 10.1016/S0169-5347(00)01910-8

Colwell, R. K., Rahbek, C., and Gotelli, N. J. (2004). The mid-domain effect and species richness patterns: what have we learned so far? *Am. Nat.* 163, E1–E23. doi: 10.1086/382056

Ellis, V. A., Collins, M. D., Medeiros, M. C. I., Sari, E. H. R. Coffey, E. D., Dickerson, R. C., et al. (2015). Local host specialization, host-switching, and dispersal shape the regional distributions of avian haemosporidian parasites. *Proc. Natl. Acad. Sci.* 112, 11294–11299. doi: 10.1073/pnas.1515309112

Feng, Y., Li, Q., Tong, X., Wang, R., Zhai, S., Gao, C., et al. (2020). Spatiotemporal spread pattern of the COVID-19 cases in China. *PLoS ONE* 15:e0244351. doi: 10.1371/journal.pone.0244351

Gleason, H. A. (1926). The individualistic concept of the plant association. *Bull. Tor. Bot. Club* 53, 7–26. doi: 10.2307/2479933

Hembry, D. H., and Weber, M. G. (2020). Ecological interactions and macroevolution: a new field with old roots. *Annu. Rev. Ecol. Evol. Syst.* 51, 215–243. doi: 10.1146/annurev-ecolsys-011720-121505

Howard, C., Stephens, P.A., Pearce-Higgins, J.W., Gregory, R.D., and Willis, S.G. (2014). Improving species distribution models: the value of data on abundance. *Methods Ecol. Evol.* 5, 506–513. doi: 10.1111/2041-210X.12184

Hubbell, S. P. (2001). *The Unified Neutral Theory of Biodiversity and Biogeography*. Princeton, NJ; Oxford: Princeton University Press.

Jablonski, D., Roy, K., and Valentine, J. W. (2006). Out of the tropics: evolutionary dynamics of the latitudinal diversity gradient. *Science* 314, 102–106. doi: 10.1126/science.1130880

Leibold, M. A., and McPeek, M. A. (2006). Coexistence of the niche and neutral perspectives in community ecology. *Ecology* 87, 1399–1410. doi: 10.1890/0012-9658(2006)871399:COTNAN2.0.CO;2

Losos, J. B. (2008). Phylogenetic niche conservatism, phylogenetic signal and the relationship between phylogenetic relatedness and ecological similarity among species. *Ecol. Lett.* 11, 995–1007 doi: 10.1111/j.1461-0248.2008.01229.x

MacArthur, R. H., and Wilson, E. O. (1967). *The Theory of Island Biogeography*. Princeton, NJ: Princeton University Press.

Milici, V. R., Dalui, D., Mickley, J. G., and Bagchi, R. (2020). Responses of plant–pathogen interactions to precipitation: implications for tropical tree richness in a changing world. *J. Ecol.* 108, 1800–1809. doi: 10.1111/1365-2745.13373

Pontarp, M., Bunnefeld, L., Cabral, J. S., Etienne, R. S., Fritz, S. A., Gillespie, R., et al. (2019). The latitudinal diversity gradient: novel understanding through mechanistic eco-evolutionary models. *Trends Ecol. Evol.* 34, 211–223. doi: 10.1016/j.tree.2018.11.009

Qian, H., Jin, Y., Leprieur, F., Wang, X., and Deng, T. (2020). Patterns of phylogenetic beta diversity measured at deep evolutionary histories across geographical and ecological spaces for angiosperms in China. *J. Biogeogr.* doi: 10.1111/jbi.14036. [Epub ahead of print].

Rahbek, C. (1995). The elevational gradient of species richness: a uniform pattern? *Ecography* 18, 200–205. doi: 10.1111/j.1600-0587.1995.tb00341.x

Ricklefs, R. E. (1987). Community diversity: relative roles of and regional processes testing predictions of local-process theories. *Science* 235, 167–171 doi: 10.1126/science.235.4785.167

Rohde, K. (1992). Latitudinal gradients in species diversity: the search for the primary cause. *Oikos* 65, 514–527. doi: 10.2307/3545569

Suo, Y., Li, S., Cao, X., Wang, X., Somerville, I., Wang, G., et al. (2020). Mesozoic-Cenozoic basin inversion and geodynamics in East China: a review. *Earth Sci. Rev.* 210:103357. doi: 10.1016/j.earscirev.2020.103357

Wang, S., Brose, U., and Gravel, D. (2019). Intraguild predation enhances biodiversity and ecosystem functioning in complex food webs. *Ecology* 100:e02616. doi: 10.1002/ecy.2616

Warren, B. H., Simberloff, D., Ricklefs, R. E., Aguilée, R., Condamine, F. L., Gravel, D., et al. (2015). Islands as model systems in ecology and evolution: prospects fifty years after MacArthur-Wilson. *Ecol. Lett.* 18, 200–217. doi: 10.1111/ele.12398

Whittaker, H. (1967). Gradient analysis of vegetation. *Biol. Rev.*4, 207–264. doi: 10.1111/j.1469-185X.1967.tb01419.x

Wiens, J. J. (1998). Combining data sets with different phylogenetic histories. *Syst. Biol.* 47, 568–581. doi: 10.1080/106351598260581

Willig, M. R., Kaufman, D. M., and Stevens, R. D. (2003). Latitudinal gradients of biodiversity: pattern, process, scale, and synthesis. *Annu. Rev. Ecol. Evol. Syst.* 34, 273–309. doi: 10.1146/annurev.ecolsys.34.012103.144032

Wu, X., Wei, Y., Fu, B., Wang, S., Zhao, Y., and Moran, E. F. (2020). Evolution and effects ofthe social-ecological system over a millennium in China's Loess Plateau. *Sci. Adv.* 6:eabc0276. doi: 10.1126/sciadv.abc0276

**Conflict of Interest:** The authors declare that the research was conducted in the absence of any commercial or financial relationships that could be construed as a potential conflict of interest.

frontiers in Ecology and Evolution

ORIGINAL RESEARCH
published: 21 April 2020
doi: 10.3389/fevo.2020.00066

# Long-Term Grazing Exclusion Reduces Species Diversity but Increases Community Heterogeneity in an Alpine Grassland

*Shanshan Song[1], Jiangling Zhu[2], Tianli Zheng[3], Zhiyao Tang[2], Fan Zhang[1], Chengjun Ji[2], Zehao Shen[2] and Jianxiao Zhu[1,2]**

[1] State Key Laboratory of Grassland Agro-Ecosystems, College of Pastoral Agriculture Science and Technology, Lanzhou University, Lanzhou, China, [2] Department of Ecology, College of Urban and Environmental Sciences, Key Laboratory for Earth Surface Processes of the Ministry of Education, Peking University, Beijing, China, [3] Environmental Science and Technology Research Center, Tianjin Research Institute for Water Transport Engineering, M.O.T., Tianjin, China

OPEN ACCESS

**Edited by:**
Marco A. Molina-Montenegro, University of Talca, Chile

**Reviewed by:**
Jianshuang Wu, Institute of Environment and Sustainable Development in Agriculture, Chinese Academy of Agricultural Sciences, China
Fernando Andrés Carrasco-Urra, University of Talca, Chile

***Correspondence:**
Jianxiao Zhu
jxzhu@lzu.edu.cn

**Specialty section:**
This article was submitted to Biogeography and Macroecology, a section of the journal Frontiers in Ecology and Evolution

**Received:** 21 October 2019
**Accepted:** 02 March 2020
**Published:** 21 April 2020

**Citation:**
Song S, Zhu J, Zheng T, Tang Z, Zhang F, Ji C, Shen Z and Zhu J (2020) Long-Term Grazing Exclusion Reduces Species Diversity but Increases Community Heterogeneity in an Alpine Grassland. Front. Ecol. Evol. 8:66. doi: 10.3389/fevo.2020.00066

Extensive grazing activity is threatening the alpine grassland of the Qinghai-Tibetan Plateau. Evidence has shown that grazing exclusion may change the composition, structure, and functions of grassland ecosystems. However, such effects depend on the intensity and duration of exclusion. We explored the effects of short-term (2 and 4 years) and long-term (9 and 11 years) grazing exclusion on plant height, coverage, and diversity and community heterogeneity in the alpine grassland of the Qinghai-Tibetan Plateau. We found no difference in plant diversity between short-term grazing exclusion and control. However, long-term grazing exclusion reduced species richness and increased the Simpson dominance index. This decrease in plant species richness was mainly attributable to the decrease in common species richness (defined as species with a relative coverage of 1∼5%). In addition, community heterogeneity (coefficient of variation, CV) was significantly higher in long-term grazing exclusion than in controlled plots. Structural equation modeling (SEM) demonstrated that long-term grazing exclusion increased the community heterogeneity mainly by reducing species diversity. These results suggest that the effects of grazing exclusion on the composition, structure, and community spatial heterogeneity of the alpine grassland ecosystem are dependent on exclusion duration. Grazing activity may maintain the high biodiversity and community stability of the alpine grassland in the harsh environment of the Qinghai-Tibetan Plateau.

**Keywords: community composition, community structure, grazing exclusion, Qinghai-Tibetan Plateau, spatial heterogeneity**

## INTRODUCTION

Spatial heterogeneity, or spatial variability (Kolasa and Rollo, 1991), represents the dissimilarity (coefficient of variation) of community properties between multiple subplots within one survey plot (Huston, 1997; Weigelt et al., 2008). Because of the impact of spatial heterogeneity on grassland ecosystem functioning (e.g., productivity) (Huston, 1997; Fukami et al., 2001), uncovering the

underlying mechanisms that cause spatial heterogeneity is a necessary step to predicting the change of ecosystem functions under global changes (Naeem et al., 1994; Weigelt et al., 2008; Grman et al., 2010). Many studies have shown that the more diverse communities have a higher probability of maintaining species and being resistant to environmental changes, i.e., more temporally stable (Tilman et al., 2006; Weigelt et al., 2008; Loreau and De Mazancourt, 2013). However, little is known about how spatial variability changes under biodiversity loss. The heterogeneity of the microclimate, such as plant coverage, has been shown to be significantly and positively correlated with biodiversity (Xu et al., 2000). Furthermore, Fukami et al. (2001) showed that biodiversity loss lowers ecosystem reliability (stability) between local communities by increasing the dissimilarity of species compositions, which indicates that biodiversity loss may lead to spatial heterogeneity among communities.

Several mechanisms have been proposed to explain community temporal stability, including compensatory dynamics (Bai et al., 2004; Song and Yu, 2015; Wilcox et al., 2017) and dominant species effects (Polley et al., 2007; Sasaki and Lauenroth, 2011; Wilsey et al., 2014). Given that the hypothesis that biodiversity increases stability can equally be applied to spatial heterogeneity (Fukami et al., 2001; Weigelt et al., 2008), these mechanisms should be applied to explain the causes of community heterogeneity. Compensatory dynamics (e.g., species asynchrony) indicates the ability of species to supplement each other under environmental changes, and higher compensatory effects can contribute to higher ecosystem stability, resulting from decreased variation in productivity (Bai et al., 2004; Song and Yu, 2015; Wilcox et al., 2017). Additionally, the stability of the dominant species is closely connected with the stability of the ecosystem, because the dominant species contributes most of the biomass in the community (Polley et al., 2007; Sasaki and Lauenroth, 2011). The effects of species asynchrony and dominant species are tightly correlated with plant diversity (Bai et al., 2004; Polley et al., 2007). Here, we hypothesize that an increase in biodiversity and asynchrony will lead to a decrease in spatial heterogeneity and that an increase in dominant species heterogeneity will lead to an increase in spatial heterogeneity. Besides biotic factors, the spatial heterogeneity of plant communities can also be influenced by abiotic factors, including pH, nutrients, water content of soils, and so on (Augustine and Frank, 2001; Wijesinghe et al., 2005; Zuo et al., 2009; Ulrich et al., 2014). Ulrich et al. (2014) found that soil variables such as pH can alter the small-scale spatial variability of the plant community structure indirectly by changing species richness. Wu et al. (2014) demonstrated that soil water content can regulate plant community productivity in the semi-arid steppes of China.

The alpine grasslands widespread on the Qinghai-Tibetan Plateau play an important role in ecosystem and water security (Su et al., 2015). The Qinghai-Tibetan Plateau is also one of the most important pastoral areas in China, supporting the production of livestock and the lives of local herdsmen. However, extensive grazing can lead to the decline of grassland productivity (Huang et al., 2007), and the alpine grassland ecosystem on the Qinghai-Tibetan Plateau is facing a series of grassland degradation problems, such as declines in biodiversity and stability (Zhou et al., 2005; Liu et al., 2018; Zhao et al., 2019). Grazing exclusion was considered as an effective measure to alleviate the degradation of the alpine grassland on the Tibetan Plateau (Yan and Lu, 2015). Given the effect of grazing exclusion on plant species diversity and soil properties (Liu et al., 2015; Xiong et al., 2016), we hypothesized that the spatial heterogeneity of plant communities under grazing exclusion would be influenced by the change in biotic and abiotic factors. However, the impact that grazing exclusion activities have on spatial heterogeneity remains controversial.

Here, we investigated the grassland abundance (coverage), height, diversity (species richness and Simpson's dominance index), and soil properties in short-term (2 and 4 years), long-term (9 and 11 years) grazing exclusion and in paired non-exclusion plots to explore the effects of grazing exclusion on species diversity and community spatial heterogeneity and their relationships in the alpine grassland of the Qinghai-Tibetan Plateau. Such knowledge will be important for policy-makers to better formulate policies to manage natural grasslands in this region.

# MATERIALS AND METHODS

## Research Sites

This study was conducted in an alpine meadow near the Haibei National Field Research Station in the Alpine Grassland Ecosystem (37° 36′–37° 37′ N, 101° 18′–101° 19′ E, 3220 m a.s.l.), located in the northeast of the Qinghai-Tibetan Plateau, China (**Table 1**). This alpine grassland has a continental monsoon climate (Wang et al., 2014; Ma et al., 2017), with a mean annual air temperature of −1.08°C and annual precipitation of 416.8 mm during the past 5 years (Wang et al., 2018). The soil type was identified as Mollisols (Liu et al., 2018). The pH of the surface soil (0–10 cm) was 7.8, and the bulk density was 0.8 g $cm^{-3}$. The alpine grassland of this area is a winter pasture, and grazing activity occurs approximately from September to May. The grazing type is free-grazing, with a grazing intensity of 5–6 sheep $ha^{-1}$ $yr^{-1}$ (**Table 1**). The dominant species in the investigated sites include *Stipa aliena* (grasses), *Tibetia himalaica* (legumes), *Saussurea pulchra*, and *S. nigrescens* (non-legume forbs) (**Supplementary Table S1**).

## Experimental Design and Field Investigation

Fenced (no grazing event occurred since being fenced) and paired non-fenced grassland with stands were investigated as grazing exclusion and control treatments, respectively. Four grazing exclusion treatments (approximately 400 $m^2$, 20 m × 20 m plot for each treatment) with different fenced durations (2, 4, 9, and 11 years) were selected and investigated. Among them, 2-year and 11-year grazing exclusion treatments and their controls (Site A, 37° 36′ 46″ N, 101° 18′ 14″ E, 3193 m a.s.l.) were within one block, and 4-year and 9-year grazing exclusion treatment and their controls (Site B, 37° 37′ 2″ N, 101° 19′ 44″ E, 3221 m a.s.l.)

**TABLE 1 |** Information on the short-term and long-term grazing plots. Numbers in parentheses indicate standard deviation.

| Duration (years) | | Site | Site area (ha) | Dominant species[a] | Grazing intensity (sheep ha$^{-1}$ yr$^{-1}$) | Grazing period | Soil pH | SWC (%) | SOC (%) | TN (%) |
|---|---|---|---|---|---|---|---|---|---|---|
| Short-term | 2 | A | 17 | *Stipa aliena*, *Tibetia himalaica*, *Taraxacum mongolicum.* | 6 | Sep. to Apr. | 7.39 (0.05) | 25.7 (0.1) | 6.89 (0.02) | 0.55 (0.03) |
| | 4 | B | 11 | *Stipa aliena*, *Tibetia himalaica*, *Taraxacum mongolicum*. | 5 | Sep. to May | 7.87 (0.04) | 27.1 (0.9) | 5.07 (0.02) | 0.40 (0.01) |
| Long-term | 9 | B | 11 | *Stipa aliena*, *Saussurea pulchra*, *Gentiana straminea*. | 5 | Sep. to May | 7.94 (0.01) | 21.9 (0.4) | 4.66 (0.12) | 0.38 (0.00) |
| | 11 | A | 17 | *Stipa aliena*, *Saussurea pulchra*, *Gentiana straminea*. | 6 | Sep. to Apr. | 7.89 (0.05) | 22.2 (0.3) | 4.31 (0.02) | 0.32 (0.01) |

[a] *The three highest-coverage species in the grazing exclusion plots. SWC, soil water content; SOC, soil organic carbon; TN, total nitrogen.*

were within another block about 3 km away. The grassland areas of these two sites were 11 ha and 17 ha, respectively.

To compare the variation in vegetation characteristics under the short-term and long-term durations of grazing exclusion, we further divided the four grazing exclusion treatments into short-term (2 and 4 years) and long-term (9 and 11 years) exclusion. The control stands were located outside the fenced grasslands (**Table 1** and **Supplementary Table S2**) and had similar community compositions and structures (**Supplementary Figure S3**). To avoid an edge influence of the fence on the growth of the plants, we randomly investigated five grassland sub-plots (1 m × 1 m) inside and outside the fence (5–10 m from the fence), respectively. We divided the 1-m$^2$ sub-plots into 16 grid cells (25 cm × 25 cm), and four of them were randomly selected for the community investigation.

We investigated species, grass height, and coverage (1 cm × 1 cm grid method, absolute coverage based on the square area) in August 2018. The total coverage of all the species was calculated as the sum of the absolute coverage of each species, and the absolute coverage of each species was divided by total coverage as the relative coverage of the species. During August 2019, we conducted a comprehensive investigation of the communities at site A and site B. We investigated species, grass height, and coverage at 75 plots (50 cm × 50 cm) in each site. The soil samples (0–10 cm) were collected after the community survey (using a 5-cm-diameter soil auger). In each 1-m$^2$ sub-plot, five soil samples were collected and were pooled together. In the laboratory, we measured soil water content (SWC), pH, soil organic content (SOC), and total nitrogen content (TN). Soil water content was measured by the oven-drying method. Air-dried samples were used to measure soil pH (pH meter, PHS-3C, INESA, China) and concentrations of C and N (elemental analyzer, FLASHEA 112 Series, Thermo Electron, United States).

The small size of the observed sub-plots (25 cm × 25 cm) might lead to imprecise estimates. To reduce this uncertainty, we performed analysis of species-area relationships. The results showed that the observed numbers of the smallest sub-plots (25 cm × 25 cm) could account for 41% (24/59) and 44% (25/57) for the whole area of site A and site B, respectively (**Supplementary Figure S10**). In addition, we compared the relationships of species richness and plot area between the two sites but found no statistical difference between these two sites.

According to Ma et al. (2017) and Liu et al. (2018), the plants in alpine grassland are divided into four functional groups, namely grasses, sedges, legumes, and non-legume forbs (**Supplementary Table S1**). The plants of the grassland community were divided into three categories according to relative dominance, including dominant species (greater than 5% of the relative coverage), common species (between 1 and 5%), and rare species (less than 1%) (Mariotte et al., 2013). As a result, four dominant species, 17 common species, and 25 rare species were identified in this study (**Supplementary Table S1**).

## Data Analysis

Species richness is the number of species in four cells. The Simpson dominance index (D) is calculated according to Eq. (1):

$$D = \sum_{s=1}^{s} p_s^2 \tag{1}$$

where $p_s$ is the relative coverage of each species (s) (Smith and Wilson, 1996).

The spatial heterogeneity of the community (and of differently dominant species) was calculated as the standard deviation of the total (and differently dominant species) coverage of four cells (σ) divided by the mean value (μ) (coefficient of variation (CV); Weigelt et al., 2008). Asynchrony of species (all species and dominant species in the community) were calculated according to Eq. (2):

$$1 - \varphi_x = \frac{1 - \sigma^2}{(\sum_{i=1}^{s} \sigma_i)^2} \tag{2}$$

where $\sigma_i$ is the standard deviation of the relative coverage of species ($i$), σ is the s.d. of community coverage, and $\varphi_x$ is species synchrony (Loreau and De Mazancourt, 2008).

One-way analysis of covariance (ANOVA) was used to test the differences in plant community characteristics (coverage, height, species richness, and Simpson's dominance index), soil properties (pH, SWC, SOC, TN), and community properties (community spatial heterogeneity, dominant species spatial heterogeneity, and species asynchrony) among the different treatments (short-term and long-term grazing exclusion and their control stands). Pearson correlation analysis was used to test the correlation between factors (biotic and abiotic) (**Supplementary Figure S1**). Non-metric multidimensional scaling (NMDS) was used

to analyze the structural differences among the communities (**Supplementary Figure S3**). First, the height data of each species were dimension-reduced to obtain the community structure under different treatments, and then an analysis of similarity (ANOSIM) was performed using the "vegan" package of R software to examine the differences in community structure between each of the two treatments. If $R = 0$ (R is the statistical value measuring the differences between and within groups, ranging from $-1$ to $+1$), then the community structure between treatments was similar. If $R > 0$ and $P < 0.05$, then the difference in community structure between treatments was significant. Analysis of covariance (ANCOVA) was used to test the existence of the species dominance effect by determining whether the slope and intercept of the regression models were significantly different among the treatments.

To explore the mechanism of grazing exclusion and its duration on plant biodiversity and community spatial heterogeneity, we first used a simple linear regression to analyze the relationship between species diversity, species asynchrony, dominant species spatial heterogeneity, and community spatial heterogeneity. We further fitted a full structural equation model (SEM) (containing all possible pathways) using the "SEM" package of R software to infer the relative importance of species richness, Simpson's dominance index, species asynchrony, and dominant species spatial heterogeneity on community spatial heterogeneity (**Supplementary Table S4**). We then obtained the final model by sequentially deleting the non-significant pathways (**Supplementary Figure S7**). The evaluation of the model was based on the criteria presented in Schermelleh-Engel et al. (2003).

# RESULTS

## Effects of Grazing Exclusion on Community Composition

The results of the ANOVA showed that short-term grazing exclusion had no significant effect on the total coverage ($F = 0.1$, $P = 0.75$) but that long-term grazing exclusion significantly reduced the total coverage ($F = 23.2$, $P < 0.001$). The total coverage decreased significantly with the increase in grazing exclusion duration (**Figure 1A**, $F = 9.9$, $P = 0.01$). Short-term grazing exclusion had no significant effect on the coverage of dominant species ($F = 0.3$, $P = 0.58$), whereas long-term grazing exclusion substantially reduced the coverage of dominant species ($F = 17.8$, $P = 0.001$). However, the divergence between them was not significant (**Figure 1B**, $F = 1.2$, $P = 0.29$). Similarly, short-term grazing exclusion had no significant effect on the coverage of common species ($F = 1.9$, $P = 0.18$), but long-term grazing exclusion significantly reduced the coverage of common species from 50.8 to 34.7% ($F = 6.4$, $P = 0.02$); the coverage of common species decreased significantly (**Figure 1C**, $F = 7.2$, $P = 0.02$) with the increase in grazing exclusion time. For the coverage of rare species, both short-term and long-term grazing exclusion showed a significant increase ($F = 14.5$, $P = 0.001$; $F = 6.8$, $P = 0.02$), but the difference between them was not significant (**Figure 1D**, $F = 0.1$, $P = 0.77$).

For the different functional groups, short-term grazing exclusion reduced but long-term grazing exclusion increased the relative coverage of grasses (**Supplementary Figure S2**). Short-term grazing exclusion resulted in a significant decrease in the relative coverage of sedge by 2.8% ($F = 8.3$, $P = 0.01$), while the relative coverage of legumes in the long-term grazing exclusion was significantly reduced by 21.9% ($F = 104.7$, $P < 0.001$). In addition, both short-term and long-term grazing exclusion increased the relative coverage of non-legume forbs.

There were no significant differences in either species richness or the Simpson's dominance index between short-term grazing exclusion and the control stands (**Figure 2**, $F = 0.2$, $P = 0.68$; $F = 0.1$, $P = 0.95$). However, long-term grazing exclusion significantly reduced species richness (**Figure 2A**, $F = 30.1$, $P < 0.001$) and increased Simpson's dominance index (**Figure 2B**, $F = 30.1$, $P < 0.001$). The duration of grazing exclusion also exerted a negative effect on species richness, with a decrease from 26 species in the short-term grazing exclusion stand to 17 in the long-term stand (**Figure 2A**, $F = 46.6$, $P < 0.001$). For the different degrees of dominance, short-term grazing exclusion has no significant effect on the diversity of the dominant and the rare species but significantly reduced the diversity of the common species (**Supplementary Figure S6**, $F = 7.9$, $P = 0.01$). Long-term grazing exclusion had significantly negative effects on dominant, common, and rare species richness ($P < 0.05$). Common species richness decreased the most (from 13 species to 8 species, **Supplementary Figure S6**).

## Effects of Grazing Exclusion on Community Structure

The ANOSIM results indicated that the greatest differences in plant community composition occurred among the durations of grazing exclusion (**Figure 3** and **Supplementary Table S3**, $R = 0.542$, $P < 0.001$). The community structure changed considerably after long-term grazing exclusion ($R = 0.461$, $P < 0.001$). There was also a significant difference in plant community between the short- and long-term grazing exclusion stands ($R = 0.542$, $P < 0.001$). Short-term grazing exclusion had a slight influence on the plant community ($R = 0.235$, $P = 0.008$). There was no statistically significant difference in plant community composition between the short-term and long-term control stands ($R = 0.060$, $P = 0.137$).

The effect of grazing exclusion on community structure was also shown by the change in plant height (**Supplementary Figures S4, S5**). For the different functional groups, the effects of grazing exclusion on plant height were different between the short-term and long-term exclusion stands. Short-term grazing exclusion significantly increased the height of the grasses, legumes, and non-legume forbs ($P < 0.05$). However, long-term grazing exclusion significantly decreased the height of the grasses, legumes, and non-legume forbs ($P < 0.05$).

## Effects of Grazing Exclusion on Community Spatial Heterogeneity

The effects of grazing exclusion on community spatial heterogeneity were also different between the short-term

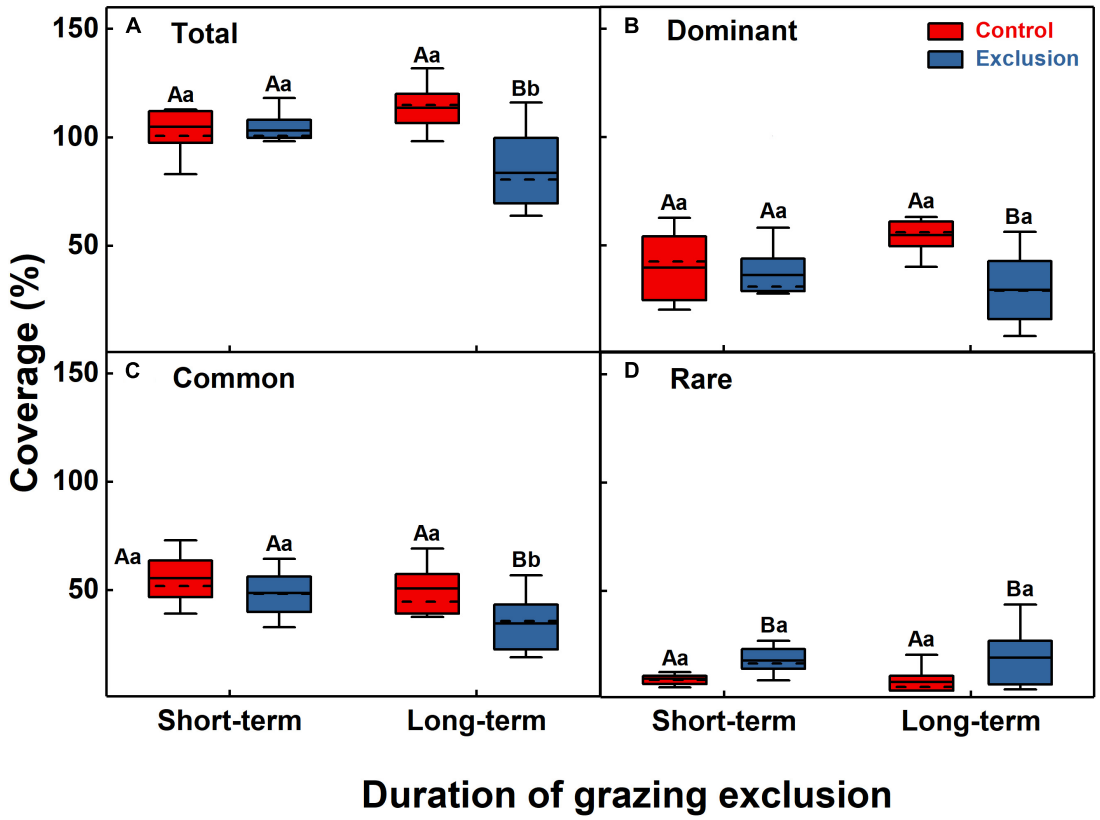


**FIGURE 1 |** Grassland coverage of the community **(A)** and dominant **(B)**, common **(C)**, and rare **(D)** species under short-term and long-term grazing exclusion and in control stands. Boxes in box plots extend from the first (25%) to third (75%) quartiles, with solid and dashed lines at the mean and the median value, respectively. Whiskers extend from the 2.5th to the 97.5th percentile ($n$ = 10). Uppercase letters indicate the differences between control and grazing exclusion under the same duration, while lowercase letters represent the differences between the short-term and long-term application of the same treatment (control or grazing exclusion).

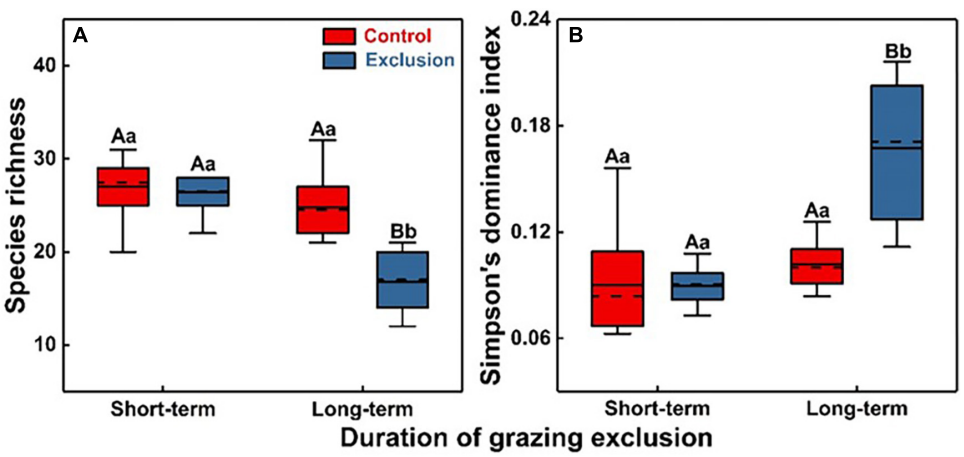


**FIGURE 2 |** Plant species diversity **(A)** and Simpson's dominance index **(B)** under short-term and long-term grazing exclusion and in control stands. Uppercase and lowercase letters indicate the differences between control (Grazing) and crazing exclusion and differences under different durations of grazing exclusion, respectively.

and long-term exclusion stands (**Figure 4**). Long-term grazing exclusion exerted a significant influence on the community heterogeneity ($F$ = 11.8, $P$ = 0.003), but the short-term effect was not significant (**Figure 4A**). Species asynchrony decreased significantly from 0.97 in the short-term grazing exclusion stands to 0.90 in the long-term grazing exclusion stands (**Figure 4C**, $F$ = 8.7, $P$ = 0.009). For dominant species, short-term grazing exclusion had no significant effect on their heterogeneity and

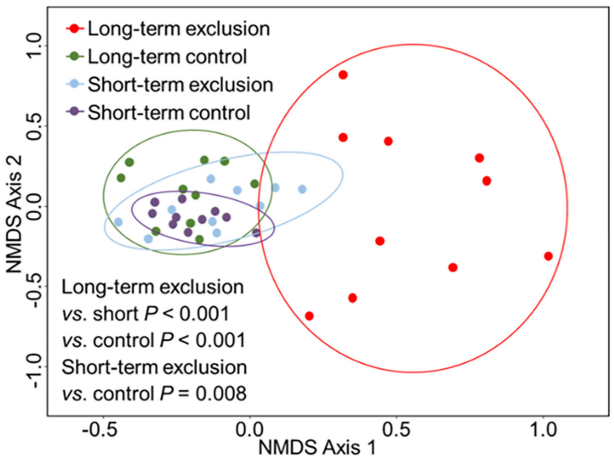


**FIGURE 3 |** Non-metric multidimensional scaling (NMDS) ordination of vegetation in plots based on the height data of different species. Ordinations were based on Bray–Curtis dissimilarities.

asynchrony ($P > 0.05$), while long-term grazing exclusion significantly increased the heterogeneity of the dominant species (**Figures 4B,D**, $F = 12.9$, $P = 0.002$).

The simple linear regression model showed that community heterogeneity was significantly and negatively correlated with species richness and species asynchrony ($P < 0.001$) but positively correlated with the Simpson's dominance index and dominant species spatial heterogeneity (**Figure 5**, $P = 0.002$; $P = 0.001$). Species asynchrony was significantly and positively correlated with species richness but negatively correlated with Simpson's dominance index (**Supplementary Figures S7A,B**). Heterogeneity of dominant species was significantly and negatively correlated with species richness but was not correlated with Simpson's dominance index (**Supplementary Figures S7C,D**). The relationship between community heterogeneity and the heterogeneity of common and rare species was non-significant (**Supplementary Figure S8**, $P = 0.768$, $P = 0.479$).

The results of the full SEM showed that the combined effect of grazing exclusion and its duration led to an increase in community heterogeneity and that this positive effect was achieved mainly by reducing species richness (**Figure 6** and **Supplementary Table S4**, Chi-square = 6.95, $P = 0.07$, AIC = 56.95, GFI = 0.98). Grazing exclusion (standardized coefficient (β) = −0.38, $P < 0.001$) and its duration (β = −0.57, $P < 0.001$) explained 47% of the variation in species diversity (species richness). Species diversity (β = −0.21, $P = 0.01$), dominant species heterogeneity (β = 0.26, $P < 0.001$), and species asynchrony (β = −0.70, $P < 0.001$) explained 89% of the variation in community heterogeneity. Although Simpson's dominance index was significantly negatively correlated with species asynchrony (**Supplementary Figure S7B**) and positively correlated with community heterogeneity (**Figure 5B**) in linear regression, it was not a significant predictor of community heterogeneity in SEM (**Figure 6** and **Supplementary Table S4** and **Supplementary Figure S9**).

# DISCUSSION

## Effects of Grazing Exclusion on Community Composition and Structure

Loss of plant diversity will lead to a reduction in ecosystem productivity and stability (Hooper et al., 2005; Oliver et al., 2015; Ren et al., 2016). In this study, we demonstrated that long-term grazing exclusion decreased plant diversity (species richness) and productivity (coverage) (**Figures 1**, **2**), which is consistent with similar experiments in the *Kobresia*-dominated meadow of the Qinghai-Tibetan Plateau and the lowland grassy ecosystems of southeast Australia (Schultz et al., 2011; Wu et al., 2009). However, the negative effect of grazing exclusion on grassland diversity and productivity was not found in the degraded *Stipa tenacissima* steppe of southern Tunisia or in the natural grassland ecosystem of western Saudi Arabia (Al-Rowaily et al., 2015; Jeddi and Chaieb, 2010). A meta-analysis in grasslands of China showed that short-term (≤5 years) grazing exclusion significantly increased species richness in alpine steppe and temperate steppe but that this phenomenon was not found in alpine meadow (Xiong et al., 2016). Our research in the alpine meadow of the Qinghai-Tibetan Plateau found that a decrease in species richness in the long-term grazing exclusion stand was mainly a result of decreases in common and rare species richness. On the one hand, in comparison to grazing grassland, grazing exclusion activity led to relatively higher grass and litter biomass, which changed the distribution of light resources in the community and then limited the existence of the common and rare species (Letts et al., 2015). On the other hand, grazing exclusion limited soil trampling, which might improve the soil properties, leading to an improvement of the conditions for vegetation (Liu et al., 2015). As a result, different durations of grazing exclusion should exert different effects on community production and plant diversity. In this study, we demonstrated that short-term grazing exclusion activities increased the height of species with different levels of dominance but did not exert any statistical effects on dominant and rare species richness (**Supplementary Figures S5, S6**). However, long-term grazing exclusion decreased the species richness of species with different levels of dominance and did not influence the height of species. The result of Pearson correlation analysis showed that soil pH, soil organic carbon, and total nitrogen content were related to Simpson's dominance index and were not related to species richness (**Supplementary Figure S1**).

Community structure in a grassland ecosystem changes with composition, and this easy-to-understand causal link has a very complex mechanism (Svenning et al., 2004; El-Keblawy, 2016). Reynolds et al. (2003) stated that changes in plant community structure were the result of plant-microbial-soil interactions. We found that long-term grazing exclusion decreased plant diversity and changed the community structure (**Figures 2**, **3**). The changed community structure can be attributed to long-term regulation among plants and between plants and the environment (Milchunas and Lauenroth, 1995). First, herbivores use a process to select food in their grazing activities, and long-term grazing selection helps to form a copromoted evolutionary model between herbivores and

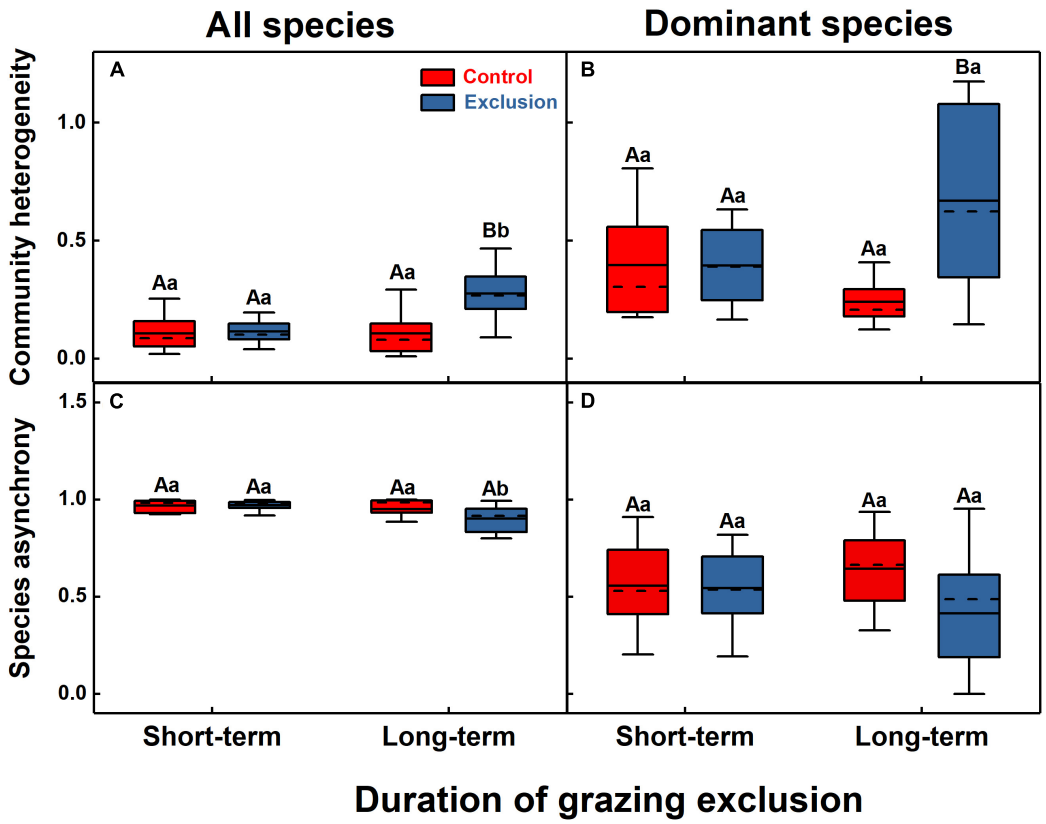


**FIGURE 4 |** Community heterogeneity **(A,B)** and species asynchrony **(C,D)** for all species **(A,C)** and dominant species **(B,D)** under short-term and long-term grazing exclusion and in control stands. Uppercase letters indicate the differences between grazing exclusion and control stands, while lowercase letters represent the differences between short-term and long-term stands.

plants (Becerra, 2007). In contrast, long-term grazing exclusion almost stops this copromoted evolution. The main interaction patterns between plant communities and the external biological environment gradually shift from aboveground (herbivores) to the surface (between plants) or below-ground (e.g., soil resources, microorganisms, and small soil-dwelling animals) (Hartnett and Wilson, 1999; Wijesinghe et al., 2005). Hartnett and Wilson (1999) demonstrated that mycorrhizal fungi drove the variation in plant community structure. Community structure characteristics may also be directly affected by nutrient availability in the soil (Huenneke et al., 1990). In addition, long-term grazing exclusion significantly reduced the coverage of dominant species but increased the coverage of rare species (**Figure 1**). This change in community composition caused by competition among species, especially competition for light resources (Brauer et al., 2012), may further change community structure.

## Increase in Community Spatial Heterogeneity

The community heterogeneity (CV) increased (a decrease of community stability in space, $\frac{1}{CV}$) significantly due to long-term grazing exclusion in this study, which is consistent with the results of a livestock exclusion experiment conducted in Colorado shortgrass steppe (Adler and Lauenroth, 2000). A simple linear model indicated that the increase of community heterogeneity could be attributed to decreases in species diversity, species asynchrony, and dominant species spatial heterogeneity (**Figure 5**), which is consistent with our hypothesis. We found that the change of community heterogeneity and biotic factors (species diversity, species asynchrony, and dominant species spatial heterogeneity) were not correlated with abiotic factors (pH, soil water content, soil organic carbon, and nitrogen content) (**Supplementary Figure S1**). So, we only consider biotic factors to discuss the mechanisms that lead to the increase of community heterogeneity under long-term grazing exclusion (based on the mechanisms that maintain community stability). The stability of community biomass is affected by the characteristics of dominant species and plant diversity (Polley et al., 2007). However, when comparing stability among communities, the change in the functional characteristics of dominant species has a greater impact on stability than the change in species diversity (Sasaki and Lauenroth, 2011). In addition, Pan et al. (2016) noted that when the compensation effect of a community is not obvious, the stability of the ecosystem is more sensitive to the loss of diversity.

Species diversity can affect not only plant productivity but also temporal stability and spatial heterogeneity (Fukami et al.,

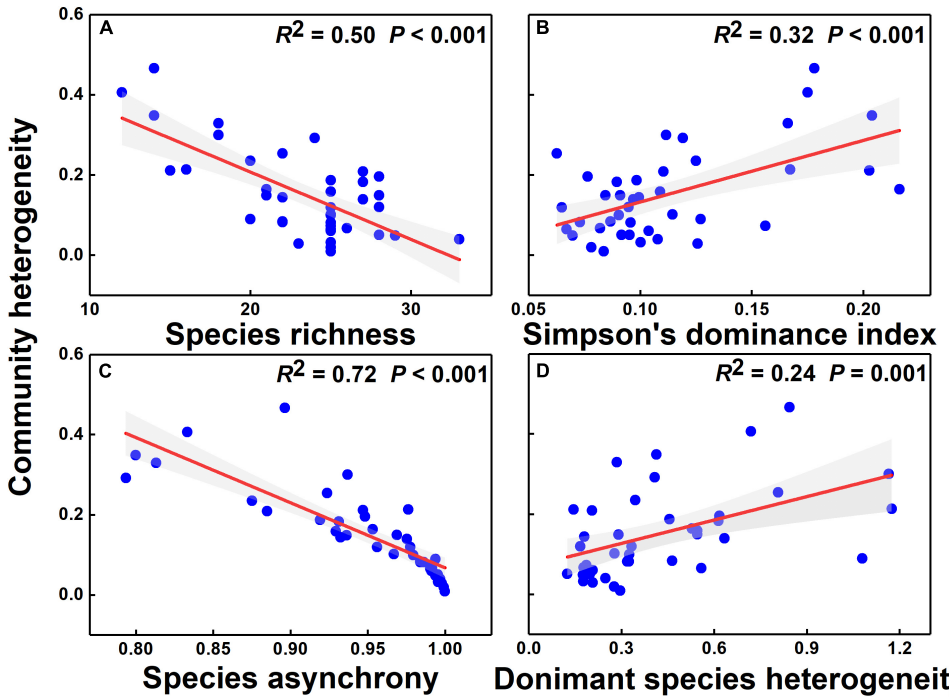


**FIGURE 5 |** The relationships of species richness **(A)**, Simpson's dominance index **(B)**, species asynchrony **(C)**, and dominant species heterogeneity **(D)** with community heterogeneity. Red solid lines represent regression lines, and gray areas are 95% confidence intervals.

2001; Eisenhauer et al., 2011; Loreau and De Mazancourt, 2013). Experimental evidence indicates that changes in environmental factors alter plant diversity and then increase or decrease the community stability of grasslands (Tilman et al., 2006; Weigelt et al., 2008). Yan and Lu (2015) revealed that a 6–8-year grazing exclusion improved the plant diversity and community stability of degraded grasslands on the Qinghai-Tibetan Plateau. In this study, long-term grazing exclusion caused the loss of species, especially the loss of common species, which led to a decline in community spatial heterogeneity (**Figure 5A** and **Supplementary Figure S6**). The full structural equation model indicated that the reduction in species richness was the most important factor affecting community spatial heterogeneity, but Simpson's dominance index was not maintained in this model as a significant factor of community spatial heterogeneity (**Figure 6**). Liu et al. (2015) demonstrated that <6 years of grazing exclusion increased plant diversity and contributed to community stability but that >11 years of grazing exclusion decreased community production and plant diversity in the sandy grassland of Ningxia. The evidence presented here suggests that long-term grazing exclusion has not improved the degradation of Qinghai-Tibetan Plateau grasslands but has decreased grassland plant diversity and increase community heterogeneity. Deléglise et al. (2011) also demonstrated that grazing exclusion may lead to an increase in the spatial variability of plant leaf dry matter content in mountain pastures in France.

Previous studies have shown that changes in the dominant species stability contributed most to changes in community stability (Polley et al., 2007; Yang et al., 2017). We found that long-term grazing exclusion significantly increased the heterogeneity of dominant species (**Figure 4B**) and that community heterogeneity increased with dominant species heterogeneity (**Figure 5D**). The full SEM demonstrated that dominant species heterogeneity was maintained in this model as a significant factor of community spatial heterogeneity and that species richness could cause the increase of community heterogeneity directly or through influencing dominant species heterogeneity (**Figure 6** and **Supplementary Figure S7**). However, after sequentially deleting the non-significant pathways from the full SEM, we found that the duration of treatment began to show an effect on dominant species heterogeneity (**Supplementary Figure S9**). One possible explanation for this phenomenon is the change in community heterogeneity with duration of grazing exclusion (**Figure 4A**).

Species asynchrony represents the interaction of species in the community. Factors that drive asynchrony among species besides environmental stress include species diversity and random effects of species (Loreau and De Mazancourt, 2008). Del Río et al. (2017) suggested that the possible mechanism for maintaining community stability is the compensatory effect between species. Zhang et al. (2016) demonstrated that the reduction of compensatory effects could explain the reduction of stability in a temperate grassland. Our experiments reinforce the idea of a compensatory effect. Interestingly, neither grazing exclusion nor its duration affected species asynchrony (all species) in the SEM, but species asynchrony exhibited significant negative relationships with community spatial heterogeneity

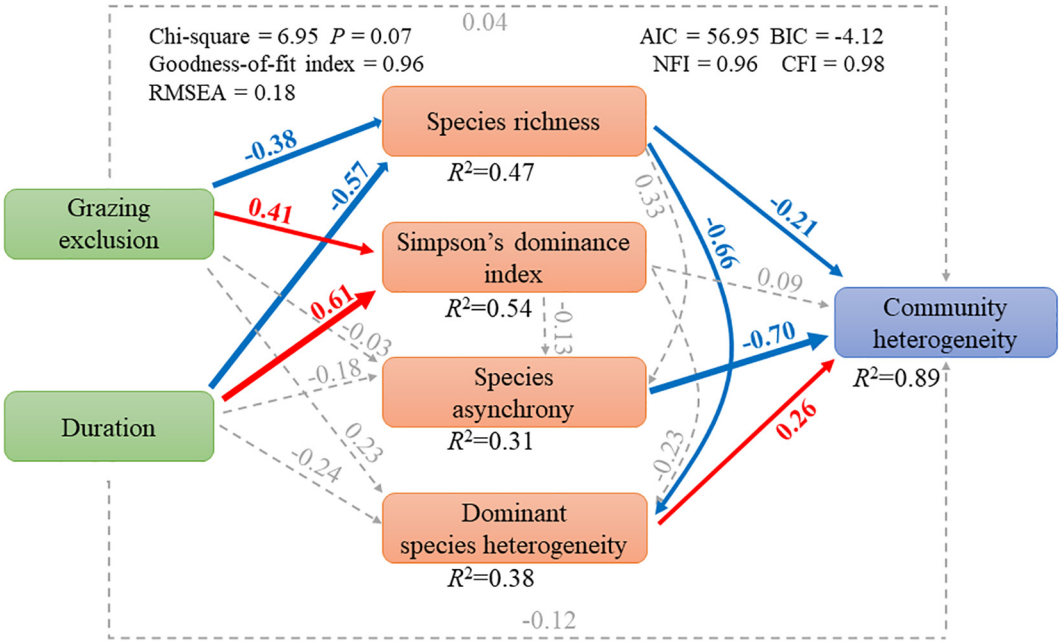


**FIGURE 6 |** A full structural equation model (SEM) of the effects of grazing exclusion and its duration of application on community spatial heterogeneity. Grazing exclusion and its duration can influence community spatial heterogeneity through species richness, Simpson's dominance index, species asynchrony, and dominant species stability. Red and blue solid arrows indicate significant positive and negative pathways, respectively. Gray dashed arrows represent the pathways that are not significant. Arrow width indicates the strength of the relationship between variables. The standard path coefficients are marked above the arrow. The magnitude of $R^2$ is proportional to the variance explained by each dependent variable in the SEM. AIC, Akaike information criterion; BIC, Bayesian information criterion; NFI, normed fit index; RMSEA, root mean square error of approximation; CFI, comparative fit index. All criteria are within acceptable scope.

**TABLE 2 |** Effect of grazing exclusion on grassland plant species richness in this and other studies.

| Study site | Latitude (°) | Longitude (') | Elevation (m) | Grassland type | Duration (years) | *RR* of SR | References |
|---|---|---|---|---|---|---|---|
| Qinghai, China | 37°36′N | 101°18′E | 3220 | Alpine meadow | 2 | 1.06 | This study |
| | 37°36′N | 101°18′E | 3220 | Alpine meadow | 4 | 1.00 | |
| | 37°36′N | 101°18′E | 3220 | Alpine meadow | 9 | 0.64 | |
| | 37°36′N | 101°18′E | 3220 | Alpine meadow | 11 | 0.73 | |
| Tibet, China | 32°19′N | 92°19′E | 4544 | Alpine meadow | 3 | 1.06 | Yan and Lu, 2015 |
| | 31°26′N | 88°20′E | 4613 | Alpine steppe | 3 | 1.01 | |
| | 31°59′N | 84°49′E | 4591 | Alpine desert steppe | 3 | 1.87 | |
| Gansu, China | 33°45′N | 102°04′E | 3500 | Alpine meadow | 8 | 0.78 | Wu et al., 2009 |
| Taif, Saudi Arabia | 21°14′N | 40°42′E | 1400 | N.A. | 25 | 3.00 | Al-Rowaily et al., 2015 |
| Sfax, Tunisia | 34°41′N | 10°30′E | 1220 | Degraded steppe | 6 | 1.85 | Jeddi and Chaieb, 2010 |
| | 34°41′N | 10°30′E | 1220 | Degraded steppe | 12 | 2.50 | |
| Western Alps, France | N.A. | N.A. | 1700 | Subalpine grassland | 22 | 1.05 | Deléglise et al., 2011 |
| | N.A. | N.A. | 1700 | Subalpine grassland | 30 | 1.19 | |
| Mitiamo, Australia | 36°13′S | 144°25′E | N.A. | Lowland grassland | 5 | 1.02 | Schultz et al., 2011 |
| Grampians, Australia | 37°03′S | 142°22′E | N.A. | Lowland grassland | 6 | 1.39 | |
| Craigieburn, Australia | 37°35′S | 144°56′E | N.A. | Lowland grassland | 8 | 1.01 | |
| Hattah Kulkyne, Australia | 34°42′S | 142°18′E | N.A. | Lowland grassland | 9 | 0.83 | |
| Pine Grove, Australia | 36°13′S | 144°25′E | N.A. | Lowland grassland | 10 | 0.86 | |
| Inverleigh, Australia | 38°05′S | 144°03′E | N.A. | Lowland grassland | 11 | 0.76 | |
| Kinypanial, Australia | 36°19′S | 143°48′E | N.A. | Lowland grassland | 12 | 0.93 | |
| Warrambeen, Australia | 37°55′S | 143°52′E | N.A. | Lowland grassland | 12 | 0.34 | |
| Murray Sunset, Australia | 34°16′S | 141°49′E | N.A. | Lowland grassland | 15 | 0.75 | |
| Wilson, Australia | 38°53′S | 146°14′E | N.A. | Lowland grassland | 16 | 0.41 | |

*RR, response ratio, ($SR_{Exclusion}/SR_{Control}$); SR, plant species richness; N.A., not available.*

(**Figures 5C**, **6**). In our study, short-term and long-term grazing exclusion had no significant effects on dominant species asynchrony (**Figure 4D**). The asynchrony of the community and of dominant species was insensitive to grazing exclusion and duration, probably because of changes in community composition, such as compensation for coverage among species with different degrees of dominance. Overall, the significant negative correlation between species asynchrony and community spatial heterogeneity emphasized the importance of species compensatory dynamics for grassland ecosystem functioning. Compared with the full SEM, we found that species richness could influence community heterogeneity indirectly through species asynchrony in the final SEM, which is consistent with the result of simple linear regression between species richness and species asynchrony (**Supplementary Figure S7A**).

In our study, two caveats limited its further application and may cause uncertainties in these results. First, there were limited repetitions in short- (two repetitions, 2 and 4 years) and long-term (two repetitions, 9 and 11 years) grazing exclusion treatments. Second, there was a lack of information about soil biotic and micro-climatic factors, which could result in biases regarding the indirect effect of grazing exclusion on community composition and structure. Despite these caveats, the results of the study still help to increase our understanding of the composition, structure, and function of plant communities under grazing exclusion in the alpine meadow of the Qinghai-Tibetan Plateau and contribute to predicting community spatial heterogeneity in other grasslands through species diversity.

### The Cross-Scale Response of Community Composition to Grazing Exclusion

We investigated the responses of community structure, such as abundance (coverage), height, diversity (species richness and Simpson's dominance index), and soil properties to short-term (2, 4 years) and long-term (9 and 11 years) grazing exclusion in the alpine meadow of the Qinghai-Tibetan Plateau. The results showed that long-term grazing exclusion could reduce species diversity. To compare the results of species richness from the alpine grassland ecosystem with the results from other grassland ecosystems, we summarized the effect of the exclusion on the species richness from related grazing exclusion experiments in different regions (**Table 2**). We found that the effects of grazing exclusion on grassland plant species richness were dependent on grassland type and exclusion duration. For example, long-term grazing exclusion has caused a loss of species richness in alpine grassland in China and lowland grassy ecosystems of southeast Australia (Wu et al., 2009; Schultz et al., 2011). However, the long-term implementation of grazing exclusion could still contribute to the maintenance of species richness in subalpine grasslands in France and degraded *Stipa tenacissima* steppe in southern Tunisia (Jeddi and Chaieb, 2010; Deléglise et al., 2011). Several abiotic and biotic factors, including climate and grassland type, could contribute to the divergent effects of grazing exclusion (Xiong et al., 2016). Temperature and precipitation can influence plant species richness after grazing exclusion (Wu et al., 2012; Xiong et al., 2016). For example, the investigations of an alpine grassland transect along the northern Tibetan Plateau indicated that growing season precipitation increased plant species richness by promoting seed germination in the local species pool (Wu et al., 2012). Long-term grazing exclusion could restore the degraded *Stipa tenacissima* steppe in southern Tunisia by promoting the growth of palatable species (Jeddi and Chaieb, 2010). However, long-term grazing exclusion decreased plant species richness, as in the non-degraded alpine grassland of the Qinghai-Tibetan Plateau (**Table 2** and **Figure 2**). The possible reason for this is the effects of the competitiveness (such as for light or nutrient resources) of dominant grasses on common and rare species under the condition of grazing exclusion (Wu et al., 2009).

## CONCLUSION

In conclusion, our results indicated that grazing exclusion, especially long-term exclusion, failed to improve grassland productivity (grassland coverage) and even reduced the community coverage and plant diversity and altered the community structure of the alpine grassland. Furthermore, our work identified decreased plant diversity as the main reason for the increased spatial heterogeneity of the grazing exclusion in the alpine grassland ecosystem. These results suggest that grazing can maintain relatively higher plant species diversity and community stability in the alpine grassland that covers much of the Qinghai-Tibetan Plateau. However, the effect is not suitable for severely degraded grassland types. Focusing on the impact of grazing exclusion on community composition and structure in different regions is necessary for the sustainable development of each grassland ecosystem.

## DATA AVAILABILITY STATEMENT

The datasets generated for this study are available on request to the corresponding author.

## AUTHOR CONTRIBUTIONS

JXZ, TZ, and SS designed the research. SS and FZ performed the field survey and data analysis. SS wrote the first draft, with inputs from all authors.

## FUNDING

This work was partly funded by the National Key Research and Development Program of China (2019YFC0507704 and 2017YF0503906), National Natural Science Foundation of China (31700374), and Fundamental Research Funds for the Central Universities (lzujbky-2018-ct02 and lzujbky-2019-76).

## ACKNOWLEDGMENTS

We are grateful to the Haibei National Field Research Station in the Alpine Grassland Ecosystem for maintaining the experimental facility.

## SUPPLEMENTARY MATERIAL

The Supplementary Material for this article can be found online at: https://www.frontiersin.org/articles/10.3389/fevo.2020.00066/full#supplementary-material

## REFERENCES

Adler, P. B., and Lauenroth, W. K. (2000). Livestock exclusion increases the spatial heterogeneity of vegetation in Colorado shortgrass steppe. *Appl. Veg. Sci.* 3, 213–222. doi: 10.2307/1479000

Al-Rowaily, S. L., El-Bana, M. I., Al-Bakre, D. A., Assaeed, A. M., Hegazy, A. K., and Ali, M. B. (2015). Effects of open grazing and livestock exclusion on floristic composition and diversity in natural ecosystem of Western Saudi Arabia. *Saudi J. Biol. Sci.* 22, 430–437. doi: 10.1016/j.sjbs.2015.04.012

Augustine, D. J., and Frank, D. A. (2001). Effects of migratory grazers on spatial heterogeneity of soil nitrogen properties in a grassland ecosystem. *Ecology* 82, 3149–3162. doi: 10.2307/2679841

Bai, Y., Han, X., Wu, J., Chen, Z., and Li, L. (2004). Ecosystem stability and compensatory effects in the Inner Mongolia grassland. *Nature* 431, 181–184. doi: 10.1038/nature02850

Becerra, J. X. (2007). The impact of herbivore-plant coevolution on plant community structure. *Proc. Natl. Acad. Sci. U.S.A.* 104, 7483–7488. doi: 10.1073/pnas.0608253104

Brauer, V. S., Stomp, M., and Huisman, J. (2012). The nutrient-load hypothesis: patterns of resource limitation and community structure driven by competition for nutrients and light. *Am. Nat.* 179, 721–740. doi: 10.1086/665650

Del Río, M., Pretzsch, H., Ruíz-Peinado, R., Ampoorter, E., Annighöfer, P., Barbeito, I., et al. (2017). Species interactions increase the temporal stability of community productivity in *Pinus sylvestris-Fagus sylvatica* mixtures across Europe. *J. Ecol.* 105, 1032–1043. doi: 10.1111/1365-2745.12727

Deléglise, C., Loucougaray, G., and Alard, D. (2011). Effects of grazing exclusion on the spatial variability of subalpine plant communities: a multiscale approach. *Basic Appl. Ecol.* 12, 609–619. doi: 10.1016/j.baae.2011.08.006

Eisenhauer, N., Milcu, A., Allan, E., Nitschke, N., Scherber, C., Temperton, V., et al. (2011). Impact of above- and below-ground invertebrates on temporal and spatial stability of grassland of different diversity. *J. Ecol.* 99, 572–582. doi: 10.1111/j.1365-2745.2010.01783.x

El-Keblawy, A. (2016). Impact of fencing and irrigation on species composition and diversity of desert plant communities in the united Arab emirates. *Land Degrad. Dev.* 28, 1354–1362. doi: 10.1002/ldr.2599

Fukami, T., Naeem, S., and Wardle, D. A. (2001). On similarity among local communities in biodiversity experiments. *Oikos* 95, 340–348. doi: 10.2307/3547380

Grman, E., Lau, J. A., Schoolmaster, D. R., and Gross, K. L. (2010). Mechanisms contributing to stability in ecosystem function depend on the environmental context. *Ecol. Lett.* 13, 1400–1410. doi: 10.1111/j.1461-0248.2010.01533.x

Hartnett, D. C., and Wilson, G. W. (1999). Mycorrhizae influence plant community structure and diversity in tallgrass prairie. *Ecology* 80, 1187–1195. doi: 10.2307/177066

Hooper, D. U., Chapin, F. S., Ewel, J. J., Hector, A., Lnchausti, P., Lavorel, S., et al. (2005). Effects of biodiversity on ecosystem functioning: a consensus of current knowledge. *Ecol. Monogr.* 75, 3–35. doi: 10.1890/04-0922

Huang, D., Wang, K., and Wu, W. L. (2007). Dynamics of soil physical and chemical properties and vegetation succession characteristics during grassland desertification under sheep grazing in an agro-pastoral transition zone in Northern China. *J. Arid Environ.* 70, 120–136. doi: 10.1016/j.jaridenv.2006.12.009

Huenneke, L. F., Hamburg, S. P., Koide, R., Mooney, H. A., and Vitousek, P. M. (1990). Effects of soil resources on plant invasion and community structure in Californian serpentine grassland. *Ecology* 71, 478–491. doi: 10.2307/1940302

Huston, M. A. (1997). Hidden treatments in ecological experiments: re-evaluating the ecosystem function of biodiversity. *Oecologia* 110, 449–460. doi: 10.1007/s004420050180

Jeddi, K., and Chaieb, M. (2010). Changes in soil properties and vegetation following livestock grazing exclusion in degraded arid environments of South Tunisia. *Flora* 205, 184–189. doi: 10.1016/j.flora.2009.03.002

Kolasa, J., and Rollo, C. D. (1991). "Introduction: the heterogeneity of heterogeneity: a glossary," in *Ecological Heterogeneity*, eds J. Kolasa, and S. T. A. Pickett, (New York, NY: Springer), 1–23. doi: 10.1007/978-1-4612-3062-5_1

Letts, B., Lamb, E. G., Mischkolz, J. M., and Romo, J. T. (2015). Litter accumulation drives grassland plant community composition and functional diversity via leaf traits. *Plant Ecol.* 216, 357–370. doi: 10.1007/s11258-014-0436-6

Liu, H., Mi, Z., Lin, L., Wang, Y., Zhang, Z., Zhang, F., et al. (2018). Shifting plant species composition in response to climate change stabilizes grassland primary production. *Proc. Natl. Acad. Sci. U.S.A.* 115, 4051–4056. doi: 10.1073/pnas.1700299114

Liu, X., Zhang, K., and Ahmad, B. (2015). Influence of fencing time on vegetation community structure and species diversity in sandy grassland of Ningxia in China. *Nat. Environ. Pollut. Technol.* 14, 703–708.

Loreau, M., and De Mazancourt, C. (2008). Species synchrony and its drivers: neutral and nonneutral community dynamics in fluctuating environments. *Am. Nat.* 172, E48–E66. doi: 10.1086/589746

Loreau, M., and De Mazancourt, C. (2013). Biodiversity and ecosystem stability: a synthesis of underlying mechanisms. *Ecol. Lett.* 16, 106–115. doi: 10.1111/ele.12073

Ma, Z., Liu, H., Mi, Z., Zhang, Z., Wang, Y., Xu, W., et al. (2017). Climate warming reduces the temporal stability of plant community biomass production. *Nat. Commun.* 8:15378. doi: 10.1038/ncomms15378

Mariotte, P., Vandenberghe, C., Kardol, P., Hagedorn, F., Buttler, A., and Schwinning, S. (2013). Subordinate plant species enhance community resistance against drought in semi-natural grasslands. *J. Ecol.* 101, 763–773. doi: 10.1111/1365-2745.12064

Milchunas, D. T., and Lauenroth, W. K. (1995). Inertia in plant community structure: state changes after cessation of nutrient-enrichment stress. *Ecol. Appl.* 5, 452–458. doi: 10.2307/1942035

Naeem, S., Thompson, L. J., Lawler, S. P., Lawton, J. H., and Woodfin, R. M. (1994). Declining biodiversity can alter the performance of ecosystems. *Nature* 368, 734–737. doi: 10.1038/368734a0

Oliver, T. H., Isaac, N. J. B., August, T. A., Woodcock, B. A., Roy, D. B., Bullock, J. M., et al. (2015). Declining resilience of ecosystem functions under biodiversity loss. *Nature* 6:10122. doi: 10.1038/ncomms10122

Pan, Q., Tian, D., Naeem, S., Auerswald, K., Elser, J. J., Bai, Y., et al. (2016). Effects of functional diversity loss on ecosystem functions are influenced by compensation. *Ecology* 97, 2293–2302. doi: 10.1002/ecy.1460

Polley, H. W., Wilsey, B. J., and Derner, J. D. (2007). Dominant species constrain effects of species diversity on temporal variability in biomass production of tallgrass prairie. *Oikos* 116, 2044–2052. doi: 10.1111/j.2007.0030-1299.16080.x

Ren, Y., Lü, Y., and Fu, B. (2016). Quantifying the impacts of grassland restoration on biodiversity and ecosystem services in China: a meta-analysis. *Ecol. Eng.* 95, 542–550. doi: 10.1016/j.ecoleng.2016.06.082

Reynolds, H. L., Packer, A., Bever, J. D., and Clay, K. (2003). Grassroots ecology: plant–microbe–soil interactions as drivers of plant community structure and dynamics. *Ecology* 84, 2281–2291. doi: 10.2307/3450134

Sasaki, T., and Lauenroth, W. K. (2011). Dominant species, rather than diversity, regulates temporal stability of plant communities. *Oecologia* 166, 761–768. doi: 10.1007/s00442-011-1916-1

Schermelleh-Engel, K., Moosbrugger, H., and Hans, M. (2003). Evaluating the fit of structural equation models: tests of significance and descriptive goodness-of-fit measures. *Methods Psychol. Res.* 8, 23–74.

Schultz, N. L., Morgan, J. W., and Lunt, I. D. (2011). Effects of grazing exclusion on plant species richness and phytomass accumulation vary across a regional productivity gradient. *J. Veg. Sci.* 22, 130–142. doi: 10.1111/j.1654-1103.2010.01235.x

Smith, B., and Wilson, J. B. (1996). A consumer's guide to evenness indices. *Oikos* 76, 70–82. doi: 10.2307/3545749

Song, M. H., and Yu, F. H. (2015). Reduced compensatory effects explain the nitrogen-mediated reduction in stability of an alpine meadow on the Tibetan Plateau. *New Phytol.* 207, 70–77. doi: 10.1111/nph.13329

Su, X. K., Wu, Y., Dong, S. K., Wen, L., Li, Y. Y., and Wang, X. X. (2015). Effects of grassland degradation and re-vegetation on carbon and nitrogen storage in the soils of the headwater area nature reserve on the Qinghai-Tibetan Plateau, China. *J. Mt. Sci.* 12, 582–591. doi: 10.1007/s11629-014-3043-z

Svenning, J. C., Kinner, D. A., Stallard, R. F., Engelbrecht, B. M. J., and Wright, S. J. (2004). Ecological determinism in plant community structure across a tropical forest landscape. *Ecology* 85, 2526–2538. doi: 10.1890/03-0396

Tilman, D., Reich, P. B., and Knops, J. M. H. (2006). Biodiversity and ecosystem stability in a decade-long grassland experiment. *Nature* 441, 629–632. doi: 10.1038/nature04742

Ulrich, W., Piwczyński, M., Zaplata, M. K., Winter, S., Schaaf, W., and Fischer, A. (2014). Small-scale spatial variability in phylogenetic community structure during early plant succession depends on soil properties. *Oecologia* 175, 985–995. doi: 10.1007/s00442-014-2954-2

Wang, Y., Liu, H., Chung, H., Yu, L., Mi, Z., Geng, Y., et al. (2014). Non-growing-season soil respiration is controlled by freezing and thawing processes in the summer monsoon-dominated Tibetan alpine grassland. *Glob. Biogeochem. Cycles* 28, 1081–1095. doi: 10.1002/2013GB004760

Wang, Y., Song, C., Yu, L., Mi, Z., Wang, S., Zeng, H., et al. (2018). Convergence in temperature sensitivity of soil respiration: evidence from the tibetan alpine grasslands. *Soil Biol. Biochem.* 122, 50–59. doi: 10.1016/j.soilbio.2018.04.005

Weigelt, A., Schumacher, J., Roscher, C., and Schmid, B. (2008). Does biodiversity increase spatial stability in plant community biomass? *Ecol. Lett.* 11, 338–347. doi: 10.1111/j.1461-0248.2007.01145.x

Wijesinghe, D. K., John, E. A., and Hutchings, M. J. (2005). Does pattern of soil resource heterogeneity determine plant community structure? An experimental investigation. *J. Ecol.* 93, 99–112. doi: 10.1111/j.0022-0477.2004.00934.x

Wilcox, K. R., Tredennick, A. T., Koerner, S. E., Grman, E., Hallett, L. M., Avolio, M. L., et al. (2017). Asynchrony among local communities stabilises ecosystem function of metacommunities. *Ecol. Lett.* 20, 1534–1545. doi: 10.1111/ele.12861

Wilsey, B. J., Daneshgar, P. P., Hofmockel, K., and Polley, H. W. (2014). Invaded grassland communities have altered stability-maintenance mechanisms but equal stability compared to native communities. *Ecol. Lett.* 17, 92–100. doi: 10.1111/ele.12213

Wu, G. L., Du, G. Z., Liu, Z. H., and Thirgood, S. (2009). Effect of fencing and grazing on a Kobresia-dominated meadow in the Qinghai-Tibetan plateau. *Plant Soil* 319, 115–126. doi: 10.1016/S0145-305X(00)00063-X

Wu, G. L., Zhang, Z. N., Wang, D., Shi, Z. H., and Zhu, Y. J. (2014). Interactions of soil water content heterogeneity and species diversity patterns in semi-arid steppes on the Loess Plateau of China. *J. Hydrol.* 519, 1362–1367. doi: 10.1016/j.jhydrol.2014.09.012

Wu, J. S., Zhang, X. Z., Shen, Z. X., Shi, P. L., Yu, C. Q., Song, M. H., et al. (2012). Species richness and diversity of alpine grasslands on the northern Tibetan Plateau: effects of grazing exclusion and growing season precipitation. *J. Resour. Ecol.* 3, 236–242. doi: 10.1016/j.jenvman.2018.10.097

Xiong, D., Shi, P., Zhang, X., and Zou, C. B. (2016). Effects of grazing exclusion on carbon sequestration and plant diversity in grasslands of China—A meta-analysis. *Ecol. Eng.* 94, 647–655. doi: 10.1016/j.ecoleng.2016.06.124

Xu, M., Qi, Y., Chen, J., and Yin, W. (2000). Effects of spatial heterogeneity of microenvironment on plant biodiversity in the Southeastern Missouri Ozarks. *Geogr. Inform. Sci.* 6, 38–47. doi: 10.1080/10824000009480532

Yan, Y., and Lu, X. (2015). Is grazing exclusion effective in restoring vegetation in degraded alpine grasslands in Tibet, China? *PeerJ* 3:e1020. doi: 10.7717/peerj.1020

Yang, Z., Zhang, Q., Su, F., Zhang, C., Pu, Z., Xia, J., et al. (2017). Daytime warming lowers community temporal stability by reducing the abundance of dominant, stable species. *Glob. Change Biol.* 23, 154–163. doi: 10.1111/gcb.13391

Zhang, Y., Loreau, M., Lü, X., He, N., Zhang, G., and Han, X. (2016). Nitrogen enrichment weakens ecosystem stability through decreased species asynchrony and population stability in a temperate grassland. *Glob. Change Biol.* 22, 1445–1455. doi: 10.1111/gcb.13140

Zhao, K., Wang, Z. Y., Li, Y. Q., Zheng, T. L., and Hu, J. B. (2019). Effect of two restorations on the grassland coverage after remediation of take-abandon soil field on the Qinghai-Tibet Plateau. *Pratacultural Sci.* 36, 2500–2507. doi: 10.11829/j.issn.1001-0629.2019-0066

Zhou, H., Zhao, X., Tang, Y., Gu, S., and Zhou, L. (2005). Alpine grassland degradation and its control in the source region of the Yangtze and Yellow Rivers, China. *Grassl. Sci.* 51, 191–203. doi: 10.1111/j.1744-697X.2005.00028.x

Zuo, X., Zhao, X., Zhao, H., Zhang, T., Guo, Y., Li, Y., et al. (2009). Spatial heterogeneity of soil properties and vegetation-soil relationships following vegetation restoration of mobile dunes in Horqin Sandy Land, Northern China. *Plant Soil* 318, 153–167. doi: 10.1007/s11104-008-9826-7

**Conflict of Interest:** The authors declare that the research was conducted in the absence of any commercial or financial relationships that could be construed as a potential conflict of interest.

frontiers in Ecology and Evolution

ORIGINAL RESEARCH
published: 30 June 2020
doi: 10.3389/fevo.2020.00181

# Diversity of Reproductive Phenology Among Subtropical Grasses Is Constrained by Evolution and Climatic Niche

*Kangxin Li[1], Jinying Wang[1], Lu Qiao[1], Ruyi Zheng[1], Yiqun Ma[1], Yuan Chen[2,3], Xiaobo Hou[4], Yanjun Du[5], Jianguo Gao[6] and Hui Liu[7,8,9]**

[1] Shanghai Minhang High School, Shanghai, China, [2] Plant Gene Expression Center, USDA-ARS, Albany, CA, United States, [3] Department of Plant and Microbial Biology, University of California, Berkeley, Berkeley, CA, United States, [4] Department of Soil, Water and Environmental Science, University of Arizona, Tucson, AZ, United States, [5] Key Laboratory of Genetics and Germplasm Innovation of Tropical Special Forest Trees and Ornamental Plants, Ministry of Education, College of Forestry, Hainan University, Haikou, China, [6] Key Laboratory for Earth Surface Processes of the Ministry of Education, Department of Ecology, College of Urban and Environmental Sciences, Peking University, Beijing, China, [7] Key Laboratory of Vegetation Restoration and Management of Degraded Ecosystems, South China Botanical Garden, Chinese Academy of Sciences, Guangzhou, China, [8] Guangdong Provincial Key Laboratory of Applied Botany, South China Botanical Garden, Chinese Academy of Sciences, Guangzhou, China, [9] Center for Plant Ecology, Core Botanical Garden, Chinese Academy of Sciences, Guangzhou, China

OPEN ACCESS

**Edited by:**
*George P. Malanson, The University of Iowa, United States*

**Reviewed by:**
*Rafael De Oliveira Xavier, University of São Paulo, Brazil*
*David R. Butler, Texas State University, United States*

***Correspondence:**
*Hui Liu*
*hui.liu@scbg.ac.cn*

**Specialty section:**
*This article was submitted to Biogeography and Macroecology, a section of the journal Frontiers in Ecology and Evolution*

**Received:** *25 December 2019*
**Accepted:** *22 May 2020*
**Published:** *30 June 2020*

**Citation:**
*Li K, Wang J, Qiao L, Zheng R, Ma Y, Chen Y, Hou X, Du Y, Gao J and Liu H (2020) Diversity of Reproductive Phenology Among Subtropical Grasses Is Constrained by Evolution and Climatic Niche. Front. Ecol. Evol. 8:181. doi: 10.3389/fevo.2020.00181*

Reproductive phenology is sensitive to climatic changes and is associated with species functional types, distribution ranges, and their corresponding climatic niches. Phylogenetic niche conservatism in reproductive phenology also constrains its diversity and the distribution of species. Therefore, we assessed the effects of photosynthetic pathway, life history, phylogeny, and climatic niche on reproductive phenology. For 190 Poaceae species in subtropical China, we compiled data on flowering onset and reproductive period, functional type (photosynthetic pathway and life history), and 18 climatic variables across the species' global distributions and used phylogenetic models to determine associations. We found strong phylogenetic signals in flowering onset but not in reproductive period. Photosynthetic pathway and life history have significant interactive effects on both flowering onset and reproductive period, such that $C_3$ annual grasses flowered the earliest and had the longest reproductive period. We found that species with wider climatic niches would flower earlier and have longer reproductive periods. Specifically, species that experience wider ranges of mean annual precipitation and coldest-month temperatures would flower earlier, and species with higher mean annual temperature and wider ranges of wettest-quarter precipitation have a longer reproductive period. This study finds that the diversity of reproductive phenology among subtropical grasses is constrained by evolution and climatic niche and that photosynthetic pathway and life history have an interactive effect on the timing and the duration of reproduction.

**Keywords: diversity, flowering phenology, geographic distribution, climatic niche, phylogenetic niche conservatism, life history, photosynthetic pathway**

## INTRODUCTION

Reproductive phenology is key to the success of individual plant reproduction and population persistence (Rathcke and Lacey, 1985; Elzinga et al., 2007; Craine et al., 2012a). Differences in reproductive phenology among co-occurring species minimize direct competition and are often important in maintaining high species diversity in communities (Craine et al., 2012b). However, the reproductive phenology of species is not fixed and may be sensitive to changes in climate (Anderson et al., 2012). Flowering onset and duration, for example, are determined by a network of signals including day length (Colasanti and Coneva, 2009), light quality (Cerdán and Chory, 2003), temperature (Fitter and Fitter, 2002; Colasanti and Coneva, 2009), atmospheric $CO_2$ concentration (Springer and Ward, 2007), and drought (Franks, 2011). In temperate grasses, vernalization, or a prolonged exposure to cold temperature, is required to induce the expression of the FLOWERING LOCUS T (FT) gene, a key gene in flower development (Corbesier et al., 2007; Tamaki et al., 2007; Lv et al., 2014). Besides environmental factors, recent studies have found that the reproductive phenology of species is also influenced by life history, photosynthetic pathway, and phylogeny (Davies et al., 2013; Du et al., 2015; Cortés-Flores et al., 2017; Munson and Long, 2017). Despite these various findings, there has not yet been a systematic study on how reproductive phenology is shaped by plant functional types, phylogeny, and climatic niches.

As the fifth largest plant family comprising ∼12,000 species, grasses (members of the Poaceae family) are an essential food source for many species, including our own, and thus any potential phenological shifts under climatic change might have huge ecological and economic consequences (Munson and Long, 2017). Phylogenetic niche conservatism (PNC) is the tendency of closely related species to share similar niches and traits (Wiens, 2004; Wiens and Graham, 2005) and has been found in flowering onset in many species from different families (Davies et al., 2013; Du et al., 2015; Li et al., 2016). Although the phenology of grasses has been studied in a small number of crops and dominant grassland species (Craine et al., 2012a; Li et al., 2016), studies that encompass the great diversity of grass species are still lacking. This may be partly due to difficulties of long-term phenological surveys on many species or distinctions between flower and fruit stages for grasses in the field (Primack and Gallinat, 2017). However, since PNC in flowering phenology has been widely found and a number of grass morphological and physiological traits show PNC (Liu et al., 2012; Liu and Osborne, 2015), we also expect to find PNC in the reproductive phenology of grasses.

Divergent structural and physiological traits among $C_3$ and $C_4$ grasses (Edwards et al., 2010; Sage et al., 2012; Taylor et al., 2014; Lundgren et al., 2019) may lead to differences in reproductive phenology. In grasses, $C_4$ species have higher photosynthetic rates, greater water use efficiencies, and faster growth under warm and dry conditions than their $C_3$ counterparts (Ehleringer, 1978; Way et al., 2014; Atkinson et al., 2016). Therefore, where $C_3$ and $C_4$ grasses coexist, $C_3$ grasses might flower earlier to gain an initial reproductive advantage before intense competition with $C_4$ grasses for space and other resources begins. In addition, the reproductive duration of $C_3$ grasses might be longer than that of $C_4$ grasses because $C_4$ grasses are adapted to warmer regions where the warm climate delays the flowering onset and shortens the duration (Sherry et al., 2011). Using herbarium records of 16 grass species, a recent study found that $C_3$ grasses indeed start to flower earlier than $C_4$ grasses (Munson and Long, 2017). However, whether this pattern in reproductive phenology between $C_3$ and $C_4$ grasses is widespread has not been tested.

Life history may be another important trait in determining phenology due to fundamental differences in resource allocation strategies across life history functional types (Lundgren and Des Marais, 2020). While annuals tend to flower once in a single growing season and die, biennials and triennials flower in their 2nd and 3rd years, respectively. In contrast, perennials persist over multiple growing seasons but may have multiple flowering periods per year (iteroparity) or flower once over multiple years (semelparity; Lundgren and Des Marais, 2020). Therefore, to ensure that their sole reproductive effort is successful and to limit competition with established perennials, annuals may flower earlier and longer than perennials. Munson and Long (2017) found that annual grasses flowered earlier than perennial grasses in a sample of 16 species, but only in regions with a higher mean annual temperature. Given that, across subtropical grasses, life history influences the diversity of several functional traits (Liu et al., 2019b), we expected that reproductive phenology would also differ between annual and perennial grasses. Therefore, as multiple environmental and functional factors will affect the reproductive phenology of grasses, more species across multiple ecosystems need to be tested to determine whether photosynthetic pathway and life history have interactive effects on grass reproductive phenology and whether the patterns depend on phylogenetic background.

Climatic niches depict where species occur over space and time and reflect their adaptive strategies (Soberón, 2007; MacLean and Beissinger, 2017). Across species, variation in climatic niche is closely related to variation in functional traits (Thuiller et al., 2004). Species with wide geographic ranges are expected to have higher adaptability and are more able to change their traits to better fit their environment than species with narrow ranges (Lavergne et al., 2004; Slatyer et al., 2013). In terms of reproductive phenology, species with larger ranges are predicted to be more able to alter the timing of reproduction in response to changes in the local environments than narrow-ranging species. For example, flowering onset is likely to be related to climatic conditions, especially temperature (Fitter and Fitter, 2002). Therefore, in climate change scenarios, knowledge of the relationships between reproductive phenology and their climatic niches is urgently needed for predicting the survival and the distribution of species.

Previous phylogenetic studies on flowering phenology have included species across multiple families (Munguía-Rosas et al., 2011; Du et al., 2015), but few have focused on many species within one family, which can assess phylogenetic effects at a more detailed scale (Staggemeier et al., 2010). Furthermore, tropical, and subtropical regions contain over half of the herbaceous species in Poaceae (except Bambusoideae and Pooideae; Watson et al., 1992; Osborne et al., 2014). Grass species in

subtropical China are diverse in life history and photosynthetic pathway and have been well surveyed and studied, providing an ideal basis for further study (Liu et al., 2019b). Here we use data on reproductive phenology, photosynthetic pathway, life history, phylogeny, and global climatic niche for 190 subtropical grasses in order to test the following hypotheses while controlling for phylogenetic effects: (1) There are strong phylogenetic signals in two reproductive phenological traits (flowering onset and reproductive period); (2) $C_3$ grasses flower earlier and have longer reproductive periods than $C_4$ grasses, and similarly, annuals flower earlier and have longer reproductive periods than perennials. Photosynthetic pathway and life history may have interactive effects on flowering onset and reproductive period; and (3) Species with wider global climatic niches might flower earlier and have longer reproductive periods, with some key climatic niche variables playing more important roles than others, for example, coldest-month temperature may be more important than mean annual temperature.

# MATERIALS AND METHODS

## Species Sampling and Reproductive Phenology

Subtropical China has a typical East Asian monsoon climate. Its central region, Guangdong Province, has a mean annual temperature of 21.2°C (13.6°C in January and 28.9°C in July) and a mean annual precipitation of ∼1,700 mm, of which 80% occurs in the wet season from April to September.

There are 316 herbaceous Poaceae species in the native flora of subtropical China, according to the "Flora of Guangdong" (South China Botanical Garden, 2009). Here we only considered herbaceous grasses and so excluded the 153 species of woody bamboos in this region to keep the same life form. We assigned photosynthetic pathway ($C_3$ or $C_4$ species) for each species based on published literature (Grass Phylogeny Working Group, 2012; Osborne et al., 2014), as well as life history (annuals or perennials) and reproductive phenology from the flora for 290 species (South China Botanical Garden, 2009). Of these species, 9.5% are $C_3$ annuals, 14.9% are $C_3$ perennials, 26.6% are $C_4$-annuals, and 49.8% are $C_4$ perennials. Furthermore, after matching species with global occurrence and phylogenetic information, we had a final sample of 190 species, which constituted 60.1% of the total native Poaceae species in subtropical China. This sample also well represented the floral pool, with 10.0% $C_3$ annuals, 12.1% $C_3$ perennials, 27.9% $C_4$ annuals, and 50.0% $C_4$ perennials (**Supplementary Table S1**).

Following previous studies on phenology using monthly data (Hart et al., 2016), we assigned the initial flowering month (e.g., May is recorded as 5) as "flowering onset" and calculated "reproductive period" as the difference between "flowering onset" and flowering and fruiting end month. For the 11 species whose reproductive period ends in the following year, we calculated the period directly (e.g., for *Heteropogon triticeus*, which flowers and fruits from October until March, the flowering onset is 10 and the reproductive period is 5). This method not only enabled the correct calculation of reproductive period but also avoided the circular problem of underestimating phylogenetic signals in plant phenology (Staggemeier et al., 2019).

## Climatic Data and Climatic Niche Calculation

For climatic data, we obtained geo-referenced locality data for each species from the Global Biodiversity Information Facility[1], using the R statistical computing environment v. 3.5.1 (R Core Team, 2018), and the *occ_download* function in the *rgbif* package (Chamberlain et al., 2014). We carefully checked each species' occurrence data to ensure that the database is representative of the distributions of the grasses (**Supplementary Figure S1**). Next, we extracted the climatic data for all occurrence points from the WorldClim database (Hijmans et al., 2005), using the function *extract* in the R package *raster* (Hijmans et al., 2015). The WorldClim dataset has climatic data at 1-km$^2$ resolution for 1950–2000. We included nine climatic variables to calculate climatic niches: mean annual temperature (MAT, bio1), temperature seasonality (Ts, bio4, standard deviation across 12 monthly temperature values), maximum temperature of the warmest month (Tmax, bio5), minimum temperature of the coldest month (Tmin, bio6), mean annual precipitation (MAP, bio12), precipitation seasonality (Ps, bio15, coefficient of variation across 12 monthly precipitation values), precipitation of the wettest and the driest quarters (Pmax and Pmin, bio16, and bio17, respectively), and mean annual solar radiation (sr). We did not use precipitation of the wettest and the driest months because the monthly precipitation values have high inter-annual fluctuations, and thus the precipitation values based on quarters are more biologically meaningful for plants. Across the 190 species, the sample size of occurrence data per species ranged from 1 to 170,647 (mean = 2,612).

We estimated climatic niches for each species using climatic variable values extracted from localities across its geographic range (Quintero and Wiens, 2013). The mean and range (maximum – minimum) of the nine climatic variables were calculated for each species, using *mean*, *max*, and *min* functions in R, giving a total of 18 indices ($9 \times 2$) to define the species' climatic niches (**Supplementary Table S1**). The indices related to temperature, precipitation, and solar radiation can set the species' climatic range limits and potential climatic tolerances.

## Phylogenetic Tree

A phylogenetic tree of the 190 study species was constructed by integrating published phylogenies based on chloroplast genes (**Supplementary Figure S2**). We first extracted 146 species from a Poaceae super tree ∼3,000 species (Edwards et al., 2010) after checking synonymies based on the GrassBase-Synonymy database[2]. We then searched published phylogenies for different genera and identified 27 more species as congeners in the super tree. Finally, we assembled the last 17 species as polytomies into the 190-species tree using the function *bind.tree* in the R package *ape* (Paradis et al., 2004). When we focused on phylogenetic

[1]https://www.gbif.org

[2]http://www.kew.org/data/grasses-syn.html

relationships rather than the exact divergence times among species, polytomies and missing branch length information only had negligible impacts on the phylogenetic signals calculated using phylogenetic generalized least square (PGLS; Münkemüller et al., 2012). Therefore, we transformed the branch lengths of the phylogenetic tree using Grafen's method to avoid the effects of setting dichotomies/polytomies (Grafen, 1989).

## Data Analysis

To determine if there are phylogenetic signals in reproductive phenology traits, we estimated Pagel's $\lambda$. This indicates the degree to which residual trait variation shows similarity based on phylogenetic relationships across species (Pagel, 1999). The $\lambda$ values vary between 0 and 1 in which, $\lambda = 0$ indicates no phylogenetic signal and thus this trait is independent of phylogeny. In contrast, $\lambda = 1$ implies that the distribution of trait values across the phylogeny is as expected under the Brownian model of trait evolution (i.e., trait variation completely depends on phylogeny). We estimated $\lambda$ for both flowering onset and reproductive period using PGLS models, using the function *pgls* in the R package *caper* (Orme and Freckleton, 2018).

To establish how reproductive phenology differed with photosynthetic type (PT) and life history (AP, annuals and perennials) and whether interactive effects existed between PT and AP, we also constructed PGLS models. PGLS performs well irrespective of the intensity of the phylogenetic signal, which is ideal for comparisons across large numbers of traits differing in their associations with phylogeny (Revell, 2010). We compared four alternative models ($y \sim$ PT $\times$ AP, $y \sim$ PT + AP, $y \sim$ PT, and $y \sim$ AP), where the response variable was either flowering onset or reproductive period, and selected the best-fitted model that had the lowest Akaike information criterion (AIC) scores (Anderson, 2007).

How reproductive phenology related to the 18 climatic niches (nine means and ranges of MAT, Ts, Tmax, Tmin, MAP, Ps, Pmax, Pmin, and sr) was analyzed using stepwise regression based on PGLS. As many factors in a stepwise regression will give redundant factors in the selected best model, we constructed four potential models and compared them. We first built a full model (M1, with all climatic variable means and ranges as factors), from which we obtained its best-fitted model (M1best) based on stepwise regressions by using function *step* in R. Next, we built a mean-value-based model (using the nine mean variables as factors) and obtained its corresponding best-fitted model M2. Similarly, a range-value-based model (nine range variables as factors) produced its corresponding best-fitted model M3. Then, we combined significant factors from M1best, M2, and M3 to construct a more comprehensive model (M4). The interactive factor PT $\times$ AP was added in M1 to M4 according to the results of the abovementioned analysis. We did not add interactive factors among climatic niches because similar previous studies had already tested and treated them as additive factors (Atkin et al., 2015). We then compared the four models to find the best-fitted model based on AIC scores and reported percentages of variation explained by each factor. Finally, we analyzed the relationships between significant climatic factors and reproductive phenology traits using standardized major axis (SMA) analysis as well as PGLS to determine the role that phylogeny plays on these relationships. In order to test the interactive effects (PT $\times$ AP) on the relationships, we ran SMAs for all data and the four PT-AP groups ($C_3$ annuals, $C_3$ perennials, $C_4$ annuals, and $C_4$-perennials) separately. SMA analysis was performed using *sma* function in the R package *smatr* (Warton et al., 2012).

# RESULTS

## Phylogenetic Signal in Reproductive Phenology Traits

Flowering onset showed a significant phylogenetic signal ($\lambda = 0.50$, $P < 0.001$ for $\lambda = 0$ or 1), whereas reproductive period had no phylogenetic signal ($\lambda = 0.00$ with $P = 1.000$ for $\lambda = 0$; **Table 1A**).

## Reproductive Phenology and Climatic Niches Among Photosynthetic and Life History Types

The 190 grass species belonged to five $C_3$ and four $C_4$ independent lineages across the phylogenetic tree, while annual and perennial species were dispersed randomly across the tree (**Supplementary Figure S2**). $C_3$ annual grasses started to flower one month earlier than $C_3$ perennials, $C_4$ annuals, and $C_4$ perennials (**Figure 1A**). $C_3$ annuals also showed the longest reproductive period and $C_3$ perennials the shortest (**Figure 1B**). Further PGLS model comparisons showed that photosynthetic pathway (PT) and life history type (AP) had significant interactive effects on both flowering onset and reproductive period. $y \sim$ PT $\times$ AP was selected as the best-fitted model (**Table 1B**). The interaction PT $\times$ AP explained 70.1 and 71.1% of total variation of flowering onset and reproductive period, respectively, far more than single factors PT and AP explained (**Table 2A**).

For climatic niches, $C_3$ annuals, and $C_3$ perennials occurred in localities with the lowest MAT, while $C_4$ perennials occurred in the highest, based on multiple comparisons (**Figure 1E**). The other three key climatic niche variables (Tmin range, MAP range, and Pmax range) did not differ among the four groups (**Figures 1C,D,F**).

## Relationships Between Reproductive Phenology Traits and Climatic Niches

Phylogenetic generalized least square stepwise model comparison on the relationships between flowering onset and climatic niches selected the range-based model (M3) as the one with the best fit (**Table 1C**). Further analyses using this model found that, among multiple factors, Tmin range, MAP range, and PT $\times$ AP were the three significant factors that explained 19.5, 34.5, and 19.2% of the total variation in flowering onset, respectively (**Table 2B**). Separate bivariate relationships showed that flowering onset was significantly earlier with both increasing Tmin range and MAP range (**Figures 2A,B**). However, the relationships were driven by $C_4$ perennials because the models on the other three groups were not significant (**Figures 2A,B** and **Supplementary Table S3A**).

**TABLE 1 |** Phylogenetic generalized least square models on the reproductive phenology traits of 190 grass species.

| | AIC values | | | | | | | | | | | | |
|---|---|---|---|---|---|---|---|---|---|---|---|---|---|
| | PT × AP | PT + AP | PT | AP | M1 Full model | M2 Mean-based | M3 Range-based | M4 Combined | Best model | $R^2$ | *P* | λ | *P* (λ = 0) | *P* (λ = 1) |
| **(A) *y* ~ 1** | | | | | | | | | | | | | | |
| Flowering onset | | | | | | | | | | | | 0.5 | <0.001 | <0.001 |
| Reproductive period | | | | | | | | | | | | 0.00 | 1.000 | <0.001 |
| **(B) *y* ~ PT × AP** | | | | | | | | | | | | | | |
| Flowering onset | **699.0** | 706.8 | 706.9 | 705.9 | | | | | **PT × AP** | 0.16 | 0.005 | 0.41 | <0.001 | <0.001 |
| Reproductive period | **666.6** | 675.5 | 675.9 | 673.7 | | | | | **PT × AP** | 0.21 | 0.004 | 0.00 | 1.000 | <0.001 |
| **(C) *y* ~ climate + PT × AP** | | | | | | | | | | | | | | |
| Flowering onset | | | | | 698.7 | 705.6 | **675.8** | 679.6 | **M3** | 0.24 | <0.001 | 0.40 | <0.001 | <0.001 |
| Reproductive period | | | | | 667.6 | 666.7 | 652.6 | **650.1** | **M4** | 0.29 | <0.001 | 0.00 | 1.000 | <0.001 |

*(A) single trait to determine the phylogenetic signals, (B) model comparisons to test the interactive effects between photosynthetic pathway and life history, and (C) stepwise model comparisons to explore the key climatic niche variables affecting the reproductive phenology traits. The Akaike information criterion (AIC), $R^2$, P, and Pagel's λ values for each model are listed. In (C), the details of the four models (M1–M4, multiple and stepwise regression analyses) are presented in* ***Supplementary Table S2****. The best models are selected based on the smallest AIC values across models and shown in bold. PT, photosynthetic type ($C_3$, $C_4$); AP, life history (annual, perennial).*

For the relationship between reproductive period and climatic niche, the best-fitted model (M4) included both mean and range values of climatic niche variables (**Table 1C**). Specifically, the significant factors of the best-fitted model were MAT mean, Pmax range, and PT × AP, which explained 20.1, 33.4, and 22.9% of the total variation of reproductive period, respectively (**Table 2B**). Bivariate relationships exhibited that reproductive period was significantly longer with increasing MAT mean and Pmax range (**Figures 2C,D**). The relationship based on MAT mean was driven by $C_4$ perennials, while the relationship of Pmax range was significant for both $C_3$ and $C_4$ perennials (**Figures 2C,D** and **Supplementary Table S3B**).

# DISCUSSION

In this study, strong phylogenetic signals in flowering onset, but not reproductive period of grasses indicate the importance of phylogeny in comparative studies on phenology. Significant interactive effects between photosynthetic pathway and life history on reproductive phenology reflect different adaptive strategies. Climatic niche affects reproductive phenology, with species with wider climatic niches flowering earlier and having a longer reproductive period than those with narrower climatic niches.

## Phylogenetic Signals in Reproductive Phenology Traits

The high phylogenetic dependence of flowering onset of grasses ($\lambda$ = 0.50) was consistent with previous studies that strong phylogenetic signals existed in flowering time across 19,631 species in China (Du et al., 2015) and in flowering onset of 62 meadow species (Li et al., 2016). Generally, it was challenging to detect phylogenetic signals within one family due to stronger PNC across families than within families (Losos, 2008), but our data illustrated clear phylogenetic patterns in reproductive phenology within the Poaceae family. Our results also suggested that during the adaptation and evolution processes of grasses, flowering onset was a key trait under stabilizing selection and was therefore phylogenetically conserved (Donoghue, 2008; Anderson et al., 2012), compared with reproductive period. A potential reason was that flowering induction and onset in response to environmental stimuli, such as vernalization, is an elaborate process that involves many molecular regulations and resource investments (Lv et al., 2014; Xu et al., 2019), which tended to be fixed once evolved as an economical strategy. Reproductive period, on the other hand, can be more labile and vary with environmental changes (de Xavier et al., 2019). Environmental stresses that may occur during the reproductive period means that growth and resource allocation to reproduction needs to be more flexible than just initiating flowering in order to ensure survival.

Furthermore, the phylogenetic signals in flowering onset indicated that non-phylogenetic methods were not appropriate due to statistical independence (Revell, 2010), as all the effects

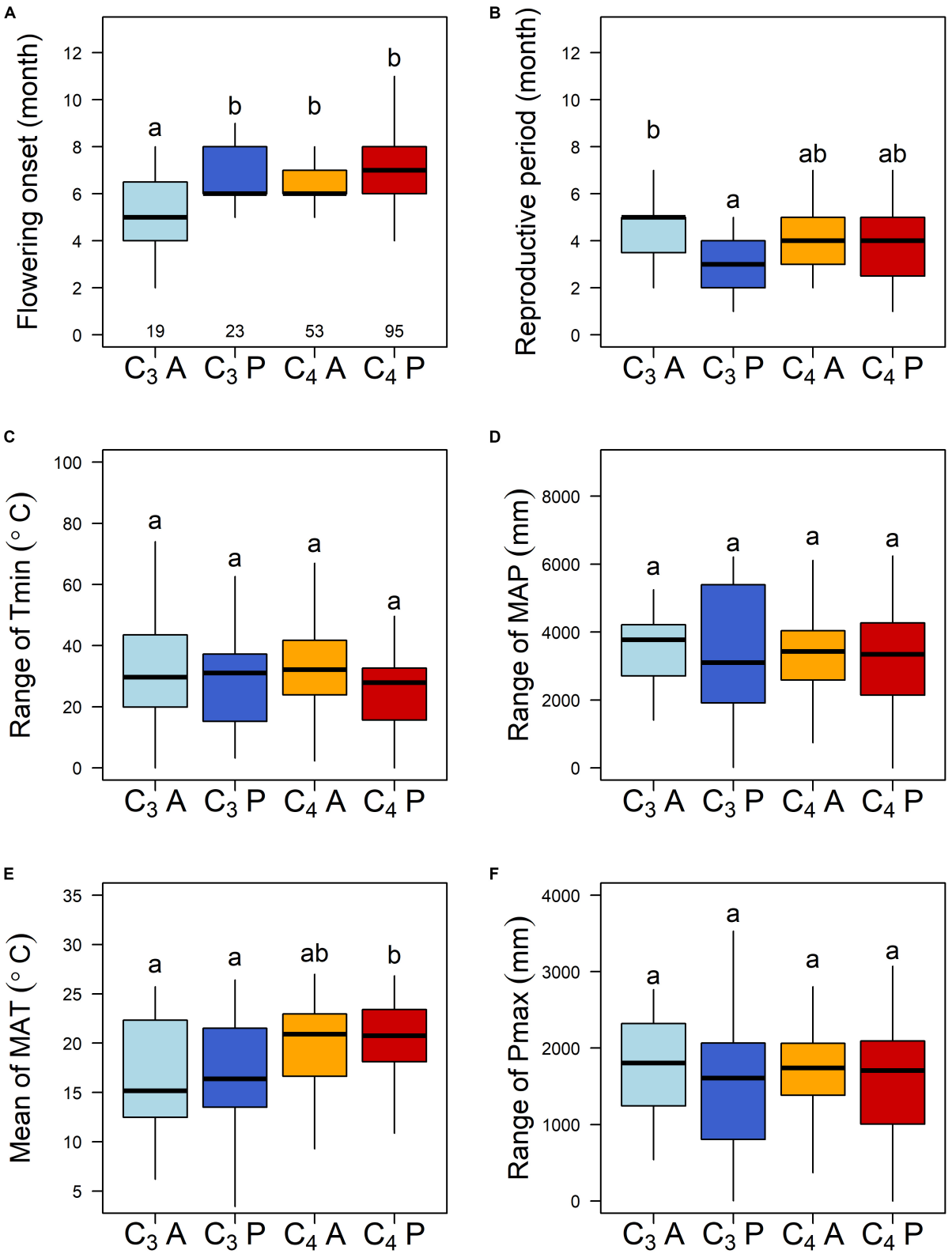


**FIGURE 1 | (A,B)** Reproductive phenology traits and key climatic niches of different photosynthetic pathways and life history types of the 190 subtropical grasses. $C_3$A, $C_3$ annuals; $C_3$P, $C_3$ perennials; $C_4$A, $C_4$ annuals; and $C_4$P, $C_4$ perennials. The sample sizes for each group are 19, 23, 53, and 95, respectively. Different letters indicate statistically significant differences. **(C–F)** Mean and range are the mean and the range values across localities of each species. Tmin, minimum temperature of the coldest month; MAP, mean annual precipitation; MAT, mean annual temperature; and Pmax, precipitation of the wettest quarter.

**TABLE 2 |** Factors and their explanatory powers in each of the best-fitting models on the reproductive phenology traits of 190 grass species.

| | | *df* | *F* | *P* | | Variation explained |
|---|---|---|---|---|---|---|
| **(A) *y* ~ PT × AP** | | | | | | |
| Flowering onset | PT | 1 | 1.08 | 0.299 | ns | 7.6% |
| | AP | 1 | 2.17 | 0.142 | ns | 15.3% |
| | **PT × AP** | **1** | **9.99** | **0.002** | ** | **70.1%** |
| | Residuals | 186 | | | | |
| Reproductive period | PT | 1 | 0.77 | 0.381 | ns | 7.1% |
| | AP | 1 | 1.35 | 0.247 | ns | 12.5% |
| | **PT × AP** | **1** | **7.68** | **0.006** | ** | **71.1%** |
| | Residuals | 186 | | | | |
| **(B) *y* ~ climate + PT × AP** | | | | | | |
| Flowering onset | MAT.range | 1 | 2.43 | 0.121 | ns | 4.8% |
| (M3, best model) | **Tmin.range** | **1** | **9.91** | **0.002** | ** | **19.5%** |
| | **MAP.range** | **1** | **17.53** | **0.001** | ** | **34.5%** |
| | Ps.range | 1 | 0.95 | 0.331 | ns | 1.9% |
| | Pmin.range | 1 | 4.81 | 0.059 | ns | 9.5% |
| | PT | 1 | 1.31 | 0.254 | ns | 2.6% |
| | AP | 1 | 3.09 | 0.080 | ns | 6.1% |
| | **PT × AP** | **1** | **9.77** | **0.002** | ** | **19.2%** |
| | Residuals | 182 | | | | |
| Reproductive period | **MAT.mean** | **1** | **8.82** | **0.003** | ** | **20.1%** |
| (M4, best model) | Ts.mean | 1 | 1.87 | 0.173 | ns | 4.3% |
| | Tmax.mean | 1 | 0.83 | 0.365 | ns | 1.9% |
| | Tmin.mean | 1 | 3.36 | 0.069 | ns | 7.7% |
| | Ps.mean | 1 | 0.13 | 0.722 | ns | 0.3% |
| | **Pmax.range** | **1** | **14.63** | **0.002** | ** | **33.4%** |
| | Pmin.range | 1 | 0.94 | 0.334 | ns | 2.1% |
| | sr.mean | 1 | 0.60 | 0.440 | ns | 1.4% |
| | PT | 1 | 0.45 | 0.505 | ns | 1.1% |
| | AP | 1 | 1.14 | 0.288 | ns | 2.6% |
| | **PT × AP** | **1** | **10.04** | **0.002** | ** | **22.9%** |
| | Residuals | 178 | | | | |

*The phylogenetic generalized least square models on (A) the interactive effects between photosynthetic pathway and life history and (B) key climatic niches affecting the reproductive phenology traits. The degree of freedom (df), F, and P values of each factor are listed. [λ]Significant factors in each of the best models are shown in bold. PT, photosynthetic type ($C_3$, $C_4$); AP, life history (annual, perennial); MAT, mean annual temperature; Ts, temperature seasonality; Tmin, minimum temperature of coldest month; Tmax, maximum temperature of warmest month; MAP, mean annual precipitation; Ps, precipitation seasonality; Pmin, precipitation of driest quarter; Pmax, precipitation of wettest quarter; sr, solar radiation; mean, mean value of each climatic niche; range, range value of each climatic niche; and ns, not significant. **P < 0.01.*

of life history, photosynthetic pathway, and climatic niches on flowering onset were significantly related to phylogeny (**Table 1**). Therefore, we suggest that phylogenetic relationships should be considered when searching for ecological drivers of reproductive phenology in comparative analyses (Davies et al., 2013; Li et al., 2016).

## Reproductive Phenology Traits Among Photosynthetic and Life History Types Reflect Their Adaptive Strategies

Due to the interactive effect between photosynthetic pathway (PT) and life history (AP), only $C_3$ annual grasses, not $C_3$ perennials, initiated flowering earlier than $C_4$ grasses (**Figure 1A**). This result agreed with previous findings that $C_3$ annual grasses started flowering the earliest in western United States (Munson and Long, 2017). $C_3$ grasses may flower earlier and reproduce longer to compensate for growth disadvantages in competing for space and resources with $C_4$ grasses (Atkinson et al., 2016). However, in our data, $C_3$ grasses did flower earlier than $C_4$ grasses, but only within annual species. Most $C_4$ grasses, which were late flowering regardless of life history, are in tropical/subtropical areas where the evolution of responses to cold/day length in early spring is not as necessary as for the $C_3$ annuals inhabiting temperate regions (Edwards et al., 2010). Our results also agreed with previous findings that annuals flower earlier than congeneric perennials in a long-term observational study of 385 plants (Fitter and Fitter, 2002). Thus, the interactive effect (PT × AP) likely arose from perennials because they had more flexibility in flowering onset and reproductive period during multiple growing seasons (Lundgren and Des Marais, 2020).

Our hypothesis that reproductive period would be associated with either PT or AP was not supported due to the interactive

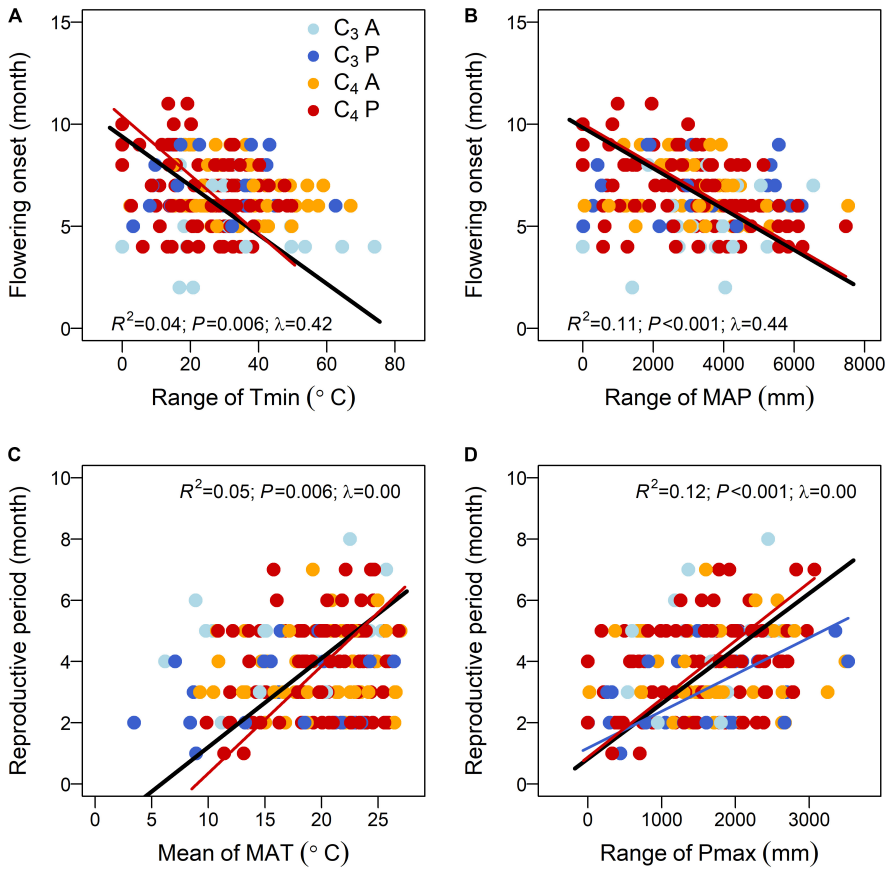


**FIGURE 2 |** Relationships between **(A,B)** flowering onset and **(C,D)** reproductive period and key climatic niche variables of the 190 subtropical grasses. Points are colored by photosynthetic pathway and life history ($C_3$A, $C_3$ annuals—blue; $C_3$P, $C_3$ perennials—dark blue; $C_4$A, $C_4$ annuals—orange; and $C_4$P, $C_4$ perennials—red). The models are tested for all data and four groups separately, but only the lines of significant models are plotted. The $R^2$, $P$, and Pagel's $\lambda$ values for the model of all data are listed, while the coefficients for the other models are presented in **Supplementary Table S3**. The four key climatic niche variables are significant factors of the best-fitted models in **Table 2**.

effect (PT × AP), with $C_3$ annuals and $C_3$ perennials showing the longest and the shortest reproductive period, respectively (**Figure 1B**). One reason for the similar reproductive period between $C_3$ and $C_4$ grasses might be their relatively narrow local climatic ranges in the study region. The local winter temperature (Dec–Mar) was 5–15°C, while vernalization requires 0–5°C for 15–30 days. Therefore, some $C_3$ grasses originally from temperate regions (**Figure 1E**) may have lost their coldness stimulation and initiated flowering just as late as $C_4$ grasses (Munson and Long, 2017), diminishing the differences between the two. We did not find any literature that directly compared the reproductive period of $C_3$ and $C_4$ plants, so it is possible that $C_3$ and $C_4$ grasses have similar reproductive lengths. Our observation on $C_3$ wheat and $C_4$ corn, which both have a reproductive period of 1 to 2 months, supports this. Another possible reason for a longer reproductive period in annuals than in perennials within $C_3$ species only is that the vegetative growth and the reproduction of annuals occur simultaneously. This might prolong the reproductive period in annuals, while the two stages are more distinct and flexible in perennials (Albani and Coupland, 2010). A longer reproductive period of annuals was consistent with the findings from 302 $C_3$ tropical tree species (Bawa et al., 2003).

Early flowering is an important strategy to occupy the cold early spring niches, particularly in temperate species (Munguía-Rosas et al., 2011). With a mean winter temperature of 5–15°C, the subtropical species studied here have rarely experienced a cold early spring; in contrast, the mean temperature of cold winter was at least below 5°C in the Western United States (Munson and Long, 2017). Thus, the early flowering of $C_3$ annuals should be an inherited trait. Indeed six out of nine $C_3$ annual species that flowered earlier than May were from the subfamily Pooideae. Members of this group are reported to flower earlier than those from other Poaceae subfamilies (Liu et al., 2019a) and are mainly distributed in temperate regions (Edwards and Smith, 2010) and acclimated to cold stress (Schubert et al., 2019). Therefore, our results reflected different ecological adaptation strategies of different photosynthetic pathways, life histories, and phylogenetic origins in grass species. Consistent with the patterns that we previously found in morphological and physiological traits (Liu et al., 2019b), life history was more important than photosynthetic pathway in explaining

differences in both flowering onset and reproductive period among subtropical grasses.

## The Four Climatic Niches Affected Reproductive Phenology After Considering Phylogeny

Our hypothesis that species with wider global climatic niches might flower earlier and have a longer reproductive period, based on geographical range theories (Lavergne et al., 2004; Thuiller et al., 2004), was supported by four key climatic niche variables. Specifically, species with wider ranges of Tmin and MAP flowered earlier, and species with higher mean MAT and a wider range of Pmax had longer reproductive periods. These relationships were mainly driven by $C_4$ perennials (**Figure 2**). After accounting for phylogenetic relationships, the effect size of models based on climatic niches was small (even for the best multiple-factor models, $R^2$ ranged from 0.16 to 0.29; **Table 1**). However, the four significant climatic niches still have important ecological implications.

The minimum temperature of the coldest month (Tmin) was a better predictor of flowering onset than other temperature variables, especially in representing the breadth of temperature niche (i.e., range). Clearly, Tmin could capture the coldness in early spring for flowering induction better than MAT. Previous studies have reported that grass species flowered earlier under lower temperatures (Evans, 1971; Fitter and Fitter, 2002; Sherry et al., 2011); however, we did not find this using our phylogenetic models. A possible reason for the contrasting results is that previous studies have matched phenological records with local temperatures, but our data were sampled across each species' global distribution (climatic niches). This partially explained the small effect sizes of all the PGLS models and revealed that, compared with local temperature as the physiological driver, the range of Tmin was the ecological driver of flowering onset.

Species spanning a wider range of precipitation tended to flower earlier. When species undergo drought, their flowering onset tends to be delayed (Craine et al., 2012a). Species of high-precipitation regions (>2,000 mm, subtropical and tropical areas; **Figure 1D**) tended to extend their reproductive period by flowering earlier and ending later. Therefore, such a flowering strategy could enhance species fitness and was an evolutionary trend based on historical phenological records (Munguía-Rosas et al., 2011; Anderson et al., 2012).

Mean temperature, but not temperature range, affected the reproductive period of grasses. Mean MAT is associated with the accumulation of temperature over time and is therefore important to plant growth and reproduction (Sherry et al., 2011). For example, compared with temperate grasses with a growth season of 6 months or less, subtropical grasses could grow for a whole year. Mean MAT was also the only factor that differed between $C_3$ and $C_4$ species (Munson and Long, 2017; **Figure 1E**).

Species experiencing a wider range of precipitation tended to have a longer reproductive period. This seemingly contrasts previous findings that reproductive phenology was more sensitive to drought rather than high-level precipitation (Franks, 2011; Craine et al., 2012a), but the drier or the wetter the localities a species occupied, the higher the range of Pmax is. The longer reproductive period is a way to increase the fitness of species with sufficient water resources (**Figures 2C,D**).

Finally, PNC in flowering onset and its relationships with climatic niche indicated that, when climate changes, a temporal shift in flowering onset was predictable and similar within the same lineage (Staggemeier et al., 2010). Meanwhile, no PNC in the relationships between reproductive period and climatic niches may mean that this aspect of reproductive phenology is less sensitive to climatic change. Although many previous studies had reported PNC in flowering phenology (Lessard-Therrien et al., 2014; Du et al., 2015; Li et al., 2016), few had done phylogenetic analyses on their relationships with climatic variables. For example, Li et al. (2016) tested phylogenetic signals in both phenological and climatic data but did not use phylogeny when examining their relationships. Thus, phylogeny was needed to interpret how reproductive phenology was related with climatic variables.

We acknowledged certain caveats about our analyses. Although we found distinct patterns among groups, more accurate flowering onset and reproductive period data (accurate to date and long-term records) would be favored for future studies. The relatively coarse classification of life history (only the two extreme life histories were considered) and the climatic niches calculated for very widely distributed species might also impede the detection of the key factors in affecting phenology. Sampling species in one family and one region might limit the generality of our results. However, phylogenetic tests within one family could be more reliable than across more distantly related families (Staggemeier et al., 2010). Given that both genetic differences and phenotypic plasticity account for plant responses to climate change (Münzbergová et al., 2017; Malanson et al., 2019), plasticity in reproductive phenology might obscure our results. However, we focused on global climatic niches, which were more stable than local climates (Petitpierre et al., 2012). Furthermore, phenological data from one region could avoid phenotypic plasticity in that measured across larger scales (although it was nearly impossible to measure the phenology of many species in all their global localities), where great plasticity in plant traits occurs (Hoffman et al., 2020). Thus, our trait variation reflected intrinsic phylogenetic differences here (Liu et al., 2015), but phenotypic plasticity should also be considered in future studies trying to assess the effects of climate change (De Kort et al., 2020). Overall, we propose that climatic niche and phylogeny constraints should be considered simultaneously in studying the reproductive phenology of subtropical grasses.

# CONCLUSION

In this study, we integrated the reproductive phenology, global-scale climatic niches, and phylogeny of 190 subtropical Poaceae species. We found strong phylogenetic signals in flowering onset but not in reproductive period, which emphasized the importance of phylogeny in comparative studies of reproductive

phenology. There were significant interactive effects between photosynthetic pathway and life history on both flowering onset and reproductive period, such that $C_3$ annual grasses flowered the earliest and had the longest reproductive period. We found four key climatic niche factors (ranges of Tmin, MAP, and Pmax and mean of MAT) associated with reproductive phenology through phylogenetic multiple stepwise regressions and demonstrated that species with wider climatic niches would flower earlier and have longer reproductive periods. Our results suggested that future studies on the role of climate on grass reproductive phenology should consider their evolutionary relationships.

## DATA AVAILABILITY STATEMENT

All datasets generated for this study are included in the article/**Supplementary Material**.

## AUTHOR CONTRIBUTIONS

HL and YC designed the study. HL collected the data. HL, KL, JW, LQ, YM, and RZ performed the analyses and drafted the first manuscript. All the authors contributed substantially to the revisions.

## FUNDING

This work was supported by the National Natural Science Foundation of China (31670411), the Pearl River S&T Nova Program of Guangzhou (201806010083), and the Youth Innovation Promotion Association of the Chinese Academy of Sciences (2019339).

## SUPPLEMENTARY MATERIAL

The Supplementary Material for this article can be found online at: https://www.frontiersin.org/articles/10.3389/fevo.2020.00181/full#supplementary-material

**FIGURE S1 |** Global distribution localities of 190 subtropical grasses.

**FIGURE S2 |** A phylogenetic tree of 190 subtropical grasses, with corresponding information on photosynthetic pathway, life history, and reproductive phenology.

**TABLE S1 |** Full dataset in this study, with definitions and descriptions for each index.

**TABLE S2 |** Phylogenetic multiple stepwise regression analyses on flowering onset and reproductive period based on 18 climatic niche variables, photosynthetic pathway, and life history.

**TABLE S3 |** Relationships between reproductive phenology and key climatic niche variables.

## REFERENCES

Albani, M. C., and Coupland, G. (2010). Comparative analysis of flowering in annual and perennial plants. *Curr. Top. Dev. Biol.* 91, 323–348. doi: 10.1016/S0070-2153(10)91011-9

Anderson, D. R. (2007). *Model Based Inference in The Life Sciences: A Primer on Evidence*. New York, NY: Springer.

Anderson, J. T., Inouye, D. W., McKinney, A. M., Colautti, R. I., and Mitchell-Olds, T. (2012). Phenotypic plasticity and adaptive evolution contribute to advancing flowering phenology in response to climate change. *Proc. R. Soc. B Biol. Sci.* 279, 3843–3852. doi: 10.1098/rspb.2012.1051

Atkin, O. K., Bloomfield, K. J., Reich, P. B., Tjoelker, M. G., Asner, G. P., Bonal, D., et al. (2015). Global variability in leaf respiration in relation to climate, plant functional types and leaf traits. *New Phytol.* 206, 614–636. doi: 10.1111/nph.13253

Atkinson, R. R. L., Mockford, E. J., Bennett, C., Christin, P. A., Spriggs, E. L., Freckleton, R. P., et al. (2016). C4 photosynthesis boosts growth by altering physiology, allocation and size. *Nat. Plants* 2, 1–5. doi: 10.1038/NPLANTS.2016.38

Bawa, K. S., Kang, H., and Grayum, M. H. (2003). Relationships among time, frequency, and duration of flowering in tropical rain forest trees. *Am. J. Bot.* 90, 877–887. doi: 10.3732/ajb.90.6.877

Cerdán, P. D., and Chory, J. (2003). Regulation of flowering time by light quality. *Nature* 423, 881–885. doi: 10.1038/nature01636

Chamberlain, S., Ram, K., Barve, V., and Mcglinn, D. (2014). *rgbif: Interface to the Global Biodiversity Information Facility API. R Packag. version 0. 7. 7*.

Colasanti, J., and Coneva, V. (2009). Mechanisms of floral induction in grasses: something borrowed, something new. *Plant Physiol.* 149, 56–62. doi: 10.1104/pp.108.130500

Corbesier, L., Vincent, C., Jang, S., Fornara, F., Fan, Q., Searle, I., et al. (2007). FT protein movement contributes to long-distance signaling in floral induction of *Arabidopsis*. *Science* 316, 1030–1033. doi: 10.1126/science.1141752

Cortés-Flores, J., Hernández-Esquivel, K. B., González-Rodríguez, A., and Ibarra-Manríquez, G. (2017). Flowering phenology, growth forms, and pollination syndromes in tropical dry forest species: influence of phylogeny and abiotic factors. *Am. J. Bot.* 104, 39–49. doi: 10.3732/ajb.1600305

Craine, J. M., Wolkovich, E. M., Gene Towne, E., and Kembel, S. W. (2012a). Flowering phenology as a functional trait in a tallgrass prairie. *New Phytol.* 193, 673–682. doi: 10.1111/j.1469-8137.2011.03953.x

Craine, J. M., Wolkovich, E. M., and Towne, E. G. (2012b). The roles of shifting and filtering in generating community-level flowering phenology. *Ecography* 35, 1033–1038. doi: 10.1111/j.1600-0587.2012.07625.x

Davies, T. J., Wolkovich, E. M., Kraft, N. J. B., Salamin, N., Allen, J. M., Ault, T. R., et al. (2013). Phylogenetic conservatism in plant phenology. *J. Ecol.* 101, 1520–1530. doi: 10.1111/1365-2745.12154

De Kort, H., Panis, B., Helsen, K., Douzet, R., Janssens, S. B., and Honnay, O. (2020). Pre-adaptation to climate change through topography-driven phenotypic plasticity. *J. Ecol.* 108, 1465–1474. doi: 10.1111/1365-2745.13365

de Xavier, R. O., Leite, M. B., and da Silva Matos, D. M. (2019). Phenological and reproductive traits and their response to environmental variation differ among native and invasive grasses in a Neotropical savanna. *Biol. Invasions* 21, 2761–2779. doi: 10.1007/s10530-019-02013-w

Donoghue, M. J. (2008). A phylogenetic perspective on the distribution of plant diversity. *Proc. Natl. Acad. Sci. U.S.A.* 105, 11549–11555. doi: 10.1073/pnas.0801962105

Du, Y., Mao, L., Queenborough, S. A., Freckleton, R. P., Chen, B., and Ma, K. (2015). Phylogenetic constraints and trait correlates of flowering phenology in the angiosperm flora of China. *Glob. Ecol. Biogeogr.* 24, 928–938. doi: 10.1111/geb.12303

Edwards, E. J., Osborne, C. P., Stromberg, C. A. E., Smith, S. A., Consortium, C. G., Bond, W. J., et al. (2010). The origins of C4 grasslands: integrating evolutionary and ecosystem science. *Science* 328, 587–591. doi: 10.1126/science.1177216

Edwards, E. J., and Smith, S. A. (2010). Phylogenetic analyses reveal the shady history of C4 grasses. *Proc. Natl. Acad. Sci. U.S.A.* 107, 2532–2537. doi: 10.1073/pnas.0909672107

Ehleringer, J. R. (1978). Implications of quantum yield differences on the distributions of C3 and C4 grasses. *Oecologia* 31, 255–267. doi: 10.1007/BF00346246

Elzinga, J. A., Atlan, A., Biere, A., Gigord, L., Weis, A. E., and Bernasconi, G. (2007). Time after time: flowering phenology and biotic interactions. *Trends Ecol. Evol.* 22, 432–439. doi: 10.1016/J.TREE.2007.05.006

Evans, L. T. (1971). Flower induction and the florigen concept. *Annu. Rev. Plant Physiol.* 22, 365–394. doi: 10.1146/annurev.pp.22.060171.002053

Fitter, A. H., and Fitter, R. S. R. (2002). Rapid changes in flowering time in British plants. *Science* 296, 1689–1691. doi: 10.1126/science.1071617

Franks, S. J. (2011). Plasticity and evolution in drought avoidance and escape in the annual plant *Brassica rapa*. *New Phytol.* 190, 249–257. doi: 10.1111/j.1469-8137.2010.03603.x

Grafen, A. (1989). The phylogenetic regression. *Philos. Trans. R. Soc. B Biol. Sci.* 326, 119–157.

Grass Phylogeny Working Group (2012). New grass phylogeny resolves deep evolutionary relationships and discovers C4 origins. *New Phytol.* 193, 304–312. doi: 10.1111/j.1469-8137.2011.03972.x

Hart, R., Georgian, E. M., and Salick, J. (2016). Fast and cheap in the fall: phylogenetic determinants of late flowering phenologies in Himalayan *Rhododendron*. *Am. J. Bot.* 103, 198–206. doi: 10.3732/ajb.1500440

Hijmans, R. J., Cameron, S. E., Parra, J. L., Jones, P. G., and Jarvis, A. (2005). Very high resolution interpolated climate surfaces for global land areas. *Int. J. Climatol.* 25, 1965–1978. doi: 10.1002/joc.1276

Hijmans, R. J., van Etten, J., Sumner, M., Cheng, J., Bevan, A., Bivand, R., et al. (2015). *Raster: Geographic Analysis and Modeling. R package version 2.8–19.* Available online at: https://cran.r-project.org/web/packages/raster/ (accessed May 30, 2019).

Hoffman, A. M., Bushey, J. A., Ocheltree, T. W., and Smith, M. D. (2020). Genetic and functional variation across regional and local scales is associated with climate in a foundational prairie grass. *New Phytol.* [Online ahead of print]. doi: 10.1111/nph.16547

Lavergne, S., Thompson, J. D., Garnier, E., and Debussche, M. (2004). The biology and ecology of narrow endemic and widespread plants: a comparative study of trait variation in 20 congeneric pairs. *Oikos* 107, 505–518. doi: 10.1111/j.0030-1299.2004.13423.x

Lessard-Therrien, M., Davies, T. J., and Bolmgren, K. (2014). A phylogenetic comparative study of flowering phenology along an elevational gradient in the *Canadian subarctic*. *Int. J. Biometeorol.* 58, 455–462. doi: 10.1007/s00484-013-0672-9

Li, L., Li, Z., Cadotte, M. W., Jia, P., Chen, G., Jin, L. S., et al. (2016). Phylogenetic conservatism and climate factors shape flowering phenology in alpine meadows. *Oecologia* 182, 419–428. doi: 10.1007/s00442-016-3666-6

Liu, H., Edwards, E. J., Freckleton, R. P., and Osborne, C. P. (2012). Phylogenetic niche conservatism in C4 grasses. *Oecologia* 170, 835–845. doi: 10.1007/s00442-012-2337-5

Liu, H., and Osborne, C. P. (2015). Water relations traits of C4 grasses depend on phylogenetic lineage, photosynthetic pathway, and habitat water availability. *J. Exp. Bot.* 66, 761–773. doi: 10.1093/jxb/eru430

Liu, H., Osborne, C. P., Yin, D., Freckleton, R. P., Jiang, G., and Liu, M. (2019a). Phylogeny and ecological processes influence grass coexistence at different spatial scales within the steppe biome. *Oecologia* 191, 25–38. doi: 10.1007/s00442-019-04475-0

Liu, H., Taylor, S. H., Xu, Q., Lin, Y., Hou, H., Wu, G., et al. (2019b). Life history is a key factor explaining functional trait diversity among subtropical grasses, and its influence differs between C3 and C4 species. *J. Exp. Bot.* 70, 1567–1580. doi: 10.1093/jxb/ery462

Liu, H., Xu, Q., He, P., Santiago, L. S., Yang, K., and Ye, Q. (2015). Strong phylogenetic signals and phylogenetic niche conservatism in ecophysiological traits across divergent lineages of Magnoliaceae. *Sci. Rep.* 5:12246. doi: 10.1038/srep12246

Losos, J. B. (2008). Phylogenetic niche conservatism, phylogenetic signal and the relationship between phylogenetic relatedness and ecological similarity among species. *Ecol. Lett.* 11, 995–1003. doi: 10.1111/j.1461-0248.2008.01229.x

Lundgren, M. R., and Des Marais, D. L. (2020). Life history variation as a model for understanding trade-offs in plant-environment interactions. *Curr. Biol.* 30, R180–R189. doi: 10.1016/j.cub.2020.01.003

Lundgren, M. R., Dunning, L. T., Olofsson, J. K., Moreno-Villena, J. J., Bouvier, J. W., Sage, T. L., et al. (2019). C4 anatomy can evolve via a single developmental change. *Ecol. Lett.* 22, 302–312. doi: 10.1111/ele.13191

Lv, B., Nitcher, R., Han, X., Wang, S., Ni, F., Li, K., et al. (2014). Characterization of Flowering Locus T1 (FT1) gene in *Brachypodium* and wheat. *PLoS One* 9:e0094171. doi: 10.1371/journal.pone.0094171

MacLean, S. A., and Beissinger, S. R. (2017). Species' traits as predictors of range shifts under contemporary climate change: a review and meta-analysis. *Glob. Chang. Biol.* 23, 4094–4105. doi: 10.1111/gcb.13736

Malanson, G. P., DeRose, R. J., and Bekker, M. F. (2019). Individual variation and ecotypic niches in simulations of the impact of climatic volatility. *Ecol. Modell.* 411:108782. doi: 10.1016/j.ecolmodel.2019.108782

Munguía-Rosas, M. A., Ollerton, J., Parra-Tabla, V., and De-Nova, J. A. (2011). Meta-analysis of phenotypic selection on flowering phenology suggests that early flowering plants are favoured. *Ecol. Lett.* 14, 511–521. doi: 10.1111/j.1461-0248.2011.01601.x

Münkemüller, T., Lavergne, S., Bzeznik, B., Dray, S., Jombart, T., Schiffers, K., et al. (2012). How to measure and test phylogenetic signal. *Methods Ecol. Evol.* 3, 743–756. doi: 10.1111/j.2041-210X.2012.00196.x

Munson, S. M., and Long, A. L. (2017). Climate drives shifts in grass reproductive phenology across the western USA. *New Phytol.* 213, 1945–1955. doi: 10.1111/nph.14327

Münzbergová, Z., Hadincová, V., Skálová, H., and Vandvik, V. (2017). Genetic differentiation and plasticity interact along temperature and precipitation gradients to determine plant performance under climate change. *J. Ecol.* 105, 1358–1373. doi: 10.1111/1365-2745.12762

Orme, D., and Freckleton, R. (2018). *Caper: Comparative Analysis of Phylogenetics and Evolution in R. R package version 1.0.1.* Available online at: https://cran.r-project.org/web/packages/caper/ (accessed May 30, 2019).

Osborne, C. P., Salomaa, A., Kluyver, T. A., Visser, V., Kellogg, E. A., Morrone, O., et al. (2014). A global database of C4 photosynthesis in grasses. *New Phytol.* 204, 441–446. doi: 10.1111/nph.12942

Pagel, M. (1999). Inferring the historical patterns of biological evolution. *Nature* 401, 877–884. doi: 10.1038/44766

Paradis, E., Claude, J., and Strimmer, K. (2004). APE: analyses of phylogenetics and evolution in R language. *Bioinformatics* 20, 289–290. doi: 10.1093/bioinformatics/btg412

Petitpierre, B., Kueffer, C., Broennimann, O., Randin, C., Daehler, C., and Guisan, A. (2012). Climatic niche shifts are rare among terrestrial plant invaders. *Science* 335, 1344–1348. doi: 10.1126/science.1215933

Primack, R. B., and Gallinat, A. S. (2017). Insights into grass phenology from herbarium specimens. *New Phytol.* 213, 1567–1568. doi: 10.1111/nph.14439

Quintero, I., and Wiens, J. J. (2013). What determines the climatic niche width of species? The role of spatial and temporal climatic variation in three vertebrate clades. *Glob. Ecol. Biogeogr.* 22, 422–432. doi: 10.1111/geb.12001

R Core Team (2018). *R: A Language and Environment for Statistical Computing*. Vienna: R Foundation for Statistical Computing.

Rathcke, B., and Lacey, E. P. (1985). Phenological patterns of terrestrial plants. *Annu. Rev. Ecol. Syst.* 16, 179–214. doi: 10.1146/annurev.es.16.110185.001143

Revell, L. J. (2010). Phylogenetic signal and linear regression on species data. *Methods Ecol. Evol.* 1, 319–329. doi: 10.1111/j.2041-210X.2010.00044.x

Sage, R. F., Sage, T. L., and Kocacinar, F. (2012). Photorespiration and the evolution of C4 photosynthesis. *Annu. Rev. Plant Biol.* 63, 19–47. doi: 10.1146/annurev-arplant-042811-105511

Schubert, M., Grønvold, L., Sandve, S. R., Hvidsten, T. R., and Fjellheim, S. (2019). Evolution of cold acclimation and its role in niche transition in the temperate grass subfamily Pooideae. *Plant Physiol.* 180, 404–419. doi: 10.1104/pp.18.01448

Sherry, R. A., Zhou, X., Gu, S., Arnone, J. A., Johnson, D. W., Schimel, D. S., et al. (2011). Changes in duration of reproductive phases and lagged phenological response to experimental climate warming. *Plant Ecol. Divers.* 4, 23–35. doi: 10.1080/17550874.2011.557669

Slatyer, R. A., Hirst, M., and Sexton, J. P. (2013). Niche breadth predicts geographical range size: a general ecological pattern. *Ecol. Lett.* 16, 1104–1114. doi: 10.1111/ele.12140

Soberón, J. (2007). Grinnellian and Eltonian niches and geographic distributions of species. *Ecol. Lett.* 10, 1115–1123. doi: 10.1111/j.1461-0248.2007.01107.x

South China Botanical Garden (2009). *Flora of Guangdong (In Chinese)*. Guangzhou: Guangdong Science and Technology Press.

Springer, C. J., and Ward, J. K. (2007). Flowering time and elevated atmospheric CO 2. *New Phytol.* 176, 243–255. doi: 10.1111/j.1469-8137.2007.02196.x

Staggemeier, V. G., Camargo, M. G. G., Diniz-Filho, J. A. F., Freckleton, R., Jardim, L., and Morellato, L. P. C. (2019). The circular nature of recurrent life cycle events: a test comparing tropical and temperate phenology. *J. Ecol.* 108, 393–404. doi: 10.1111/1365-2745.13266

Staggemeier, V. G., Diniz-Filho, J. A. F., and Morellato, L. P. C. (2010). The shared influence of phylogeny and ecology on the reproductive patterns of Myrteae (Myrtaceae). *J. Ecol.* 98, 1409–1421. doi: 10.1111/j.1365-2745.2010.01717.x

Tamaki, S., Matsuo, S., Hann, L. W., Yokoi, S., and Shimamoto, K. (2007). Hd3a protein is a mobile flowering signal in rice. *Science* 316, 1033–1036. doi: 10.1126/science.1141753

Taylor, S. H., Ripley, B. S., Martin, T., De-Wet, L. A., Woodward, F. I., and Osborne, C. P. (2014). Physiological advantages of C4 grasses in the field: a comparative experiment demonstrating the importance of drought. *Glob. Chang. Biol.* 20, 1992–2003. doi: 10.1111/gcb.12498

Thuiller, W., Lavorel, S., Midgley, G., Lavergne, S., and Rebelo, T. (2004). Relating plant traits and species distributions along bioclimatic gradients for 88 Leucadendron taxa. *Ecology* 85, 1688–1699. doi: 10.1890/03-0148

Warton, D. I., Duursma, R. A., Falster, D. S., and Taskinen, S. (2012). smatr 3-an R package for estimation and inference about allometric lines. *Methods Ecol. Evol.* 2, 257–259. doi: 10.1111/j.2041-210x.2011.00153.x

Watson, L., Macfarlane, T. D., and Dallwitz, M. J. (1992). *The Grass Genera of The World*. Available online at: http://delta-intkey.com/ (accessed March 30, 2019).

Way, D. A., Katul, G. G., Manzoni, S., and Vico, G. (2014). Increasing water use efficiency along the C3 to C4 evolutionary pathway: a stomatal optimization perspective. *J. Exp. Bot.* 65, 3683–3693. doi: 10.1093/jxb/eru205

Wiens, J. J. (2004). Speciation and ecology revisited: phylogenetic niche conservatism and the origin of species. *Evolution* 58, 193–197. doi: 10.1554/03-447

Wiens, J. J., and Graham, C. H. (2005). Niche conservatism: integrating evolution, ecology, and conservation biology. *Annu. Rev. Ecol. Evol. Syst.* 36, 519–539. doi: 10.1146/annurev.ecolsys.36.102803.095431

Xu, S., Xiao, J., Yin, F., Guo, X., Xing, L., Xu, Y., et al. (2019). The protein modifications of O-GlcNAcylation and phosphorylation mediate vernalization response for flowering in winter wheat. *Plant Physiol.* 180, 1436–1449. doi: 10.1104/pp.19.00081

**Conflict of Interest:** The authors declare that the research was conducted in the absence of any commercial or financial relationships that could be construed as a potential conflict of interest.

frontiers in Ecology and Evolution

ORIGINAL RESEARCH
published: 16 July 2020
doi: 10.3389/fevo.2020.00224

# Resource Heterogeneity, Not Resource Quantity, Plays an Important Role in Determining Tree Species Diversity in Two Species-Rich Forests

*Liwen Zhang[1,2], Xiangcheng Mi[2]*, Rhett D. Harrison[3], Bo Yang[4], Xingxing Man[2], Haibao Ren[2] and Keping Ma[2]*

*[1] CAS Key Laboratory of Coastal Environmental Processes and Ecological Remediation, Yantai Institute of Coastal Zone Research (YIC), Chinese Academy of Sciences (CAS), Yantai, China, [2] State Key Laboratory of Vegetation and Environmental Change, Institute of Botany, Chinese Academy of Sciences, Beijing, China, [3] World Agroforestry Centre (ICRAF), Eastern and Southern Africa Regional Office, Lusaka, Zambia, [4] Key Laboratory of Plant Resources and Biodiversity of Jiangxi Province, Jingdezhen University, Jingdezhen, China*

OPEN ACCESS

**Edited by:**
*Zehao Shen,*
*Peking University, China*

**Reviewed by:**
*Tiago Vasconcelos,*
*São Paulo State University, Brazil*
*Mingxi Jiang,*
*Chinese Academy of Sciences, China*

***Correspondence:**
*Xiangcheng Mi*
*mixiangcheng@ibcas.ac.cn*

**Specialty section:**
*This article was submitted to Biogeography and Macroecology, a section of the journal Frontiers in Ecology and Evolution*

**Received:** *21 January 2020*
**Accepted:** *18 June 2020*
**Published:** *16 July 2020*

**Citation:**
*Zhang L, Mi X, Harrison RD, Yang B, Man X, Ren H and Ma K (2020) Resource Heterogeneity, Not Resource Quantity, Plays an Important Role in Determining Tree Species Diversity in Two Species-Rich Forests. Front. Ecol. Evol. 8:224. doi: 10.3389/fevo.2020.00224*

There is still considerable debate about the relative importance of resource heterogeneity and resource quantity in the maintenance of species diversity in a community. The resource heterogeneity hypothesis proposes that spatial heterogeneity of limiting resources and inter-specific differences in resource requirements will determine species richness. In contrast, the resource quantity hypothesis predicts that average resource supply rates contribute to species richness by their effects on plant density and stochastic population dynamics. However, the evaluation of the two hypotheses in observational studies is associated with a major methodological challenge as average resource supply rate often covaries with resource heterogeneity. Using a novel approach derived from the relationships between average resource supply rate, resource heterogeneity (calculated as the standard deviation of environmental factors) and plant density in the resource hypotheses, we evaluated the relative importance of resource quantity and resource heterogeneity with a variation partitioning model in Gutianshan (GTS) forest plot, China, and Barro Colorado Island (BCI) forest plot, Central Panama. We found that resource quantity explained much less of the variation in species richness than resource heterogeneity in both GTS and BCI (44.5% vs. 4.9% in GTS and 20.4% vs. 0.8% in BCI at the 20 × 20 m scale, 57.5% vs. 3.4% in GTS at the 40 × 40 m scale, and 34.5% vs. 2.6% in BCI at the 50 × 50 m scale). We also found that resource heterogeneity governed species richness in GTS, whereas spatial processes dominated species diversity in BCI. Moreover, most of the effect of resource heterogeneity and resource quantity on species richness overlapped with that of spatial processes. This result indicates that most effects of resources could also be explained by spatial processes, such as dispersal limitation. Therefore, resource heterogeneity and spatial processes, but not resource quantity, played an important role in determining species diversity in these two old-growth forests. This is in contrast to the results

of several manipulative studies, which found that resource quantity governed species diversity when one or a limited number of resources were considered. This suggests that the processes determining species richness along ecological gradients are complicated and determined by the interaction of various processes.

**Keywords: resource quantity, resource heterogeneity, variation partitioning, species richness, ecological niche, plant density, spatial covariation**

## INTRODUCTION

Disentangling the importance of different processes in determining the species diversity of biotic communities has been an enduring challenge for ecologists (Ricklefs and Schluter, 1993; Abrams, 1995; Barot, 2004). For example, at opposite ends of a spectrum, the resource quantity hypothesis proposes that the species richness is determined by the average supply rates of limiting resources, through stochastic population dynamics (Wright, 1983; Stevens and Carson, 2002), while the resource heterogeneity hypothesis suggests that species richness is a function of the spatial heterogeneity in resource supply and inter-specific differences in resource requirements (Ricklefs, 1977; Huston, 1979; Stein et al., 2014). The importance of these two hypotheses for regulating plant species richness has been evaluated experimentally in grasslands (Stevens and Carson, 2002; Bakker et al., 2003; Baer et al., 2004; Eilts et al., 2011), where it was found that patterns of resource quantity (Stevens and Carson, 2002; Bakker et al., 2003) or resource heterogeneity (Eilts et al., 2011; Yang et al., 2015) or both (Questad and Foster, 2008; Cardinale et al., 2009) played crucial roles in shaping species richness. However, observational studies have rarely examined the relative contributions of resource quantity and resource heterogeneity to the maintenance of species richness in natural communities.

Testing the two resource hypotheses in observational studies is associated with a major methodological obstacle. Variation in resource supply rates among sites not only includes variation in the imbalance in resource supply rates among sites with different limiting resources (i.e., resource heterogeneity) but also contains the variation of resource quantity among sites with the same limiting resources. Hence, assessment of resource heterogeneity using solely within-site heterogeneity will lead to underestimation, whereas assessment of resource heterogeneity using both within-site heterogeneity and among-site resource supply rate will result in an inflated estimation (Lundholm, 2009). The close spatial covariation of resource quantity and resource heterogeneity has presented an enduring challenge in measuring their separate effects on species diversity (Stevens and Carson, 2002) and has hampered our ability to draw general conclusions regarding the mechanisms of diversity maintenance.

The resolution to the challenge in separating the effects of resource quantity and resource heterogeneity appears to lie with how resource supply rate covaries with plant density and how plant density influences species richness. It is widely appreciated that resource quantity and resource heterogeneity have a qualitatively different impact on species richness. The resource quantity hypothesis predicts that as the resource supply rates increase, the productivity and the density of plants in a community are either a monotonically increasing function (but may level off, more individuals hypothesis) (Srivastava and Lawton, 1998) or a unimodal function of resource supply rate (assemblage-level thinning hypothesis) (Stevens and Carson, 1999). Thus, species richness should also appear to be a monotonically increasing or a unimodal function of average resource supply rate, because increased plant density leads to a reduced risk of stochastic extinction for rare species (Stevens and Carson, 1999; Cardinale et al., 2009). Thus, the variation of species richness in natural communities explained by resource quantity should largely overlap with that explained by plant density. In contrast, the resource heterogeneity hypothesis predicts that spatial turnover in species composition will increase when resource heterogeneity (spatial niche dimensionality) increases within the same species pool and species differ in resource utilization (Questad and Foster, 2008; Eilts et al., 2011). The resource heterogeneity hypothesis does not necessarily rely on assumptions about the relationship among resource supply rate, plant density, and species richness. Therefore, it is possible to separate the effects of resource quantity and resource heterogeneity among sites using the joint effect of plant density and resource supply rate to estimate the effect of resource quantity.

Using a novel approach, we examined the relative importance of resource heterogeneity and resource quantity in explaining species diversity in two large-scale species-rich forest plots in Gutianshan (GTS) Nature Reserve, Southeast China, and Barro Colorado Island (BCI), Central Panama. The two plots are ideal for testing the relative importance of the two hypotheses, because the rugged terrain of GTS and relatively uniform topography of BCI represent two extreme ends of resource heterogeneity (Harms et al., 2001; Legendre et al., 2009), and the soil resources and species distribution in the two plots have been mapped at high resolution (John et al., 2007; Zhang et al., 2011). To test the two hypotheses, we first partitioned the variation of species richness into components explained by resource quantity, resource heterogeneity, and plant density. We further evaluated the relative importance of resource quantity and resource heterogeneity by accounting for the effect of space.

## MATERIALS AND METHODS

### Study Site

We conducted research at two species-rich sites: (i) the 24-ha subtropical forest plot in GTS (29.25°N, 118.12°E, alt.

446–715 m), Zhejiang Province, East China; (ii) the 50-ha forest plot on BCI (09.15°N, 79.84°E, alt. 120–160 m), Central Panama. GTS is a subtropical evergreen broad-leaved forest supporting 159 species and 140,700 individuals (DBH $\geq$ 1cm). *Castanopsis eyrei* (Fagaceae), *Schima superba* (Theaceae), and *Pinus massoniana* (Pinaceae) are dominant species in this forest (Zhu et al., 2008). The soil is a subtropical red soil (equivalent to Ultisols in United States soil taxonomy).

Barro Colorado Island forest is a lowland semi-deciduous moist forest sustaining 299 species and 208, 400 individuals in the sixth census carried out in 2005. The soils in BCI are mostly well-weathered Kaolintic Oxisols (John et al., 2007).

## Soil Sampling and Analysis

Soils were sampled and analyzed at GTS and BCI following the same protocol of soil survey but with different grid sizes (John et al., 2007; Zhang et al., 2011). The soils of the BCI plot were sampled in a previous study (John et al., 2007) using a grid of 50 × 50 m, and one additional point was added to each intersection point at 2 m, 8 m, or 20 m in a random compass direction from the grid. Soils in GTS were sampled with a regular grid of 30 × 30 m in an area of 390 × 600 m. Each regular point was associated with two additional sampling points at 2 m, 5 m, or 15 m in a random compass direction. The remaining area was divided into 10 × 30 m grid and sampled the cross points. Thus, 893 points in GTS and 300 points in BCI were sampled. The soil sampling and analysis methods are available in John et al. (2007) and Zhang et al. (2011).

We applied Ordinary Kriging to obtain average values of soil variables for 10 × 10 m, 20 × 20 m, 40 × 40 m quadrats (in GTS), and 50 × 50 m quadrats (in BCI). We chose 40 × 40 m quadrats in GTS instead of 50 × 50 m quadrats at larger scale due to sufficient sample size at 40 × 40 m (150 quadrats at 40 × 40 m vs. 96 quadrats at 50 × 50 m).

## Data Analysis

### Plant Richness and Density

Species richness was the number of species in a sampled quadrat. We used the number of individuals (plant density) in each quadrat as an explanatory factor due to the relationship between species richness and plant density predicted by the resource quantity hypothesis (Srivastava and Lawton, 1998; Stevens and Carson, 1999).

### Environmental Factors

Environmental factors used in the analysis included soil nutrients and topographic variables. Available ions (Al, B, Ca, Cu, Fe, K, Mg, Mn, N, Na, Si, Zn), N mineralization rate ($N_{min}$), pH, moisture, Total C (TC), Total N (TN), Total P (TP) for GTS, and available ions (Al, B, Ca, Cu, Fe, K, Mg, Mn, P, Zn, N), $N_{min}$, pH for BCI were included in the analysis. Topographic variables (mean elevation, convexity, slope, and aspect) of both GTS and BCI were also included in the analysis. Topographic variables were calculated from elevation data following methods in Harms et al. (2001) and Legendre et al. (2009). Before the analysis, the soil nutrient except pH value was standardized by dividing the maximum value of each soil nutrient in the plot; pH value, mean elevation, convexity, and slope were centralized, while aspect was sine and cosine transformed to express east and north (Harms et al., 2001; John et al., 2007; Legendre et al., 2009). To assess the effects of resource heterogeneity and resource quantity on species diversity patterns, we combined soil nutrients and topographic variables as resource variables, because topographic factors can partly represent the light availability, soil temperature, or soil moisture in local communities.

### Spatial Factors

Spatial structure of species richness among quadrats was represented by dbMEM (distance-based Moran's eigenvector mapping) (Borcard and Legendre, 2002; Dray et al., 2006), which has also been called PCNM (principal coordinate of neighbor matrices). A truncated geographic distance matrix among quadrats was computed using the coordinates of quadrats, then principal coordinate analysis (PCoA) was employed to transform this matrix to dbMEMs (Borcard and Legendre, 2002). The dbMEMs were employed as explanatory variables to model spatial structures of species richness. Details of dbMEMs have been demonstrated in Legendre et al. (2009). Using function *forward.sel()* in R package *packfor* (Dray et al., 2012), we perform forward selection to choose significant dbMEMs representing spatial factors.

## Statistical Analysis

We used a variation partitioning method (Borcard et al., 1992; Peres-Neto et al., 2006; Cao et al., 2019) to partition the variation of species richness into fractions that were explained by resource heterogeneity, resource quantity (mean resource level), and spatial structure. We used function *varpart()* in R package "*vegan*" to calculate the variation fractions (Oksanen et al., 2007).

We used the standard deviation of environmental factors in 4 and 16 sub-quadrats of 10 × 10 m to represent resource heterogeneity within a 20 × 20 m or a 40 × 40 m quadrat (within-quadrat resource heterogeneity) for GTS, respectively. Similarly, we used the standard deviation of environmental factors in 4 and 25 sub-quadrats of 10 × 10 m to represent within-quadrat resource heterogeneity within a 20 × 20 m or a 50 × 50 m quadrat for BCI (Tilman, 1982; Stevens and Carson, 2002). To estimate average resource supply rate, we used the mean values of environmental factors at the same scales (Stevens and Carson, 2002).

We first partitioned the variation of species richness into fractions explained by resource quantity, resource heterogeneity, and plant density as shown in **Figure 1**. The fraction explained by within-quadrat resource heterogeneity is represented by fractions [1] + [5] + [6] in **Figure 1**. To disentangle the effect of resource heterogeneity and resource quantity, we used the joint effect of average resource supply rate and plant density to estimate the effect of resource quantity on species richness (fractions [4] + [7] in **Figure 1**) and used the other parts of the fraction explained by average resource supply rate to estimate resource heterogeneity among quadrats (among-quadrat resource heterogeneity) (fractions [2] + [5] in **Figure 1**).

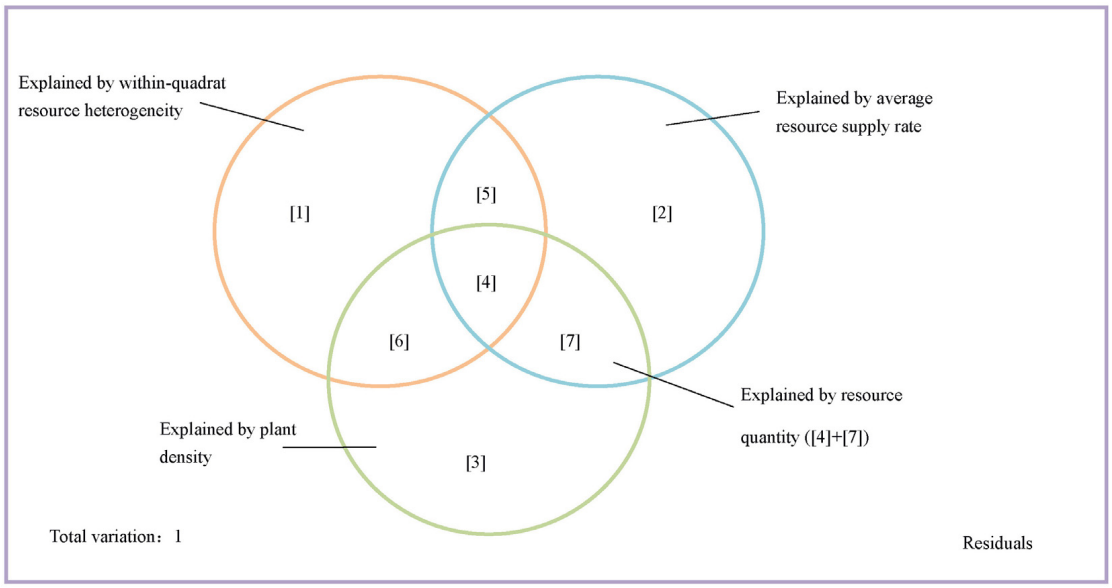


**FIGURE 1 |** Variation partitioning model for testing predictions of the resource quantity hypothesis and the resource heterogeneity hypothesis. The box encompasses the total variation in species richness of the studied plot. Circles stands for the fractions of variation that within-quadrat resource heterogeneity, average resource supply rate, and plant density could explain. [1]~[7] represent the fractions of variation in species richness that could be explained by different variables. [1], [2], and [3] are the fraction of variation that could be explained by one factor controlling other factors, respectively. [4]~[7] represent the intersection of variation that could be explained by joint effect of two or three variables.

Thus, the effect of resource heterogeneity can be estimated as the sum of within-quadrat resource heterogeneity and among-quadrat resource heterogeneity (fractions [1] + [2] + [5] + [6] in **Figure 1**).

Next, we further evaluated the effect of resource quantity and resource heterogeneity on species richness by accounting for the effect of space. We partitioned the variation in species richness into fractions explained by resource heterogeneity, average resource supply rate, plant density, and dbMEMs as shown in **Supplementary Figure S1**. Similarly, the variation in species richness explained by resource quantity is the sum of fractions [7], [10], [12], and [15], and the fractions explained by resource heterogeneity is the sum of fractions [1], [2], [5], [8], [9], and [14]. The joint effect of resource quantity and space is the sum of fractions [12] and [15], and the joint effect of resource heterogeneity and space is the sum of fractions [8], [9], and [14]. The pure effect of space is [4].

To model non-linear relationships between species richness and resource heterogeneity, average resource supply rate, and plant density, a third-order polynomial equation was applied to these factors to obtain monomials (Legendre et al., 2009). We used forward selection (with permutation tests, at the 5% significance level, of the increase in the adjusted $R^2$) to eliminate high collinearity among these variables and select a parsimonious subset of variables that significantly affect the distribution of species richness.

Spatial structure variables (dbMEMs) were produced by "*PCNM*" package (Legendre et al., 2012), forward selection was computed by "*packfor*" package (Dray et al., 2012), and variation partitioning method was performed using the "*vegan*" package (Oksanen et al., 2007). All the analysis was conducted in the open source software R 2.15.2 (R Development Core Team, 2012), and the R code was shown in the supporting information (**Supplementary Text S1**).

## RESULTS

The present work asked a central question: what is the relative contribution of resource quantity and resource heterogeneity to species diversity maintenance? We first addressed this question by partitioning the variation in species richness at GTS and BCI into fractions explained by resource heterogeneity, resource quantity, and plant density (**Figures 2A,B** and **Table 1**). In GTS plot, 60.0% of the variation in species richness could be explained by all variables at the 20 × 20 m scale, but only 21.6% at the same scale in BCI. However, we found consistent results across both plots, in terms of the relative importance of resource quantity and resource heterogeneity. Resource quantity could explain very little of variation in species richness. In GTS only 4.9% of the variation in species richness was explained by resource quantity, which contrasted markedly with 44.5% of the variation explained by resource heterogeneity (including both within-quadrat and among-quadrat resource heterogeneity) at the 20 × 20 m scale (**Figure 2A** and **Table 1**). Similarly, in BCI only 0.8% of the variation in species richness could be explained by resource quantity compared with 20.4% of the variation explained by resource heterogeneity at the 20 × 20 m scale (**Figure 3A** and **Table 1**). We found the similar results at the 40 × 40 m scale in

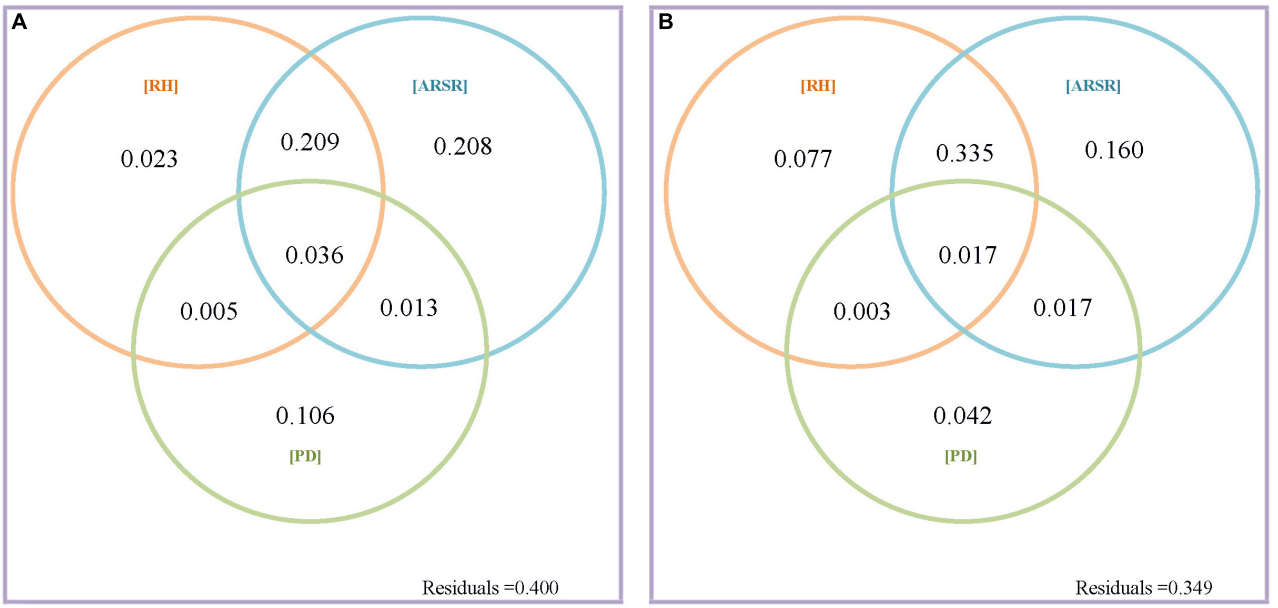


**FIGURE 2 |** Venn diagrams of variation partitioning results of variation in species richness explained by resource heterogeneity, average resource supply rate, and plant density at grain size 20 × 20 m **(A)** and 40 × 40 **(B)** for GTS; "RH" is the fraction explained by within-quadrat resource heterogeneity; "ARSR" is the fraction explained by average resource supply rate including the effect of resource quantity and among-quadrat resource heterogeneity; and "PD" is the fraction explained by plant density.

GTS and at the 50 × 50 m scale in BCI (**Figures 2B**, **3B** and **Table 1**).

We further evaluated the relative importance of resource quantity and resource heterogeneity on species richness while accounting for the effect of space (**Supplementary Table S1** and **Supplementary Figure S2**). We found that most of the effect of resource quantity and resource heterogeneity on species richness overlapped with the effect of space (**Supplementary Table S1** and **Supplementary Figure S2**). In GTS, we found that 61.2% of the effect of resource quantity and 99.8% of the effect of resource heterogeneity on species richness could be explained by space at the 20 × 20 m scale (**Supplementary Table S1** and **Supplementary Figures S2A,B**). Likewise, in BCI almost 100% of effect of both resource quantity and resource heterogeneity could be explained by space at the 20 × 20 m scale (**Supplementary Table S1** and **Supplementary Figures S2C,D**). We found the similar results at larger scales in both plots (**Supplementary Table S1** and **Supplementary Figure S2**). Moreover, we found that the effect of resource heterogeneity (44.5% for the effect of resource heterogeneity vs. 9.2% for the pure effect of space and 3.4% for the effect of resource quantity) governed species richness in GTS at the 20 × 20 m scale, whereas the pure effect of space (31.4% for the pure effect of space vs. 20.4% for the effect of resource heterogeneity and 0.8% for the effect of resource quantity) dominated the species diversity in BCI at the same scale (**Supplementary Figure S2** and **Supplementary Table S1**). Again, results at the larger scales were similar (**Supplementary Figure S2** and **Supplementary Table S1**).

**TABLE 1 |** Results of partitioning the variation of species richness explained by resource heterogeneity and resource quantity in Gutianshan (GTS) and Barro Colorado Island (BCI).

| Plot | Grain size | Resource quantity (%) [4] + [7] | Resource heterogeneity (%) [1] + [2] + [5] + [6] | All factors (%) 1-Residuals |
|---|---|---|---|---|
| GTS | 20 × 20 m | 4.9 | 44.5 | 60.0 |
| GTS | 40 × 40 m | 3.4 | 57.5 | 65.1 |
| BCI | 20 × 20 m | 0.8 | 20.4 | 21.6 |
| BCI | 50 × 50 m | 2.6 | 34.5 | 41.7 |

*The reported fractions are the adjusted $R^2$ statistics. [1]~[7] is the fraction of variation in species richness explained by variables shown in **Figure 1**.*

## DISCUSSION

The resource quantity hypothesis and the resource heterogeneity hypothesis are two contrasting views developed to explain the maintenance of species richness in the forest ecosystems (Tilman, 1982; Wright, 1983). However, the close spatial covariation in average resource supply rate and resource heterogeneity in natural communities make it difficult to isolate the effect of resource quantity and resource heterogeneity (Stevens and Carson, 2002). Using an approach derived from the relationship among resource quantity, resource heterogeneity, and plant density in the resource hypotheses, we found that resource quantity played a limited role in maintaining species diversity in two species-rich forests.

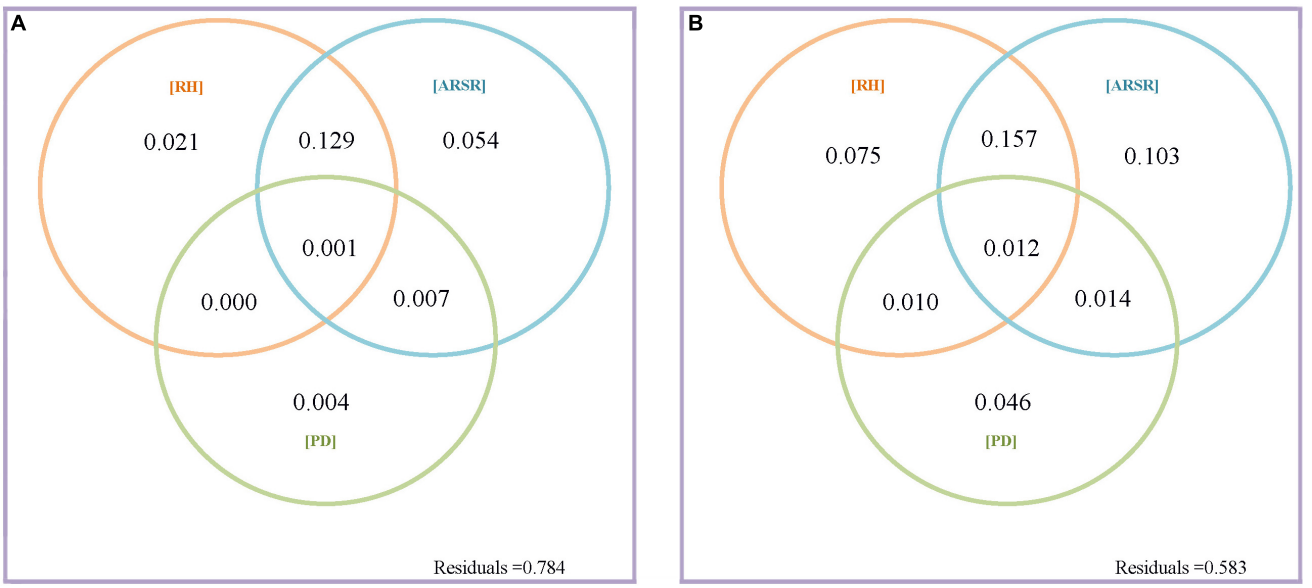


**FIGURE 3 |** Venn diagrams of variation partitioning results of variation in species richness explained by resource heterogeneity, average resource supply rate, and plant density at grain size 20 × 20 m **(A)** and 50 × 50 m **(B)** for BCI; "RH" is the fraction explained by within-quadrat resource heterogeneity; "ARSR" is the fraction explained by average resource supply rate including the effect of resource quantity and among-quadrat resource heterogeneity; and "PD" is the fraction explained by plant density.

We found that resource quantity could explain much less of the variation in species richness than resource heterogeneity in both of GTS and BCI. Thus, our results confirmed the resource heterogeneity hypothesis, but failed to support the resource quantity hypothesis. This suggests that resource heterogeneity may play a more important role in maintaining plant species diversity than resource quantity, at least in these two old-growth forests. This result is consistent with the findings that confirmed resource heterogeneity hypothesis in heterogeneous habitats (Bell et al., 2000; Balvanera and Aguirre, 2006; Douda et al., 2012; Ortega et al., 2018; Liu et al., 2019). In experimental studies, Stevens and Carson (2002) and Baer et al. (2004) showed that resource quantity contributes to species richness in artificially created uniform niches, such as light availability. Kumar et al. (2018) also found that mean light level was more important than light heterogeneity in explaining the understory species richness. Our results and above-mentioned studies may collectively support Bartels and Chen (2010)'s hypothesis that resource quantity determines species richness along a particular niche, whereas resource heterogeneity dominates species diversity across niches.

When spatial factors were included into the analysis, we found that most of the effect of resource heterogeneity and resource quantity on species richness overlapped with the effect of space, and the pure effects of resource quantity and resource heterogeneity were small (**Supplementary Figure S2** and **Supplementary Table S1**). This result indicates that most effects of resources could also be explained by spatial processes, such as dispersal limitation, invalidating the default assumption in both hypotheses that all appropriate species can reach all suitable habitats (Lundholm, 2009). On the other hand, the spatial arrange of habitats such as mountain ridge, hillside, or valley which related to the spatial distribution of resources also played an important role in regulating species richness pattern of these two forests (Harms et al., 2001; Lai et al., 2009; Legendre et al., 2009). This paralleled findings from experimental studies that propagule supply and resource heterogeneity jointly determine the species diversity of a community (Questad and Foster, 2008; Eilts et al., 2011; Myers and Harms, 2011). We also found that the effect of resource heterogeneity governed species richness in GTS, whereas the pure effect of space dominated the species diversity in BCI (**Supplementary Figure S2** and **Supplementary Table S1**). As we included soil nutrients and within-quadrat resource heterogeneity into analysis in GTS, we found that the effect of resource heterogeneity on species richness (44.5 and 57.5% at the 20 × 20 m and 40 × 40 m scales) was larger than that found by Legendre et al. (2009) (25.8 and 36.2% at the 20 × 20 m and 40 × 40 m scales, **Table 1**). It also suggested that the positive effect of the resource heterogeneity on species richness was more important at the larger scale. This may be because larger units encompassed more variability and species turnover (Stein et al., 2014).

In studies, the sum of pure effect of resource heterogeneity and the joint of resource heterogeneity and space was interpreted as the outcome of resource heterogeneity, while the pure effect of space was interpreted as the effect of spatial processes such as dispersal limitation (Jones et al., 2008; Legendre et al., 2009). However, caution should be excised when attributing fractions of

variation partitioning to the consequences of these processes even though soil nutrients were measured to a high resolution in both plots. The effect of resource quantity and resource heterogeneity may be underestimated, because the effect space may include the effects of unmeasured habitat factors, such as light availability; while the effect of space may be underestimated, because limited dispersal often correlates with spatial arrangement of habitats (Gilbert and Bennett, 2010; Smith and Lundholm, 2010).

Additionally, it is difficult to manipulate the resource heterogeneity and average resource supply rate to test the related hypotheses in the forest ecosystem. However, the method used in our study is novel, which could address this problem. Above all, the variation partitioning was used to separate the impacts of resources heterogeneity and resource quantity with *in situ* observational data, which could be a more appropriate way to reveal the assembly rule of the forests. Secondly, the variation partitioning could account for the spatial effect which is one crucial factor contributed importantly to the community assembly of the forests, and it makes the analysis more robust (Hu et al., 2018).

In summary, we evaluated the relative importance of resource quantity and resource heterogeneity in determining species richness in a subtropical forest plot in China. Using a novel approach to partition the effects of resource quantity and resource heterogeneity, we found that resource quantity played a limited role in structuring species diversity in two species-rich forests. To the best our knowledge, our study is the first evaluation of the relative contribution of resource quantity and resource heterogeneity in natural forest communities. We also found that resource heterogeneity governed species richness in GTS, whereas spatial processes such as dispersal limitation dominated species diversity in BCI. Our results, together with experimental and observational studies, suggest that the processes determining variation in species richness along ecological gradients in natural communities may be more complicated than can be represented by a single hypothesis. In the future, other types of forest ecosystem such as temperate forests could be tested using this method to gain more general results in the forest ecosystem. Moreover, the temporal pattern of the relative importance of resource heterogeneity and resource quantity also needs to be examined and compared, and it may help to deepen the understanding of community assembly rules in the forests.

## DATA AVAILABILITY STATEMENT

The datasets generated for this study are available on request to the corresponding author.

## AUTHOR CONTRIBUTIONS

LZ, XMi, and RH contributed to the experiment performance, data collection, data analysis and interpretation, and manuscript writing. BY and XMan contributed to the experiment performance and data collection. HR and KM contributed to the experimental design and interpretation. All authors contributed to the article and approved the submitted version.

## FUNDING

Soil work in the BCI plot was supported by NSF DEB 021104, 021115, 0212284, 0212818, and OISE 0314581, and the STRI soils initiative. This research was funded by the National Science and Technology Support Program (2012BAC01B05), the NSFC Project (31170401), and the Youth Innovation Promotion Association CAS (2018247).

## ACKNOWLEDGMENTS

The authors are grateful to Pierre Legendre and Kyle Harms for their valuable comments on data analysis and manuscript revision.

## SUPPLEMENTARY MATERIAL

The Supplementary Material for this article can be found online at: https://www.frontiersin.org/articles/10.3389/fevo.2020.00224/full#supplementary-material

## REFERENCES

Abrams, P. A. (1995). Monotonic or unimodal diversity productivity gradients - what does competition theory predict. *Ecology* 76, 2019–2027. doi: 10.2307/1941677

Baer, S. G., Blair, J. M., Collins, S. L., and Knapp, A. K. (2004). Plant community responses to resource availability and heterogeneity during restoration. *Oecologia* 139, 617–629. doi: 10.1007/s00442-004-1541-3

Bakker, C., Blair, J. M., and Knapp, A. K. (2003). Does resource availability, resource heterogeneity or species turnover mediate changes in plant species richness in grazed grasslands? *Oecologia* 137, 385–391. doi: 10.1007/s00442-003-1360-y

Balvanera, P., and Aguirre, E. (2006). Tree diversity, environmental heterogeneity, and productivity in a Mexican tropical dry forest. *Biotropica* 38, 479–491. doi: 10.1111/j.1744-7429.2006.00161.x

Barot, S. (2004). Mechanisms promoting plant coexistence: can all the proposed processes be reconciled? *Oikos* 106, 185–192. doi: 10.1111/j.0030-1299.2004.13038.x

Bartels, S. F., and Chen, H. Y. H. (2010). Is understory plant species diversity driven by resource quantity or resource heterogeneity? *Ecology* 91, 1931–1938. doi: 10.1890/09-1376.1

Bell, G., Lechowicz, M. J., and Waterway, M. J. (2000). Environmental heterogeneity and species diversity of forest sedges. *J. Ecol.* 88, 67–87. doi: 10.1046/j.1365-2745.2000.00427.x

Borcard, D., and Legendre, P. (2002). All-scale spatial analysis of ecological data by means of principal coordinates of neighbour matrices. *Ecol. Model.* 153, 51–68. doi: 10.1016/s0304-3800(01)00501-4

Borcard, D., Legendre, P., and Drapeau, P. (1992). Partialling out the Spatial Component of Ecological Variation. *Ecology* 73, 1045–1055. doi: 10.2307/1940179

Cao, K., Mi, X. C., Zhang, L. W., Ren, H. B., Yu, M. J., Chen, J. H., et al. (2019). Examining residual spatial correlation in variation partitioning of beta diversity in a subtropical forest. *J. Plant Ecol.* 12, 636–644. doi: 10.1093/jpe/rty058

Cardinale, B. J., Bennett, D. M., Nelson, C. E., and Gross, K. (2009). Does productivity drive diversity or vice versa? A test of the multivariate

productivity-diversity hypothesis in streams. *Ecology* 90, 1227–1241. doi: 10.1890/08-1038.1

Douda, J., Doudova-Kochankova, J., Boublik, K., and Drasnarova, A. (2012). Plant species coexistence at local scale in temperate swamp forest: test of habitat heterogeneity hypothesis. *Oecologia* 169, 523–534. doi: 10.1007/s00442-011-2211-x

Dray, S., Legendre, P., and Blanchet, G. (2012). *packfor: R package for forward selection, version 0.0-8*. Available online at: http://R-Forge.R-project.org (accessed July, 2013).

Dray, S., Legendre, P., and Peres-Neto, P. R. (2006). Spatial modelling: a comprehensive framework for principal coordinate analysis of neighbour matrices (PCNM). *Ecol. Model.* 196, 483–493. doi: 10.1016/j.ecolmodel.2006.02.015

Eilts, J. A., Mittelbach, G. G., Reynolds, H. L., and Gross, K. L. (2011). Resource Heterogeneity, Soil Fertility, and Species Diversity: Effects of Clonal Species on Plant Communities. *Am. Nat.* 177, 574–588. doi: 10.1086/659633

Gilbert, B., and Bennett, J. R. (2010). Partitioning variation in ecological communities: do the numbers add up? *J. Appl. Ecol.* 47, 1071–1082. doi: 10.1111/j.1365-2664.2010.01861.x

Harms, K. E., Condit, R., Hubbell, S. P., and Foster, R. B. (2001). Habitat associations of trees and shrubs in a 50-ha neotropical forest plot. *J. Ecol.* 89, 947–959. doi: 10.1111/j.1365-2745.2001.00615.x

Hu, Y. H., Johnson, D. J., Mi, X. C., Wang, X. G., Ye, W. H., Li, Y. D., et al. (2018). The relative importance of space compared to topography increases from rare to common tree species across latitude. *J. Biogeogr.* 45, 2520–2532. doi: 10.1111/jbi.13420

Huston, M. (1979). A general hypothesis of species diversity. *Am. Nat.* 113, 81–101. doi: 10.1086/283366

John, R., Dalling, J. W., Harms, K. E., Yavitt, J. B., Stallard, R. F., Mirabello, M., et al. (2007). Soil nutrients influence spatial distributions of tropical tree species. *Proc. Natl. Acad. Sci. U.S.A.* 104, 864–869. doi: 10.1073/pnas.0604666104

Jones, M. M., Tuomisto, H., Borcard, D., Legendre, P., Clark, D. B., and Olivas, P. C. (2008). Explaining variation in tropical plant community composition: influence of environmental and spatial data quality. *Oecologia* 155, 593–604. doi: 10.1007/s00442-007-0923-8

Kumar, P., Chen, H. Y. H., Thomas, S. C., and Shahi, C. (2018). Linking resource availability and heterogeneity to understorey species diversity through succession in boreal forest of Canada. *J. Ecol.* 106, 1266–1276. doi: 10.1111/1365-2745.12861

Lai, J. S., Mi, X. C., Ren, H. B., and Ma, K. P. (2009). Species-habitat associations change in a subtropical forest of China. *J. Veget. Sci.* 20, 415–423. doi: 10.1111/j.1654-1103.2009.01065.x

Legendre, P., Borcard, D., Blanchet, F. G., Caceres, M. D., and Dray, S. (2012). *PCNM: MEM spatial eigenfunction and principal coordinate analyses, Version: 2.1-2*. Available online at: http://r-forge.r-project.org/ (accessed July, 2013).

Legendre, P., Mi, X. C., Ren, H. B., Ma, K. P., Yu, M. J., Sun, I. F., et al. (2009). Partitioning beta diversity in a subtropical broad-leaved forest of China. *Ecology* 90, 663–674. doi: 10.1890/07-1880.1

Liu, Y. J., De Boeck, H. J., Li, Z. Q., and Nijs, I. (2019). Unimodal relationship between three-dimensional soil heterogeneity and plant species diversity in experimental mesocosms. *Plant Soil* 436, 397–411. doi: 10.1007/s11104-019-03938-w

Lundholm, J. T. (2009). Plant species diversity and environmental heterogeneity: spatial scale and competing hypotheses. *J. Veget. Sci.* 20, 377–391. doi: 10.1111/j.1654-1103.2009.05577.x

Myers, J. A., and Harms, K. E. (2011). Seed arrival and ecological filters interact to assemble high-diversity plant communities. *Ecology* 92, 676–686. doi: 10.1890/10-1001.1

Oksanen, J., Kindt, R., Legendre, P., and O'hara, R. B. (2007). *vegan: community ecology package. R package version 1.9-25*. Available online at: http://cran.r-project.org/ (accessed July, 2013).

Ortega, J. C. G., Thomaz, S. M., and Bini, L. M. (2018). Experiments reveal that environmental heterogeneity increases species richness, but they are rarely designed to detect the underlying mechanisms. *Oecologia* 188, 11–22. doi: 10.1007/s00442-018-4150-2

Peres-Neto, P. R., Legendre, P., Dray, S., and Borcard, D. (2006). Variation partitioning of species data matrices: estimation and comparison of fractions. *Ecology* 87, 2614–2625. doi: 10.1890/0012-9658(2006)87[2614:vposdm]2.0.co;2

Questad, E. J., and Foster, B. L. (2008). Coexistence through spatio-temporal heterogeneity and species sorting in grassland plant communities. *Ecol. Lett.* 11, 717–726. doi: 10.1111/j.1461-0248.2008.01186.x

R Development Core Team (2012). *R: A Language and Environment for Statistical Computing*. Vienna: The R Foundation for Statistical Computing.

Ricklefs, R. E. (1977). Environmental heterogeneity and plant species diversity: a hypothesis. *Am. Nat.* 111, 376–381. doi: 10.1086/283169

Ricklefs, R. E., and Schluter, D. (1993). *Species Diversity in Ecological Communities: Historical and Geographical Perspectives*. Chicago, IL: University of Chicago Press.

Smith, T. W., and Lundholm, J. T. (2010). Variation partitioning as a tool to distinguish between niche and neutral processes. *Ecography* 33, 648–655. doi: 10.1111/j.1600-0587.2009.06105.x

Srivastava, D. S., and Lawton, J. H. (1998). Why more productive sites have more species: An experimental test of theory using tree-hole communities. *Am. Nat.* 152, 510–529. doi: 10.1086/286187

Stein, A., Gerstner, K., and Kreft, H. (2014). Environmental heterogeneity as a universal driver of species richness across taxa, biomes and spatial scales. *Ecol. Lett.* 17, 866–880. doi: 10.1111/ele.12277

Stevens, M. H. H., and Carson, W. P. (1999). The significance of assemblage-level thinning for species richness. *J. Ecol.* 87, 490–502. doi: 10.1046/j.1365-2745.1999.00374.x

Stevens, M. H. H., and Carson, W. P. (2002). Resource quantity, not resource heterogeneity, maintains plant diversity. *Ecol. Lett.* 5, 420–426. doi: 10.1046/j.1461-0248.2002.00333.x

Tilman, D. (1982). *Resource Competition and Community Structure*. Princeton: Princeton University Press.

Wright, D. H. (1983). Species energy theory: an extension of species-area theory. *Oikos* 41, 496–506.

Yang, Z. Y., Liu, X. Q., Zhou, M. H., Ai, D., Wang, G., Wang, Y. S., et al. (2015). The effect of environmental heterogeneity on species richness depends on community position along the environmental gradient. *Sci. Rep.* 5:15723.

Zhang, L. W., Mi, X. C., Shao, H. B., and Ma, K. P. (2011). Strong plant-soil associations in a heterogeneous subtropical broad-leaved forest. *Plant Soil* 347, 211–220. doi: 10.1007/s11104-011-0839-2

Zhu, Y., Zhao, G. F., Zhang, L. W., Shen, G. C., Mi, X. C., Ren, H. B., et al. (2008). Community composition and structure of Gutianshan forest dynamic plot in a mid-subtropical evergreen broad-leaved forest, east China. *J. Plant Ecol.* 32, 262–273.

**Conflict of Interest:** The authors declare that the research was conducted in the absence of any commercial or financial relationships that could be construed as a potential conflict of interest.

frontiers in Ecology and Evolution

ORIGINAL RESEARCH
published: 31 July 2020
doi: 10.3389/fevo.2020.00245

# Temporal and Spatial Pattern of *Holcoglossum* Schltr. (Orchidaceae), an East Asian Endemic Genus, Based on Nuclear and Chloroplast Genes

*Jiahong Zhao[1], Peng Zhou[1], Xiaoqian Li[1,2], Liguo Zhang[1], Xiaohua Jin[2] and Xiaoguo Xiang[1]**

*[1] Jiangxi Province Key Laboratory of Watershed Ecosystem Change and Biodiversity, Institute of Life Science and School of Life Sciences, Nanchang University, Nanchang, China, [2] State Key Laboratory of Systematic and Evolutionary Botany, Institute of Botany, Chinese Academy of Sciences, Beijing, China*

East Asia is one of the plant diversity and endemism centers in the world, and the temporal and spatial patterns and processes of vascular plants attracted ecologists' and biogeographers' attention. However, the biogeographic patterns of endemic epiphytic plants in East Asia are still unclear. Here, we investigated the historical biogeography of an East Asian endemic epiphytic genus *Holcoglossum* Schltr. (Orchidaceae). Using DNA sequences of eleven chloroplast genes and one nuclear gene, we reconstructed a robust phylogenetic framework for *Holcoglossum* and used a relaxed-clock method to estimate divergent times for the genus. We inferred the ancestral range of lineages under the statistical dispersal-extinction cladogenesis (S-DEC) and statistical dispersal-vicariance analysis (S-DIVA), respectively. Biogeographical analysis suggested that the most recent common ancestor of *Holcoglossum* occurred in the Palaeotropical region in the late Miocene (6.33 Ma). Four dispersal events were inferred to explain the *Holcoglossum* expansion to Sino-Himalayan, Sino-Japanese, and Taiwan regions from the latest Miocene to Quaternary. The episodes of these events were associated with intensification of East Asian monsoon around 3.6–2.6 Ma and global cooling since the latest Pliocene. The disjunct distribution between mainland China and Taiwan was attributed by the sea-level fluctuations and climate changes during the late Pliocene. This study shed light on the biogeographic processes of endemic epiphytic plants in East Asia.

**Keywords: biogeography, East Asia, *Holcoglossum*, molecular dating, phylogeny**

OPEN ACCESS

***Edited by:***
*Meng Yao,*
*Peking University, China*

***Reviewed by:***
*Xin Zhou,*
*China Agricultural University, China*
*Xiaolei Huang,*
*Fujian Agriculture and Forestry University, China*

***Correspondence:**
*Xiaoguo Xiang*
*xiangxg2010@163.com*

***Specialty section:***
*This article was submitted to Biogeography and Macroecology, a section of the journal Frontiers in Ecology and Evolution*

***Received:*** *03 February 2020*
***Accepted:*** *06 July 2020*
***Published:*** *31 July 2020*

***Citation:***
*Zhao J, Zhou P, Li X, Zhang L, Jin X and Xiang X (2020) Temporal and Spatial Pattern of Holcoglossum Schltr. (Orchidaceae), an East Asian Endemic Genus, Based on Nuclear and Chloroplast Genes. Front. Ecol. Evol. 8:245. doi: 10.3389/fevo.2020.00245*

## INTRODUCTION

East Asia is well-known for its vascular plant diversity and endemic (Qian et al., 2005). The flora of East Asia harbors ca. 258 families and more than 3000 genera, of which approximately 8.2% are endemic (Wu and Wu, 1998; Chen et al., 2018). Understanding the historical origins and processes of the plant richness of East Asia has been of major interest for ecologists and biogeographers. In the Cenozoic, East Asia underwent the uplift of the Himalaya–Tibetan Plateau (An et al., 2001) and the establishment and intensification of the Asian monsoon (Sun and Wang, 2005).

A great deal of phytogeographic research on plants in East Asia has been published. East Asia is suggested as both a "Cradle" and a "Museum" for vascular plants since the Cretaceous (e.g., Wu and Wu, 1998; Wen, 1999; Jiang et al., 2019). Xiang et al. (2019) combined molecular and fossil data and inferred that the ancestors of Hamamelidaceae occurred in tropical Asia during the mid-Cretaceous and subsequently migrated to Europe, Africa, and America during the Late Cretaceous and Early Tertiary. Luo et al. (2015) carried out phylogeographic analysis of four perennial herbs in Hengduan Mountains and showed that these species originated during the Late Pliocene or early–mid-Pleistocene and diverged by climate-induced habitat fragmentation. Further, during the glacial periods of Quaternary, East Asia acted as refugia for vascular plants' survival and evolution, especially for more recent divergent lineages (Tiffney, 1985; Ying, 2001; Qiu et al., 2011; Chen et al., 2018). However, the biogeographic patterns and processes of endemic epiphytic plants in East Asia are still poorly known.

Aeridinae is the largest and horticulturally important subtribe in Orchidaceae, which consisted of 83 genera and 1550 species (Pridgeon et al., 2014; Chase et al., 2015). The subtribe is mainly composed of epiphytes and distributed in tropical and subtropical Asia and northern Australia with some extended to northeast Asia (Hidayat et al., 2012; Chase et al., 2015). Among these, nearly 33 genera occurred across tropical Asia to temperate Asia. *Holcoglossum* Schltr. (Aeridinae, Orchidaceae) is used here as a typical case to illustrate the biogeographic processes of endemic epiphytic plants in East Asia. This genus encompasses ca. 16 currently accepted species (Xiang et al., 2012), mainly distributed in southwestern China and neighboring regions (Schlechter, 1919; Christenson, 1998; Jin and Wood, 2009; Xiang et al., 2012). These species are diverse in morphology, especially the structure of the flower (**Figure 1**). Xiang et al. (2012) employed three DNA markers (ITS, *matK*, and *trnH-psbA*) to resolve the relationship of 16 *Holcoglossum* species and found that *Holcoglossum* is monophyletic, which contains three clades, alpine clade (AC), tropical clade (TC), and the intermediate group (HC). Li et al. (2019) used the whole chloroplast genomes of 12 *Holcoglossum* species and obtained the same result of Xiang et al. (2012). Of *Holcoglossum* species, TC includes six species that occur in Southeast Asia, and AC contains five species that are mainly found in the Hengduan Mountains (**Figure 2**). Within HC, two species are restricted to Taiwan, and another two species are distributed in the mainland China (**Figure 2**). Previous studies show that the stem age of *Holcoglossum* was 7.71 Ma [95% highest posterior density (HPD): 4.12–12.04] (Xiang et al., 2016) with two *Holcoglossum* samplings. Without time estimation and biogeographic analyses, Fan et al. (2009) postulated that *Holcoglossum* originated in tropical Asia and migrated from the tropics to the temperate regions. Therefore, when and how the genus *Holcoglossum* formed current biogeographic patterns is still unclear.

In this study, we reconstruct a time-calibrated phylogenetic tree with samples of nearly all species. We also reconstruct the biogeographic history of *Holcoglossum*. Our specific objectives were to infer (1) the spatial and temporal pattern of *Holcoglossum* and (2) the possible impacts of past geological and climatic oscillations on the distribution of these species.

# MATERIALS AND METHODS

## Taxon Sampling

In this study, we sampled 15 species of *Holcoglossum*, representing the three clades of this genus. Based on Topik et al. (2005) and Xiang et al. (2012), the phylogenetic relationships of *Aerides* alliance is not all resolved, so ten species from *Aerides* alliance were used as outgroups (*Aerangis calligera*, *Aeranthes ramosus*, *Aerides multiflora*, *Angraecum eburneum*, *Ascocentrum ampullaceum*, *Diaphananthe odoratissima*, *Neobenthamia gracilis*, *Neofinetia falcata*, *Phalaenopsis aphrodite*, *Vanda coerulescens*). Voucher information and GenBank accession numbers are listed in **Supplementary Table 1**.

## Molecular Data

Total genomic DNA was extracted from silica gel-dried leaves of a living plant using total DNA extraction kit (CWBIO, Beijing). One nuclear markers (ITS) and eleven chloroplast DNA markers (*atpH-I*, *matK*, *psbA-trnH*, *psbK-I*, *rbcL*, *rpoB*, *rpoC1*, *rpS12-rpL20*, *trnL-F*, *trnS-fM*, and *trnS-G*) were employed in this study. The primers for amplification and sequencing are listed in **Supplementary Table 2**. The PCR procedure of *atpH-I* is followed by Shaw et al. (2007); procedures of *psbK-I*, *rpoB*, and *rpoC1* are followed by CBOL Plant Working Group (2009); procedures of *rpS12-rpL20* and *trnS-G* are followed by Shaw et al. (2005); the procedure of *rbcL* is followed by Goldman et al. (2001); and the procedure of *trnS-fM* is followed by Demesure et al. (1995).

## Phylogenetic Analysis

DNA sequences were aligned using the default parameters in Clustal X v.1.83 (Thompson et al., 1997) and subsequently manually adjusted with BioEdit (Hall, 1999). Topological congruence between the chloroplast and nuclear data was evaluated using the incongruence length difference (ILD) test (Farris et al., 1994).

Phylogenetic reconstruction was performed using maximum parsimony (MP), maximum likelihood (ML) in PAUP* 4.0b10 (Swofford, 2003), and Bayesian inference (BI) methods in MrBayes v.3.2 (Ronquist et al., 2012), respectively. All characters were unordered and had equal weight. Gaps were treated as missing data.

For MP analyses, heuristic searches were conducted with 1000 replicates of random addition, in combination with tree bisection–reconnection (TBR) branch-swapping, Multrees in effect, and steepest descent off. Bootstrap support values were conducted with 1000 replicates with 10 random taxon additions and heuristic search options.

Before performing ML and BI analyses, the best-fit nucleotide substitution model for each DNA region was chosen based on the Akaike information criterion (AIC) as calculated using

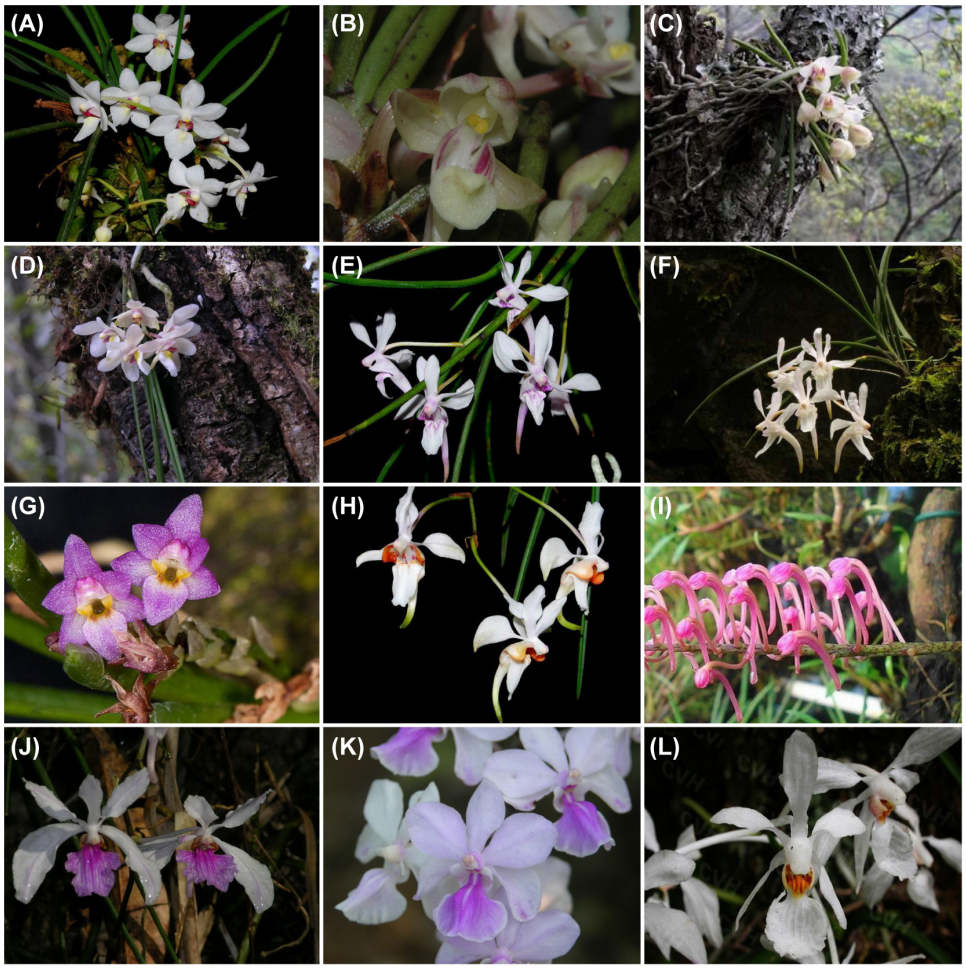


**FIGURE 1 |** Habitat and diversity of *Holcoglossum*. **(A)** *H. rupestre*; **(B)** *H. sinicum*; **(C)** *H. flavescens*; **(D)** *H. nujiangense*; **(E)** *H. lingulatum*; **(F)** *H. omeiense*; **(G)** *H. pumilum*; **(H)** *H. quasipinifolium*; **(I)** *H. himalaicum*; **(J)** *H. kimballianum*; **(K)** *H. amesianum*; **(L)** *H. subulifolium*. Photo by Xiaohua Jin.

Modeltest v.3.7 (Posada and Crandall, 1998). For ML analyses, we conducted a rapid bootstrap analysis (1000 replicates) and searched for the best-scoring ML tree simultaneously. Each DNA region was assigned the best-fit model, and other parameters followed the default settings.

For BI analyses, each DNA region was assigned its own model of nucleotide substitution. Four Markov-chain Monte Carlo (MCMC) were run, sampling one tree every 1000 generations for 3,000,000 generations. Runs started with a random tree. Majority-rule (>50%) consensus trees were constructed after removing the "burn-in" samples (the first 20% of the sampled trees).

## Molecular Age Estimation

We first conducted a likelihood ratio test to determine whether our sequence data were evolved in a clock-like fashion. The result rejected a constant rate ($\delta$ = 246.55, d.f. = 24, $P < 0.001$); we used a relaxed lognormal clock model in BEAST v.1.7.4 (Drummond and Rambaut, 2007) to generate a dated phylogeny of *Holcoglossum*. There are no fossil for *Holcoglossum* and subtribe Aeridinae, so we used the age of 33.97 Ma (95% HPD: 25.67–42.33) for the tree root prior to our analysis based on our recent broader study of Orchidaceae (Xiang et al., 2016). Following the suggestion of Ho (2007), we assigned a prior normal distribution for the calibration, with a standard deviation of 4. The YULE process was chosen as the speciation prior, and the BEAST analysis was run on the GTR + I + $\Gamma$ model for each DNA region, respectively. MCMC searches were run for 100,000,000 generations, sampled every 5000 generations. Convergence was monitored using Tracer v.1.5 (Rambaut and Drummond, 2007). The effective sampling sizes (ESSs) for all parameters were more than 200. The maximum clade credibility tree was computed using TreeAnnotator v.1.7.4 (Drummond and Rambaut, 2007).

## Ancestral Range Reconstruction

According to the extant distribution of *Holcoglossum* and outgroups, four main regions were categorized based on the floristic regions of Wu and Wu (1998) and Wu et al. (2003): A, Sino-Japanese region; B, Sino-Himalayan region; C,

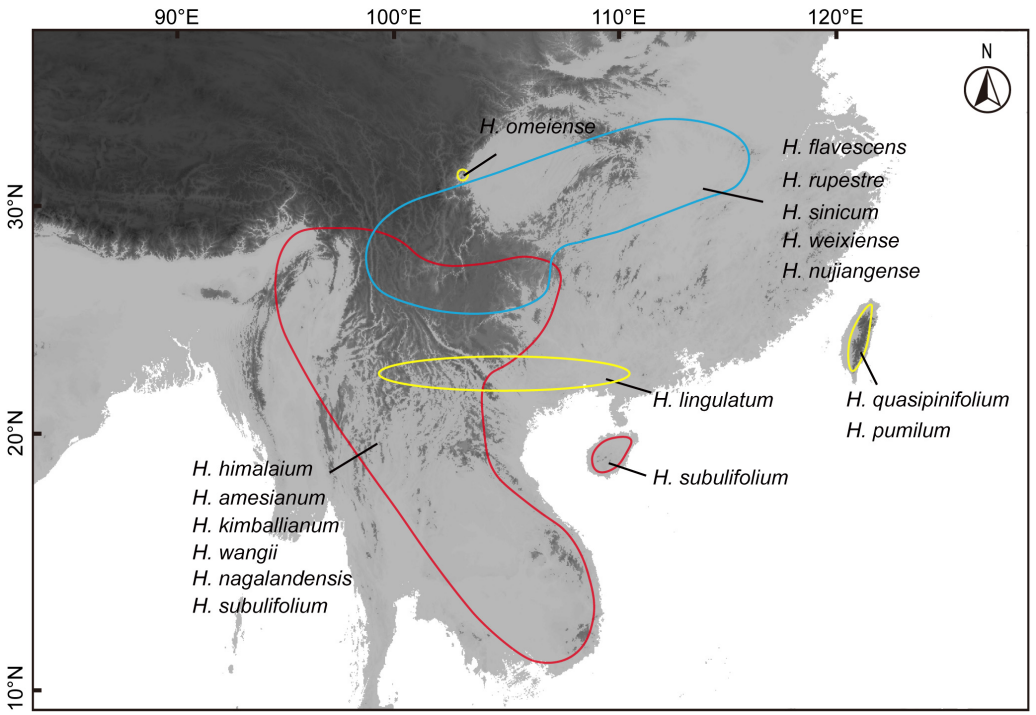


**FIGURE 2 |** Geographical distribution of *Holcoglossum*. The red region represents the range of tropical clade (TC), the blue region is for temperate alpine clade (AC), and the yellow region is for the group between the first two clades (HC).

Palaeotropical region; and D, Taiwan. The ancestral range reconstruction was inferred using the statistical dispersal-extinction cladogenesis (S-DEC) model and statistical dispersal-vicariance analysis (S-DIVA) as implemented in RASP (Yu et al., 2015), respectively. The maximum clade credibility tree obtained from BEAST was chosen as the input tree. The random 1000 trees from BEAST trees after burn-in were input to estimate the probabilities of the ancestral range at each node.

# RESULTS

## Phylogenetic Relationships Within *Holcoglossum*

A total of 103 new sequences for *atpH-I*, *rbcL*, *psbK-I*, *rpoB*, *rpoC1*, *rpS12-rpL20*, *trnS-fM*, and *trnS-G* were generated in this study (**Supplementary Table 2**). The total length of the combined chloroplast and nuclear DNA sequences was 11,176 bp, of which 1117 characters were variable, and 433 were parsimony informative (**Supplementary Table 3**). The result of ILD suggested that there is congruence between chloroplast and nuclear data ($P$ = 1.00). The monophyly of *Holcoglossum* and the three clades previously proposed (Fan et al., 2009; Xiang et al., 2012) was strongly supported (**Figure 3**). The TC was basal to *Holcoglossum* (BI-PP: 1.00; ML-BS: 79%; MP-BS: 82%), and the AC and the group between the first two clades (HC) formed a sister group (BI-PP: 1.00; ML-BS: 100%; MP-BS: 100%). The most nodes within *Holcoglossum* were supported by moderate to high supporting values, except for interrelationships in the AC clade (**Figure 3**).

## Divergent Time Estimation

The likelihood ratio test showed that our sequence data were evolving in a non-clock-like model, and a chronogram of *Holcoglossum* based on the relaxed-clock model is presented in **Figure 4**. Our time estimates suggested that *Holcoglossum* might have originated during the Late Tertiary (8.53 Ma, 95% HPD: 4.19–14.02, node 1). The crown age of *Holcoglossum* was 6.33 Ma (95% HPD: 3.3–10.6, node 2). The TC clade, containing *Holcoglossum himalaicum*, *H. nagalandensis*, *H. kimballianum*, *H. wangii*, *H. amesianum*, and *H. subulifolium*, diverged first during the Early Pliocene (5.31 Ma, 95% HPD: 2.5–8.81, node 3). Then, the HC clade and AC clade diverged during the Late Pliocene (3.63 Ma, 95% HPD: 1.64–6.24, node 4). The crown age of the HC clade, containing *Holcoglossum ligulatum*, *H. omeiense*, *H. pumilum*, and *H. quasipinifolium*, was at latest Pliocene (2.7 Ma, 95% HPD: 1.16–4.78, node 5), and then the two Taiwan species (*H. pumilum*, *H. quasipinifolium*) were divergent from their sister group. The AC clade might have started to diversify around Middle Pleistocene (1.22 Ma, 95% HPD: 0.5–2.39, node 8), and its five species (*Holcoglossum nujiangense*, *H. weixiense*, *H. rupestre*, *H. sinicum*, *H. flavescens*) rapidly differentiated since then.

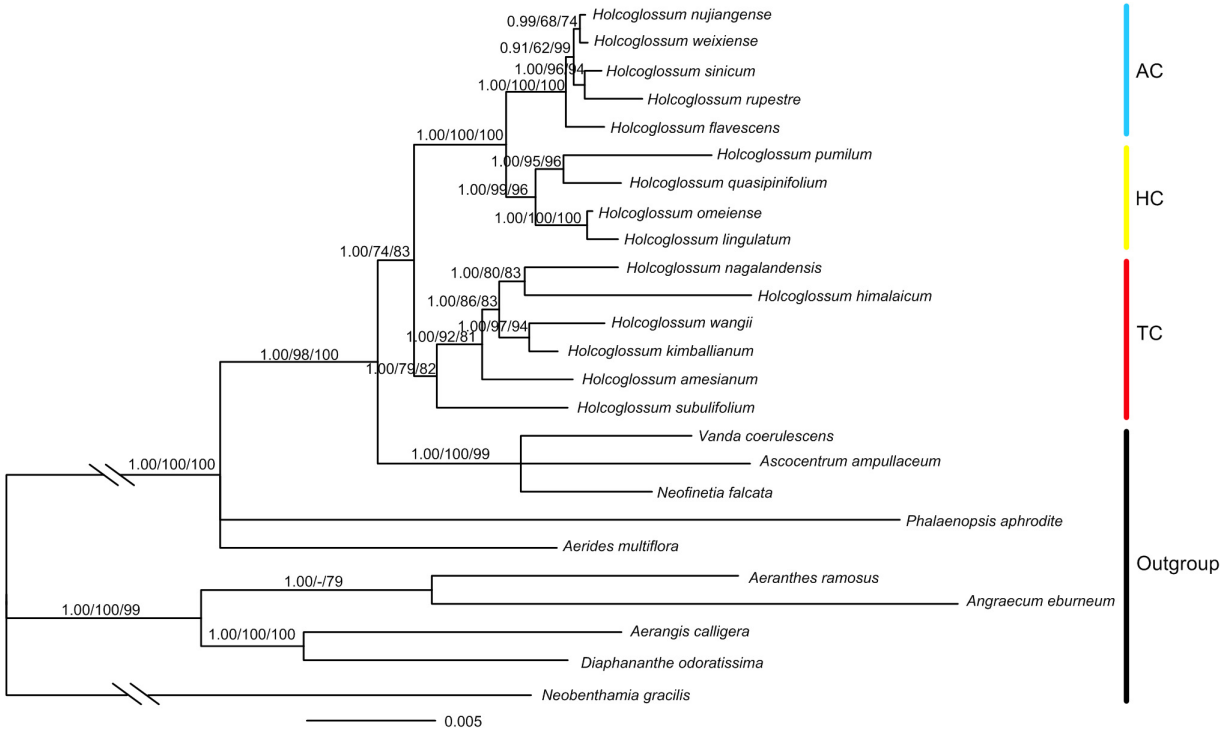


**FIGURE 3 |** Chronogram obtained from Bayesian inference analysis based on combined nrDNA and cpDNA data. Numbers on the branches are supporting values of Bayesian inference, maximum likelihood, and maximum parsimony, respectively. Dash indicates that the node was not supported.

## Ancestral Range Reconstruction

The ancestral range reconstruction of *Holcoglossum* based on S-DEC and S-DIVA is shown in **Figure 4**. Both S-DEC and S-DIVA inferred that the most recent common ancestor (MRCA) of *Holcoglossum* was probably distributed in the Palaeotropical region (node 2). The MRCA of TC was also in the Palaeotropical region (node 3). The MRCA of HC distributed in the Palaeotropical region and Taiwan (node 5), which were later split into mainland China and Taiwan. The MRCA of AC was inferred at the Sino-Japanese region and Sino-Himalayan region by S-DEC, and Sino-Himalayan by S-DIVA (node 8), which subsequently diversified in the Sino-Himalayan region.

# DISCUSSION

## Phylogenetic Relationship of *Holcoglossum*

A robust phylogenetic framework is needed for biogeographical analyses. In this study, the phylogenetic result based on combined chloroplast and nuclear data strongly supported *Holcoglossum* as monophyletic, which included three clades, i.e., TC, HC, and TC, which is consistent with Xiang et al. (2012) and Li et al. (2019). However, the phylogenetic relationships within TC and AC are slightly different. For example, *Holcoglossum naglandensis* and *H. himalaicum* among TC are sisters in this study and Xiang et al. (2012), while *H. naglandensis* is close to *H. amesianum* and *H. himalaicum* is close to *H. wangii* due to different DNA sequences. Nevertheless, these species of TC and AC are distributed in the same floristic region, respectively, and there is no influence on subsequently biogeographic analyses.

## Temporal and Spatial Patterns of *Holcoglossum*

Both S-DEC and S-DIVA analyses detected that the modern distribution of *Holcoglossum* is attributed to four dispersal events (**Figure 4**). Here, we adopted the S-DEC result to explain the temporal and spatial patterns of *Holcoglossum*. The biogeographical analyses indicate that the stem and crown of *Holcoglossum* most likely occurred in the Palaeotropical region, partly in agreement with the conclusion from Fan et al. (2009) that *Holcoglossum* was dispersed from the tropical region.

Within TC, all six currently recognized species distribute in the Asian tropical region. The crown group of TC happened in the Palaeotropical region since 5.31 Ma (95% HPD: 4.19–14.02, node 3) and then six species diversified there among 5.31–1.63 Ma. The weather in Southeast Asia had no distinct seasonality, and the climate is constantly moist and warm since Pliocene (Clements et al., 2006), which is beneficial for *Holcoglossum* colonization in tropical forests. Further, a putative abrupt intensification of the East Asian monsoon system during 3.6–2.6 Ma (Zhang et al., 2012) brought abundant precipitation, which provided favorable climatic conditions for the survival of epiphytic species in East Asia.

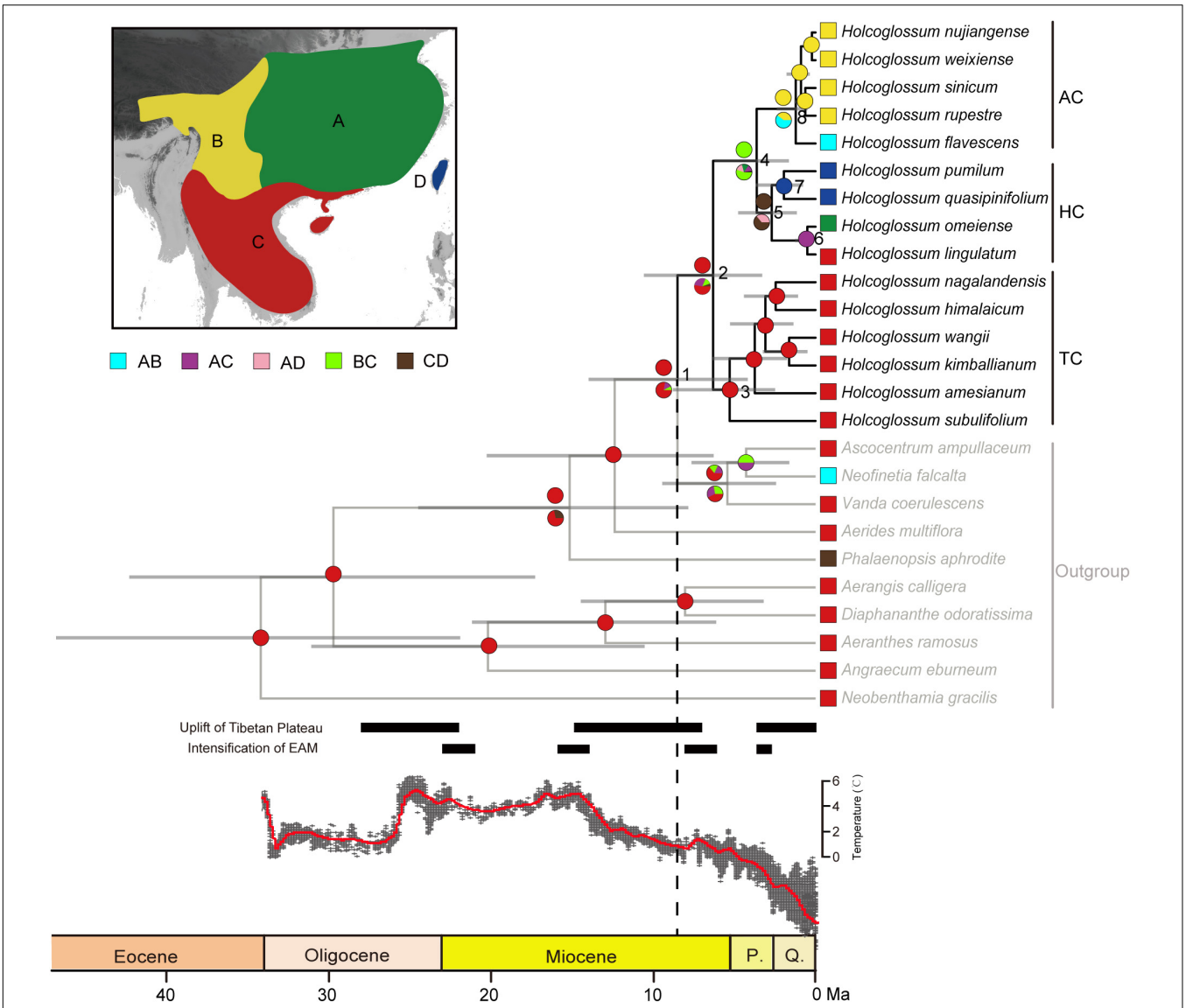


**FIGURE 4 |** Ancestral range reconstruction of *Holcoglossum* in RASP. The same results of S-DEC and S-DIVA are marked by one circle at the node. Colored circles at nodes above branches for S-DIVA and below branches for S-DEC. A, Sino-Japanese region; B, Sino-Himalayan region; C, Palaeotropical region; D, Taiwan. The global temperature curve is modified from Zachos et al. (2008).

After TC diverged from AC and HC, a subsequent dispersal from the Palaeotropical region to the Sino-Himalayan region occurred since the Late Miocene (3.63 Ma, 95% HPD: 1.64–6.24, node 4). Within HC, the ancestor of HC dispersed from the Palaeotropical region and Sino-Himalayan region into Taiwan (2.7 Ma, 95% HPD: 1.16–4.78, node 5). Taiwan island formed at 5–6 Ma and had been long linked to the Chinese mainland via Fujian-Taiwan land bridge (Teng, 1990; Zeng, 1993), which led to the close relationship between flora of Taiwan and mainland China (e.g., Zeng, 1993; Hsieh, 2002; Nie et al., 2007; Ying and Chen, 2011; Xiang et al., 2017). Wang (1992) proposed that plant lineages could extend from Southwest China eastward along the Nanling Corridor and along other mountain chains in Central China to East China or Taiwan. The biogeography of *Cycas taitungensis* (Huang et al., 2001), *Sassafras tzumu* (Nie et al., 2007), and *Dichocarpum basilare* (Xiang et al., 2017) showed that dispersal is attributed to the disjunct distribution between Asian mainland and Taiwan. *Holcoglossum* lineages may also have dispersed eastward along the same route to east China and then across the Fujian-Taiwan land bridge to Taiwan. Conversely, the global cooling and the subsequent rise of sea level caused the interruption of the continuous distribution of *Holcoglossum* since the latest Pliocene. The Palaeotropical *Holcoglossum lingulatum* and Sino-Japanese *H. omeiense* split at 0.56 Ma (95%: 0.11–1.17, node 6) (**Figure 4**). The global cooling and frequently glacial periods happened at Quaternary, which resulted in *H. omeiense* being restricted in Omei Mountains in China and *H. lingulatum* in Southeast Asia.

Within AC, the ancestor of AC migrated from the Palaeotropical region and Sino-Himalayan region to the Sino-Japanese region (1.22 Ma, 95% HPD: 0.5–2.36, node 8). All five currently recognized species distribute in Hengduan Mountains, except for *H. flavescens*, which extend to the Sino-Japanese region. These species are inferred to diverge rapidly during a short time interval (<1 Ma; **Figure 4**). The time is markedly later than the time of the Hengduan Mountains Region uplift (around 4–3 Ma; Chen, 1992, 1996; Shi et al., 1998). However, the uplift of the Hengduan Mountains formed a complex range of topographies, climates, and habitats (Hoorn et al., 2013), and many areas of this region are ice-free during Quaternary glaciations (Zheng et al., 1998), which can allow immigrations and survivals of plant lineages. *Holcoglossum* species of AC clade grow on the trees of evergreen broad-leaved forests, especially *Quercus* section *Heterobalanus* (Jin, 2003). The continuous uplift of Himalaya-Hengduan Mountains in the Late Miocene to Early Pliocene triggered the diversification of *Quercus* section *Heterobalanus* (Meng et al., 2017), which provided suitable habits for *Holcoglossum* in the Hengduan Mountains. Extensive biogeographical researches proved that the uplift of the Hengduan Mountains directly or indirectly plays vital roles in the species diversification in multiple lineages, such as *Rhodiola* (Crassulaceae; Zhang et al., 2014), *Rhododendron* (Eriaceae; Xing and Ree, 2017), *Saxifraga* (Saxifragaceae; Ebersbach et al., 2017), and alpine bamboo (Ye et al., 2019). The divergence of *Holcoglossum* still supported that the Hengduan Mountains Region is an adaptive plant diversification center in the Quaternary climate oscillations (Boufford, 2014; Jian et al., 2015; Xing and Ree, 2017).

## CONCLUSION

In this study, we reconstructed a phylogenetic tree and estimated divergent times of *Holcoglossum*, a genus endemic to East Asia. Our biogeographic inference indicated that the MRCA of *Holcoglossum* occurred in the Palaeotropical region. Four dispersal events happened from the Palaeotropical region to the Sino-Himalayan region at ca. 3.63 Ma, from Chinese Mainland to Taiwan at ca. 2.7 Ma, from the Sino-Himalayan and Palaeotropical to Sino-Japanese regions at ca. 1.22 Ma, and from the Palaeotropical to Sino-Japanese regions at ca. 0.5 Ma. During Quaternary, the global cooling climate caused the *H. pumilum* and *H. quasipinifolium* endemic in Taiwan and the restriction *H. omeiense* in the Omei Mountains of China. The temporal and spatial patterns of *Holcoglossum* shed light on the divergence and diversification of recently evolved epiphytic plants within East Asia.

## DATA AVAILABILITY STATEMENT

The datasets analyzed for this study can be found in the GenBank Database under the accession numbers listed in the **Supplementary Material**.

## AUTHOR CONTRIBUTIONS

XX and XJ conceived and designed the experiments. XX performed the experiments. XX, JZ, XL, PZ, and LZ analyzed the data. JZ, XX, XL, PZ, and LZ wrote the manuscript. XX, JZ, XL, PZ, LZ, and XJ revised the draft. All authors contributed to the article and approved the submitted version.

## FUNDING

This research was supported by the National Natural Science Foundation of China (31300181 and 31670212) and the National Natural Science Foundation of China–Yunnan Joint Fund Project (U1802242). XX is supported by the Youth Innovation Promotion Association Foundation of the Chinese Academy of Sciences.

## SUPPLEMENTARY MATERIAL

The Supplementary Material for this article can be found online at: https://www.frontiersin.org/articles/10.3389/fevo.2020.00245/full#supplementary-material

## REFERENCES

An, Z. S., Kutzbach, J. E., Prell, W. L., and Porter, W. L. (2001). Evolution of Asian monsoons and phased uplift of the himalaya-tibetan plateau since late miocene times. *Nature* 411, 62–66. doi: 10.1038/35075035

Boufford, D. (2014). Biodiversity hotspot: China's hengduan mountains. *Arnoldia* 72, 24–35.

CBOL Plant Working Group (2009). A DNA barcode for land plants. *Proc. Natl. Acad. Sci. U.S.A.* 106, 12794–12797.

Chase, M. K., Cameron, K. M., Freudenstein, J. V., Pridgeon, A. M., Salazar, G., van den Berg, C., et al. (2015). An updated classification of *Orchidaceae*. *Bot. J. Linn. Soc.* 177, 151–174. doi: 10.1111/boj.12234

Chen, F. B. (1992). Hengduan event: an important tectonic event of the late Cenozoic in Eastern Asia. *Mountain Res.* 10, 195–202.

Chen, F. B. (1996). Second discussion on the Hengduan movement. *Mountain Res.* 17, 14–22.

Chen, Y. S., Deng, T., Zhou, Z., and Sun, H. (2018). Is the East Asian flora ancient or not? *Natl. Sci. Rev.* 5, 920–932. doi: 10.1093/nsx/nwx156

Christenson, E. A. (1998). Two new species of *Holcoglossum* Schltr. (*Orchidaceae*: *Aeridinae*) from China. *Lindleyana* 13, 121–124.

Clements, R., Sodhi, N. S., Schilthuizen, M., and Ng, P. K. (2006). Limestone karsts of southeast Asia: imperiled arks of biodiverisity. *BioScience* 56, 733–742.

Demesure, B., Sodzi, N., and Pettit, R. J. (1995). A set of universal primers for amplification of polymorphic non-coding regions of mitochondrial and chloroplast DNA in plants. *Mol. Ecol.* 4, 129–131. doi: 10.1111/j.1365-294x.1995.tb00201.x

Drummond, A. J., and Rambaut, A. (2007). BEAST: bayesian evolutionary analysis by sampling trees. *BMC Evol. Biol.* 7:214. doi: 10.1186/1471-2148-7-214

Ebersbach, J., Schnitzler, J., Favre, A., and Muellner-Riehl, A. N. (2017). Evolutionary radiations in the species-rich mountain genus *Saxifraga* L. *BMC Evol. Biol.* 17:119. doi: 10.1186/s12862-017-0967-2

Fan, J., Qin, H. N., Li, D. Z., and Jin, X. H. (2009). Molecular phylogeny and biogeography of *Holcoglossum* (*Orchidaceae*: *Aeridinae*) based on nuclear ITS,

and chloroplast *trnL-F* and *matK*. *Taxon* 58, 849–861. doi: 10.1371/journal.pone.0024864

Farris, J. S., Källersjö, M., Kluge, A. G., and Bult, C. (1994). Testing significance of incongruence. *Cladistics* 10, 315–319. doi: 10.1006/clad.1994.1021

Goldman, D. H., Freudenstein, J. V., Kores, P. J., Molvray, M., Jarrell, D. C., Whitten, W. M., et al. (2001). Phylogenetics of Arethuseae (*Orchidaceae*) based on plastid *matK* and *rbcL* sequences. *Syst. Bot.* 2, 670–695. doi: 10.1043/0363-6445-26.3.670

Hall, T. A. (1999). BioEdit: a user-friendly biological sequence alignment editor and analysis program for Windows 95/98/NT. *Nucl. Acid. S.* 41, 95–98.

Hidayat, T., Weston, P. H., Yukawa, T., Ito, M., and Rice, R. (2012). Phylogeny of subtribe *Aeridinae* (*Orchidaceae*) inferred from DNA sequences data: advanced analyses including Australasian genera. *J. Teeknol.* 59, 87–95. doi: 10.11113/jt.v59.1591

Ho, S. Y. W. (2007). Calibrating molecular estimates of substitution rates and divergence times in bird. *J. Avian Biol.* 38, 409–414. doi: 10.1111/j.0908-8857.2007.04168.x

Hoorn, C., Mosbrugger, V., Mulch, A., and Antonelli, A. (2013). Biodiversity from mountain building. *Nat. Geosci.* 6, 154–154. doi: 10.1038/ngeo1742

Hsieh, C. F. (2002). Composition, endemism and phytogeographical affinities of the Taiwan flora. *Taiwannia* 47, 298–310.

Huang, S., Chiang, Y. C., Schaal, B. A., Chou, C. H., and Chiang, T. Y. (2001). Organelle DNA phylogeography of *Cycas taitungensis*, a relict species in Taiwan. *Mol. Ecol.* 10, 2669–2681. doi: 10.1046/j.0962-1083.2001.01395.x

Jian, H. Y., Tang, K. X., and Sun, H. (2015). Phylogeography of *Rosa soulieana* (*Rosaceae*) in the Hengduan mountains: refugia and 'melting' pots in the Quaternary climate oscillations. *Plant. Syst. Evol.* 301, 1819–1830. doi: 10.1007/s00606-015-1195-0

Jiang, D. C., Klaus, S., Zhang, Y. P., Hillis, D. M., and Li, J. T. (2019). Asymmetric biotic interchange across the Bering land bridge between Eurasia and North America. *Nat. Sci. Rev.* 6, 739–754. doi: 10.1093/nsr/nwz035

Jin, X. H. (2003). *Systematics on the Genus Holcgolossum Schltr. (Orchidaceae)*. Thesis, Chinese Academy of Sciences, Beijing.

Jin, X. H., and Wood, J. J. (2009). "Holcoglossum," in *Flora of China*, eds Z. Y. Wu and P. H. Raven (Beijing: Missouri Botanical Garden Press), 499–502.

Li, Z. H., Ma, X., Wang, D. Y., Li, Y. X., Wang, C. W., and Jin, X. H. (2019). Evolution of plastid genomes of *Holcoglossum* (*Orchidaceae*) with recent radiation. *BMC Plant Biol.* 19:63. doi: 10.1186/s12862-019-1384-5

Luo, D., Yue, J. P., Sun, W. G., Xu, B., Li, Z. M., Comes, H. P., et al. (2015). Evolutionary history of the subnival flora of the Himalaya-Hengduan mountains: first insights from comparative phylogeography of four perennial herbs. *J. Biogeogr.* 43, 31–43. doi: 10.1111/jbi.12610

Meng, H. H., Su, T., Gao, X. Y., Li, J., Jiang, X. L., Sun, H., et al. (2017). Warm-cold colonization: response of oaks to uplift of the Himalaya-Hengduan Mountains. *Mol. Ecol.* 26, 3276–3294. doi: 10.1111/mec.14092

Nie, Z. L., Wen, J., and Sun, H. (2007). Phylogeny and biogeography of *Sassafras* (Lauraceae) disjunct between eastern Asia and eastern North America. *Pl. Syst. Evol.* 267, 191–203. doi: 10.1007/s00606-007-0550-1

Posada, D. L., and Crandall, K. A. (1998). Modeltest: testing the model of DNA substitution. *Bioinformatics* 14, 817–818. doi: 10.1093/bioinformatics/14.9.817

Pridgeon, A. M., Cribb, P. J., Chase, M. W., and Rasmussen, F. N. (2014). *Genera Orchidacearum Epidendroideae, Part III*. Vol. 6. Oxford: Oxford University Press.

Qian, H., Ricklefs, R. E., and White, P. S. (2005). Beta diversity of angiosperms in temperate floras of eastern Asia and eastern North America. *Ecol. Lett.* 8, 15–22. doi: 10.1111/j.1461-0248.2004.00682.x

Qiu, Y. X., Fu, C. X., and Comes, H. P. (2011). Plant molecular phylogeography in China and adjacent regions: tracing the genetic imprints of Quaternary climate and environmental change in the world's most diverse temperate flora. *Mol. Phylogenet. Evol.* 59, 225–244. doi: 10.1016/j.ympev.2011.01.012

Rambaut, A., and Drummond, A. J. (2007). *Tracer v1.5 [online]*. Available online at: http://beast.bio.ed.ac.uk/Tracer (accessed November 30, 2009).

Ronquist, F., Teslenko, M., Van der Mark, P., Ayres, D. L., Darling, A., Höhna, S., et al. (2012). MrBayes 3.2: efficient Bayesian phylogenetic inference and model choice across a large model space. *Syst. Biol.* 61, 539–542. doi: 10.1093/sysbio/sys029

Schlechter, R. (1919). Orchideologiae Sino-Japonicae Prodromus. *Feddes. Repert. Spec. Nov. Regni. Veg. Beih.* 4:285.

Shaw, J., Lickey, E. B., Beck, J. T., Farmer, S. B., Liu, W. S., Miller, J., et al. (2005). The tortoise and the hare II: relative utility of 21 noncoding chloroplast DNA sequences for phylogenetic analysis. *Amer. J. Bot.* 92, 142–166. doi: 10.3732/ajb.92.1.142

Shaw, J., Lickey, E. B., Schilling, E. E., and Small, R. L. (2007). Comparison of whole chloroplast genome sequences to choose noncoding regions for phylogenetic studies in angiosperms: the tortoise and the hare III. *Amer. J. Bot.* 94, 275–288. doi: 10.3732/ajb.94.3.275

Shi, Y. F., Li, J. J., and Li, B. Y. (1998). *Uplift and Environmental Changes of Qinghai-Tibetan Plateau in the Late Cenozoic*. Guangzhou: Guangdong Science and Technology Press.

Sun, X. J., and Wang, P. X. (2005). How old is the Asian monsoon system? – Palaeobotanical records from China. *Palaeogeogr. Palaeoclimat. Palaeoecol.* 222, 181–222. doi: 10.1016/j.palaeo.2005.03.005

Swofford, D. L. (2003). *PAUP*: Phylogenetic Analysis Using Parsimony (* and related methods), Version 4.0b10*. Sunderland: Sinauer Associates.

Teng, L. S. (1990). Geotectonic evolution of late Cenozoic arc-continent collision in Taiwan. *Tectonophysics* 183, 57–76. doi: 10.1016/0040-1951(90)90188-e

Thompson, J. D., Gibson, T. J., Plewniak, F., Jeanmougin, F., and Higgins, D. G. (1997). The CLUSTAL_X windows interface: flexible strategies for multiple sequence alignment aided by quality analysis tools. *Nucleic. Acids. Res.* 25, 4876–4882. doi: 10.1093/nar/25.24.4876

Tiffney, B. H. (1985). Perspectives on the origin of the floristic similarity between eastern Asia and eastern North America. *J. Arnold Arbor.* 66, 73–94. doi: 10.5962/bhl.part.13179

Topik, H., Yukawa, T., and Ito, M. (2005). Molecular phylogenetics of subtribe *Aeridinae* (*Orchidaceae*): insights from plastid *matK* and nuclear ribosomal ITS sequences. *J. Plant. Res.* 118, 271–284. doi: 10.1007/s10265-005-0217-3

Wang, W. T. (1992). On some disjunction patterns and some migration routes found in the east Asiatic region. *Acta Phytotax. Sin.* 30, 1–24.

Wen, J. (1999). Evolutionary of eastern Asian and eastern North American disjunct distributions in flowering plants. *Annu. Rev. Ecol. Syst.* 30, 421–455. doi: 10.1146/annurev.ecolsys.30.1.421

Wu, Z. Y., and Wu, S. (1998). "A proposal for a new floristic kingdom (realm) the East Asiatic Kingdom, its delineation and characteristics," in *Floristic Characteristics and diversity of East Asian Plants*, eds A. L. Zhang and S. G. Wu (Beijing: Higher Education Press and Springer Verlag Press), 1–42.

Wu, Z. Y., Zhou, Z. K., Li, D. Z., Peng, H., and Sun, H. (2003). The areal types of the world families of seed plants. *Acta Bot. Yunnanica* 25, 245–257. doi: 10.1023/A:1022289509702

Xiang, K. L., Zhao, L., Erst, A. S., Yu, S. X., Jabbour, F., and Wang, W. (2017). A molecular phylogeny of *Dichocarpum* (*Ranunculaceae*): implications for eastern Asian biogeography. *Mol. Phylogenet. Evol.* 107, 594–604. doi: 10.1016/j.ympev.2016.12.026

Xiang, X. G., Li, D. Z., Jin, X. H., Hu, H., Zhou, H. L., Jin, W. T., et al. (2012). Monophyly or paraphyly-the taxonomy of *Holcoglossum* (*Aeridinae*: *Orchidaceae*). *PLoS One* 7:e52050. doi: 10.1371/journal.pone.0052050

Xiang, X. G., Mi, X. C., Zhou, H. L., Li, J. W., Chung, S. W., Li, D. Z., et al. (2016). Biogeographical diversification of mainland Asian *Dendrobium* (*Orchidaceae*) and its implications for the historical dynamics of evergreen broad-leaved forests. *J. Biogeogr.* 43, 1310–1323. doi: 10.1111/jbi.12726

Xiang, X. G., Xiang, K. L., Ortiz, R. D. C., Jabbour, F., and Wang, W. (2019). Intergrating palaeontological and molecular data uncovers multiple ancient and recent dispersals in the pantropical *Hamamelidaceae*. *J. Biogeogr.* 46, 2622–2631. doi: 10.1111/jbi.13690

Xing, Y., and Ree, R. H. (2017). Uplift-driven diversification in the Hengduan Mountains, a temperate biodiversity hotspot. *Proc. Natl. Acad. Sci. U.S.A.* 114, E3444–E3451. doi: 10.1073/pnas.161606311

Ye, X. Y., Ma, P. F., Yang, G. Q., Guo, C., Zhang, Y. X., Chen, Y. M., et al. (2019). Rapid diversification of alpine bamboos associated with the uplift of the Hengduan Mountains. *J. Biogeogr.* 46, 2678–2689. doi: 10.1111/jbi.13723

Ying, T. S. (2001). Species diversity and distribution pattern of seed plants in China. *Biodiver. Sci.* 9, 393–398. doi: 10.17520/biods.1999021

Ying, T. S., and Chen, M. L. (2011). *Plant Geography of China*. Shanghai: Shanghai Scientific & Technical Publishers, 290–342.

Yu, Y., Harris, A. J., Blair, C., and He, X. (2015). RASP (reconstruct ancestral state in phylogenies): a tool for historical biogeography. *Mol. Phylogenet. Evol.* 87, 46–49. doi: 10.1016/j.ympev.2015.03.008

Zachos, J. C., Dickens, G. R., and Zeebe, R. E. (2008). An early Cenozoic perspective on greenhouse warming and carbon-cycle dynamics. *Nature* 451, 279–283. doi: 10.1038/nature06588

Zeng, W. B. (1993). The passageway of the flora migration on both sides of the Taiwan strait in Pleistocene epoch. *Acta Bot. Yunnanica* 16, 107–110.

Zhang, J. Q., Meng, S. Y., Allen, G. A., Wen, J., and Rao, G. Y. (2014). Rapid radiation and dispersal out of the Qinghai-Tibetan Plateau of an alpine plant lineage *Rhodiola* (*Crassulaceae*). *Mol. Phylogenet. Evol.* 77, 147–158. doi: 10.1016/j.ympev.2014.04.013

Zhang, Q. Q., Ferguson, D. K., Mosbrugger, V., Wang, Y. F., and Li, C. S. (2012). Vegetation and climatic changes of SW China in response to the uplift of Tibetan Plateau. *Palaeogeogr. Palaeocl.* 363, 23–36. doi: 10.1016/j.palaeo.2012.08.009

Zheng, Z., Yuan, B. Y., and Petit-Maire, N. (1998). Paleoenvironments in China during the last glacial maximum and the Holocene optimum. *Episodes* 21, 152–158. doi: 10.18814/epiiugs/1998/v21i3/003

**Conflict of Interest:** The authors declare that the research was conducted in the absence of any commercial or financial relationships that could be construed as a potential conflict of interest.

frontiers in Ecology and Evolution

ORIGINAL RESEARCH
published: 31 July 2020
doi: 10.3389/fevo.2020.00244

# The Importance of Including Soil Properties When Disentangling the Drivers of Species Richness: The Case of the Alpine Genus *Saxifraga* L. in China

*Lian Liu[1], Ying Xu[1], Yigong Tang[1], Weihua Du[2], Chen Shao[1], Jianyong Wu[3], Lina Zhao[4], Lei Zhang[1], Jianquan Liu[1] and Xiaoting Xu[1]**

[1] Key Laboratory of Bio-Resource and Eco-Environment of Ministry of Education, College of Life Sciences, Sichuan University, Chengdu, China, [2] Chengdu Institute of Biology, Chinese Academy of Sciences, Chengdu, China, [3] Nanjing Institute of Environmental Sciences, Ministry of Environmental Protection, Nanjing, China, [4] State Key Laboratory of Systematic and Evolutionary Botany, Institute of Botany, Chinese Academy of Sciences, Beijing, China

OPEN ACCESS

**Edited by:**
*Meng Yao,*
*Peking University, China*

**Reviewed by:**
*Zhiheng Wang,*
*Peking University, China*
*Mauro Fois,*
*University of Cagliari, Italy*

***Correspondence:**
*Xiaoting Xu*
*xiaotingxu@scu.edu.cn;*
*xiaotingxu@pku.edu.cn*

**Specialty section:**
*This article was submitted to Biogeography and Macroecology, a section of the journal Frontiers in Ecology and Evolution*

**Received:** *04 February 2020*
**Accepted:** *06 July 2020*
**Published:** *31 July 2020*

**Citation:**
*Liu L, Xu Y, Tang Y, Du W, Shao C, Wu J, Zhao L, Zhang L, Liu J and Xu X (2020) The Importance of Including Soil Properties When Disentangling the Drivers of Species Richness: The Case of the Alpine Genus Saxifraga L. in China. Front. Ecol. Evol. 8:244. doi: 10.3389/fevo.2020.00244*

Despite the numerous studies on the large-scale patterns of species richness, the spatial variation and determinants of species richness for the alpine plants are still an outstanding question and critical to future biodiversity conservation. The genus *Saxifraga* is a typical alpine plant group with high species richness in the Himalaya-Hengduan Mountain (HHM) regions, China. We performed simple regression models and variance partitioning to assess the importance of different factors, especially soil-related ones, in driving *Saxifraga* richness patterns. The results showed that environmental energy, habitat heterogeneity, and soil heterogeneity together dominated the spatial variation of species richness. The coarse fragment volume (CRFVOL) of soil, elevation range, and soil heterogeneity are positively related to *Saxifraga* richness. Soil slightly outperforms habitat heterogeneity in predicting the spatial variation of *Saxifraga* species richness with an explanatory power of 39.3% and 36.6%, respectively. Environmental energy, such as the maximum temperature of the warmest quarter, is negatively correlated with species richness and explains 44.8% of spatial variation of *Saxifraga* richness. Multiple regression models, including three variables, each representing energy, soil, and habitat heterogeneity, can only explain 53.1% variation of species richness. Variance partitioning outscored 26% of the shared effects of the three variables, while the independent effect of each variable is less than 10%. These results indicated that the energy, soil, and habitat heterogeneity together are primary determinants of the spatial variation of *Saxifraga* species richness. However, there are probably other hidden factors predicting species richness variation due to the low explanatory power of the multiple regression models. Our study emphasizes the significance of soil properties in determining species

richness patterns in China, especially for alpine plant groups. The negative association of species richness with temperature suggests a potential threat of alpine biodiversity loss in HHM from future warming.

**Keywords: alpine, habitat heterogeneity, rock cliff, *Saxifraga*, soil fertility, soil texture, species richness, temperature**

## INTRODUCTION

The mechanisms of large-scale patterns of species richness are one of the central and controversial issues in macroecology and biogeography (Gaston et al., 1995; Brown et al., 2004). Previous studies in large-scale species richness patterns focus on the effects of contemporary climate, habitat heterogeneity, and evolutionary history and have proposed productivity hypothesis, water–energy dynamic hypothesis, and niche conservatism hypothesis (Rosenzweig, 1995; O'Brien et al., 2000; Currie and Francis, 2004; Wiens and Donoghue, 2004; Wiens and Graham, 2005). China, spanning from tropical rainforest to boreal coniferous forest, harbors over 30,000 vascular plants. Southwestern China, especially the Himalaya-Hengduan Mountain (HHM) regions, holds the highest species richness and an extraordinary diversity in alpine plants. It was regarded as one of the global biodiversity hotspots (Myers et al., 2000). Despite the numerous studies on the patterns and determinants of species richness in China (Wang et al., 2009, 2011a,b; Shrestha et al., 2018a), the large-scale patterns, and determinants of alpine plant richness are still poorly understood.

The evolution of mountains can influence species richness through speciation, immigration, and extinction (Antonelli et al., 2018), especially in the HHM regions (Sun et al., 2017). First of all, the orogenic process in HHM regions since the Neogene increased the topography complexity and habitat heterogeneity; henceforth, it encouraged allopatric speciation and provided different climatic niches to promote the coexistence of more species (Du et al., 2017; Rahbek et al., 2019b). Shrestha et al. (2018b) found that habitat heterogeneity will increase species diversification and then increase species richness for a plant genus *Rhododendron*. Secondly, climate heterogeneity increased with topography complexity, and the uplift of HHM facilitated species movement along the altitudinal gradient. Therefore, HHM can play a role in refugium when climate change events happened. Previous studies found that habitat heterogeneity is also the primary determinant of spatial variation of plant species richness in drylands (Liu et al., 2019), Tibetan Plateau (Mao et al., 2013), and European mountains (Svenning and Skov, 2004; Svenning et al., 2006). These results are probably caused by the refugia effects, subsequent speciation events, and limited dispersals for species in the mountains. However, contemporary climate (e.g., climate seasonality) and climate change since last glacial maximum (LGM) are the primary determinants for the spatial variation of species richness for the herbaceous family Gesneriaceae in China (Liu et al., 2017) and palms in Madagascar (Rakotoarinivo et al., 2013). Similar results were found for other biological groups, e.g., *tetrapods* in Asia mountain regions (Antonelli et al., 2018). Other studies also found that habitat heterogeneity has negative or insignificant effects on species richness (Cramer and Willig, 2005; Lundholm, 2009; Laanisto et al., 2013; Coyle and Hurlbert, 2016). Thus, the relative importance of habitat heterogeneity and other environmental factors on the spatial variation of species richness is still controversial and has rarely been studied for herbaceous plants at a large scale.

Recently, Rahbek et al. (2019a) suggested that orogeny can promote soil formation and then fodder the species richness by affecting plant physiology, vegetation composition, and primary productivity. Soil attributes, e.g., soil heterogeneity, soil texture and structure, and soil fertility, varied with the uplift of mountains and the erosion of bedrocks (Antonelli et al., 2018). Soil heterogeneity usually positively correlates with the elevation range in mountain regions suggesting a high niche diversity (Stein et al., 2014; Antonelli et al., 2018). In mountain regions of Asia and Europe, soil heterogeneity even explains more on species richness than elevation range (Antonelli et al., 2018). The high content of cliff, shallow depth, and relative infertile are unique characters of mountain soil due to the limited biological activities, soil genesis, and evolution under low temperatures (Romeo et al., 2015). Where the slope becomes steeper, the soil becomes thinner and infertile because precipitation or surface runoff washes away topsoil easily in the mountains. Rising temperatures in alpine regions will promote soil moisture transpiration, result in soil water stress, and thus affect species survival (Zhu et al., 2016). Despite the harsh and diversified environment, alpine plant species have adapted well in the mountain soils and even diversified faster than other regions (Hughes and Atchison, 2015). However, soil effect on the spatial variation of species richness in mountain regions, especially the HHM, remains an outstanding question.

*Saxifraga* L. (Saxifragaceae) is a smallish herb, most of which are typical alpine plants and endemic to the HHM and adjacent regions (Yang et al., 2013; Ebersbach et al., 2017a; Rawat et al., 2019). Phylogenetic studies suggested that *Saxifraga* radiated rapidly in montane and alpine habitats. Along with the persistent uplift of mountains, *Saxifraga* species evolved two critical innovations of cushion life form and lime-secreting hydathodes to adapt to the colder and colder environment and exhibited a high diversification rate in the habitat of rock cliffs (de Casas et al., 2016; Ebersbach et al., 2017a). Meanwhile, sky islands and climate oscillation during the Quaternary period probably contributed to the high species diversity of *Saxifraga* through the allopatric speciation process and refugium effects in HHM as well (Ebersbach et al., 2017b). Therefore, the diversification of *Saxifraga* is connected tightly with the uplift of HHM, and the effects of the topographic factors and soil properties

(e.g., the rock cliff content of the soil) are expected to be the primary determinants on the present species richness patterns.

Here, we evaluated the relative importance of habitat heterogeneity, soil factors, climate change since the LGM, and contemporary climate on the spatial variation of *Saxifraga* species richness based on county-level species distribution data in China. We specifically intend to comprehensively assess the effects of different soil properties on the species richness patterns for alpine plants. We performed an evaluation quantitatively to partition the effects of habitat heterogeneity, soil properties, climate change, and contemporary climate on *Saxifraga* richness patterns across China.

# MATERIALS AND METHODS

## Species Distribution Data

The distribution of *Saxifraga* at county level in China was compiled from published flora and regional and local plant checklists, peer-reviewed articles, online databases, and herbarium specimens (**Supplementary Appendix S1**). Due to the broad area of several counties in northwest China, we divided the 12 large counties into 24 subcounties to reduce the effect of area on species richness (Wang et al., 2011a). The final geographic database based on county boundaries classified the whole of China into 2411 geographic units. We standardized and georeferenced the recorded geographical names from different literature following Xue (2014) and the global geographical names database (GeoNames[1]). Then, we assigned species distribution records to these subcounties according to data availability. All species names were standardized according to the Flora of China[2]. We merged intraspecific taxa to species level and excluded hybrids. In total, our database included 3532 distribution records for 224 species from 994 geographic units with an average area of 5648 $km^2 \pm 12{,}250$ $km^2$.

For each geographic unit, the number of species was counted, and the area was calculated in ArcGIS (version 10.4.1) using the Albers equal-area conic projection. The area has low explanatory power (*adjusted*-$R^2$ = 0.09, modified *t*-test $p = 0.013$) on the spatial variation of *Saxifraga* species richness (**Supplementary Figure S1** in **Supplementary Appendix S2**). Therefore, we exclude the area from subsequent analysis.

## Environmental Variables

To estimate the relative importance of habitat heterogeneity, soil, contemporary climate, and change since LGM on *Saxifraga* species richness, we first included 54 potential environmental variables in our preliminary analysis (**Supplementary Table S1** in **Supplementary Appendix S3**).

The contemporary climate factors include all 19 bioclimatic variables derived from monthly temperature and precipitation, moisture index (*Im*), aridity index (AI), potential evapotranspiration (PET), annual actual evapotranspiration (AET), and water deficit (WD) in our study. We classified all variables into environmental energy including temperature-related variables, water availability including precipitation-related variables, *Im* and AET, climate seasonality including temperature seasonality (TSN), and precipitation seasonality (PSN). The 19 bioclimatic variables were downloaded from CHELSA[3] at a spatial resolution of 30 arc seconds. *Im* was calculated following Fang and Yoda (1990) using monthly temperature and monthly precipitation obtained from WorldClim[4] at a spatial resolution of 2.5 arc minutes. AI, PET, and AET with the resolution of 30 arc seconds were downloaded from the Consortium of International Agricultural Research Centers consortium for spatial information[5]. WD was calculated as the difference between PET and AET. For each climatic variable, we estimated the value of each geographic unit by averaging all grid cells within it.

Habitat heterogeneity was measured by elevation range (ELER), mean annual temperature range (MATR), and mean annual precipitation range (MAPR) within each geographic unit. ELER, MATR, and MAPR were calculated as the difference between the maximum and minimum values across all grids within each geographic unit, respectively. ELER was used to represent the topographic relief while MATR and MAPR were used to represent the climate heterogeneity. Elevation with 2.5 arc minutes of resolution was also downloaded from WorldClim[4].

We included 25 soil variables in our preliminary analysis and classified them into soil texture, soil fertility, and soil heterogeneity (**Supplementary Table S1** in **Supplementary Appendix S3**). Soil texture included six variables and represented the fractions of each soil separate, e.g., the coarse fragments volume, silt, sand, and clay content of the soil. Bulk density and depth to the bedrock were also classified into soil texture. Soil fertility included six variables related to nutrient availability of soil, including available water capacity (AWCh3), cation exchange capacity (CECSOL), organic carbon density (OCDENS), organic carbon stock (OCSTHA), organic carbon content (ORCDRC), and pH of the soil. Soil heterogeneity was calculated as the standard deviation of all grid cells in each geographic unit for each of all 12 soil variables. The number of soil types within each geographic unit was counted as one factor of soil heterogeneity.

We downloaded soil variables at four depths (0, 5, 15, and 30 cm) from the global soil geographic database (SoilGrids[6]) at a spatial resolution of 1 km (Hengl et al., 2014, 2017). The mean value of four soil layers was estimated (Soil_mean) and applied in our study. Depth to bedrock (BDRICM), soil organic carbon stock (OCSTHA), and soil types variables (TAXNWRB) have no soil layer data.

Climate change since the LGM was represented by temperature anomaly (ANOM MAT, °C) and precipitation anomaly (ANOM MAP, mm). ANOM MAT and ANOM MAP were calculated as the absolute values of the contemporary minus the LGM mean annual temperature and mean annual

[1]http://www.geonames.org/

[2]http://www.efloras.org//

[3]http://chelsa-climate.org/, version 1.2.

[4]www.worldclim.org, version 1.4.

[5]http://www.cgiar-csi.org/

[6]https://soilgrids.org/, access date: April, 2018.

**TABLE 1 |** Climate and soil variables and their abbreviations used in the analyses.

| Groups | Abbreviations | Environmental variables |
|---|---|---|
| Energy | MTWQ | Mean temperature of the warmest quarter (°C) |
| Water | PDM | Precipitation of driest month (mm) |
| Habitat heterogeneity | ELER | Elevation range (m) |
| Soil texture | CRFVOL | Coarse fragment volume (%) |
| Soil fertility | CECSOL | Cation exchange capacity (cmolc/kg) |
| Soil heterogeneity | STD_BDRICM | Standardized deviation of depth to bedrock (R horizon) up to 200 cm |

precipitation, respectively. To account for the uncertainty in past climate simulations, the mean annual temperature and precipitation of LGM reconstructed based on the Community Earth System Model (CCSM4) and the Model for Interdisciplinary Research on Climate Earth System Model (MIROC-ESM) were used in our analysis. These data were downloaded from WorldClim[4] at 2.5 arc minutes of spatial resolution.

We used zonal statistics in ArcGIS (version 10.4.1) to calculate the mean, range, and standard deviation values of each variable within each geographical unit. The spatial variation of each soil factor was mapped using ArcMap in ArcGIS (version 10.4.1). The latitudinal and longitudinal trends of each soil factor were plotted and estimated by "lowess" function, and Spearman's correlations among each two variables were calculated by "cor" function in R with the "stats" package.

## Statistical Analyses

We first used linear regression models (LM) to assess the effect of each potential factor on spatial variation of *Saxifraga* richness. Species richness was natural logarithm transformed [log (species richness)] in all statistical analyses. Owing to the high spatial autocorrelation of the spatial patterns of species richness, which can inflate the type I error, we performed a modified *t*-test (Dutilleul et al., 1993) to estimate the significance level of all regression models. Then, for each environmental group, we only selected one best variable explaining the highest explanatory power in LM and significant in the modified *t*-test (**Table 1**). Due to the low explanatory power and insignificant effects (modified *t*-test $p > 0.1$) of the climate change since LGM and climate seasonality on spatial variation of *Saxifraga* species richness, we removed variables from these two groups in the following analysis (**Supplementary Table S2** in **Supplementary Appendix S3**).

To compare the relative importance of each environmental group on the spatial variation of species richness, we first built multiple regression models of species richness against the selected six variables. Because of the collinearity among these six factors (**Supplementary Table S3** in **Supplementary Appendix S3**), we applied a hierarchical partitioning method to decompose the variation in species richness into the independent effect for each variable and conjoint effects with all other variables on species richness patterns (Chevan and Sutherland, 1991; Nally, 1996). Hierarchical multivariate regression was set in hierarchical partitioning considering all possible models for the response variable and predictors. By the incorporation of a given variable or combination of variables, hierarchical partitioning involves the calculation of the increased goodness of fit in models, and these are averaged over all combinations to provide measures of the effects of independent variables and their combinations (Chevan and Sutherland, 1991; Mac Nally and Walsh, 2004). For the three variables with the highest independent effect identified by hierarchical partitioning, we performed multiple regression and variance partition to estimate the independent effect of each variable and shared effects among variables.

We performed LM analysis using the "lm" function in the R package "stats" (Chambers and Hastie, 1992), modified *t*-tests using the R package "SpatialPack" (Dutilleul et al., 1993), hierarchical partitioning using the R package "hier.part" (Chevan and Sutherland, 1991; Mac Nally and Walsh, 2004), and variance partitioning using the R package "vegan" (Peres-Neto et al., 2006).

# RESULTS

The species richness patterns of *Saxifraga* were highly consistent with the topographical structure of China with a high striking species richness in the HHM regions (**Figure 1**). The Qinghai-Tibetan Plateau also harbors high species richness, whereas *Saxifraga* species were rarely distributed in the eastern part of China. Soil properties also showed clear spatial patterns and highly correlated with climate and elevation (**Supplementary Table S3** in **Supplementary Appendix S3**).

Soil properties showed distinct geographical patterns and are closely related to temperature and elevation range (**Figure 2**, **Supplementary Figure S2** in **Supplementary Appendix S2**, and **Supplementary Table S3** in **Supplementary Appendix S3**). CRFVOL and a standard deviation of depth to bedrock (STD_BDRICM) increase from east to west and are high in the Hengduan mountains and Qinghai-Tibet Plateau. Cation exchange capacity (CECSOL) is high in Hengduan Mountains; Daxinganling, Xiaoxinganling, and Changbai Mountains; Altai Mountains, and Tianshan Mountains and low in lowland regions (**Figure 2**). All these three variables were positively correlated with elevation range and negatively correlated with mean temperature in the warmest quarter (**Figure 2** and **Supplementary Table S3** in **Supplementary Appendix S3**). Mean temperature in the warmest quarter showed the highest association with CRFVOL, followed by the STD_BDRICM and CECSOL with Spearman's ρ of −0.645, −0.6, and −0.57, respectively. The elevation range showed the highest correlation with a STD_BDRICM, followed by CRFVOL and CECSOL with Spearman's ρ of 0.809, 0.688, and 0.39, respectively.

As expected, results of simple linear regression analysis showed that CRFVOL representing soil texture and elevation

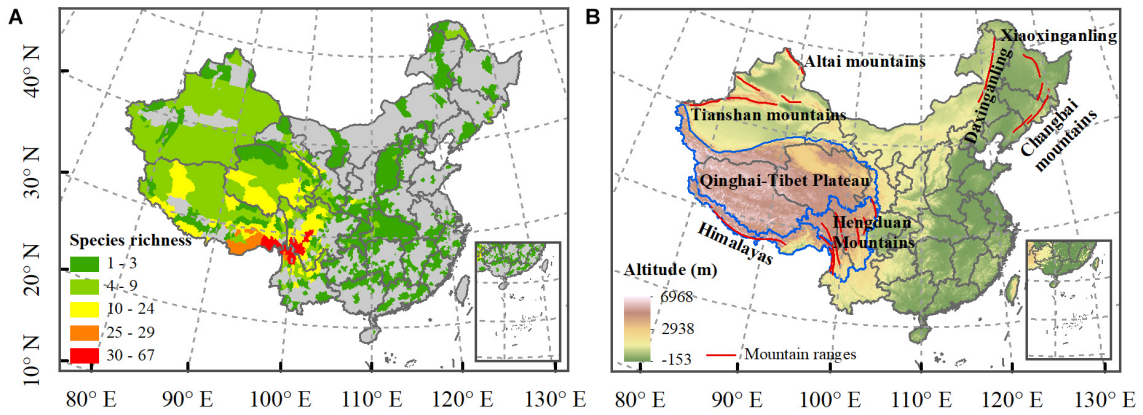


**FIGURE 1 |** Spatial patterns of *Saxifraga* L. species richness in China **(A)**. The maps of the Hengduan Mountains region, Himalayas region, QTP, and main mountain ranges **(B)**.

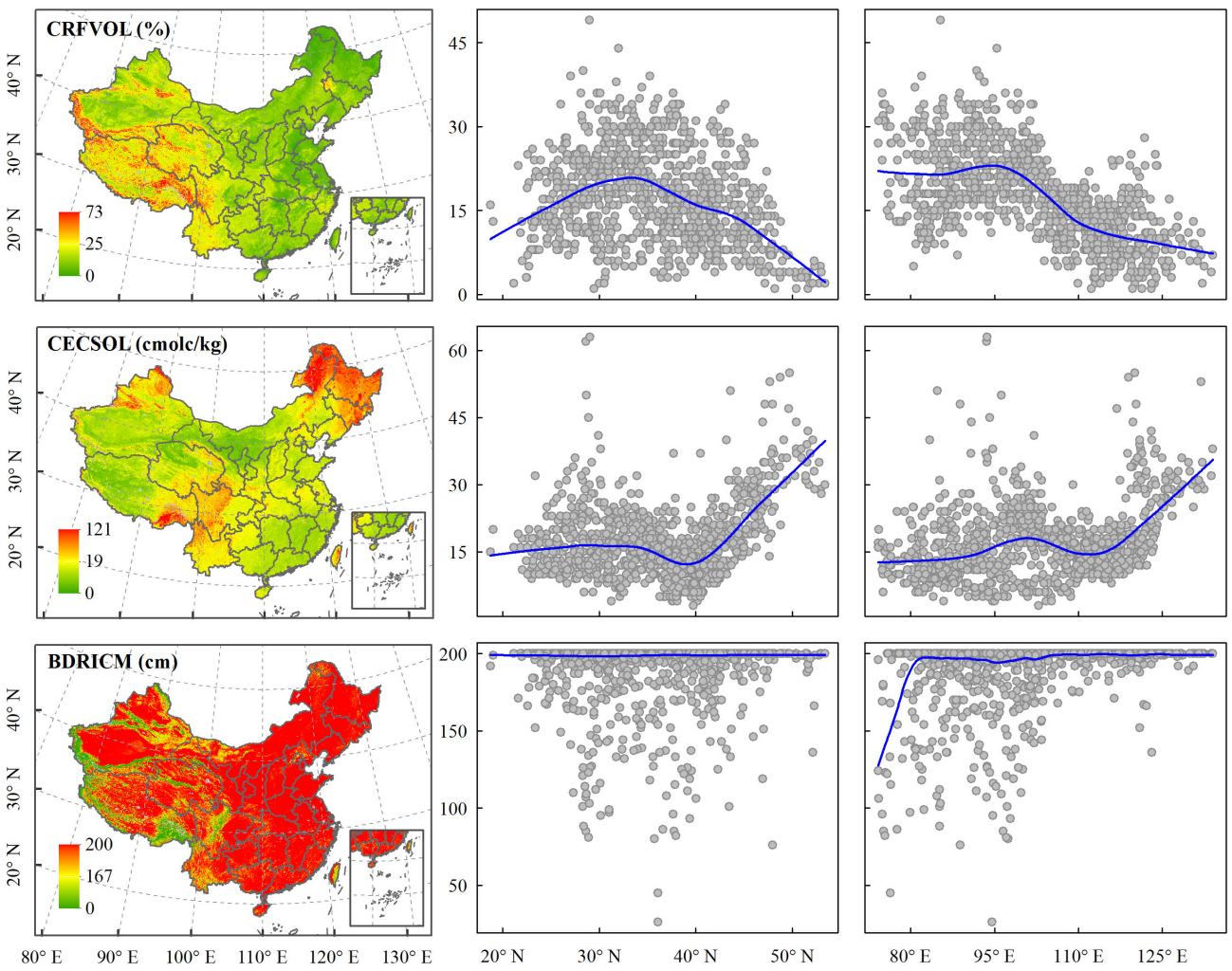


**FIGURE 2 |** Spatial patterns, latitudinal and longitudinal gradients of the coarse fragment volume (CRFVOL), cation exchange capacity (CECSOL), and depth to the bedrock (BDRICM) at the resolution of 1 km. The scatter plot was drawn based on 992 randomly sampled points.

**TABLE 2 |** The regression coefficients, *p*-values, and *adjusted-$R^2$* of two regression models based on the variables which were used by the hierarchical partitioning analyses and the variance partition analyses, respectively.

| Predictors | Coefficients | *P* | *Adjusted-$R^2$* | AIC |
|---|---|---|---|---|
| Intercept | 0.157 (0.683) | 0.436 | | |
| MTWQ | −0.005 (−0.293) | $<10^{-5}$ | | |
| PDM | 0.001 (0.024) | 0.391 | | |
| ELER | $<10^{-3}$ (0.264) | $<10^{-5}$ | 0.567 | 1843.487 |
| CRFVOL | 0.035 (0.202) | $<10^{-5}$ | | |
| CECSOL | 0.039 (0.199) | $<10^{-5}$ | | |
| STD_BDRICM | −0.007 (−0.077) | 0.053 | | |
| Intercept | 1.033 (0.683) | $<10^{-5}$ | | |
| MTWQ | −0.005 (−0.344) | $<10^{-5}$ | 0.531 | 1919.954 |
| ELER | $<10^{-3}$ (0.230) | $<10^{-5}$ | | |
| CRFVOL | 0.034 (0.195) | $<10^{-5}$ | | |

*Numbers in parentheses are standard coefficients of respective variables.*

range representing habitat heterogeneity are positively related and explained 39.3% and 36.6% of the spatial variation of species richness, respectively. The soil heterogeneity, represented by the standardized deviation of depth to bedrock, and the soil fertility, represented by CECSOL, are positively related to the spatial variations of the species richness with the explanatory power of 31.7% and 23.9%, respectively (**Figure 2** and **Supplementary Table S2** in Appendix S3). Out of expectation, the environmental energy represented by the mean temperature of the warmest quarter showed the highest but negative effect (*adjusted-$R^2$* = 44.75%, modified *t*-test $p < 0.001$) on the spatial variation of species richness among all examined variables. Environmental water availability is also negatively correlated with species richness but with a relatively low explanatory power (the best variable PDM *adjusted-$R^2$* = 18%, modified *t*-test $p < 0.1$).

The multiple regression model, including six variables, can explain 56.7% of species richness variation (**Table 2**). Hierarchical partitioning analyses showed consistent results with simple LM analyses. MTWQ had the highest independent and conjoint effects on species richness followed by CRFVOL and ELER, representing soil texture and habitat heterogeneity, respectively (**Figure 3**). Despite relatively low independent effects (<5% of the total $R^2$), we found a high conjoint effect of soil heterogeneity (>10% of the total $R^2$) on species richness (**Figure 4**).

The multiple regression model, including three variables with the highest independent effect, has almost equal predictive power with the six variable multiple regression model (*adjusted-$R^2$* = 53.1%) (**Table 2**). The results of variance partition analysis showed that the conjoint effects of energy, habitat heterogeneity, and soil texture on *Saxifraga* species richness were 26% and higher than the independent explanatory power of each variable. The independent effect of MTWQ is the highest but only explains 6% of the species richness variation. The independent effects of elevation range and soil texture were almost equally low to 3% and 2%, respectively. The conjoint effects of energy and soil texture were 8% and higher than that of soil texture and elevation range and that of energy and elevation range (**Figure 5**).

# DISCUSSION

Our results supported the role of environmental energy, soil texture, and habitat heterogeneity in determining the species richness patterns of the alpine genus *Saxifraga* in China. With a particular high species richness in HHM regions, the habitat heterogeneity accounted for 36.6% of the species richness variation, which is lower than the explanatory power of the mean temperature of warmest quarter (MTWQ, *adjusted-$R^2$* = 44.75%) and the coarse fragments volume of soil (CRFVOL, *adjusted-$R^2$* = 39.3%). Results of variance partitioning confirm that environmental energy, soil, and habitat heterogeneity are the primary determinants of the *Saxifraga* species richness patterns. We further established a negative relationship of energy–alpine species richness and an insignificant relationship of water–species richness, which suggested considerable discrepancy of climate impacts on species richness between alpine herbs and woody plants/lowland regions at large scale (Wang et al., 2009, 2018; Liu et al., 2017). In comparison with other landforms, orogenic dynamics promoted habitat heterogeneity and fostered the distinctive soil properties and novel habitats in mountain regions by surface uplift, runoff, and erosions, thereby resulting in the increase in diversification rate and exceptionally high species richness (Rahbek et al., 2019a).

## Habitat Heterogeneity Effects on Alpine Species Richness

Habitat heterogeneity is widely accepted as a primary driver of the high species richness in mountain regions by increasing speciation and decreasing extinction and niche space for species coexistence (Stein et al., 2014; Favre et al., 2016; Ebersbach et al., 2017b). During the uplift of the mountains, habitat heterogeneity increases with the increase in elevation, which raised a large number of sky islands and modified the species dispersal barriers (Hughes and Eastwood, 2006; Ebersbach et al., 2017b). The unique north–south orientation of the Hengduan Mountain and its parallel valleys form numerous and complex ecological niches, which promote the exchange of species in the north–south direction but also strengthen the isolation of species in the east–west direction (Sun et al., 2017). These processes together promoted the allopatric speciation rate in mountain regions. Meanwhile, the increasing elevation range and diversified microclimates and habitats during the mountain building process result in many refugia, which can buffer the species extinction rate when global climate oscillations happened (Qian and Ricklefs, 2000; Ebersbach et al., 2017b). The buffering effect of habitat heterogeneity probably is one reason for the insignificant impact of the historical climate change on species richness in Asia (Wang et al., 2011b; Xu et al., 2019). Furthermore, the increased habitat heterogeneity also offers numerous empty niches for species to occupy and increases the number of coexistence species (Stein et al., 2014). Albeit the previous findings of an insignificant topographic relief effect on species richness in High Asia (Antonelli et al., 2018), our study confirmed the importance of habitat heterogeneity in giving rise to

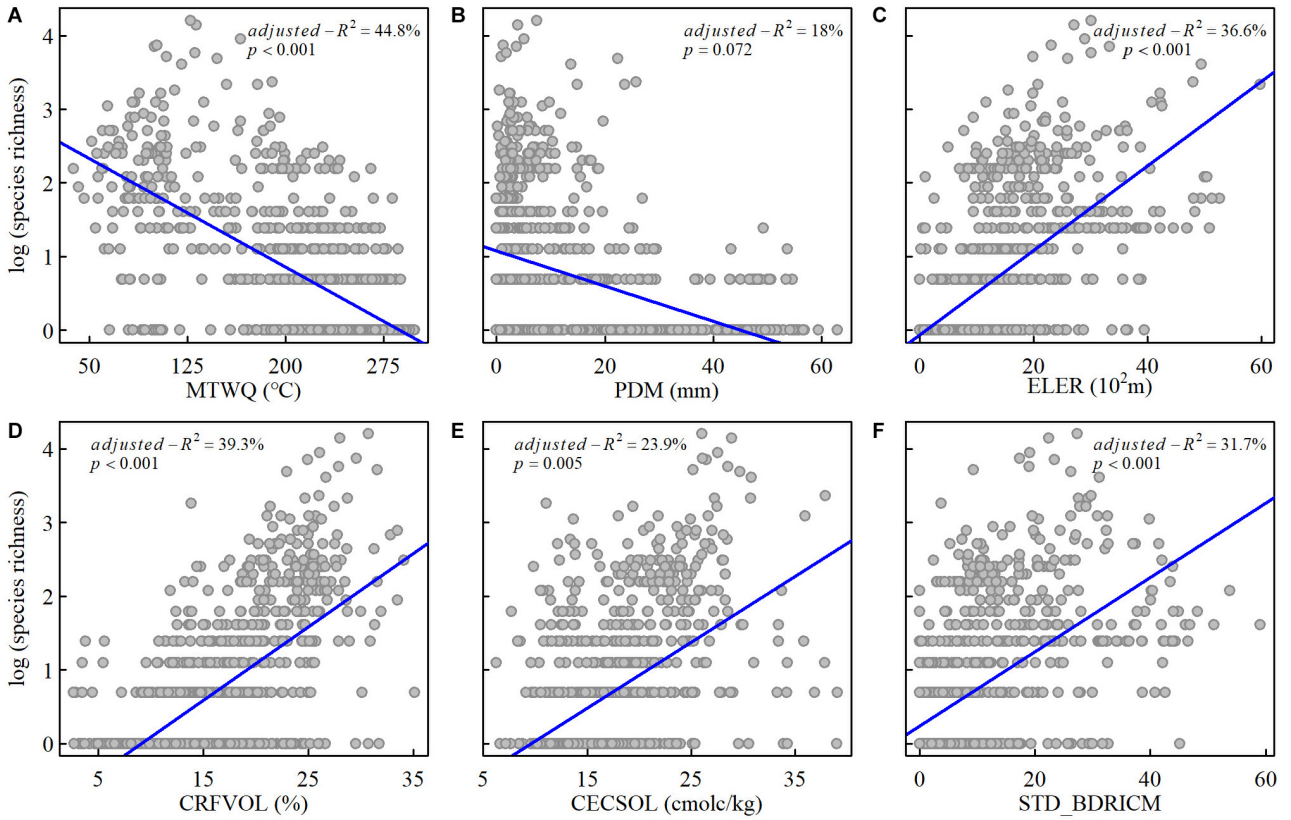


**FIGURE 3 |** Relationships between the log-transformed species richness of *Saxifraga* L. in China and mean temperature of warmest quarter (MTWQ) **(A)**, precipitation of driest month (PDM) **(B)**, elevation range (ELER) **(C)**, coarse fragment volume (CRFVOL) **(D)**, cation exchange capacity (CECSOL) **(E)**, and standard deviation of depth to the bedrock (STD_BDRICM) **(F)**, respectively.

the high diversity in the HHM regions in southwest China, as well as the previous researches for other plant groups (Shrestha et al., 2018a,b).

## Soil Effects on Large-Scale Alpine Species Richness

However, in contrast to the well-acknowledged significance of habitat heterogeneity, the striking effects of soil on the high species richness mostly focused on restricted areas or at a local scale (Kutiel and Danin, 1987; Harrison and Rajakaruna, 2011; Escudero et al., 2015; Abdelaal et al., 2019; Kontopanou and Panitsa, 2020). Most studies suggested that soil can take effect on plant species richness at the local scale because of the direct impact on water and nutrient supplies (Huston, 1980; Kammer et al., 2013; Dingaan et al., 2017). The large-scale variation of soil properties might not be able to capture the real effects of soil on plants. However, our results showed that soil effects on species richness at the large scale are almost equal to climate and habitat heterogeneity.

On the one hand, soils derived from the mafic and ultramafic rocks harbor high plant diversity by the radiation of a lineage specialized for such edaphic niche (Rahbek et al., 2019a). For example, serpentine habitat specialists are remarkably rich in California and can adapt to low levels of phosphorus and high content of magnesium. Recent studies have found a high speciation rate and species richness of the Gesneriaceae in the karst limestone mountainous areas in southern China (Liu et al., 2017). Consistent with the above studies, the *Saxifraga* species are well adapted to rock crevices and showed a higher diversification rate in rock cliffs than in other habitats (de Casas et al., 2016; Ebersbach et al., 2017b). These probably are reasons for the high explanatory power of CRFVOL of soil on species richness in our study.

On the other hand, soil heterogeneity, as one part of habitat heterogeneity, showed consistent positive impacts on species richness in mountain regions by creating the novel habitat and ecological niche (Antonelli et al., 2018). Previous studies found that the physical structure and chemical composition of the cliffs, as well as their relation position, provide more habitats to promote plants' coexistence (Cooper, 1997). Consistent with these studies, our result also showed that all soil heterogeneity factors are positively correlated with *Saxifraga* species richness. In our study, all soil heterogeneity factors are positively correlated with elevation range (Spearman's $p$ range from 0.34 to 0.8), suggesting that the uplift of mountains in the HHM regions increased both the elevation range and soil heterogeneity, thereby contributing to the increase of species richness.

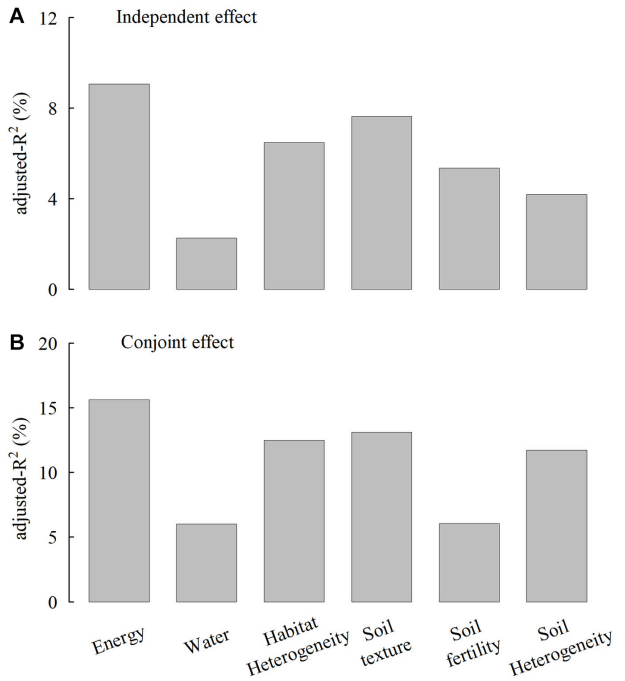


**FIGURE 4 |** Comparisons of the independent effects **(A)** and conjunct effects **(B)** (*adjusted-*$R^2$, %, given as the percentage of the total explained variance) of six environmental factor groups on the species richness. The *adjusted-*$R^2$ was estimated based on the hierarchical partitioning method. Energy, water, habitat heterogeneity, soil texture, soil fertility, and soil heterogeneity were represented by the mean temperature of the warmest quarter (MTWQ), precipitation of the driest month (PDM), elevation range (ELER), coarse fragment volume (CRFVOL), cation exchange capacity (CECSOL), and the standard deviation of depth to bedrock (STD_BDRICM).

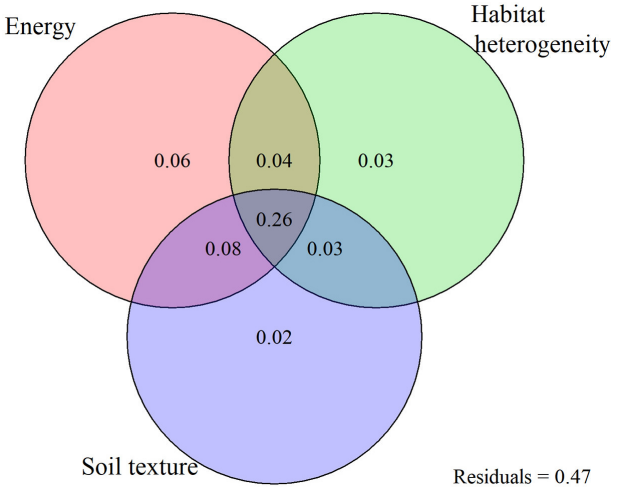


**FIGURE 5 |** The unique and shared variance of environmental energy, habitat heterogeneity, and soil texture to *Saxifraga* species richness using the variance partitioning analysis. The proportions of explained variances and the unexplained variance add up to one. Energy, habitat heterogeneity, and soil texture were represented by the mean temperature of the warmest quarter (WTWQ), elevation range (ELER), and coarse fragment volume (CRFVOL), respectively.

Finally, the significant correlations between soil properties, climate, and elevation range and the high conjoint effect on species richness are probably due to the direct impact of climate and topographic structure on soil development. These also suggested that climate and elevation range can indirectly influence species richness through soils. Although Laliberte et al. (2013) proposed a framework by using the structural equation modeling to explore the soil effects on latitudinal species richness patterns, further study is still needed.

## The Negative Effect of Temperature on Alpine Species Richness

Although climate shapes the main patterns of diversity in mountain regions all over the world (Rahbek et al., 2019b), the negative temperature–richness climate has been rarely established and may be the outcome of the evolutionary history of this alpine genus and available cold habitat with the uplift of Hengduan Mountains. Despite the climate-based hypothesis supporting a positive association between species richness with environmental energy (Currie, 1991), the temperature–richness relationship probably depends on the evolutionary history of the specific groups based on niche conservatism hypothesis (Wiens and Donoghue, 2004; Wiens and Graham, 2005; Xu et al., 2013, 2019). Niche conservatism suggested that the positive associations of energy and species richness for all flowering plants are the result of their warm ancestral niche. Due to the tendency of the descendants to occupy a similar niche with their ancestors, most flowering plants cannot adapt to the cold environment (Wiens and Donoghue, 2004). Research on Asian oaks also found that a striking difference in temperature impacts on species richness between subtropical and temperate lineage supported niche conservatism hypothesis (Xu et al., 2013). The phylogenetic study found that *Saxifraga* originated in a temperate habitat around 74 Mya, e.g., the ancestor of Saxifragaceae and Grossulariaceae had occupied temperate habitat since 81 Mya. With the continuous cooling since Late Paleocene, *Saxifraga* colonized Europe and the QTP region as global temperatures declines in the Late Eocene and diversified rapidly since Mid-Miocene when continuous climatic cooling and oscillation occurred (Ebersbach et al., 2017a). During these dispersal and colonization processes, niche conservatism probably promoted speciation of *Saxifraga* by geographic isolation and accumulated high species richness in a cold environment, which is also supported by theoretical simulations (Hua and Wiens, 2013).

Except for niche conservatism, niche divergence might also contribute to a negative richness–temperature relationship. Based on macroevolution analysis, niche lability of most clades in Saxifragales has increased since ca. 5 Mya when climatic cooling and oscillations occurred and showed to be greater in the clade originated in cooler environment. Consequently, the *Saxifraga* with a cold ancestral habitat developed cold-associated phenotypic traits and adapted to the freezing climate with global cooling through niche divergence. For example, the trichomes of *Saxifraga* may be helpful in tolerance to drought,

high UV radiations, and low temperature at high altitudes (Rawat et al., 2019). *Saxifraga cernua* growing at 10°C has a higher dark respiration rate than 20°C (Mcnulty and Cummins, 1987). Thereby, the deep time niche conservatism and recent niche divergence to freezing climate together may contribute to the negative richness–temperature relationship.

## CONCLUSION

In summary, our results suggest that environmental energy, soil, and habitat heterogeneity all acted as the essential determinants for the richness patterns of *Saxifraga* L. in China. Our results might be generalized to other alpine plant groups due to their similar evolutionary history and environmental adaptations. Our study emphasizes the significance of soil in determining the high alpine species richness, which even outperformed the habitat heterogeneity. The negative species richness–temperature relationship might be the result of the cold adaptation of alpine plants, which suggests that climate warming might threaten the species loss of alpine diversity.

## DATA AVAILABILITY STATEMENT

The datasets generated for this study are available on request to the corresponding author.

## AUTHOR CONTRIBUTIONS

XX conceived and designed the study. LL, WD, YT, LiZ, LeZ, JW, YX, and CS compiled the data. LL, YX, YT, and CS analyzed the data. XX and LL led the writing. All authors contributed to the writing and agreed to be accountable for all aspects of the work.

## FUNDING

This study was supported by the National Natural Science Foundation of China (31770566), the National Key Research Development Program of China (2017YFC0505200), the Fundamental Research Funds for the Central Universities of China (YJ201721), and Biodiversity Survey, Observation and Assessment Program of Ministry of Ecology and Environment of China.

## ACKNOWLEDGMENTS

We thank Professor Kangshan Mao from Sichuan University for valuable feedback and discussion.

## SUPPLEMENTARY MATERIAL

The Supplementary Material for this article can be found online at: https://www.frontiersin.org/articles/10.3389/fevo.2020.00244/full#supplementary-material

**APPENDIX S1 |** Data sources for the compilation of *Saxifraga* L. distributions.

**APPENDIX S2 |** Supplementary figures.

**APPENDIX S3 |** Supplementary tables.

## REFERENCES

Abdelaal, M., Ahmed, D., Fois, M., Fenu, G., and Bacchetta, G. (2019). Floristic patterns and ecological drivers of sand dune ecosystem along the Mediterranean coast of Egypt. *Arid Land Res. Manage.* 33, 388–411. doi: 10.1080/15324982.2018.1564147

Antonelli, A., Kissling, W. D., Flantua, S. G., Bermúdez, M. A., Mulch, A., Muellner-Riehl, A. N., et al. (2018). Geological and climatic influences on mountain biodiversity. *Nat. Geosci.* 11, 718–725. doi: 10.1038/s41561-018-0236-z

Brown, J. H., Gillooly, J. F., Allen, A. P., Savage, V. M., and West, G. B. (2004). Toward a metabolic theory of ecology. *Ecology* 85, 1771–1789. doi: 10.1890/03-9000

Chambers, J., and Hastie, T. (1992). "Linear models," in *Statistical Models in S*, (Pacific Grove, CA: Wadsworth & Brooks/Cole).

Chevan, A., and Sutherland, M. (1991). Hierarchical partitioning. *Am. Stat.* 45, 90–96.

Cooper, A. (1997). Plant species coexistence in cliff habitats. *J. Biogeogr.* 24, 483–494. doi: 10.1111/j.1365-2699.1997.00128.x

Coyle, J. R., and Hurlbert, A. H. (2016). Environmental optimality, not heterogeneity, drives regional and local species richness in lichen epiphytes. *Glob. Ecol. Biogeogr.* 25, 406–417. doi: 10.1111/geb.12420

Cramer, M. J., and Willig, M. R. (2005). Habitat heterogeneity, species diversity and null models. *Oikos* 108, 209–218. doi: 10.1111/j.0030-1299.2005.12944.x

Currie, D. J. (1991). Energy and large-scale patterns of animal-and plant-species richness. *Am. Nat.* 137, 27–49. doi: 10.1086/285144

Currie, D. J., and Francis, A. P. (2004). Regional versus climatic effect on taxon richness in angiosperms: reply to Qian and Ricklefs. *Am. Nat.* 163, 780–785. doi: 10.1086/383596

de Casas, R. R., Mort, M. E., and Soltis, D. E. (2016). The influence of habitat on the evolution of plants: a case study across Saxifragales. *Ann. Bot.* 118, 1317–1328. doi: 10.1093/aob/mcw160

Dingaan, M. N. V., Tsubo, M., Walker, S., and Newby, T. (2017). Soil chemical properties and plant species diversity along a rainfall gradient in semi-arid grassland of South Africa. *Plant Ecol. Evol.* 150, 35–44. doi: 10.5091/plecevo.2017.1260

Du, F. K., Hou, M., Wang, W., Mao, K., and Hampe, A. (2017). Phylogeography of *Quercus aquifolioides* provides novel insights into the Neogene history of a major global hotspot of plant diversity in southwest China. *J. Biogeogr.* 44, 294–307. doi: 10.1111/jbi.12836

Dutilleul, P., Clifford, P., Richardson, S., and Hemon, D. (1993). Modifying the t test for assessing the correlation between two spatial processes. *Biometrics* 49, 305–314.

Ebersbach, J., Muellner-Riehl, A. N., Michalak, I., Tkach, N., Hoffmann, M. H., Röser, M., et al. (2017a). In and out of the Qinghai-Tibet Plateau: divergence time estimation and historical biogeography of the large arctic-alpine genus *Saxifraga* L. *J. Biogeogr.* 44, 900–910. doi: 10.1111/jbi.12899

Ebersbach, J., Schnitzler, J., Favre, A., and Muellner-Riehl, A. N. (2017b). Evolutionary radiations in the species-rich mountain genus *Saxifraga* L. *Bmc. Evol. Biol.* 17:119. doi: 10.1186/s12862-017-0967-2

Escudero, A., Palacio, S., Maestre, F. T., and Luzuriaga, A. L. (2015). Plant life on gypsum: a review of its multiple facets. *Biol. Rev.* 90, 1–18. doi: 10.1111/brv.12092

Fang, J., and Yoda, K. (1990). Climate and vegetation in China III water balance and distribution of vegetation. *Ecol. Res.* 5, 9–23. doi: 10.1007/bf02348460

Favre, A., Michalak, I., Chen, C.-H., Wang, J.-C., Pringle, J. S., Matuszak, S., et al. (2016). Out-of-Tibet: the spatio-temporal evolution of *Gentiana* (Gentianaceae). *J. Biogeogr.* 43, 1967–1978. doi: 10.1111/jbi.12840

Gaston, K. J., Williams, P. H., Eggleton, P., and Humphries, C. J. (1995). Large scale patterns of biodiversity: spatial variation in family richness. *P. Roy. Soc. Lond. B. Bio.* 260, 149–154. doi: 10.1098/rspb.1995.0072

Harrison, S., and Rajakaruna, N. (2011). *Serpentine: The Evolution and Ecology of a Model System. Berkeley*. Los Angeles, CA: University of California Press.

Hengl, T., de Jesus, J. M., MacMillan, R. A., Batjes, N. H., Heuvelink, G. B., Ribeiro, E., et al. (2014). SoilGrids1km-global soil information based on automated mapping. *PLoS One* 9:e0105992. doi: 10.1371/journal.pone.0105992

Hengl, T., Mendes de Jesus, J., Heuvelink, G. B., Ruiperez Gonzalez, M., Kilibarda, M., Blagotic, A., et al. (2017). SoilGrids250m: global gridded soil information based on machine learning. *PLoS One* 12:e0169748. doi: 10.1371/journal.pone.0169748

Hua, X., and Wiens, J. J. (2013). How does climate influence speciation? *Am. Nat.* 182, 1–12. doi: 10.1086/670690

Hughes, C., and Eastwood, R. (2006). Island radiation on a continental scale: exceptional rates of plant diversification after uplift of the Andes. *Proc. Natl. Acad. Sci. U.S.A.* 103, 10334–10339. doi: 10.1073/pnas.0601928103

Hughes, C. E., and Atchison, G. W. (2015). The ubiquity of alpine plant radiations: from the andes to the hengduan mountains. *New Phytol.* 207, 275–282. doi: 10.1111/nph.13230

Huston, M. (1980). Soil nutrients and tree species richness in costa rican forests. *J. Biogeogr.* 7, 147–157.

Kammer, P. M., Schöb, C., Eberhard, G., Gallina, R., Meyer, R., and Tschanz, C. (2013). The relationship between soil water storage capacity and plant species diversity in high alpine vegetation. *Plant Ecol. Divers.* 6, 457–466. doi: 10.1080/17550874.2013.783142

Kontopanou, A., and Panitsa, M. (2020). Habitat islands on the Aegean Islands (Greece): elevational gradient of chasmophytic diversity, endemism, phytogeographical patterns and need for monitoring and conservation. *Diversity* 12:33. doi: 10.3390/d12010033

Kutiel, P., and Danin, A. (1987). Annual-species diversity and aboveground phytomass in relation to some soil properties in the sand dunes of the northern Sharon Plains. *Israel. Vegetatio.* 70, 45–49.

Laanisto, L., Tamme, R., Hiiesalu, I., Szava-Kovats, R., Gazol, A., and Pärtel, M. (2013). Microfragmentation concept explains non-positive environmental heterogeneity–diversity relationships. *Oecologia* 171, 217–226. doi: 10.1007/s00442-012-2398-5

Laliberte, E., Grace, J. B., Huston, M. A., Lambers, H., Teste, F. P., Turner, B. L., et al. (2013). How does pedogenesis drive plant diversity? *Trends Ecol. Evol.* 28, 331–340. doi: 10.1016/j.tree.2013.02.008

Liu, Y., Shen, Z., Wang, Q., Su, X., Zhang, W., Shrestha, N., et al. (2017). Determinants of richness patterns differ between rare and common species: implications for Gesneriaceae conservation in China. *Divers. Distrib.* 23, 235–246. doi: 10.1111/ddi.12523

Liu, Y., Su, X., Shrestha, N., Xu, X., Wang, S., Li, Y., et al. (2019). Effects of contemporary environment and Quaternary climate change on drylands plant diversity differ between growth forms. *Ecography* 42, 334–345. doi: 10.1111/ecog.03698

Lundholm, J. T. (2009). Plant species diversity and environmental heterogeneity: spatial scale and competing hypotheses. *J. Veg. Sci.* 20, 377–391. doi: 10.1111/j.1654-1103.2009.05577.x

Mac Nally, R., and Walsh, C. J. (2004). Hierarchical partitioning public-domain software. *Biodivers. Conserv.* 13, 659–660. doi: 10.1023/b:bioc.0000009515.11717.0b

Mao, L. F., Chen, S. B., Zhang, J. L., Hou, Y. H., Zhou, G. S., and Zhang, X. S. (2013). Vascular plant diversity on the roof of the world: spatial patterns and environmental determinants. *J. Syst. Evol.* 51, 371–381. doi: 10.1111/j.1759-6831.2012.00240.x

Mcnulty, A. K., and Cummins, W. R. (1987). The relationship between respiration and temperature in leaves of the arctic plant *Saxifraga cernua*. *Plant Cell Environ.* 10, 319–325. doi: 10.1111/j.1365-3040.1987.tb01612.x

Myers, N., Mittermeier, R. A., Mittermeier, C. G., da Fonseca, G. A. B., and Kent, J. (2000). Biodiversity hotspots for conservation priorities. *Nature* 403, 853–858. doi: 10.1038/35002501

Nally, R. M. (1996). Hierarchical partitioning as an interpretative tool in multivariate inference. *Aust. J. Ecol.* 21, 224–228. doi: 10.1111/j.1442-9993.1996.tb00602.x

O'Brien, E. M., Field, R., and Whittaker, R. J. (2000). Climatic gradients in woody plant (tree and shrub) diversity: water-energy dynamics, residual variation, and topography. *Oikos* 89, 588–600. doi: 10.1034/j.1600-0706.2000.890319.x

Peres-Neto, P. R., Legendre, P., Dray, S., and Borcard, D. (2006). Variation partitioning of species data matrices: estimation and comparison of fractions. *Ecology* 87, 2614–2625. doi: 10.1890/0012-9658(2006)87[2614:vposdm]2.0.co;2

Qian, H., and Ricklefs, R. E. (2000). Large-scale processes and the Asian bias in species diversity of temperate plants. *Nature* 407, 180–182. doi: 10.1038/35025052

Rahbek, C., Borregaard, M. K., Antonelli, A., Colwell, R. K., Holt, B. G., Nogues-Bravo, D., et al. (2019a). Building mountain biodiversity: geological and evolutionary processes. *Science* 365, 1114–1119. doi: 10.1126/science.aax0151

Rahbek, C., Borregaard, M. K., Colwell, R. K., Dalsgaard, B., Holt, B. G., Morueta-Holme, N., et al. (2019b). Humboldt's enigma: what causes global patterns of mountain biodiversity? *Science* 365, 1108–1113. doi: 10.1126/science.aax0149

Rakotoarinivo, M., Blach-Overgaard, A., Baker, W. J., Dransfield, J., Moat, J., and Svenning, J.-C. (2013). Palaeo-precipitation is a major determinant of palm species richness patterns across Madagascar: a tropical biodiversity hotspot. *P. Roy. Soc. B Biol. Sci.* 280:20123048. doi: 10.1098/rspb.2012.3048

Rawat, D. S., Uniyal, P., and Chandra, S. (2019). Micromorphology and distribution of trichome in *Saxifraga* L. species from Western Indian Himalaya and its taxonomic implications. *Taiwania* 64, 13–22.

Romeo, R., Vita, A., Manuelli, S., Zanini, E., Freppaz, M., and Stanchi, S. (2015). *Understanding Mountain soils: A Contribution From Mountain Areas to the International Year of Soils 2015*. Rome: FAO.

Rosenzweig, M. L. (1995). *Species Diversity in Space and Time*. Cambridge, MA: Cambridge University Press.

Shrestha, N., Su, X., Xu, X., and Wang, Z. (2018a). The drivers of high *Rhododendron* diversity in southwest China: does seasonality matter? *J. Biogeogr.* 45, 438–447. doi: 10.1111/jbi.13136

Shrestha, N., Wang, Z., Su, X., Xu, X., Lyu, L., Liu, Y., et al. (2018b). Global patterns of *Rhododendron* diversity: the role of evolutionary time and diversification rates. *Glob. Ecol. Biogeogr.* 27, 913–924. doi: 10.1111/geb.12750

Stein, A., Gerstner, K., and Kreft, H. (2014). Environmental heterogeneity as a universal driver of species richness across taxa, biomes and spatial scales. *Ecol. Lett.* 17, 866–880. doi: 10.1111/ele.12277

Sun, H., Zhang, J., Deng, T., and Boufford, D. E. (2017). Origins and evolution of plant diversity in the Hengduan Mountains. *China. Plant Divers.* 39, 161–166. doi: 10.1016/j.pld.2017.09.004

Svenning, J.-C., Normand, S., and Skov, F. (2006). Range filling in European trees. *J. Biogeogr.* 33, 2018–2021. doi: 10.1111/j.1365-2699.2006.01630.x

Svenning, J. C., and Skov, F. (2004). Limited filling of the potential range in European tree species. *Ecol Lett.* 7, 565–573. doi: 10.1111/j.1461-0248.2004.00614.x

Wang, Q., Wu, S., Su, X., Zhang, L., Xu, X., Lyu, L., et al. (2018). Niche conservatism and elevated diversification shape species diversity in drylands: evidence from Zygophyllaceae. *Proc. Biol. Sci.* 285:20181742. doi: 10.1098/rspb.2018.1742

Wang, Z., Brown, J. H., Tang, Z., and Fang, J. (2009). Temperature dependence, spatial scale, and tree species diversity in eastern Asia and North America. *Proc. Natl. Acad. Sci. U.S.A.* 106, 13388–13392. doi: 10.1073/pnas.0905030106

Wang, Z., Fang, J., Tang, Z., and Lin, X. (2011a). Patterns, determinants and models of woody plant diversity in China. *P. Roy. Soc. B Biol. Sci.* 278, 2122–2132. doi: 10.1098/rspb.2010.1897

Wang, Z., Fang, J., Tang, Z., and Lin, X. (2011b). Relative role of contemporary environment versus history in shaping diversity patterns of China's woody plants. *Ecography* 34, 1–10. doi: 10.1111/j.1600-0587.2011.06781.x

Wiens, J. J., and Donoghue, M. J. (2004). Historical biogeography, ecology and species richness. *Trends Ecol. Evol.* 19, 639–644. doi: 10.1016/j.tree.2004.09.011

Wiens, J. J., and Graham, C. H. (2005). Niche conservatism: integrating evolution, ecology, and conservation biology. *Annu. Rev. Ecol. Evol. Syst.* 36, 519–539. doi: 10.2307/30033815

Xu, X., Wang, Z., Rahbek, C., Lessard, J.-P., Fang, J., and Burns, K. C. (2013). Evolutionary history influences the effects of water-energy dynamics on oak diversity in Asia. *J. Biogeogr.* 40, 2146–2155. doi: 10.1111/jbi.12149

Xu, X., Dimitrov, D., Shrestha, N., Rahbek, C., Wang, Z., and Jordan, G. (2019). A consistent species richness–climate relationship for oaks across the northern hemisphere. *Glob. Ecol. Biogeogr.* 28, 1051–1066. doi: 10.1111/geb.12913

Xue, G. (2014). *Ancient and Contemporary Geographical Names in China*. Shanghai: Lexicographical Publishing House.

Yang, A. M., Wu, R., Li, J. Y., and Guo, W. J. (2013). Chemical constituents of *Saxifraga umbellulata*. *Adv. Mater. Res.* 781-784, 2289–2291. doi: 10.4028/www.scientific.net/AMR.781-784.2289

Zhu, J., Zhang, Y., and Wang, W. (2016). Interactions between warming and soil moisture increase overlap in reproductive phenology among species in an alpine meadow. *Biol. Lett.* 12:20150749. doi: 10.1098/rsbl.2015.0749

**Conflict of Interest:** The authors declare that the research was conducted in the absence of any commercial or financial relationships that could be construed as a potential conflict of interest.

frontiers in Ecology and Evolution

ORIGINAL RESEARCH
published: 11 August 2020
doi: 10.3389/fevo.2020.00234

# Species Delimitation and Evolutionary History of Tree Frogs in the *Hyla chinensis* Group (Hylidae, Amphibian)

*Peng Yan[1†], Tao Pan[1†], Guiyou Wu[2], Xing Kang[2], Izaz Ali[1], Wenliang Zhou[3], Jiatang Li[4], Xiaobing Wu[1]* and Baowei Zhang[1,2]**

[1] Anhui Provincial Key Laboratory of the Conservation and Exploitation of Biological Resources, College of Life Sciences, Anhui Normal University, Wuhu, China, [2] School of Life Sciences, Anhui University, Hefei, China, [3] Key Lab of Animal Ecology and Conservation Biology, Institute of Zoology, Chinese Academy of Sciences, Beijing, China, [4] Chengdu Institute of Biology, Chinese Academy of Sciences, Chengdu, China

OPEN ACCESS

**Edited by:**
Zehao Shen,
Peking University, China

**Reviewed by:**
Zhenghuan Wang,
East China Normal University, China
Xiaolei Huang,
Fujian Agriculture and Forestry University, China

***Correspondence:**
Xiaobing Wu
wuxb@ahnu.edu.cn
Baowei Zhang
zhangbw@ahu.edu.cn

[†] These authors have contributed equally to this work

**Specialty section:**
This article was submitted to Biogeography and Macroecology, a section of the journal Frontiers in Ecology and Evolution

**Received:** 07 January 2020
**Accepted:** 26 June 2020
**Published:** 11 August 2020

**Citation:**
Yan P, Pan T, Wu G, Kang X, Ali I, Zhou W, Li J, Wu X and Zhang B (2020) Species Delimitation and Evolutionary History of Tree Frogs in the Hyla chinensis Group (Hylidae, Amphibian). Front. Ecol. Evol. 8:234. doi: 10.3389/fevo.2020.00234

Species are the cornerstone in many domains of biology research, which make accurate species delimitation critically important. In this study, the systematics and biogeography of the *Hyla chinensis* group were analyzed based on phylogeny, species delimitation, and ancestral area reconstruction methods. The phylogenetic results showed that six specific clusters existed in the *H. chinensis* group. Bayesian Phylogenetics and Phylogeography (BPP) analysis indicated that six distinct species exist due to the high probability values (>0.95), which were also supported by the Bayes factor (BF) analysis. The divergence time of the *H. chinensis* group was estimated to date back to 18.84 million years ago (Mya) in the early Miocene. Combining the results of ancestral area reconstruction, the *H. chinensis* group might have originated from Guangxi-Hainan, then spread eastwardly and reached Nanling Mountains, Wuyi Mountains, Huangshan Mountain, and Taiwan. In right-about colonization, it was gradually extended to the Yunnan-Guizhou Plateau, Sichuan Basin, Qinling Mountains, and Dabie Mountains. Considering the geological movement from early Miocene to Pliocene, the colonization pattern of the *H. chinensis* group may be closely related to the progressive uplift of the Qinghai-Tibetan Plateau (QTP) and historical climate change. Our study provided evidence for species delimitation and speciation process within the *H. chinensis* group. Our study supported the hypothesis that the evolutionary divergence in this species group was a consequence of the progressive uplift of the QTP and environmental change.

**Keywords: *Hyla chinensis* group, species delimitation, phylogeny, biogeography, evolutionary history**

## INTRODUCTION

For biogeography, abiotic factors (e.g., climate changes and tectonic events) and biological factors (e.g., interspecific or intraspecific interactions, competition, and predation) act as the major drivers temporally and geographically for biological evolution and diversification (Benton, 2009). Generally, for mountainous landscapes, the interactions of those factors provided beneficial

conditions for the various microhabitats. Herein, those species endemic to mountain habitats often exhibit special phylogeographic patterns, such as the relatively small populations with well-defined geographical boundaries (Shepard and Burbrink, 2011; Huang et al., 2017; Pan et al., 2019). In southern China, many mountains (e.g., Hengduan Mountains, Qinling Mountains, Daba Mountains, Wuyi Mountains, and Dabie Mountains) are scattered, which form potential spatially isolated sky islands, providing various microhabitats with beneficial conditions for the speciation process of endemic species (Gao et al., 2015; Zhen et al., 2016). For example, due to the various microhabitats under climate and tectonic events, the Qinghai-Tibetan Plateau (QTP) had significant influence on the evolution of many animal groups (Päckert et al., 2012; Favre et al., 2015).

Species are considered the cornerstone of research in biology fields (e.g., evolutionary biology, biogeography) (Aldhebiani, 2018), which makes appropriate and accurate species delimitation increasingly meaningful (Yang and Rannala, 2010; Grummer et al., 2014; Blair and Bryson, 2017; Kajtoch et al., 2017; Kotsakiozi et al., 2018; Sheridan and Stuart, 2018). The genus *Hyla* (Hylidae, Anura) comprised 35 recent described species (19 species distributed in Eurasia; 16 species distributed in North and Central America) (Frost, 2014; Li et al., 2015). *Hyla chinensis* group, mainly distributed in China, is one of the species complexes in *Hyla*. As for the number of species identified in the *H. chinensis* group, it is controversial (Hua et al., 2009; Li et al., 2015). One supported that it included seven species (*Hyla annectans*, *H. chinensis*, *Hyla hallowelli*, *Hyla sanchiangensis*, *Hyla simplex*, *Hyla tsinlingensis*, and *Hyla zhaopingensis*) (Hua et al., 2009); the other study supported only six species (*H. annectans*, *H. chinensis*, *H. simplex*, *H. sanchiangensis*, *H. tsinlingensis*, and *H. zhaopingensis*) and five subspecies in *H. annectans* (*H. a. chuanxiensis, H. a. gongshanensis, H. a. jingdongensis, H. a. tengchongensis*, and *H. a. wulingensis*) (Li et al., 2015). Combining those results, it is more urgent to solve the problem of determined number of species and subspecies within this species complex based on species delimitation methods.

On the other hand, Li et al. (2015) had demonstrated that the *Hyla* originated from North America, then diffused to China *via* Beringia during the Middle Eocene to Early Oligocene (Smith et al., 2005; Wiens et al., 2006), which may be inferred that the speciation of *H. chinensis* group may be from northern China to southern China. However, the phylogenetic tree in the study by Li et al. (2015) disclosed that the base clades of *H. chinensis* group were all located in southern China, which may be a hint of another expansion route of the *H. chinensis* group.

Using genetic data and multiple analysis methods to solve taxonomic uncertainties enables us to disclose phylogenetic topology and speciation process. Here, we reveal a phylogeny of the *H. chinensis* group based on multiple mitochondrial and nuclear genes covering currently described species or subspecies within the *H. chinensis* group (Li et al., 2015). On the basis of species delimitation methods, we aim to clarify systematic and taxonomic matters bound up with species within the *H. chinensis* group. Meanwhile, we evaluate whether orogeny and climate oscillations affected the speciation and evolutionary history of *H. chinensis* group.

# MATERIALS AND METHODS

## Ethics Statement

In this study, the sample collection of *H. tsinlingensis* and *H. chinensis* was conducted by a long-term investigation project on amphibian diversity in Dabie Mountains and Huangshan Mountain. This investigation project and sample collection were approved by the Anhui Normal University Academic Ethics Committee, Anhui Province, China.

## Taxon Sampling

Based on previous study, we embraced almost all currently recognized species (76 individuals) within the *H. chinensis* group (Li et al., 2015) and chose two species (*Hyla arborea*, *Hyla orientalis)* as outgroups. Additionally, our own specimens (17 *H. tsinlingensis* individuals and two *H. chinensis* individuals) were collected from Dabie Mountains and Huangshan Mountain during 2011 to 2014, all samples were non-invasive sampling and the specimens were stored in School of Life Sciences, Anhui University, China (**Figure 1**). Details on specimen vouchers and GenBank accession numbers and specimen sites are listed in **Table 1**.

## Laboratory Methods

The proteinase K digestion and phenol/chloroform extraction method were used to extract total genomic DNA (Sambrook et al., 1989). For combined previous sequence data (Li et al., 2015), the same genes were selected based on published primers and new primers (**Supplementary Table S1**), including four mitochondrial genes (12S ribosomal small subunit gene/12S rRNA, NADH dehydrogenase subunit 1 gene/ND1, tRNA-Leu, and the partial 16S ribosomal large subunit gene/16S) and one nuclear protein-coding gene (proopiomelanocortin A/POMC) (Wiens et al., 2005).

All PCRs were performed within the same conditions in 30 μl volume: 10–40 ng of genomic DNA, 15 μl 2 × EasyTaq PCR SuperMix polymerase (containing 1 U Ex Taq, 0.4 mM dNTP, 3 mM $Mg^{2+}$; TransGen Biotech) and 0.2 μM of primers. PCRs were performed by the following protocol: an initial denaturing step of 5 min at 94°C, followed by 32 cycles with denaturing 30 s at 94°C, annealing 30 s at 50°C and 55°C (for mitochondrial gene and nuclear gene, respectively), extending 40 and 100 s (for mitochondrial gene and nuclear gene, respectively) at 72°C, and a final extension step of 10 min conducted at 72°C. PCR samples were checked on a 1% agarose gel. Subsequently, PCR products were purified by EasyPure PCR Purification Kit (TransGene), and each fragment was sequenced in both directions on the ABI 3730 semiautomated sequencer (PE Applied Biosystems).

## Sequence Processing and Phylogenetic Analyses

The DNA analysis package DNASTAR Lasergene Seqman and EditSeq v.7.1 were used to proofread or assemble the resulting

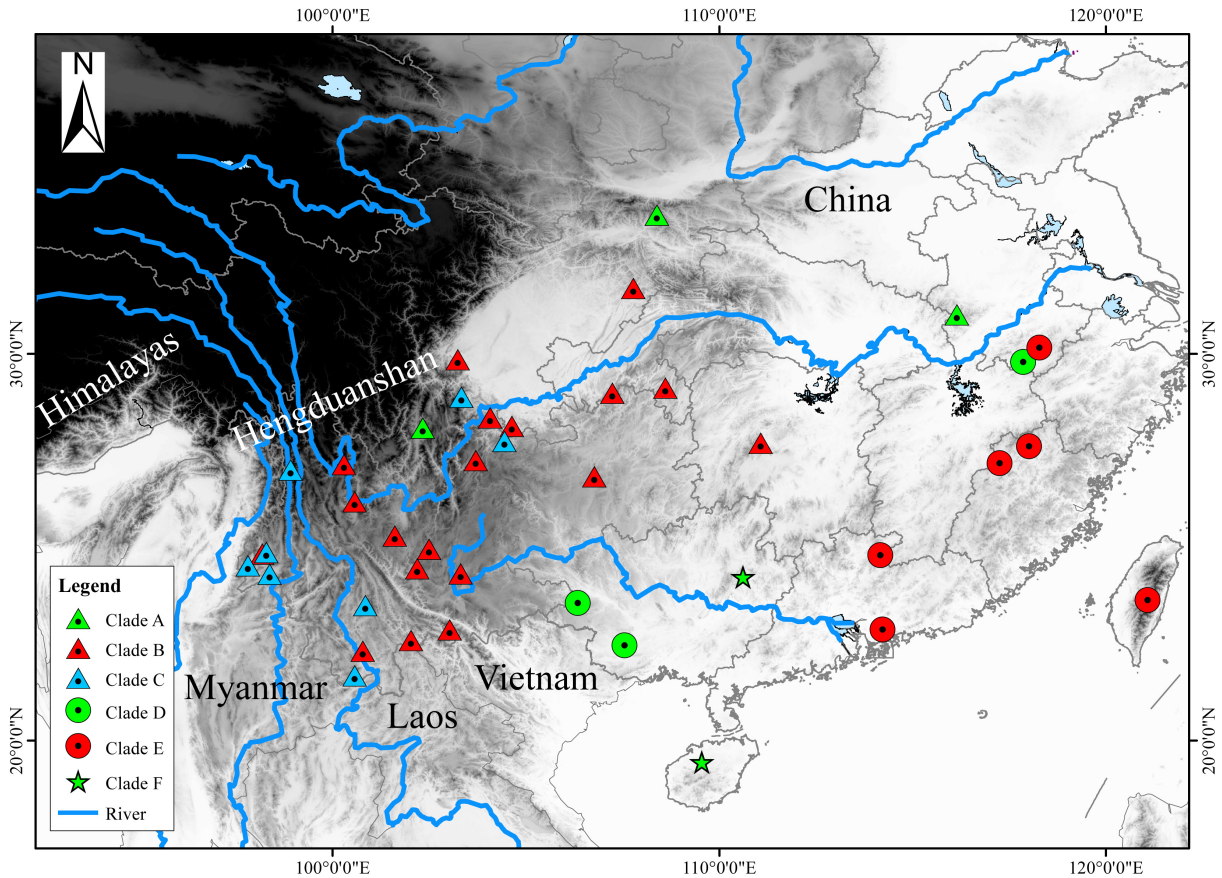


**FIGURE 1 |** Map with the locality samples of the *Hyla chinensis* group in this study. The sampling sites of each clade **(A–F)** were marked with different triangles or dots in different colors. These clades **(A–F)** correspond to the clades in **Figures 2**, **3**. The black and white coloration represents elevation.

sequences of all genes (Burland, 1999) with default parameters, and the nucleotide sequences were checked by eyes. All the genes were concatenated for analysis and aligned in MEGA v.7.0 (Tamura et al., 2011). Aligned sequences had a total length of 2,474 bp (12S rRNA, 815 bp; 16S+tRNA+ND1, 1,172 bp; POMC, 487 bp). Two datasets were applied in phylogenetic analyses: (1) a data set consisting of the combined mtDNA genes (12S rRNA+16S+tRNA+ND1) was used to conduct species tree, Bayes factor (BF) delimitation (BFD) analyses (Sullivan and Joyce, 2005), infer divergence times, phylogenetic network, and genetic distance analysis; (2) the entire set of mitochondrial and nuclear genes (12S rRNA+16S+tRNA+ND1+POMC) was used to conduct the phylogenetic reconstruction [maximum likelihood (ML); Bayesian] and Bayesian Phylogenetics and Phylogeography (BPP) analysis (Rannala and Yang, 2003; Yang and Rannala, 2010).

Before phylogenetic analysis, the software jModeltest v.2 (Darriba et al., 2012) was used to find the best-fit nucleotide substitution model of each gene using Bayesian information criterion (BIC), and this optimal model (GTR+G, 12S; GTR+I+G, 16S+tRNA+ND1+POMC) was selected and implemented in all downstream analyses. Bayesian phylogenetic analysis was performed on different partitions of mitochondrial and nuclear datasets with a mixed-model approach separated into using MrBayes v.3.2.2 (Ronquist and Huelsenbeck, 2003). The homologous sequence of *H. arborea* and *H. orientalis* was used as outgroups. Two independent runs of Markov Chain Monte Carlo (MCMC) analyses for 10 million generations were conducted. The run was sampled every 1,000 generations, and 10% of the initial samples were discarded as "burn-in." The ML tree was generated with RAxML v.7.0.3 (Stamatakis, 2008) using the GTR model for mitochondrial and nuclear datasets. Support of nodes was calculated with 1,000 bootstrap replicates with the fast bootstrapping algorithm. Aside from the above analysis, we also operated "net between putative species mean distance" between the *H. chinensis* group species with 1,000 bootstrap replicates by Kimura two-parameter model on mitochondrial genes in MEGA v.7.0 (Tamura et al., 2011).

## Divergence Time Estimation

Mitochondrial genes were used to estimate divergence times among *H. chinensis* group in BEAST v.1.8.0 (Drummond et al., 2012). An MCMC approach with uncorrelated lognormal relaxed molecular clock for rate variation was set. Two independent runs were performed, consisting of 10 million generations, each run sampling every 1,000 generations with a burn-in set to 10% of

**TABLE 1 |** Samples, with sampling site, museum voucher nos., and GenBank accession nos. of corresponding sequences.

| Taxon | Locality | Specimen voucher no./ isolate no. | GenBank No. (MtDNA: 12S, 16S, tRNA-Leu and ND1; NuDNA: POMC) | | | | | Distribution areas | Source |
|---|---|---|---|---|---|---|---|---|---|
| | | | 12S | 16S | tRNA-Leu | ND1 | POMC | | |
| Hylidae | | | | | | | | | |
| Hylinae | | | | | | | | | |
| *Hyla* | | | | | | | | | |
| *Hyla annectans* | China: Binchuan, Yunnan | KIZDL100502 | KP742535 | KP742664 | KP742664 | KP742664 | – | Y | Li et al., 2015 |
| *Hyla annectans* | China: Binchuan, Yunnan | KIZBC100601 | KP742552 | KP742681 | KP742681 | KP742681 | – | Y | Li et al., 2015 |
| *Hyla annectans* | China: Yulong, Yunnan | KIZLJ100602 | KP742540 | KP742669 | KP742669 | KP742669 | – | Y | Li et al., 2015 |
| *Hyla annectans* | China: Fugong, Yunnan | CAS215021 | AY819421 | DQ055813 | DQ055813 | DQ055813 | DQ055786 | Y | Li et al., 2015 |
| *Hyla annectans* | China: Weixi, Yunnan | KIZ200905320 | KP742522 | KP742651 | KP742651 | KP742651 | – | Y | Li et al., 2015 |
| *Hyla annectans* | China: Lvchun, Yunnan | KIZ200905639 | KP742523 | KP742652 | KP742652 | KP742652 | – | Y | Li et al., 2015 |
| *Hyla annectans* | China: Yuanyang, Yunnan | KIZ200905641 | KP742524 | KP742653 | KP742653 | KP742653 | – | Y | Li et al., 2015 |
| *Hyla annectans* | China: Shuifu, Yunnan | KIZ270806034 | KP742525 | KP742654 | KP742654 | KP742654 | – | Y | Li et al., 2015 |
| *Hyla annectans* | China: Shuifu, Yunnan | KIZ270806035 | KP742526 | KP742655 | KP742655 | KP742655 | – | Y | Li et al., 2015 |
| *Hyla annectans* | China: Yuexi, Sichuan | KIZLZY20090172 | KP742527 | KP742656 | KP742656 | KP742656 | – | Y | Li et al., 2015 |
| *Hyla annectans* | China: Yongde, Yunnan | KIZ200701067 | KP742528 | KP742657 | KP742657 | KP742657 | – | Y | Li et al., 2015 |
| *Hyla annectans* | China: Jinggu, Yunnan | KIZJG125 | KP742529 | KP742658 | KP742658 | KP742658 | – | Y | Li et al., 2015 |
| *Hyla annectans* | China: Tengchong, Yunnan | KIZGLGS3481 | KP742530 | KP742659 | KP742659 | KP742659 | KP742498 | Y | Li et al., 2015 |
| *Hyla annectans* | China: Tengchong, Yunnan | KIZGLGS3729 | KP742531 | KP742660 | KP742660 | KP742660 | KP742499 | Y | Li et al., 2015 |
| *Hyla annectans* | China: Shiwuli, Yunnan | KIZGLGS2658 | KP742532 | KP742661 | KP742661 | KP742661 | KP742500 | Y | Li et al., 2015 |
| *Hyla annectans* | China: Hongya, Sichuan | CIBLJT070504 | KP742533 | KP742662 | KP742662 | KP742662 | KP742491 | Y | Li et al., 2015 |
| *Hyla annectans* | China: Jinping, Yunnan | KIZ060821f | KP742534 | KP742663 | KP742663 | KP742663 | – | Y | Li et al., 2015 |
| *Hyla annectans* | China: Tengchong, Yunnan | KIZTC100501 | KP742536 | KP742665 | KP742665 | KP742665 | – | Y | Li et al., 2015 |
| *Hyla annectans* | China: Sangzhi, Hunan | KIZSZ100602 | KP742537 | KP742666 | KP742666 | KP742666 | – | Y | Li et al., 2015 |
| *Hyla annectans* | China: Sangzhi, Hunan | KIZSZ100603 | KP742538 | KP742667 | KP742667 | KP742667 | – | Y | Li et al., 2015 |
| *Hyla annectans* | China: Yunlong, Yunnan | KIZDL100504 | KP742539 | KP742668 | KP742668 | KP742668 | – | Y | Li et al., 2015 |
| *Hyla annectans* | China: Menglian, Yunnan | KIZML100602 | KP742541 | KP742670 | KP742670 | KP742670 | – | Y | Li et al., 2015 |
| *Hyla annectans* | China: Menghai, Yunnan | KIZMH100601 | KP742542 | KP742671 | KP742671 | KP742671 | – | Y | Li et al., 2015 |
| *Hyla annectans* | China: Menghai, Yunnan | KIZMH100602 | KP742543 | KP742672 | KP742672 | KP742672 | – | Y | Li et al., 2015 |
| *Hyla annectans* | China: Kunming, Yunnan | KIZKM060501 | KP742544 | KP742673 | KP742673 | KP742673 | – | Y | Li et al., 2015 |
| *Hyla annectans* | China: Mile, Yunnan | KIZMLE080502 | KP742545 | KP742674 | KP742674 | KP742674 | – | Y | Li et al., 2015 |
| *Hyla annectans* | China: Yuexi, Sichuan | CIBLJT101186 | KP742546 | KP742675 | KP742675 | KP742675 | KP742494 | Y | Li et al., 2015 |
| *Hyla annectans* | China: Yuexi, Sichuan | CIBJT101187 | KP742547 | KP742676 | KP742676 | KP742676 | KP742495 | Y | Li et al., 2015 |
| *Hyla annectans* | China: Zhaotong, Yunnan | KIZSK100801 | KP742548 | KP742677 | KP742677 | KP742677 | – | Y | Li et al., 2015 |
| *Hyla annectans* | China: Zhaotong, Yunnan | KIZMLZ100801 | KP742549 | KP742678 | KP742678 | KP742678 | – | Y | Li et al., 2015 |
| *Hyla annectans* | China: Lvfeng, Yunnan | KIZCX101001 | KP742550 | KP742679 | KP742679 | KP742679 | – | Y | Li et al., 2015 |
| *Hyla annectans* | China: Ningliang, Yunnan | KIZNL100901 | KP742551 | KP742680 | KP742680 | KP742680 | – | Y | Li et al., 2015 |
| *Hyla annectans* | China: Youyang, Chongqing | CIB20120440 | KP742553 | KP742682 | KP742682 | KP742682 | KP742489 | Y | Li et al., 2015 |
| *Hyla annectans* | China: Nanchuan, Chongqing | CIBZYC776 | KP742554 | KP742683 | KP742683 | KP742683 | KP742490 | Y | Li et al., 2015 |
| *Hyla annectans* | China: Nanchuan, Chongqing | CIBZYC777 | KP742555 | KP742684 | KP742684 | KP742684 | – | Y | Li et al., 2015 |
| *Hyla annectans* | China: Nanchuan, Chongqing | CIBGP263 | KP742556 | KP742685 | KP742685 | KP742685 | – | Y | Li et al., 2015 |
| *Hyla annectans* | China: Nanchuan, Chongqing | CIBGP273 | KP742557 | KP742686 | KP742686 | KP742686 | – | Y | Li et al., 2015 |
| *Hyla annectans* | China: Nanchuan, Chongqing | CIBGP274 | KP742558 | KP742687 | KP742687 | KP742687 | – | Y | Li et al., 2015 |
| *Hyla annectans* | China: Xuanhan, Sichuan | CIB201105129 | KP742559 | KP742688 | KP742688 | KP742688 | – | Y | Li et al., 2015 |
| *Hyla annectans* | China: Xuanhan, Sichuan | CIB201105130 | KP742560 | KP742689 | KP742689 | KP742689 | – | Y | Li et al., 2015 |
| *Hyla annectans* | China: Xuanhan, Sichuan | CIB201105131 | KP742561 | KP742690 | KP742690 | KP742690 | – | Y | Li et al., 2015 |
| *Hyla annectans* | China: Xuanhan, Sichuan | CIB201105132 | KP742562 | KP742691 | KP742691 | KP742691 | – | Y | Li et al., 2015 |
| *Hyla annectans* | China: Xuanhan, Sichuan | CIB201105133 | KP742563 | KP742692 | KP742692 | KP742692 | – | Y | Li et al., 2015 |
| *Hyla annectans* | China: Lijiang, Yunnan | CIB3LW0019 | KP742564 | KP742693 | KP742693 | KP742693 | KP742493 | Y | Li et al., 2015 |
| *Hyla annectans* | China: Yuexi, Sichuan | SCUM060486L | KP742565 | KP742694 | KP742694 | KP742694 | – | Y | Li et al., 2015 |
| *Hyla annectans* | China: Yuexi, Sichuan | SCUM060487L | KP742566 | KP742695 | KP742695 | KP742695 | – | Y | Li et al., 2015 |
| *Hyla annectans* | China: Junlian, Sichuan | CIBGP298 | KP742567 | KP742696 | KP742696 | KP742696 | – | Y | Li et al., 2015 |
| *Hyla annectans* | China: Junlian, Sichuan | CIBGP299 | KP742568 | KP742697 | KP742697 | KP742697 | KP742492 | Y | Li et al., 2015 |
| *Hyla annectans* | China: Guizhou | CIBGZ080537 | KP742569 | KP742698 | KP742698 | KP742698 | – | Y | Li et al., 2015 |
| *Hyla annectans* | China: Guizhou | CIBGZ080538 | KP742570 | KP742699 | KP742699 | KP742699 | – | Y | Li et al., 2015 |
| *Hyla chinensis* | China: Taiwan | HL1 | – | DQ055817 | DQ055817 | DQ055817 | DQ055789 | W | Li et al., 2015 |
| *Hyla chinensis* | China: Zhaowu, Fujian | IOZCAS4796 | KP742571 | KP742700 | KP742700 | KP742700 | KP742503 | W | Li et al., 2015 |
| *Hyla chinensis* | China: Longmen, Guangdong | CIB200905260 | KP742572 | KP742701 | KP742701 | KP742701 | – | W | Li et al., 2015 |

*(Continued)*

**TABLE 1 |** Continued

| Taxon | Locality | Specimen voucher no./ isolate no. | GenBank No. (MtDNA: 12S, 16S, tRNA-Leu and ND1; NuDNA: POMC) | | | | | Distribution areas | Source |
|---|---|---|---|---|---|---|---|---|---|
| | | | 12S | 16S | tRNA-Leu | ND1 | POMC | | |
| *Hyla chinensis* | China: Wuyihshan, Fujian | WYS100602 | KP742573 | KP742702 | KP742702 | KP742702 | KP742502 | W | Li et al., 2015 |
| *Hyla chinensis* | China: Chebaling, Guangdong | CIB20120429 | KP742574 | KP742703 | KP742703 | KP742703 | – | W | Li et al., 2015 |
| *Hyla chinensis* | China: Chebaling, Guangdong | CIB20120430 | KP742575 | KP742704 | KP742704 | KP742704 | KP742505 | W | Li et al., 2015 |
| *Hyla chinensis* | China: Chebaling, Guangdong | CIB20120431 | KP742576 | KP742705 | KP742705 | KP742705 | – | W | Li et al., 2015 |
| *Hyla chinensis* | China: Chebaling, Guangdong | CIB20120432 | KP742577 | KP742706 | KP742706 | KP742706 | – | W | Li et al., 2015 |
| *Hyla chinensis* | China: Chebaling, Guangdong | CIB20120433 | KP742578 | KP742707 | KP742707 | KP742707 | | W | Li et al., 2015 |
| *Hyla chinensis* | China: Chebaling, Guangdong | CIB20120434 | KP742579 | KP742708 | KP742708 | KP742708 | – | W | Li et al., 2015 |
| *Hyla chinensis* | China: Nanling, Guangdong | CIBGP400 | KP742580 | KP742709 | KP742709 | KP742709 | KP742504 | W | Li et al., 2015 |
| *Hyla chinensis* | China: Nanling, Guangdong | CIBGP409 | KP742581 | KP742710 | KP742710 | KP742710 | – | W | Li et al., 2015 |
| *Hyla chinensis* | China: Tanjiaqiao, Anhui | AHU20140801 | MK880293 | | | | MK883719 | W | This study |
| *Hyla chinensis* | China: Tanjiaqiao, Anhui | AHU20140802 | MK880294 | | | | MK883720 | W | This study |
| *Hyla sanchiangensis* | China: Xiuning, Anhui | CIB20120435 | KP742636 | KP742755 | KP742755 | KP742755 | KP742506 | W | Li et al., 2015 |
| *Hyla sanchiangensis* | China: Xiuning, Anhui | CIB20120436 | KP742637 | KP742756 | KP742756 | KP742756 | – | W | Li et al., 2015 |
| *Hyla sanchiangensis* | China: Xiuning, Anhui | CIB20120437 | KP742638 | KP742757 | KP742757 | KP742757 | – | W | Li et al., 2015 |
| *Hyla sanchiangensis* | China: Xiuning, Anhui | CIB20120438 | KP742639 | KP742758 | KP742758 | KP742758 | – | W | Li et al., 2015 |
| *Hyla sanchiangensis* | China: Xiuning, Anhui | CIB20120439 | KP742640 | KP742759 | KP742759 | KP742759 | – | W | Li et al., 2015 |
| *Hyla sanchiangensis* | China: Chongzuo, Guangxi | CIBGP1936 | KP742641 | KP742760 | KP742760 | KP742760 | – | S | Li et al., 2015 |
| *Hyla sanchiangensis* | China: Nonggang, Guangxi | – | KP742761 | KP742761 | KP742761 | KP742507 | – | S | Li et al., 2015 |
| *Hyla tsinlingensis* | China: Ningshan, Shaanxi | CIBLJT070511 | KP742645 | KP742764 | KP742764 | KP742764 | KP742496 | Z | Li et al., 2015 |
| *Hyla tsinlingensis* | China: Ningshan, Shaanxi | CIBLJT070512 | KP742646 | KP742765 | KP742765 | KP742765 | KP742497 | Z | Li et al., 2015 |
| *Hyla tsinlingensis* | China: Ningshan, Shaanxi | SCUM06060005 | GQ374901 | GQ374905 | GQ374905 | GQ374905 | GQ374917 | Z | Li et al., 2015 |
| *Hyla tsinlingensis* | China: Yaoluoping, Anhui | AHU20140601 | MK862405 | MK876185 | MK876185 | MK876185 | MK876202 | Z | This study |
| *Hyla tsinlingensis* | China: Yaoluoping, Anhui | AHU20140602 | MK862406 | MK876186 | MK876186 | MK876186 | MK876203 | Z | This study |
| *Hyla tsinlingensis* | China: Yaoluoping, Anhui | AHU20140603 | MK862407 | MK876187 | MK876187 | MK876187 | MK876204 | Z | This study |
| *Hyla tsinlingensis* | China: Yaoluoping, Anhui | AHU20140604 | MK862408 | MK876188 | MK876188 | MK876188 | MK876205 | Z | This study |
| *Hyla tsinlingensis* | China: Yaoluoping, Anhui | AHU20140605 | MK862409 | MK876189 | MK876189 | MK876189 | MK876206 | Z | This study |
| *Hyla tsinlingensis* | China: Yaoluoping, Anhui | AHU20140606 | MK862410 | MK876190 | MK876190 | MK876190 | MK876207 | Z | This study |
| *Hyla tsinlingensis* | China: Yaoluoping, Anhui | AHU20140607 | MK862411 | MK876191 | MK876191 | MK876191 | MK876208 | Z | This study |
| *Hyla tsinlingensis* | China: Yaoluoping, Anhui | AHU20140608 | MK862412 | MK876192 | MK876192 | MK876192 | MK876209 | Z | This study |
| *Hyla tsinlingensis* | China: Yaoluoping, Anhui | AHU20140609 | MK862413 | MK876193 | MK876193 | MK876193 | MK876210 | Z | This study |
| *Hyla tsinlingensis* | China: Yaoluoping, Anhui | AHU20140610 | MK862414 | MK876194 | MK876194 | MK876194 | MK876211 | Z | This study |
| *Hyla tsinlingensis* | China: Yaoluoping, Anhui | AHU20140611 | MK862415 | MK876195 | MK876195 | MK876195 | MK876212 | Z | This study |
| *Hyla tsinlingensis* | China: Yaoluoping, Anhui | AHU20140612 | MK862416 | MK876196 | MK876196 | MK876196 | MK876213 | Z | This study |
| *Hyla tsinlingensis* | China: Yaoluoping, Anhui | AHU20140613 | MK862417 | MK876197 | MK876197 | MK876197 | MK876214 | Z | This study |
| *Hyla tsinlingensis* | China: Yaoluoping, Anhui | AHU20140614 | MK862418 | MK876198 | MK876198 | MK876198 | MK876215 | Z | This study |
| *Hyla tsinlingensis* | China: Yaoluoping, Anhui | AHU20140615 | MK862419 | MK876199 | MK876199 | MK876199 | MK876216 | Z | This study |
| *Hyla tsinlingensis* | China: Yaoluoping, Anhui | AHU20140616 | MK862420 | MK876200 | MK876200 | MK876200 | MK876217 | Z | This study |
| *Hyla tsinlingensis* | China: Yaoluoping, Anhui | AHU20140617 | MK862421 | MK876201 | MK876201 | MK876201 | MK876218 | Z | This study |
| *Hyla zhaopingensis* | China: Zhaoping, Guangxi | CIBZP100601 | KP742647 | KP742766 | KP742766 | KP742766 | – | N | Li et al., 2015 |
| *Hyla zhaopingensis* | China: Zhaoping, Guangxi | CIBZP100602 | KP742648 | KP742767 | KP742767 | KP742767 | – | N | Li et al., 2015 |
| *Hyla zhaopingensis* | China: Danzhou, Hainan | CIBGP641 | KP742649 | KP742768 | KP742768 | KP742768 | – | N | Li et al., 2015 |
| *Hyla zhaopingensis* | China: Danzhou, Hainan | CIBGP642 | KP742650 | KP742769 | KP742769 | KP742769 | KP742508 | N | Li et al., 2015 |
| Outgroup | | | | | | | | | |
| Hylidae | | | | | | | | | |
| Hylinae | | | | | | | | | |
| *Hyla* | | | | | | | | | |
| *Hyla arborea* | Croatia: Split–Dalmatia County, Kamesnica, Mountain, pool in Donja Korita village | – | DQ055835 | DQ055814 | DQ055814 | DQ055814 | DQ055787 | | |
| *Hyla orientalis* | Russia | CIB20120455 | KP742630 | KP742751 | KP742751 | KP742751 | KP742509 | | |

*"–" represents no molecular data. The distribution areas were consistent with that within* ***Figure 3****.*

the samples. Tracer v.1.6 was used to check the stationarity of results (Rambaut and Drummond, 2007). TreeAnnotator v.1.8.0 (Rambaut and Drummond, 2007) and FigTree v. 1.4.2 (Rambaut, 2014) was used to annotate and visualize tree information. In the absence of appropriate fossils, we selected several calibration points information from previous work (Li et al., 2015), assuming a normal distribution for the divergence time between *H. arborea* group and the *H. chinensis* group, with a mean of 23 million years ago (Mya) and standard deviation of 3.04 (18–28 Mya).

## Bayes Factor Delimitation

The BF is a common species delimitation selection tool in phylogenetics (Sullivan and Joyce, 2005) based on the marginal-likelihood estimates (MLE) *via* path-sampling (PS) and stepping-stone sampling (SS) analyses (Fan et al., 2011; Xie et al., 2011; Li and Drummond, 2012). The scopes of BF are as follows: $0 < BF < 2$ is not worth more than a bare mention, $2 < BF < 6$ is positive evidence, $6 < BF < 10$ is strong support, and $BF > 10$ is decisive (Drummond et al., 2012). Coupled with the former studies (Hua et al., 2009; Li et al., 2015) and the above phylogenetic analysis inference, six ingroup species in the *H. chinensis* group were assumed and four species delimitation scenarios (True, Lump, Split, and Reassign) were generated to disclose the inner species number in *BEAST (Heled and Drummond, 2010). For "True" scenario, individuals were assigned to six ingroup species in the *H. chinensis* group as prior set. For the "Lump" scenario, we inferred that two ingroup species were regarded as a single species, corresponding to the ingroup number of species from six to five. In contrast, the "Split" scenario suggested two ingroup species each split into two species, which indicated the total number of ingroup species from six to eight. As to the "Reassign" scenario, a total of three individuals were "incorrectly" reassigned to different ingroup species than in the "True" tree. PS and SS analyses were each run, totaling $10^8$ generations with a chain length of $10^6$ generations for 100 path steps.

## Bayesian Phylogenetics and Phylogeography

In contrast to the results of our BFD method and to a commonly used method of species delimitation, we performed species delimitation analysis with the phased dataset for the two mitochondrial loci and one nuclear locus implemented in BPP v.3.0 (Rannala and Yang, 2003; Yang and Rannala, 2010). This method utilizes a reversible jump MCMC (rjMCMC) algorithm to calculate the posterior probabilities to speciation events that contain more or less lineages (Yang and Rannala, 2010). Between all BPP analyses, probability values $\geq$0.95 were considered a strong support in favor of a speciation event (Leaché and Fujita, 2010). The guide tree was generated from the species tree.

The priors of ancestral population size ($\theta$) and root age ($\tau$) are directly related to the posterior probabilities of each result for the models. For example, the combination of large values for $\theta$ and small values for $\tau$ is assumed to be the most conservative, leading to a lower number of speciation events (Leaché and Fujita, 2010; Yang and Rannala, 2010). We evaluated three schemes of the prior of the $\theta$ and $\tau$: (1) $\theta$ = G (1:2,000) and $\tau$ = G (1:10), (2) $\theta$ = G (1:2,000) and $\tau$ = G (1:100), (3) $\theta$ = G (2:2,000) and $\tau$ = G (1:10). The parameters of the rjMCMC analyses were set as 500,000 generations with sampling every 50 steps and 100,000 burn-in steps.

## Species Tree Inference

The coalescent-based method implemented in *BEAST was used to construct the species tree (Heled and Drummond, 2010) based on mitochondrial genes. Two independent runs of 20 million generations were conducted. The sample frequency was set as 10,000 generations, and 10% of the total samples were discarded as burn-in. The other models and prior specification applied were set as follows: the nucleotide substitution model: HKY; Relaxed Uncorrelated Lognormal Clock (estimate); Yule process of speciation; random starting tree; alpha Uniform (0, 10). The convergence was checked by examining trace plots and histograms in Tracer. Runs were combined using LogCombiner. In addition, we tended to construct an uncorrected p-distances phylogenetic network with heterozygous ambiguities averaged and normalized by Splitstree v. 4.13.1 (Huson and Bryant, 2006). The neighbor-net ordinary least squares variance and equal angle algorithm were used, and 1,000 bootstrap replicates were calculated to assess branch support.

## Ancestral Area Reconstruction

Geographical regions were delimited in terms of the current distribution area of the sequenced species of the *H. chinensis* group, at the same time, the information coming from the relevant literatures (Tang and Zhang, 1984; Li and Yang, 1985; Fei et al., 2009; Frost, 2014). The five areas were as follows: N, the southern China (Guangxi-Hainan provinces), which is a main distribution area of *H. zhaopingensis*; W, Eastern China; S, the southern Guangxi province in China, which is an important distribution range about *H. sanchiangensis*; Y, the eastern of the Tibetan Plateau (Yunnan-Guizhou Plateau and Sichuan Basin); Z, the Tsinling-Dabie Mountains (**Figures 1**, **3**). LAGRANGE is a deep-time biogeographical model-based method that allows the incorporation of paleogeographical data (Ree and Smith, 2008; Chacón and Renner, 2014). Taking the effect of the LAGRANGE model components into account, we designed experiments that transform the adjacency matrix, hence, resulting in a total of three experiments (M0, M1, and M2). This is according to the assumption that the *H. chinensis* group, like all organisms, has a lower possibility to disperse over non-adjacent areas than adjacent areas. For this reason, no ranges were forbidden for M0; WZ, SZ, and NZ were forbidden for M1; WZ, NZ, SZ, and NY were forbidden for M2. To select the optimal model, we compared their log-likelihood (the data presented by LAGRANGE); meanwhile, we used the standard cutoff value of two log-likelihood units as indicating a conspicuous imbalance between models, with the less negative likelihood being preferred (Chacón and Renner, 2014). Ancestral areas were reconstructed by dispersal-extinction-cladogenesis model (Garzione et al., 2000) as carried out in the software Lagrange v.20130526 (Ree and Smith, 2008), and the chronogram obtained in BEAST was the starting component of the analyses.

## RESULTS

Phylogenetic analysis of concatenated sequences (mtDNA data and nuclear gene) recovered a well-resolved tree with six major clades (labeled A–F) within the *H. chinensis* group (**Figures 2**, **3**). Clade A corresponds to *H. tsinlingensis* and *H. annectans chuanxiensis*, which are mainly located in the Qinling-Dabie mountains; Clade B included *H. annectans*, *H. a. wulingensis*,


**FIGURE 2 |** Phylogenetic relationship of the *Hyla chinensis* group by Bayesian phylogenetic and maximum likelihood (ML) analysis based on concatenated sequences (mtDNA and nuclear genes). Values above branches indicate Bayesian posterior probabilities, below bootstrap values of the ML analysis. **(A–F)** represents the six clades within the *H. chinensis* group.

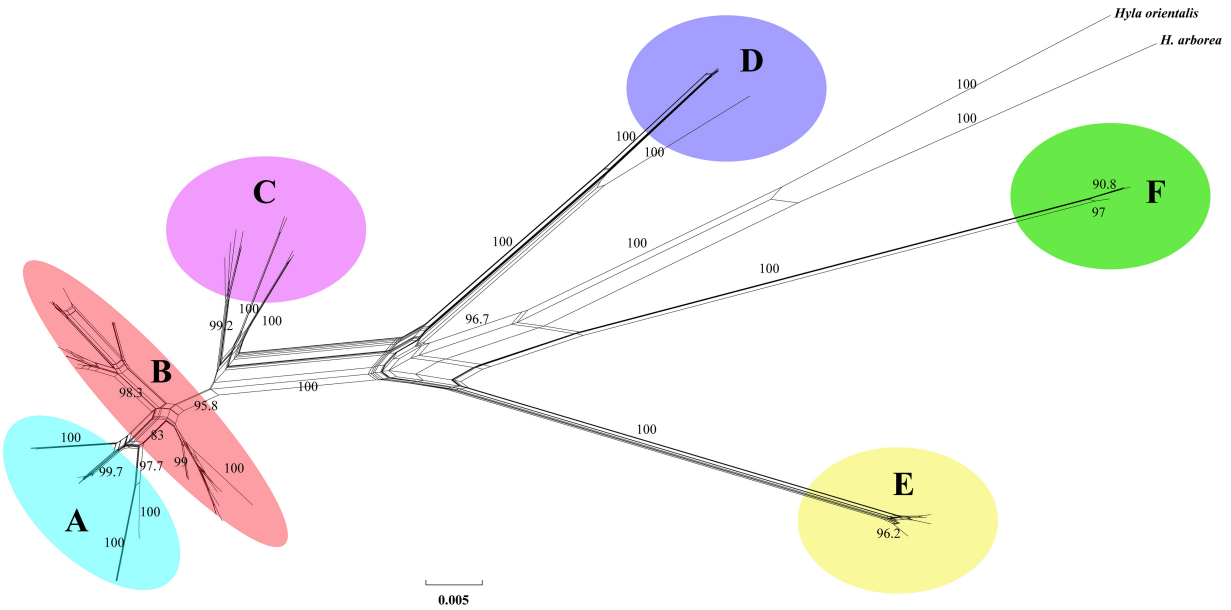


**FIGURE 3 |** Network constructed from the mtDNA genes of the *Hyla chinensis* group based on uncorrected p-distances using SPLITSTREE. The values on nodes indicate bootstrap support (only values above 75% are shown). **(A–F)** represents the six clades within the *H. chinensis* group.

and *H. a. jingdongensis*, while *H. a. gongshanensis* and *H. a. tengchongensis* are within clade C, and they are all distributed in the Yunnan-Guizhou Plateau and Sichuan Basin. The remaining clade D (i.e., *H. sanchiangensis*), E (i.e., *H. chinensis*), and F (i.e., *H. zhaopingensis*) are located in the Guangxi province, Hainan province, and the Eastern China, respectively (**Figures 2**, **3**). The phylogenetic network of the *H. chinensis* group showed the consistent groupings compared with the phylogenetic methods (**Figure 4**). Dating analyses indicated that the most recent common ancestor (MRCA) of the *H. chinensis* group dates back to 18.84 Mya [95% of the highest posterior density (HPD), 19.50–17.18 Mya] in the mid-Miocene. The divergence time between clades within the *H. chinensis* group was taken place from late Miocene (11.88 Mya) to the early Pleistocene (around 4.82 Mya) (**Figure 3**).

The BFD based on PS (BF, 12.62) and SS (BF, 20.84) models decisively supported six species in the *H. chinensis* group (**Table 2**), corresponding to the six clades disclosed by the phylogenetic tree (**Figures 2**, **3**). BPP methods also supported six separated species due to higher than 0.95 probability values (**Table 3**). Species tree, consistent with BPP tree topology, recovered a concordant, robust phylogenetic topology (**Figure 5**). Pairwise sequence divergence (p uncorrected distance) between hidden species in the *H. chinensis* group ranged from 2.1% (A vs. B) to 11.4% (E vs. F) (**Table 4**).

In the ancestral area reconstruction, the best model for the *H. chinensis* group was M2, which supported that it was dispersed from southern China to the Qinling-Dabie mountains and to the Eastern of the Tibetan Plateau was restricted (**Table 5**). The analyses supported the Southern China (Guangxi-Hainan provinces, Area N) and Eastern China (Area W) as the ancestral area of the *H. chinensis* group, and most speciation events were attributed to the progressive uplift of the Himalayas (**Figure 3** and **Supplementary Table S2**). Additionally, *H. tsinlingensis* originated from the Eastern of the Tibetan Plateau (Yunnan-Guizhou Plateau and Sichuan Basin, Area Y).

## DISCUSSION

The phylogenetic analysis identified all the individuals of the *H. chinensis* group formed into six genetically distinct population clusters (i.e., Clades A–F) (**Figures 2–4**). Based on BF and BPP methods, the species delimitation suggested that these six genetically distinct clades could be regarded as hidden separated species in the *H. chinensis* group, which also got the support from genetic distance (**Table 4**). In brief, clade A corresponds to *H. tsinlingensis* and *H. annectans chuanxiensis*; clade B included *H. annectans*, *H. a. wulingensis*, and *H. a. jingdongensis*; while *H. a. gongshanensis* and *H. a. tengchongensis* are within clade C. The remaining clades (D–F) corresponded to three putative species (*H. sanchiangensis*, *H. chinensis*, and *H. zhaopingensis*), respectively (**Figures 2**, **3**), which were supported by the various species delimitation analyses. Overall, compared with the study of Li et al. (2015), some minor differences exist: *H. annectans chuanxiensis* belongs to *H. tsinlingensis*, not *H. annectans*; two subspecies of *H. annectans* (*H. a. gongshanensis* and *H. a. tengchongensis*) were regarded as separated species. As for the species not involved (*H. simplex*), we cannot give corresponding conclusions due to missing key samples in our research. As mentioned by previous researchers, further clarification of the relationship of *H. simplex* and *H. zhaopingensis* can be resolved only based on the *H. simplex* from its type locality in Vietnam and in-depth analysis (Li et al., 2015).

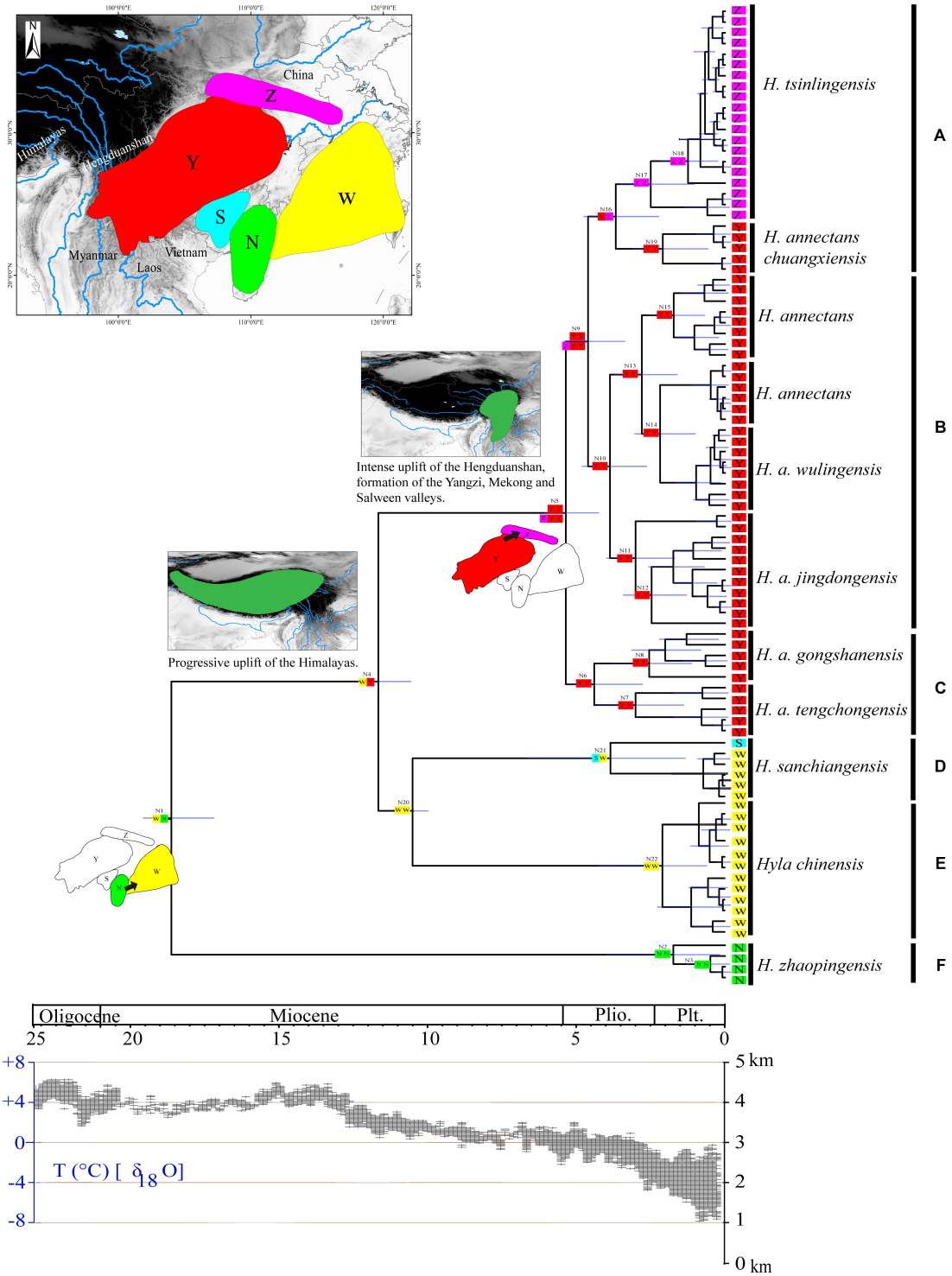


**FIGURE 4 |** Chronogram and ancestral reconstructions of the *Hyla chinensis* group. **Top panel:** time-calibrated phylogeny of the *H. chinensis* group based on mitochondrial dataset [the light blue bars through the nodes indicate 95% highest posterior densities (HPDs)] and ancestral area reconstruction by a dispersal-extinction-cladogenesis model (colored squares), two extensive dispersal events were shown for the origin of N1 and N5 (arrows represent the direction of dispersal), geological sequence of events related to the diversification of the *H. chinensis* group including a graphical representation of the extent of uplift of the Tibetan Plateau (TP) through time green shades indicate the portion of the Qinghai-Tibetan Plateau that had achieved altitudes comparable to present day (adapted from Favre et al., 2015). Areas divided for reconstructing ancestral areas are displayed in the top left: N, Southern China (Guangxi-Hainan provinces); W, Eastern China; S, the southern Guangxi province in China; Y, the eastern of the Tibetan Plateau (Yunnan-Guizhou Plateau and Sichuan Basin); Z, the Tsinling-Dabie mountains. **Lower panel:** temperature changes (Zachos et al., 2001, 2008). **(A–F)** represents the six clades within the *H. chinensis* group.

**TABLE 2 |** Species delimitation results of the *Hyla chinensis* group.

| Model | Species | MLE Path Sampling (PS) | MLE Stepping Stone (SS) | Rank | BF (PS) | BF (SS) |
|---|---|---|---|---|---|---|
| True | 6 | −7908.64 | −7875.13 | 1 | 12.62 | 20.84 |
| Lump | 5 | −7966.71 | −7937.86 | 4 | – | – |
| Split | 8 | −7914.95 | −7885.55 | 2 | – | – |
| Reassign | 6 | −7964.56 | −7934.90 | 3 | – | – |

*MLE, marginal likelihood estimate; BF, Bayes factor; PS, path sampling; SS, stepping stone.*

**TABLE 3 |** The species delimitation results of the *Hyla chinensis* group based on mtDNA and nuclear gene data in Bayesian Phylogenetics and Phylogeography (BPP).

| Scheme | Prior distribution | | Posterior probabilities |
|---|---|---|---|
| | Θ | τ | |
| Scheme 1 | G (1, 100) | G (1, 2,000) | 0.98393 |
| Scheme 2 | G (1, 10) | G (1, 2,000) | 0.98877 |
| Scheme 3 | G (1, 10) | G (2, 2,000) | 0.98607 |

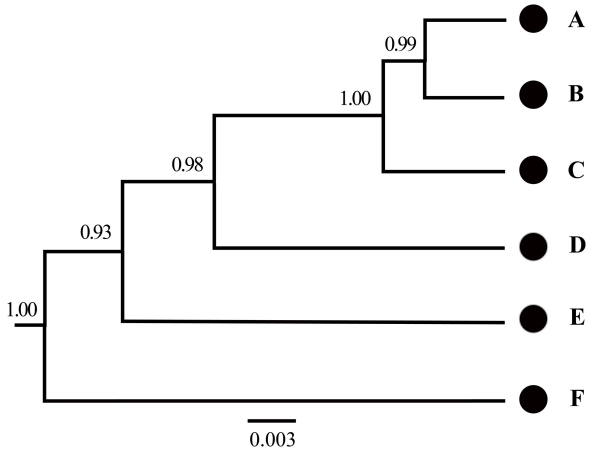


**FIGURE 5 |** Species tree estimated using BEAST based on mtDNA genes in the *Hyla chinensis* group. The letters **(A–F)** correspond to the clades in **Figures 2**, **3**. The values on nodes are Bayesian posterior probabilities.

**TABLE 4 |** Average genetic distances by Kimura two−parameter model among six candidate species within the *Hyla chinensis* group based on mtDNA genes.

| Clade | A | B | C | D | E | F |
|---|---|---|---|---|---|---|
| A | | | | | | |
| B | 0.010* | | | | | |
| C | 0.015* | 0.015* | | | | |
| D | 0.066* | 0.063* | 0.056* | | | |
| E | 0.082* | 0.073* | 0.071* | 0.090* | | |
| F | 0.100* | 0.096* | 0.096* | 0.105* | 0.110* | |

*Significant tests are indicated with an asterisk (*P < 0.01).*

**TABLE 5 |** Comparison of different dispersal models in Lagrange.

| Model | −lnL | Extinction rate | Dispersal rate |
|---|---|---|---|
| M0 | 20.80 | 5.595e−3 | 4.285e−09 |
| M1 | 20.40 | 6.724e−3 | 4.285e−09 |
| M2 | 20.38 | 8.422e−3 | 4.285e−09 |

*M0, unconstrained; M1, dispersal from southern China to the Qinling−Dabie mountains were restricted from W, N, S to Z; M2, dispersal from southern China to the Qinling−Dabie mountains and to the eastern of the Tibetan Plateau were restricted from W, N, S to Z and from N to Y. N, the southern China (Guangxi−Hainan provinces); W, Eastern China; S, the southern Guangxi province in China; Y, the eastern of the Tibetan Plateau (Yunnan−Guizhou Plateau and Sichuan Basin); Z, the Tsinling-Dabie mountains.*

In addition, for the distribution pattern of the clade D, this clade includes samples from Anhui and Guangxi; it seems that a large geographic gap exists between these places, which may hint the sampling incompleteness within this clade (Fei et al., 2012). These results represent a definitive molecular evidence for the taxonomic revision of each clade within the *H. chinensis* group. Nevertheless, in order to revise the group from a comprehensive perspective, a thorough quantitative multivariate analysis of the diagnostic morphological features and more key samples of unexplored species (e.g., *H. simplex*) is still required, and ideally, additional ecological evidence is required. During the Middle Eocene to Early Oligocene (45–34 Mya), the *Hyla* originated from North America, then diffused to China through the Bering Land Bridge, thus forming a branch of *Hyla* (Smith et al., 2005; Wiens et al., 2006; Li et al., 2015). In this study, the dated phylogenetic tree indicated that the Clade F (about 18.84 Mya) is at the base of the *H. chinensis* group and contains *H. zhaopingensis* in Southern China (Guangxi province). Six putative hidden species in the *H. chinensis* group (Clade A to F) approximately correspond to the three areas of China: the Eastern of Qinghai-Tibetan Plateau (i.e., the Yunnan-Guizhou Plateau and Sichuan Basin), the Eastern and Southern China, and the Qinling-Dabie mountains. Additionally, the first stage of speciation (e.g., split between Clades D and E) in the *H. chinensis* group occurs in Southern and Eastern in China during the Middle Miocene (ca. 18–10 Ma). *Hyla* is a small, arboreal, and semiaquatic frog; prefers to live in warm and damp environments, which widely inhabits boscages, paddy fields, or edges of rivers; and breeds in still water in ponds or paddy fields (Fei, 2005). During this period, the southern China humid climate is conducive to the survival of the species. For example, paleobotanical data indicated that the southeastern of the QTP has a warm and humid climate, was dominated by subtropical vegetation during the Miocene (Jacques et al., 2011), which had provided an opportunity for the first stage of speciation in the *H. chinensis* group.

The second stage of speciation in the *H. chinensis* group occurs in the Southwest of China (Yunnan Province and Sichuan Province) and the Qinling Mountains–Dabie Mountains in China from the late Miocene to Pliocene (5.57∼4.82 Mya). During the Late Miocene to Pliocene, the progressive uplift of the QTP particularly at its eastern and northern margins (mostly province of Yunnan, Sichuan, and Qinghai) led to the formation of some rivers; the Hengduanshan hot spot of biodiversity was composed of

those areas (Favre et al., 2015). In addition, the upheaval of the QTP had a significant impact on the atmospheric circulation in Asia and promoted the development of the Asian monsoon system (Kutzbach et al., 1993; Tang et al., 2013). The East Asian Monsoon system has controlled China's climate at that time, and this condition brought moisture air from the ocean to East China (Liu et al., 2009). Combining the geological events, they may be contributed to the second stage of speciation in the *H. chinensis* group.

In conclusion, although a previous study had demonstrated that the *Hyla* originated from North America, then diffused to China *via* Beringia during the Middle Eocene to Early Oligocene (Smith et al., 2005; Wiens et al., 2006; Li et al., 2015), it did not mean that the speciation of the *H. chinensis* group may be from northern China to southern China. Under the framework of speciation time within the *H. chinensis* group, the rapid uplifting mountain ranges (the Tibetan Plateau and its adjacent mountain) formed a blocky orographic barrier for many endemic species (Favre et al., 2015), which also played an important role in the formation of the Asian monsoon system (Guo et al., 2008; Song et al., 2010; Tang et al., 2013). Additionally, three East Asian monsoon intensification periods (∼15 Ma, ∼8 Ma, and 4–3 Ma) (Wan et al., 2007; Molnar et al., 2010; Jacques et al., 2011) also had urged the formation of humid and warm climates in south China (Sun and Wang, 2005), which was favorable for geographical dispersal, especially for amphibians (Che et al., 2010; Wu et al., 2013; Yan et al., 2013; Ye et al., 2013). More dispersal events often means that these species had more opportunities for allopatric divergence, which greatly affected the high levels of inter-population genetic divergence and unique patterns of genetic structure (Che et al., 2010; Wu et al., 2013; Yan et al., 2013; Ye et al., 2013; Favre et al., 2015). Therefore, based on those results, unlike the history of the *Hyla* evolution (North America→Beringia→China) (Smith et al., 2005; Wiens et al., 2006; Li et al., 2015), we can infer that the speciation and diffusion in the *H. chinensis* group had been from Guangxi-Hainan provinces to Guangxi province and Eastern China, and then to the Yunnan-Guizhou Plateau and Sichuan Basin, finally spread to Qinling-Dabie mountains. The diversification and speciation in the *H. chinensis* group also may be related to the special geological deformations and the climatic history.

## CONCLUSION

As one of the species complexes in *Hyla*, the determined species number in the *H. chinensis* group was full of competing. Until now, no research focuses on the species delimitation based on the genetic data. In this study, different species delimitation approaches revealed that multiple species exist in the *H. chinensis* group. These methods indicated that there are six distinct species (from Clades A to F, respectively) in this species group. The progressive uplift of QTP and climate change led to the dispersal progress and formation of hidden species diversity in the *Hyla chinensis* group. Nevertheless, diagnostic morphological characters and other ecological evidences are still needed to supply for providing the integrative revision of this species group.

## DATA AVAILABILITY STATEMENT

The accession number(s) can be found in the table within this article.

## ETHICS STATEMENT

The animal study was reviewed and approved by the Anhui Normal University.

## AUTHOR CONTRIBUTIONS

BZ, JL, and XW conceived the study. PY and TP contributed to sample collection. PY, GW, TP, XK, IA, and WZ carried out the laboratory work. PY, GW, TP, and XK analyzed the data and wrote the manuscript with contributions from BZ, XW, JL, PY, and TP. IA corrected the language. All authors approved the final version of the manuscript and agreed to be held accountable for its content.

## FUNDING

This work is supported by the Anhui Natural Science Foundation (Youth, 1908085QC127), 2018 Funding for research activities of postdoctoral researchers in Anhui Province in the design of study, fieldwork, sample collection, lab work, and data analysis. The writing and publishing were supported by the Anhui Province Academic and Technical Leader & Backup Candidate Academic Research Activities Fund (2017H130).

## ACKNOWLEDGMENTS

We are grateful to Chaochao Hu, Lifu Qian, Ke Fang, Chengcheng Wang, Yanan Zhang, and Xiaonan Sun for their help in the wild survey and data analysis. This manuscript has been released as a preprint at Research Square.

## SUPPLEMENTARY MATERIAL

The Supplementary Material for this article can be found online at: https://www.frontiersin.org/articles/10.3389/fevo.2020.00234/full#supplementary-material

## REFERENCES


Aldhebiani, A. Y. (2018). Species concept and speciation. *Saudi J. Biol. Sci.* 25, 437–440. doi: 10.1016/j.sjbs.2017.04.013

Benton, M. J. (2009). The Red Queen and the Court Jester: species diversity and the role of biotic and abiotic factors through time. *Science* 323, 728–732. doi: 10.1126/science.1157719

Blair, C., and Bryson, J. R. (2017). Cryptic diversity and discordance in single-locus species delimitation methods within horned lizards (Phrynosomatidae: *Phrynosoma*). *Mol. Ecol. Res.* 17, 1–15.

Burland, T. G. (1999). "DNASTAR's Lasergene sequence analysis software," in *Bioinformatics Methods and Protocols*, eds S. Misener, and S. A. Krawetz (Totowa, NJ: Humana Press), 71–91. doi: 10.1385/1-59259-192-2:71

Chacón, J., and Renner, S. S. (2014). Assessing model sensitivity in ancestral area reconstruction using lagrange: a case study using the Colchicaceae family. *J. Biogeogr.* 41, 1414–1427. doi: 10.1111/jbi.12301

Che, J., Zhou, W. W., Hu, J. S., Yan, F., Papenfuss, T. J., Wake, D. B., et al. (2010). Spiny frogs (*Paini*) illuminate the history of the Himalayan region and Southeast Asia. *Proc. Natl. Acad. Sci. U.S.A.* 107, 13765–13770. doi: 10.1073/pnas.1008415107

Darriba, D., Taboada, G. L., Doallo, R., and Posada, D. (2012). JModelTest 2: more models, new heuristics and parallel computing. *Nat. Methods* 9:772. doi: 10.1038/nmeth.2109

Drummond, A. J., Suchard, M. A., Xie, D., and Rambaut, A. (2012). Bayesian phylogenetics with BEAUti and the BEAST 1.7. *Mol. Biol. Evol.* 29, 1969–1973. doi: 10.1093/molbev/mss075

Fan, Y., Wu, R., Chen, M. H., Kuo, L., and Lewis, P. O. (2011). Choosing among partition models in Bayesian phylogenetics. *Mol. Biol. Evol.* 28, 523–532. doi: 10.1093/molbev/msq224

Favre, A., Päckert, M., Pauls, S. U., Jähnig, S. C., Uhl, D., Michalak, I., et al. (2015). The role of the uplift of the Qinghai-Tibetan Plateau for the evolution of Tibetan biotas. *Biol. Rev.* 90:236. doi: 10.1111/brv.12107

Fei, L. (2005). *An Illustrated Key to Chinese Amphibians*. Chengdu: Sichuan Publ. Group.

Fei, L., Hu, S. Q., Ye, C. Y., and Huang, Y. Z. (2009). *Fauna Sinica. Amphibia Vol. 2 Anura*. Beijing: Science Press.

Fei, L., Ye, C. Y., and Jiang, J. P. (2012). *Colored Atlas of Chinese Amphibians and their Distributions*. Chengdu: Sichuan Publishing House of Science and Technology.

Frost, D. R. (2014). *Amphibian Species of the World: An Online Reference. Version 6.0*. New York, NY: American Museum of Natural History.

Gao, Y., Ai, B., Kong, H. H., Kang, M., and Huang, H. W. (2015). Geographical pattern of isolation and diversification in karst habitat islands: a case study in the *Primulina eburnea* complex. *J. Biogeogr.* 42, 2131–2144.

Garzione, C. N., Dettman, D. L., Quade, J., Decelles, P. G., and Butler, R. F. (2000). High times on the Tibetan Plateau: paleoelevation of the *Thakkhola graben*. *Nepal Geol.* 28, 339–342. doi: 10.1130/0091-7613(2000)028<0339:htottp>2.3.co;2

Grummer, J. A., Bryson, R. W., and Reeder, T. W. (2014). Species delimitation using Bayes factors: simulations and application to the *Sceloporus scalaris* species group (Squamata: Phrynosomatidae). *Syst. Biol.* 63, 119–133. doi: 10.1093/sysbio/syt069

Guo, Z. T., Sun, B., Zhang, Z. S., Peng, S. Z., Xiao, G. Q., Ge, J. Y., et al. (2008). A major reorganization of Asian climate by the early Miocene. *Clim. Past* 4, 153–174. doi: 10.5194/cp-4-153-2008

Heled, J., and Drummond, A. J. (2010). Bayesian inference of species trees from multilocus data. *Mol. Biol. Evol.* 27, 570–580. doi: 10.1093/molbev/msp274

Hua, X., Fu, C. Z., Li, J. T., De Oca, A. N. M., and Wiens, J. J. (2009). A revised phylogeny of Holarctic treefrogs (genus *Hyla*) based on nuclear and mitochondrial DNA sequences. *Herpetologica* 65, 246–259. doi: 10.1655/08-058r1.1

Huang, Z. S., Yu, F. L., Gong, H. S., Song, Y. L., Zeng, Z. G., and Zhang, Q. (2017). Phylogeographical structure and demographic expansion in the endemic alpine stream salamander (Hynobiidae: *Batrachuperus*) of the Qinling Mountains. *Sci. Rep.* 7, 1–13.

Huson, D. H., and Bryant, D. (2006). Application of phylogenetic networks in evolutionary studies. *Mol. Biol. Evol.* 23, 254–267. doi: 10.1093/molbev/msj030

Jacques, F. M. B., Guo, S. X., Su, T., Xing, Y. W., Huang, Y. J., Liu, Y. S., et al. (2011). Quantitative reconstruction of the Late Miocene monsoon climates of southwest China: a case study of the Lincang flora from Yunnan Province. *Palaeogeogr. Palaeocl.* 304, 318–327. doi: 10.1016/j.palaeo.2010.04.014

Kajtoch, Ł, Montagna, M., and Wanat, M. (2017). Species delimitation within the *Bothryorrhynchapion weevils*: multiple evidence from genetics, morphology and ecological associations. *Mol. Phylogenet. Evol.* 120, 354–363. doi: 10.1016/j.ympev.2017.12.022

Kotsakiozi, P., Jablonski, D., Ilgaz, Kumlutaş, Y., Avcı, A., Meiri, S., et al. (2018). Multilocus phylogeny and coalescent species delimitation in Kotschy's gecko, *Mediodactylus kotschyi*: hidden diversity and cryptic species. *Mol. Phylogenet. Evol.* 125, 177–187. doi: 10.1016/j.ympev.2018.03.022

Kutzbach, J. E., Prell, W. L., and Ruddiman, W. F. (1993). Sensitivity of Eurasian climate to surface uplift of the Tibetan Plateau. *J. Geol.* 101, 177–190. doi: 10.1086/648215

Leaché, A. D., and Fujita, M. K. (2010). Bayesian species delimitation in West African forest geckos (*Hemidactylus fasciatus*). *Proc. R. Soc. Lond. B Biol.* 277, 3071–3077. doi: 10.1098/rspb.2010.0662

Li, J. T., Wang, J. S., Nian, H. H., Litvinchuk, S. N., Wang, J. C., Li, Y., et al. (2015). Amphibians crossing the Bering Land Bridge: evidence from holarctic treefrogs (*Hyla*, Hylidae, Anura). *Mol. Phylogenet. Evol.* 87, 80–90. doi: 10.1016/j.ympev.2015.02.018

Li, S. M., and Yang, D. T. (1985). The description of a new subspecies *Hyla annectanus* gongshanensis from Yunnan. *Zool. Res.* 6, 23–28.

Li, W. L. S., and Drummond, A. J. (2012). Model averaging and Bayes factor calculation of relaxed molecular clocks in Bayesian phylogenetics. *Mol. Biol. Evol.* 29, 751–761. doi: 10.1093/molbev/msr232

Liu, L. P., Eronen, J. T., and Fortelius, M. (2009). Significant mid-latitude aridity in the middle Miocene of East Asia. *Palaeogeogr. Palaeocl.* 279, 201–206. doi: 10.1016/j.palaeo.2009.05.014

Molnar, P., Boos, W. R., and Battisti, D. S. (2010). Orographic controls on climate and paleoclimate of Asia: thermal and mechanical roles for the Tibetan Plateau. *Annu. Rev. Earth Publ. Sci.* 38, 77–102. doi: 10.1146/annurev-earth-040809-152456

Päckert, M., Martens, J., Sun, Y. H., Severinghaus, L. L., Nazarenko, A. A., Ting, J., et al. (2012). Horizontal and elevational phylogeographic patterns of Himalayan and Southeast Asian forest passerines (Aves: Passeriformes). *J. Biogeogr.* 39, 556–573. doi: 10.1111/j.1365-2699.2011.02606.x

Pan, T., Sun, Z. L., Lai, X. L., Orozcoterwengeld, P., Yan, P., Wu, G. Y., et al. (2019). Hidden species diversity in *Pachyhynobius*: a multiple approaches species delimitation with mitogenomes. *Mol. Phylogenet. Evol.* 137, 138–145. doi: 10.1016/j.ympev.2019.05.005

Rambaut, A. (2014). *FigTree. Version 1.4. 2*.

Rambaut, A., and Drummond, A. J. (2007). *Tracer v1.5*.

Rannala, B., and Yang, Z. H. (2003). Bayes estimation of species divergence times and ancestral population sizes using DNA sequences from multiple loci. *Genetics* 164, 1645–1656.

Ree, R. H., and Smith, S. A. (2008). Maximum likelihood inference of geographic range evolution by dispersal, local extinction, and cladogenesis. *Syst. Biol.* 57, 4–14. doi: 10.1080/10635150701883881

Ronquist, F., and Huelsenbeck, J. P. (2003). MrBayes 3: bayesian phylogenetic inference under mixed models. *Bioinformatics* 19, 1572–1574. doi: 10.1093/bioinformatics/btg180

Sambrook, J., Fritsch, E. F., and Maniatis, T. (1989). *Molecular Cloning*. New York, NY: Cold spring harbor laboratory press.

Shepard, D. B., and Burbrink, F. T. (2011). Local-scale environmental variation generates highly divergent lineages associated with stream drainages in a terrestrial salamander, *Plethodon caddoensis*. *Mol. Phylogenet. Evol.* 59, 399–411. doi: 10.1016/j.ympev.2011.03.007

Sheridan, J. A., and Stuart, B. L. (2018). Hidden species diversity in *Sylvirana nigrovittata* (Amphibia: Ranidae) highlights the importance of taxonomic revisions in biodiversity conservation. *PLoS One* 13:e0192766. doi: 10.1371/journal.pone.0192766

Smith, S. A., Stephens, P. R., and Wiens, J. J. (2005). Replicate patterns of species richness, historical biogeography, and phylogeny in Holarctic treefrogs. *Evolution* 59, 2433–2450. doi: 10.1111/j.0014-3820.2005.tb00953.x

Song, J. H., Kang, H. S., Byun, Y. H., and Hong, S. Y. (2010). Effects of the Tibetan Plateau on the Asian summer monsoon: a numerical case study using a regional climate model. *Int. J. Climatol.* 30, 743–759.

Stamatakis, A. (2008). *The RAxML 7.0. 3 Manual*. Heidelberg: Heidelberg Institute for Theoretical Studies.

Sullivan, J., and Joyce, P. (2005). Model selection in phylogenetics. *Annu. Rev. Ecol. Sci.* 36, 445–466.

Sun, X. G., and Wang, P. X. (2005). How old is the Asian monsoon system?—Palaeobotanical records from China. *Palaeogeogr. Palaeocl.* 222, 181–222. doi: 10.1016/j.palaeo.2005.03.005

Tamura, K., Peterson, D., Peterson, N., Stecher, G., Nei, M., and Kumar, S. (2011). MEGA5: molecular evolutionary genetics analysis using maximum likelihood, evolutionary distance, and maximum parsimony methods. *Mol. Biol. Evol.* 28, 2731–2739. doi: 10.1093/molbev/msr121

Tang, H., Micheels, A., Eronen, J. T., Ahrens, B., and Fortelius, M. (2013). Asynchronous responses of East Asian and Indian summer monsoons to mountain uplift shown by regional climate modelling experiments. *Clim. Dyn.* 40, 1531–1549. doi: 10.1007/s00382-012-1603-x

Tang, Y. X., and Zhang, Z. J. (1984). A new species of amphibians from Guangxi. *Acta Zootaxon. Sin.* 4:23.

Wan, S. M., Li, A. C., Clift, P. D., and Stuut, J. B. W. (2007). Development of the East Asian monsoon: mineralogical and sedimentologic records in the northern South China Sea since 20 Ma. *Palaeogeogr. Palaeocl.* 254, 561–582. doi: 10.1016/j.palaeo.2007.07.009

Wiens, J. J., Fetzner, J. W., Parkinson, C. L., and Reeder, T. W. (2005). Hylid frog phylogeny and sampling strategies for speciose clades. *Syst. Biol.* 54, 778–807. doi: 10.1080/10635150500234625

Wiens, J. J., Graham, C. H., Moen, D. S., Smith, S. A., and Reeder, T. W. (2006). Evolutionary and ecological causes of the latitudinal diversity gradient in hylid frogs: treefrog trees unearth the roots of high tropical diversity. *Am. Nat.* 168, 579–596. doi: 10.1086/507882

Wu, Y. K., Wang, Y. Z., Jiang, K., and Hanken, J. (2013). Significance of pre-Quaternary climate change for montane species diversity: insights from Asian salamanders (Salamandridae: *Pachytriton*). *Mol. Phylogenet. Evol.* 66, 380–390. doi: 10.1016/j.ympev.2012.10.011

Xie, W. G., Lewis, P. O., Fan, Y., Kuo, L., and Chen, M. H. (2011). Improving marginal likelihood estimation for Bayesian phylogenetic model selection. *Syst. Biol.* 60, 150–160. doi: 10.1093/sysbio/syq085

Yan, F., Zhou, W. W., Zhao, H. T., Yuan, Z. Y., Wang, Y. Y., Jiang, K., et al. (2013). Geological events play a larger role than Pleistocene climatic fluctuations in driving the genetic structure of *Quasipaa boulengeri* (Anura: Dicroglossidae). *Mol. Ecol.* 22, 1120–1133. doi: 10.1111/mec.12153

Yang, Z. H., and Rannala, B. (2010). Bayesian species delimitation using multilocus sequence data. *Proc. Natl. Acad. Sci. U.S.A.* 107, 9264–9269. doi: 10.1073/pnas.0913022107

Ye, S. P., Huang, H., Zheng, R. Q., Zhang, J. Y., Yang, G., and Xu, S. X. (2013). Phylogeographic analyses strongly suggest cryptic speciation in the giant spiny frog (Dicroglossidae: *Paa spinosa*) and interspecies hybridization in *Paa*. *PLoS One* 8:e70403. doi: 10.1371/journal.pone.0070403

Zachos, J., Pagani, M., Sloan, L., Thomas, E., and Billups, K. (2001). Trends, rhythms, and aberrations in global climate 65 Ma to present. *Science* 292, 686–693. doi: 10.1126/science.1059412

Zachos, J. C., Dickens, G. R., and Zeebe, R. E. (2008). An early Cenozoic perspective on greenhouse warming and carbon-cycle dynamics. *Nature* 451, 279–283. doi: 10.1038/nature06588

Zhen, Y., Chen, P. P., and Bu, W. J. (2016). Terrestrial mountain islands and Pleistocene climate fluctuations as motors for speciation: a case study on the genus *Pseudovelia* (Hemiptera: Veliidae). *Sci. Rep.* 6:33625.

**Conflict of Interest:** The authors declare that the research was conducted in the absence of any commercial or financial relationships that could be construed as a potential conflict of interest.

frontiers in Ecology and Evolution

ORIGINAL RESEARCH
published: 14 August 2020
doi: 10.3389/fevo.2020.00255

# Diversity of Fagaceae on Hainan Island of South China During the Middle Eocene: Implications for Phytogeography and Paleoecology

*Xiaoyan Liu[1,2,3]*, Hanzhang Song[2] and Jianhua Jin[2]**

[1] School of Geography, South China Normal University, Guangzhou, China, [2] State Key Laboratory of Biocontrol and Guangdong Provincial Key Laboratory of Plant Resources, School of Life Sciences, Sun Yat-sen University, Guangzhou, China, [3] Key Laboratory of Economic Stratigraphy and Palaeogeography, Nanjing Institute of Geology and Palaeontology, Chinese Academy of Sciences, Nanjing, China

The Fagaceae family is currently widespread throughout tropical and temperate regions of South America and the Northern Hemisphere, especially East Asia, and has likely been so since the Eocene, according to fossil records. In China, Fagaceae fossils are rare in the lowest latitudes of South China. Here, we describe 12 species in 5 genera of Fagaceae (i.e., *Berryophyllum*, *Castaneophyllum*, *Quercus, Castanopsis*, and *Lithocarpus*) based on leaf morphology and trichomes. These fossils are recovered from the Changchang Formation of Changchang Basin, Hainan Island, South China, indicating that Fagaceae has been distributed in the tropical low latitudes since the Eocene. Given that our fossils are closely related to the tropical and subtropical extant species, we speculate that Fagaceae lineages have likely diverged since the Eocene and that each extant lineage, such as *Quercus* sect. *Cyclobalanopsis*, became highly differentiated no later than middle Eocene. Based on the current living conditions of the extant species, we further speculate that the climate of Hainan Island was warm and wet during the middle Eocene, suitable for the growth and differentiation of the family.

**Keywords: Fagaceae, Eocene, South China, phytogeography, paleoecology**

OPEN ACCESS

***Edited by:***
*Zehao Shen,*
*Peking University, China*

***Reviewed by:***
*Min Deng,*
*Yunnan University, China*
*Yaowu Xing,*
*Xishuangbanna Tropical Botanical Garden (CAS), China*

****Correspondence:***
*Xiaoyan Liu*
*lxy_0628@163.com*
*Jianhua Jin*
*lssjjh@mail.sysu.edu.cn*

***Specialty section:***
*This article was submitted to Biogeography and Macroecology, a section of the journal Frontiers in Ecology and Evolution*

***Received:*** *10 April 2020*
***Accepted:*** *13 July 2020*
***Published:*** *14 August 2020*

***Citation:***
*Liu X, Song H and Jin J (2020) Diversity of Fagaceae on Hainan Island of South China During the Middle Eocene: Implications for Phytogeography and Paleoecology. Front. Ecol. Evol. 8:255. doi: 10.3389/fevo.2020.00255*

## INTRODUCTION

The woody angiosperms family Fagaceae, which includes beeches and oaks, defines the structure of subtropical and tropical evergreen forests (Tang, 2015; Wilf et al., 2019). The family is subdivided into ten extant genera: *Fagus* L., *Formanodendron* Nixon et Crepet, *Trigonobalanus* Forman, *Colombobalanus* Nixon et Crepet, *Castanopsis* (D. Don) Spach, *Castanea* Miller, *Notholithocarpus* Manos, Cannon et S. Oh, *Lithocarpus* Bl., *Quercus* L., and *Chrysolepis* Hjelmqvist (Larson-Johnson, 2016). Widely distributed in temperate, subtropical, and tropical regions of the Northern Hemisphere and South America (Huang et al., 1999; Chen, 2007), Fagaceae is most diverse in South and Southeast Asia and North America (Zhou, 1999; Chen, 2007; Denk et al., 2017; Xu et al., 2019). Of the approximately 927 species in 10 genera, China hosts 294 species in 6 genera: *Fagus*, *Formanodendron*, *Castanopsis*, *Castanea*, *Lithocarpus*, and *Quercus*, most of which are found in South and Southwest China (Li, 1996; Huang et al., 1999). Characterizing the evolution and distribution of Fagaceae in this region is important for understanding this keystone family.

Fagaceae has several distinct features that help define the family, as well as its genera. Its diagnostic leaf characteristics are simple leaves with obliquely-oriented tertiary veins, anomocytic and/or cyclocytic stomatal complexes, and specific trichome complements (Jones, 1986). Of the nine main morphotypes, the two most common are the craspedodromous "chestnut"-like forms or the coarsely round-toothed, deciduous forms, both found among the genera *Castanopsis*, *Castanea*, *Lithocarpus, and Quercus*. Trichome is one of the important characteristics of Fagaceae and can be divided into glandular, intermediate, and non-glandular. Simple uniseriate trichome, a glandular trichome, usually occurs in *Lithocarpus*, *Notholithocarpus* and few species of *Q.* sect. *Cyclobalanopsis* (Luo and Zhou, 2001; Liu et al., 2009; Deng et al., 2013). Stellate trichomes are widely present in *Castanopsis*, *Castanea*, *Quercus*, and *Lithocarpus*, representing a symplesiomorphic feature (Liu et al., 2009). Appressed parallel tufts (APT) trichome is unique trichome type in the genus *Lithocarpus*. Therefore, above genera are distinguishable based on the combining characters of venation, tooth type and trichomes.

The Cenozoic is arguably the most important geologic era for the evolution of global angiosperms (Xing et al., 2015) and although the earliest fagaceous fossils were found in the Late Cretaceous, it wasn't until later in the Cenozoic that the family evolved and spread. These earliest fagaceous fossils include *Antiquacupula sulcata* Sims, Herendeen et Crane and *Protofagacea allonensis* Herendeen, Crane et Drinnan with inflorescences and fruit characteristics similar to some taxa of Fagaceae and Nothofagaceae (Herendeen et al., 1995; Sims et al., 1998). From a single Cretaceous site in Georgia USA into the Paleocene, the family became widely distributed in Europe, Asia, and North America (**Figure 1**). Fagaceous fossils from this epoch are mainly assigned to extinct fossil genera, e.g., *Berryophyllum* Jones et Dilcher, *Castaneophyllum* Jones et Dilcher, and *Trigonobalanoidea* Crepet et Nixon (Takhtajan, 1982; Jones and Dilcher, 1988; Crepet and Nixon, 1989a; Kvaček and Walther, 2010). Although *Trigonobalanoidea* has some similar fruits with the extant *Trigonobalanus doichangensis* (A. Camus) Forman and *T. excels* Loz.-Contr., Hern.Com. et Henao-S., there remain many differences (Crepet and Nixon, 1989a) and there is currently no convincing evidence for modern genera Fagaceae during the Paleocene.

The warm and wet climate of the Eocene was critical for the diversification, differentiation, and formation of modern flora, including Fagaceae. Based on numerous reports of leaves, fruits, and dispersed pollen, the fossil record of Fagaceae is well known in for the Northern Hemisphere (**Figure 1**) and one record from the early Eocene in South Argentina (Wilf et al., 2019). Fagaceae became more diverse and widely distributed with the appearance of many modern genera including *Fagus*, *Trigonobalanus*, *Castanopsis*, *Castanea*, *Lithocarpus*, and *Quercus* (**Figure 1**; MacGinitie, 1953, 1969; Axelrod, 1966a,b, 1998a; Writing Group of Cenozoic Plants of China [WGCPC], 1978; Crepet and Daghlian, 1980; Takhtajan, 1982; Mai and Walther, 1985; Kvaček and Walther, 1989; Manchester, 1994; Zhou, 1996; Manchester and Dillhoff, 2004; Vikulin, 2011), as well as two extinct genera (*Berryophyllum* Jones et Dilcher and *Castaneophyllum* Jones et Dilcher). Into the Oligocene, however, the distribution of other genera has been reduced with the exception of *Quercus* which remain widely distributed in Europe, Asia, and North America (**Figure 1**, Writing Group of Cenozoic Plants of China [WGCPC], 1978; Takhtajan, 1982; Daghlian and Crepet, 1983; Manchester and Crane, 1983; Crepet and Nixon, 1989b; Kvaček and Walther, 1989, 2004, 2010; Meyer and Manchester, 1997). From the Miocene, some extant genera had begun to flourish in Europe, Asia, and North America while *Berryophyllum* and *Castaneophyllum* had almost disappeared (**Figure 1**, Axelrod, 1956, 1962; Wolfe and Tanai, 1980; Takhtajan, 1982; Kvaček and Walther, 1989; Palamarev and Tsenov, 2004; Hably, 2013).

In China, previously reported Fagaceae fossils were mainly recovered from the Eocene to Pleistocene strata in the northern and southwestern regions, including Liaoning, Shandong, Tibet, Sichuan, and Yunnan (Writing Group of Cenozoic Plants of China [WGCPC], 1978; Liu et al., 1995; Tao et al., 2000; Xiao et al., 2006; Xing et al., 2013; He et al., 2014; Wu et al., 2014; Li et al., 2015). Reports on Fagaceae fossils from the tropical low latitudes of South China are rare. The fossil history and its biogeographic implications of Fagaceae have been previously discussed (Zhou, 1999; Chen, 2007) given the continuous increase of this family's fossil record in recent years (Mindall et al., 2007, 2009; Vikulin, 2011; Xing et al., 2013; He et al., 2014; Wu et al., 2014; Jia et al., 2015; Li et al., 2015; Xu et al., 2016; Wilf et al., 2019), the diversity, and phytogeographic history of the family need to be further studied.

In this study, we studied 41 leaf fossils of Fagaceae recovered from the middle Eocene of Changchang Formation, Changchang Basin, Hainan Island, South China. Twelve species within 5 genera (*Berryophyllum* Jones et Dilcher, *Castaneophyllum* Jones et Dilcher, *Castanopsis*, *Lithocarpus,* and *Quercus*) have been described based on the leaf morphology and trichomes via Scanning Electron Microscopy (SEM). The present discovery documents a tropical low latitude distribution of Fagaceae in the middle Eocene. Moreover, our fossils are closely related to the extant tropical and subtropical elements, providing an important contribution to the understanding of the historical biogeography of this family and the paleoecology of Hainan Island during the middle Eocene.

## MATERIALS AND METHODS

The present fossils were collected from the Changchang Formation of Changchang Basin (**Figure 2**, 19°38′03″N, 110°27″04″E), located near Jiazi Town, Qiongshan County, in the northeastern part of Hainan Island, South China and housed in the Museum of Biology, Sun Yat-sen University, Guangzhou, China.

The Changchang Formation is composed of two parts: the lower coal-bearing part is ca. 52–54 m thick and consists of clastic terrigenous and coal deposits with mudstone, coaly shale, oil-bearing shale, muddy siltstone, and sandstone, and coal; the upper part is ca. 37–40 m thick and consists predominantly of lacustrine and fluvial mudstones, siltstones, and sandstones (Spicer et al., 2014). Numerous well-preserved plant macrofossils,

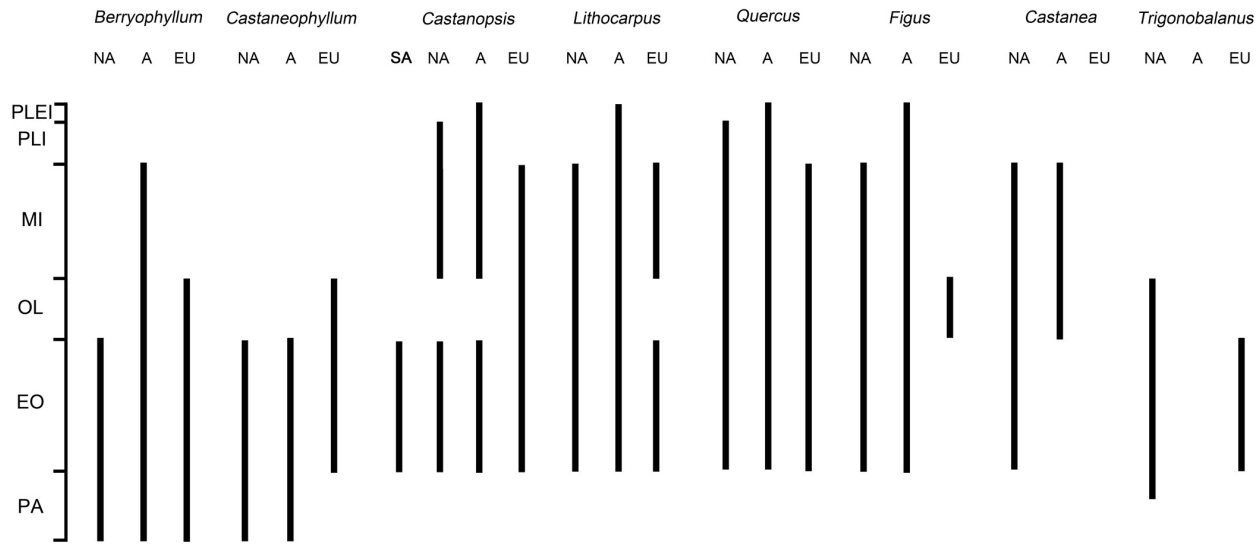


**FIGURE 1 |** Fossil records of Fagaceae in the Cenozoic. PA, Paleocene; EO, Eocene; OL, Oligocene; MI, Miocene; PLI, Pliocene; PLEI, Pleistocene; SA, South America; NA, North America; A, Asia; EU, Europe. References for the fossil records are listed in S1 (**Supplementary Material**).

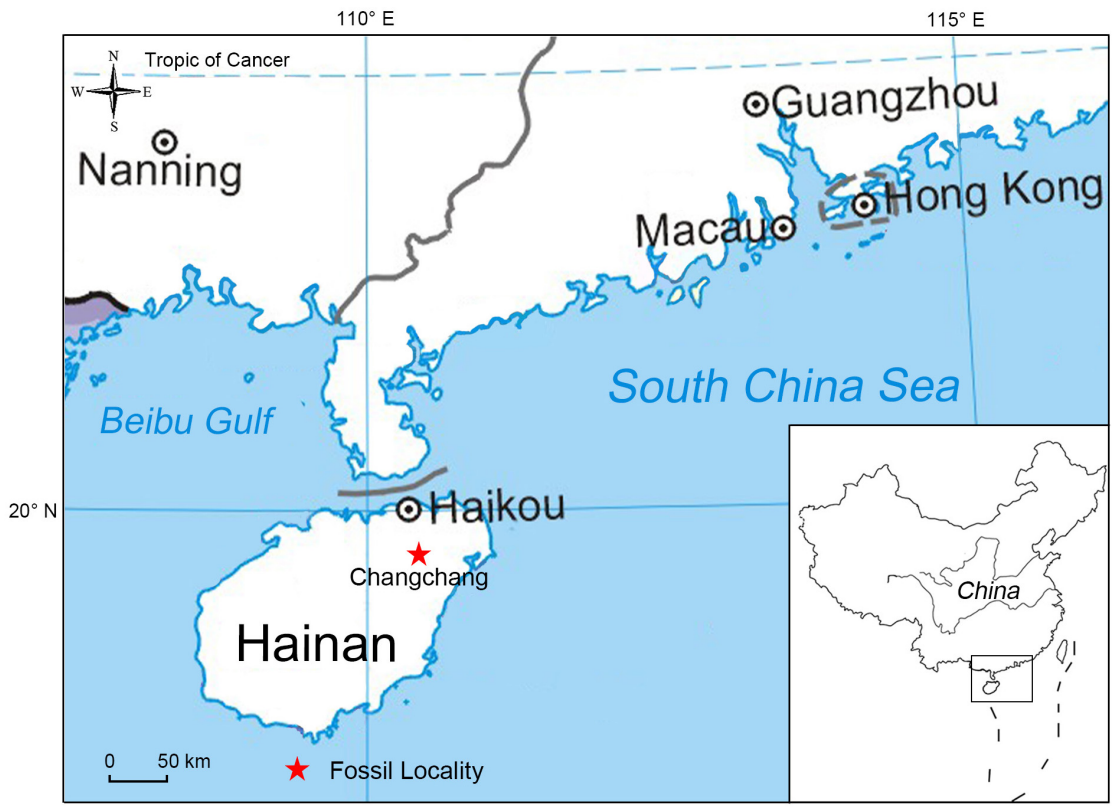


**FIGURE 2 |** Geographic map of the fossil locality. Base map modified after the Standard Map Service of the National Administration of Surveying, Mapping and Geoinformation of China (http://bzdt.ch.mnr.gov.cn/).

including the fagaceous leaf fossils investigated here, were mainly collected from the lower part of the Changchang Formation. These deposits also contain diverse pollen and spore assemblages (Zhang, 1980; Lei et al., 1992; Yao et al., 2009; Hofmann et al., 2019), as well as bivalve and gastropod remains, and fish bones and scales. The age of the Changchang Formation was originally

considered to be the late Palaeocene to early/middle Eocene based on floral composition (Guo, 1979). Later, the Changchang Formation is dated on the basis of palynological data as the middle Oligocene (Zhang, 1980), the late early Eocene to early late Eocene (Lei et al., 1992), and early middle Eocene (Yao et al., 2009). Recently, Spicer et al. (2014) dates the Changchang Formation as middle Eocene (Lutetian–Bartonian, ca.48–38 Ma) based on comprehensive analysis on the macrofossil flora, its similarity with the adjacent deposit Youganwo Formation in Maoming Basin, Guangdong Province, South China, and previously published palynological data. Here we followed the age assessment by Spicer et al. (2014).

Leaf fossils were photographed using a Canon EOS 500D digital camera (Canon, Tokyo, Japan). Small cuticular fragments of some species were recovered from the leaf fossils. Remnant rock particles adhering to the leaf fossils were removed using 40% HF for 24 h. The specimens were then rinsed in distilled water and mounted on stubs, coated with gold, and then examined and photographed using a JSM-6330F SEM (JSM, Tokyo, Japan).

We examined the extant specimens of *Quercus*, *Lithocarpus*, and *Castanopsis* represented in herbaria of the South China Botanical Garden, Chinese Academy of Sciences (IBSC, Guangzhou), Sun Yat-sen University (SYS, Guangzhou), Harvard University (HUH, Boston) and the University of Florida (FLAS, Gainesville). Leaf terminology follows Ellis et al. (2009). The following states and abbreviations are used for interpreting tooth types: convex (CV), straight (ST), concave (CC), retroflexed (RT; tooth flank is basally concave and apically convex). Tooth shape is described in terms of the distal and proximal flank curvatures relative to the midline of the tooth. The distal flank shape is always given first, e.g.: CV-ST indicates that the tooth is concave on the distal flank and straight on the proximal flank.

## RESULTS

**Order** Fagales Engl. 1892

**Family** Fagaceae Dumort. 1829

**Genus** *Berryophyllum* Jones et Dilcher, 1988

**Species** *Berryophyllum relongtanense* (Colani) Z. K. Zhou (**Figure 3**)

**Specimens examined** CC-998 (a, b), CC-1107

**Description** Leaf lanceolate (**Figure 3A**), 4.6–5.4 cm long, 1.5–1.6 cm wide, base cuneate (**Figure 3B**). Margin entire near base, serrate from > 1/3 of the leaf to the apex (**Figure 3A**), teeth CC-ST with rounded sinus (**Figure 3C**). Midvein thick, straight or slightly bend; secondary veins pinnate, opposite at base, alternate from the third pairs to apex, craspedodromous, with angles 30–40° between the midvein and secondary veins (**Figure 3A**); Tertiary veins mostly opposite percurrent; Quaternaries regular, rectangular to polygonal reticulate (**Figure 3C**). Leaf surface rugose with solitary trichomes and stomata (**Figures 3D–F**).

**Comparison** The present specimens are assigned to *Berryophyllum* because they have lanceolate leaves, cuneate bases, serrate margins with CC-ST teeth and craspedodromous secondary veins (**Figures 3A–C**). They are similar to *Dryophyllum puryearensis* Berry, *D. anomalum* Berry, and *B. tennesseensis* (Berry) Jones et Dilcher from the early Eocene of southeastern North America on the leaf shape (Berry, 1916; Jones and Dilcher, 1988), but they are different on venations. The present fossils are distinguished with *B. dewalquei* (Sap. et Mar.) Zhou (1996) and *B. yunnanense* (Colani) Zhou (1996) by the leaf shape, the trend and angle of secondary veins and the teeth (Writing Group of Cenozoic Plants of China [WGCPC], 1978; Zhou, 1996). Our specimens conform to the diagnosis of *B. relongtanense* (Colani) Z. K. Zhou previously recognized from Writing Group of Cenozoic Plants of China [WGCPC] (1978) and Zhou (1996).

**Species** *Berryophyllum hainanensis* X-Y Liu et J-H Jin sp. nov. (**Figure 4**).

**Diagnosis** Leaf narrowly lanceolate, apex elongate, acuminate or caudate bending to the right. Margin serrate up to the apex, teeth CC-ST to CC-CV with rounded sinus. Midvein straight to slightly bend in apex; secondary veins pinnate, nearly opposite, craspedodromous, bend inward in margin, with angles 40–50° between the midvein and secondary veins; Tertiary veins mixed percurrent; Quaternaries regular, rectangular to polygonal reticulate. Leaf surface rugose with verrucae.

**Holotype** CC-1244 (a, b)

**Paratypes** CC-1103, CC-1118 (a, b)

**Etymology** The specific epithet "*hainanensis*" refers to the Hainan Island from which the specimens were collected.

**Description** Leaf narrowly lanceolate (**Figures 4A–E**), preserved part 4.3–9.0 cm long, 1.5–1.6 cm wide, apex elongate, acuminate or caudate bending to the right (**Figures 4A,E**). Margin serrate up to the apex, irregular spaced (**Figures 4A,B,D,E**), teeth CC-ST to CC-CV with rounded sinus (**Figures 4B–D,F**). Midvein straight to slightly bend in apex; secondary veins pinnate, nearly opposite, craspedodromous, bend inward in margin, with angles 40–50° between the midvein and secondary veins (**Figures 4A,C,D**); Tertiary veins mixed percurrent; Quaternaries regular, rectangular to polygonal reticulate (**Figure 4C**). Leaf surface rugose with verrucae (**Figure 4G**).

**Comparison** The present specimens are distinguished from *B. relongtanense* which is also known from the same site, because they are narrowly lanceolate in shape while *B. relongtanense* is lanceolate. The present fossils are also different from the linear or extremely narrowly lanceolate leaves of *Berryophyllum tenuifolia* Jones and Dilcher (1988) and the lanceolate leaves of *B. dewalquei*, *B. yunnanense,* and *B. relongtanense* (Writing Group of Cenozoic Plants of China [WGCPC], 1978; Zhou, 1996). Our fossils are similar to *Dryophyllum berendtianum* (Goepp.) Kirchh. from the Eocene of Ukraine and Kaliningrad, Russia (Takhtajan, 1982) on having elongate acuminate or caudate apex with clear teeth. However, the teeth of our fossils have more irregular spaced teeth and narrower leaves than *D. berendtianum*. The features of narrowly lanceolate leaf shape with elongate acuminate or caudate apex, irregularly spaced CC-ST to CC-CV teeth and pinnate secondary veins without forming a loop convinced us to assign these fossils to a new species *B. hainanensis* sp. nov (**Figure 4**).

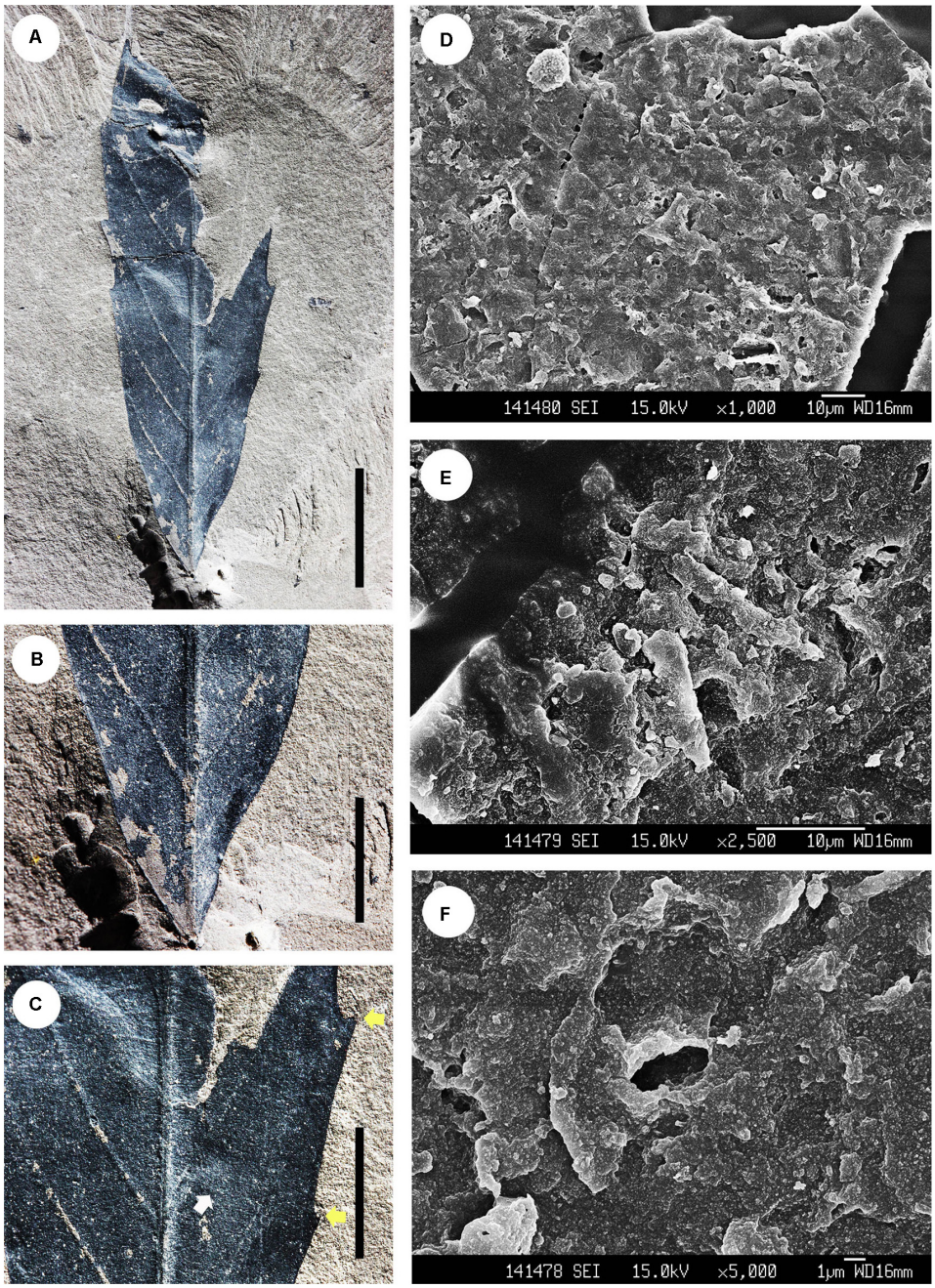


**FIGURE 3 |** Morphology of *Berryophyllum relongtanense* (Colani) Z.K. Zhou. **(A)** Specimen No. CC-998, showing leaf morphology; **(B)** enlargement of **(A)**, showing the base of the specimen; **(C)** enlargement of **(A)**, yellow arrows indicate leaf margin with teeth, white arrow indicates the tertiary and quaternary venations; **(D)** SEM image showing rugose structures on the outer surface of leaf; **(E)** showing solitary trichomes on the outer surface of leaf; **(F)** showing stomata on the outer surface of leaf. Scale bars: 10 mm **(A)**; 5 mm **(B,C)**.

**Genus** *Castaneophyllum* Jones et Dilcher, 1988

**Species** *Castaneophyllum hainanensis* X-Y Liu et J-H Jin sp. nov. (**Figure 5**)

**Diagnosis** Leaf lanceolate, base cuneate, symmetric. Margin entire near base, serrate from > 1/3 of the leaf to the apex, teeth ST-CC to CC-CC with rounded sinus; Tip slightly bend inward. Midvein thick, straight; secondary veins at least 10 pairs, pinnate, nearly opposite, craspedodromous, bend in ward near the margin; Tertiary veins mixed percurrent; Quaternaries regular, rectangular to polygonal reticulate. Leaf surface rugose with solitary trichomes.

**Holotype** CC-1260

**Paratypes** CC-1111, CC-1117, CC-1242, CC-1250

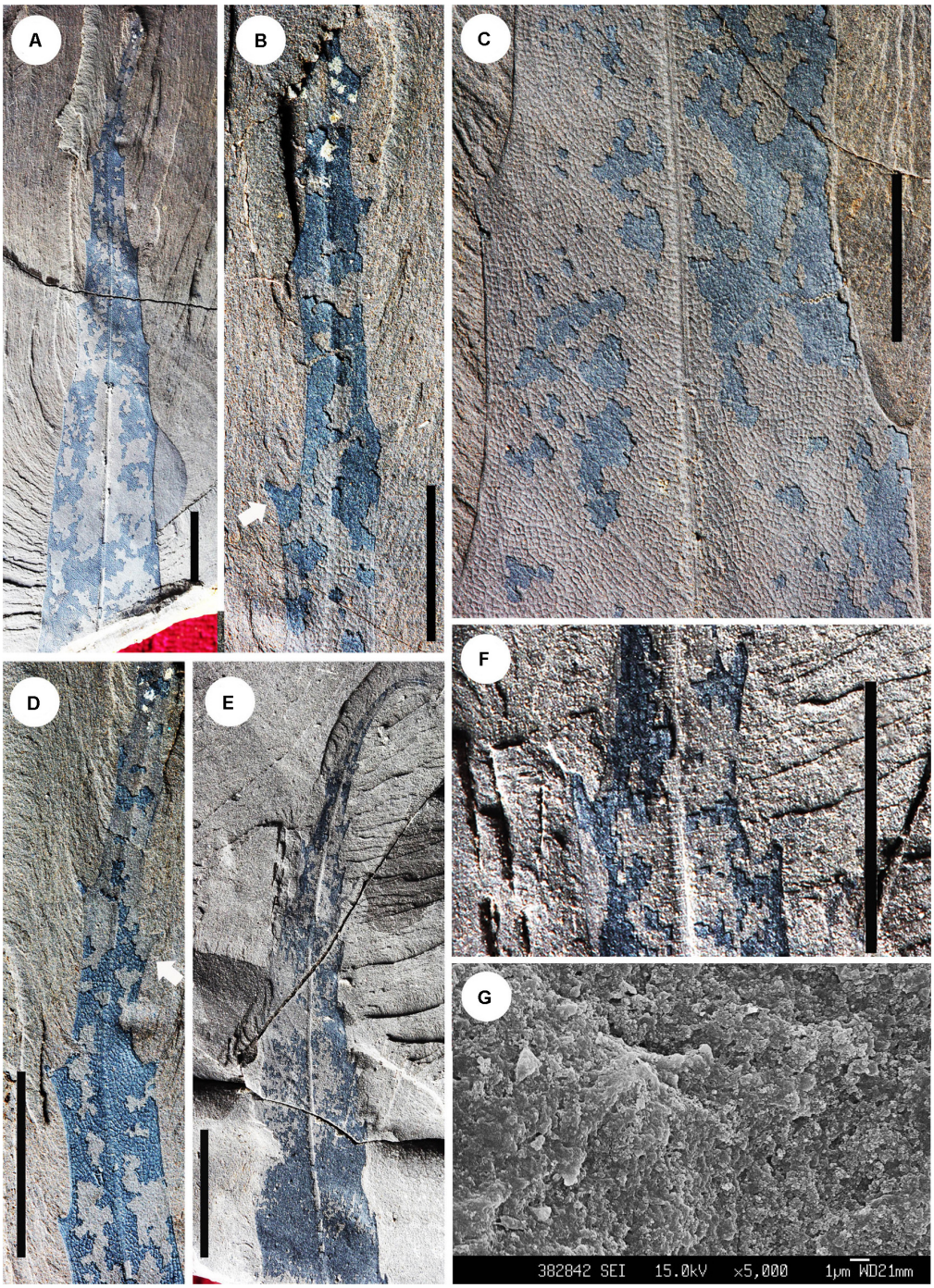


**FIGURE 4 |** Morphology of *Berryophyllum hainanensis* sp. nov. **(A)** Holotype. Specimen No. CC-1244a, showing leaf morphology; **(B)** specimen No. CC-1244b, arrow indicates the tooth; **(C)** enlargement of **(A)**, showing the tooth and venation; **(D)** enlargement of **(A)**, showing the apex with teeth (white arrow); **(E)** paratype. Specimen No. CC-1118a, showing the leaf shape; **(F)** enlargement of **(E)**, showing the teeth; **(G)** granular microstructure on the surface. Scale bars: 10 mm **(A,C,D)**; 5 mm **(B,E,F)**.

**Etymology** The specific epithet "*hainanensis*" refers to the Hainan Island from which the specimens were collected.

**Description** Leaf lanceolate (**Figure 5A**), preserved part 3.2–10.1 cm long, 1.2–2.0 cm wide, base cuneate, symmetric (**Figure 5A**). Margin entire near base, serrate from > 1/3 of the leaf to the apex (**Figure 5A**), teeth ST-CC to CC-CC with rounded sinus; Tip slightly bend inward (**Figure 5B**). Midvein thick, straight;

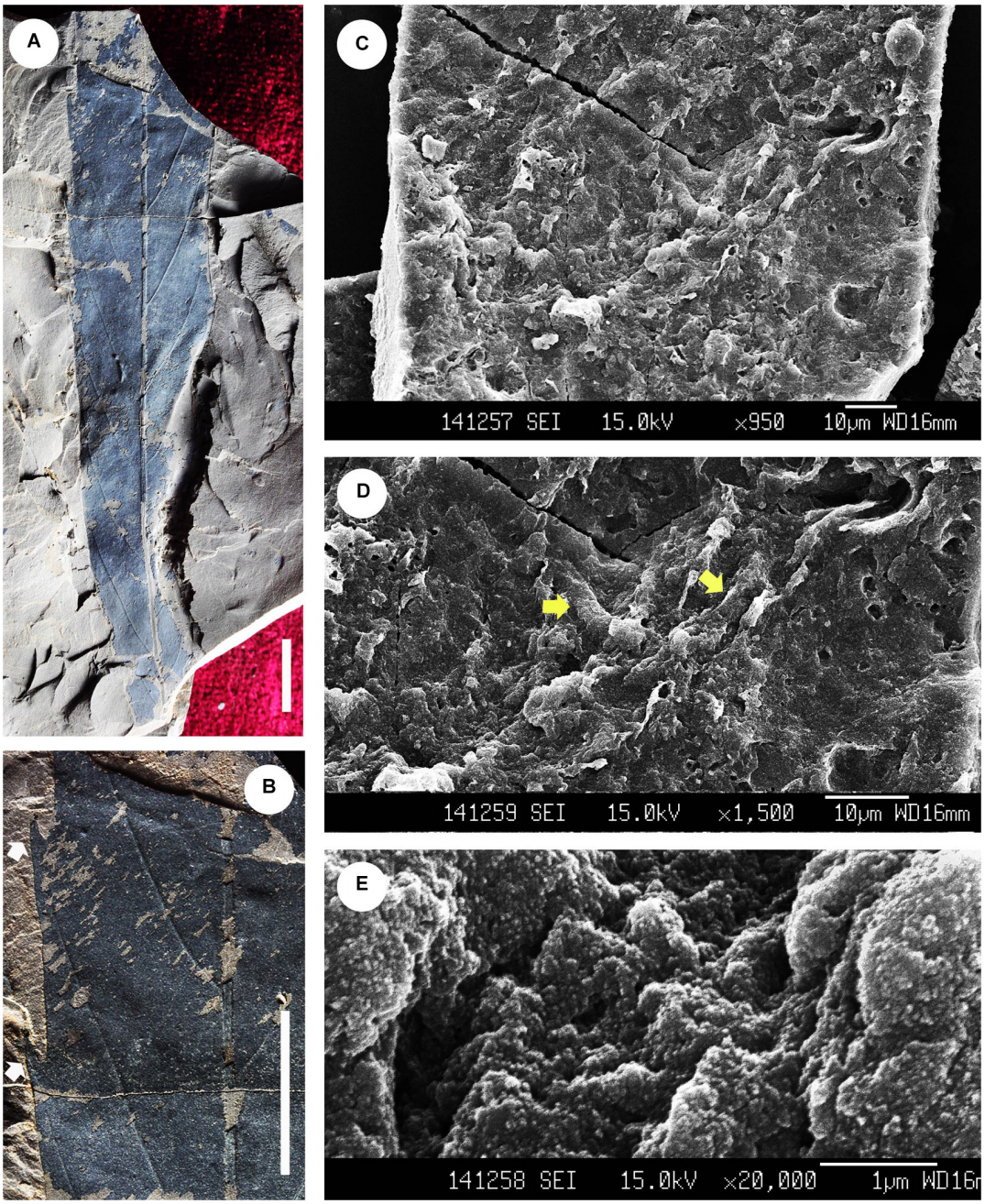


**FIGURE 5 |** Morphology of *Castaneophyllum hainanensis* sp. nov. **(A)** Holotype. Specimen No. CC-1260, showing leaf morphology; **(B)** enlargement of **(A)**, showing the venation, arrows indicate teeth; **(C)** SEM image showing the structures on the outer surface of leaf; **(D)** yellow arrows indicate the solitary trichomes on the outer surface of leaf; **(E)** SEM image showing rugose structures on the outer surface of leaf. Scale bars: 10 mm **(A,B)**.

secondary veins at least 10 pairs, pinnate, nearly opposite, craspedodromous, bend inward near the margin, with angles 50° between the midvein and secondary veins (**Figure 5A**); Tertiary veins mixed percurrent; Quaternaries regular, rectangular to polygonal reticulate (**Figure 5B**). Leaf surface rugose with solitary trichomes, 20.6–35.6 μm (mean = 27.6 μm) long, 2.0–5.1 μm (mean = 4.3 μm) wide (**Figures 5C,D**).

**Comparison** The present specimens are attributed to the *Castaneophyllum* rather than *Castanea* because their lanceolate leaf shape, craspedodromous and bend inward secondary veins and mixed percurrent tertiary veins are consistent with the *Castaneophyllum* (**Figures 5A,B**). Our specimens differ to *Castanea* on the secondary and tertiary veins. The secondary veins of *Castanea* are decurved near the midribs with two adjacent secondary veins near the midribs closer than those

near the margin. The tertiary veins of *Castanea* are opposite percurrent. This new species is similar to *Castaneophyllum tennesseense* (Berry) Jones et Dilcher (1988) from the Eocene of Tennessee, North America on the lanceolate leaf shape, but it is different on the teeth characters and arrangement of the secondary veins. Our specimens are distinguished from *C. moorii* (Lesq.) Jones et Dilcher (1988) which is elliptic to narrowly elliptic, 23 cm long and secondary veins closely spaced from the Eocene of Tennessee, by the leaf shape, size and venations. Our fossils greatly differ from *C. fushunense* (Chen et Wang) Z.K. Zhou from the Eocene of Fushun, Liaoning Province in teeth type and angles between midvein and secondary veins (Writing Group of Cenozoic Plants of China [WGCPC], 1978; Zhou, 1996).

**Species** *Castaneophyllum lanceolata* X-Y Liu et J-H Jin sp. nov. (**Figure 6**)

**Diagnosis** Leaf lanceolate, apex elongate acuminate, base cuneate. Margin entire near base, serrate from > 1/3 of the leaf to the apex, teeth ST-CV to CC-CV with rounded sinus. Midvein thick, straight; secondary veins 15 pairs, opposite from base to middle, pinnate from middle to apex, craspedodromous, bend in ward near the margin; Tertiary veins opposite percurrent; Quaternaries unclear. Leaf surface rugose with solitary trichomes.

**Holotype** CC-1106 (a, b)

**Etymology** The epithet "*lanceolata*" refers to the specimen has elongate lanceolate leaf.

**Description** Leaf lanceolate (**Figure 6A**), preserved part 12.6 cm long, 1.8 cm wide, length/width ratio 7, apex elongate acuminate with the angle 15°, base cuneate with the angle 30° (**Figures 6B,C**). Margin entire near base, serrate from > 1/3 of the leaf to the apex (**Figure 6A**), teeth ST-CV to CC-CV with rounded sinus (**Figures 6D–F**). Midvein thick, straight; secondary veins 15 pairs, opposite from base to middle, pinnate from middle to apex, craspedodromous, bend in ward near the margin, with angles 45° from base to the 3/4 of the leaf and declining up to the apex (**Figures 6A,E**); Tertiary veins opposite percurrent (**Figure 6F**); Quaternaries unclear. Leaf surface rugose with solitary trichomes, 15.6–18.8 μm (mean = 17.2 μm) long, 1.3–2.5 μm (mean = 1.9 μm) wide (**Figures 6G,H**).

**Comparison** The present fossil is attributed to *Castaneophyllum* because its leaves lanceolate with elongate acuminate apex, cuneate base, and serrate margin, secondary and tertiary veins (**Figures 6A–F**). This new species differs from *C. hainanensis*, described above, by the venation and tooth type. The present fossil is very similar to *C. tennesseense* (Jones and Dilcher, 1988), for both having lanceolate leaf and variable teeth type, but the present fossil has more elongate acuminate apex and smaller leaf than *C. tennesseense*. Our specimen with the length of 12.6 cm is much smaller than *C. moorii* and *C. fushunense* (Writing Group of Cenozoic Plants of China [WGCPC], 1978; Zhou, 1996).

**Species** *Castaneophyllum* cf. *moorii* (Lesq.) Jones et Dilcher (**Figure 7**)

**Specimen examined** CC-1136

**Description** Leaf lanceolate, symmetric, preserved part 4.4 cm long, 1.6 cm wide (**Figure 7A**). Margin serrate (**Figure 7A**), teeth ST-ST with rounded sinus (**Figure 7B**). Midvein thick, straight; secondary veins more than 9 pairs irregularly spaced, nearly opposite, craspedodromous, with stable angles 55° (**Figure 7A**); Tertiary and quaternaries veins unclear. Leaf surface rugose with stellate trichomes with 9 solitary branches; Branches 22.7–32.7 μm (mean = 27.7 μm) long, 1.8–2.3 μm (mean = 2.1 μm) wide (**Figures 7C–E**).

**Comparison** The present fossil is confirmed to *Castaneophyllum* because its lanceolate leaf shape, serrate margin, secondary and tertiary veins (**Figures 7A,B**). It is closest to *C. moorii* by having consistent characteristics of teeth type, similar angles between the midvein and secondary veins and the arrangement of secondary veins, but they are different in leaf shape and size. The present specimens are similar to *Q. relongtanense* Colani and *Quercus* cf. *relongtanense* Colani from the Miocene-Pliocene of To-tang, Yunnan Province, Southwest China (Colani, 1920) in venation, but our specimens have ST-ST teeth with rounded sinus and stellate trichomes, while the To-Tang species are lacking the details of leaf margin and surface.

**Genus** *Castanopsis* (D. Don) Spach, 1842

**Species** *Castanopsis* sp. (**Figure 8**)

**Specimen examined** CC-343, CC-401, CC-1276

**Description** Leaf lanceolate, preserved part 5.2–6.7 cm long, 2.9–3.2 cm wide (**Figure 8A**, apex acuminate (**Figure 8F**). Margin serrate, teeth irregularly spaced (**Figures 8F,G**). apex acuminate (**Figure 8F**). Margin serrate, teeth regularly spaced (**Figures 8A,F,G**), ST-RT with rounded sinus (**Figures 8B,C,H,I**). Midvein thick, straight; secondary veins more than 12 pairs regularly spaced, nearly opposite, craspedodromous, slightly bend in ward near the margin, with angles 40–50° (**Figures 8A,B**). Tertiary and quaternaries veins unclear. Leaf surface rugose with stellate trichomes with 6–10 solitary branches; Branches 22.7–29.1 μm (mean = 25.9 μm) long, 2.0–4.5 μm (mean = 3.25 μm) wide (**Figures 8D,E**).

**Comparison** we decided to assign the present specimen to *Castanopsis* based on the venation and ST-RT teeth with rounded sinus (**Figures 8A–C**). Our fossils resemble the extant *C. sclerophylla* on the tooth type and secondary veins, but they are different in the arrangement of the teeth. Our specimens have teeth from base to apex, while only the top 1/3 part of *C. sclerophylla* has teeth. This new species is similar with the extant *C. sclerophylla* (Lindl. et Paxton) Schottky in the characteristic of leaf shape and teeth type, but they are obviously different in secondary veins and trichomes. Our specimen has stellate trichomes (**Figures 8D,E**), while *C. sclerophylla* has thin-walled peltate trichomes. Our fossil has similar stellate trichomes with *C. mekongensis* A. Camus, but their leaf shape, size and angles between midvein and secondary veins are quite different. The present specimen is also distinctive from the previously fossil records of *Castanopsis* in the Cenozoic of China and North America (Wolfe, 1968; Tao et al., 2000; Wu et al., 2014; Li et al., 2015) by the teeth arrangement and small angle between midvein and secondary veins. Although *Castaneophyllum* cf. *moorii* also has stellate trichomes, these specimens are assigned to *Castanopsis* rather

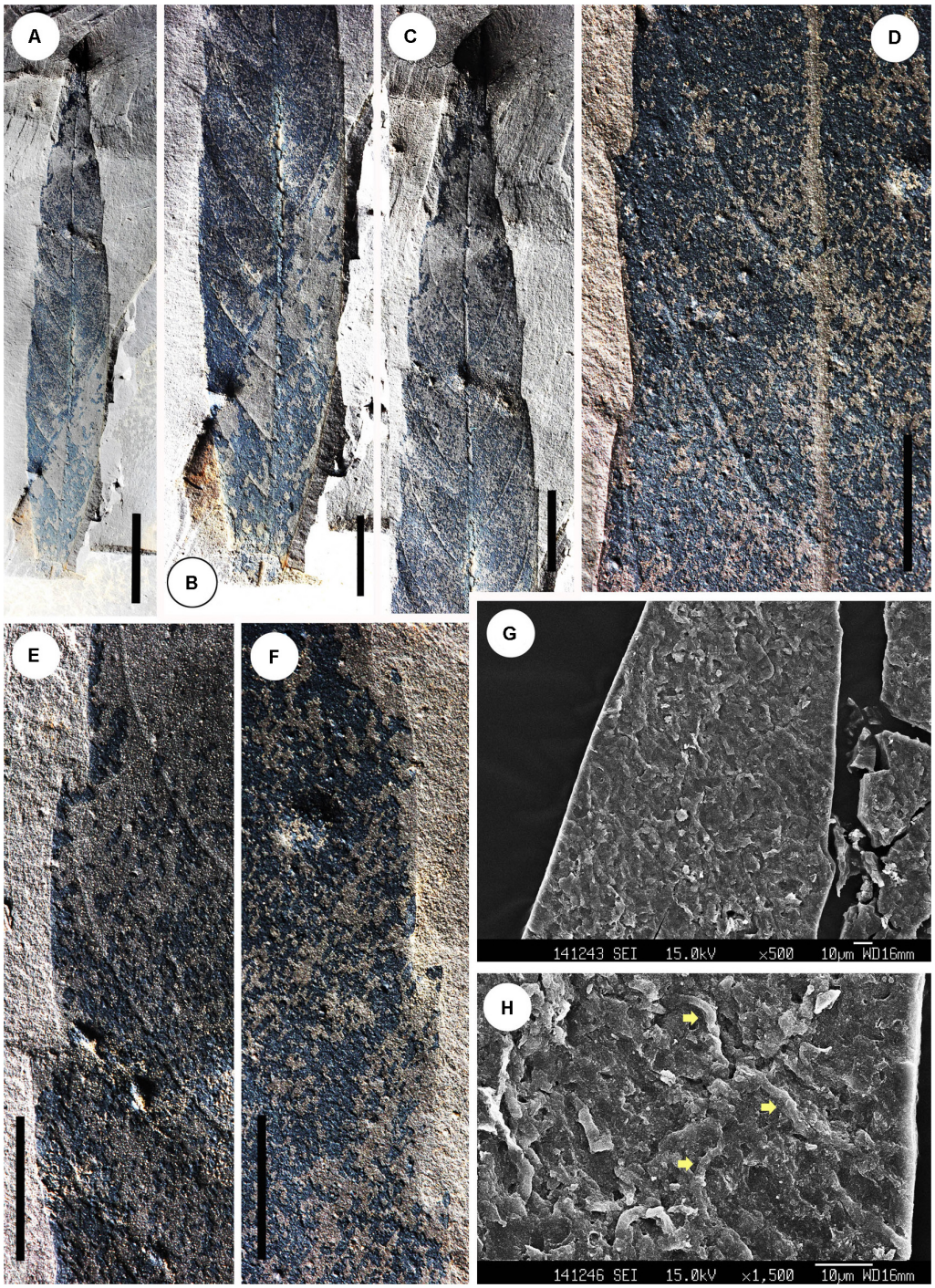


**FIGURE 6 |** Morphology of *Castaneophyllum lanceolata* sp. nov. **(A)** Holotype. Specimen No. CC-1106a, showing leaf morphology; **(B)** enlargement of **(A)**, showing the secondary veins from middle to base; **(C)** enlargement of **(A)**, showing the secondary veins from middle to apex; **(D)** enlargement of **(A)**, showing the teeth; **(E)** enlargement of **(A)**, showing the secondary veins end to the margin; **(F)** enlargement of **(A)**, showing the tertiary veins; **(G)** SEM showing rugose outer surface; **(H)** yellow arrows indicate solitary trichomes. Scale bars: 10 mm **(A–C)**; 5 mm **(D–F)**.

than *Castaneophyllum* for their ST-RT teeth and regularly spaced secondary veins.

**Genus** *Lithocarpus* Bl., 1826

**Species** *Lithocarpus changchangensis* X-Y Liu et J-H Jin sp. nov. (**Figure 9**)

**Diagnosis** Leaf elliptic, base cuneate with a short petiole. Margin serrate from 1/4 of the leaf to apex, teeth regularly

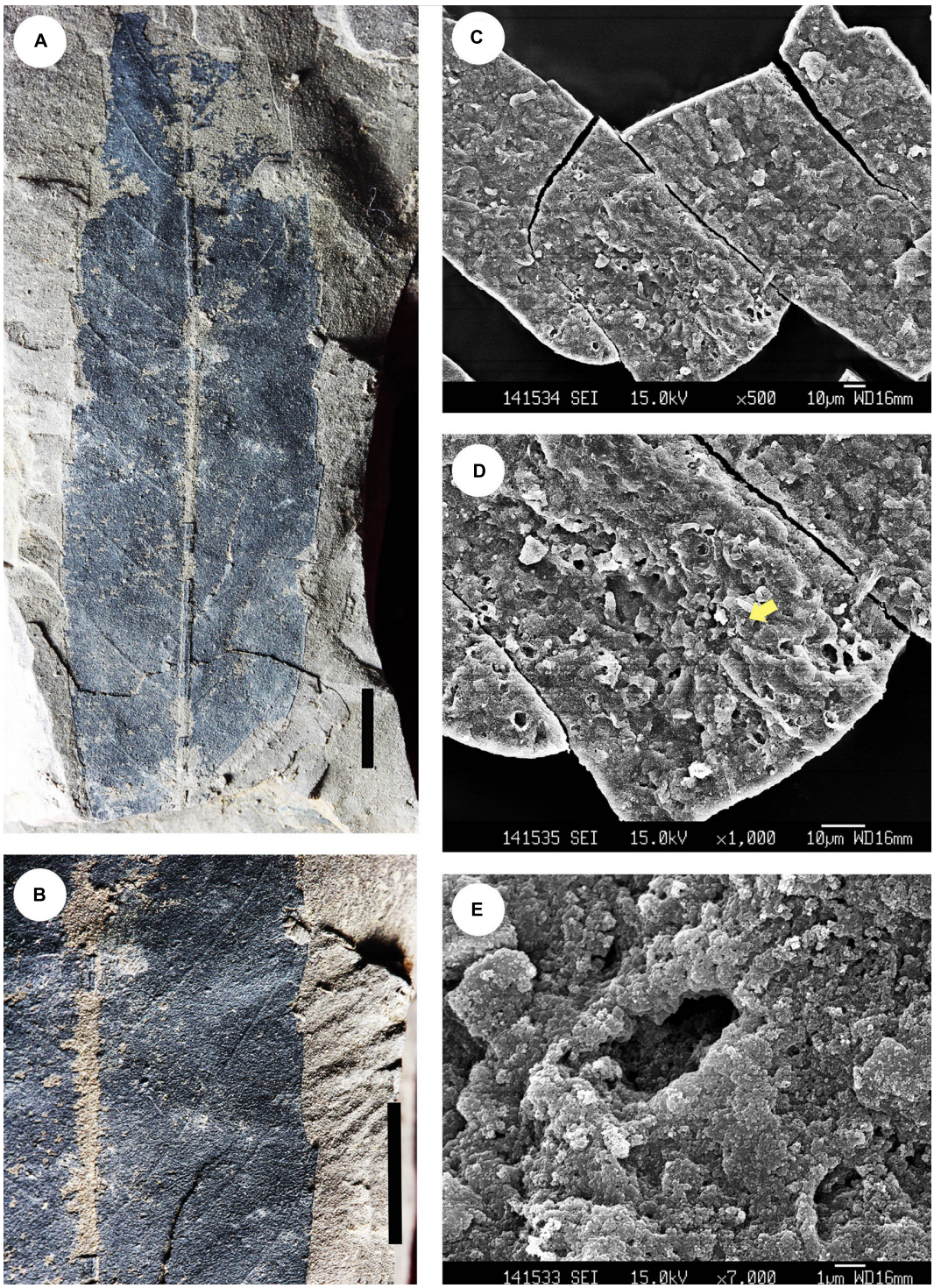


**FIGURE 7 |** Morphology of *Castaneophyllum* cf. *moorii* (Lesq.) Jones et Dilcher. **(A)** Specimen No. CC-1136, showing leaf morphology; **(B)** enlargement of **(A)**, showing teeth, tertiary veins and quaternary veins; **(C)** stellate trichomes and rugose structures on the outer surface; **(D)** yellow arrow indicates stellate trichomes; **(E)** SEM image showing stomata. Scale bars: 10 mm **(A)**; 5 mm **(B)**.

spaced, ST-ST or CV-CV with rounded sinus. Midvein straight; secondary veins thin, secondary veins more than 8 pairs regularly spaced, pinnate, craspedodromous. Tertiary veins opposite percurrent; Quaternaries unclear. Leaf surface rugose with appressed parallel tufts (APT) trichomes.

**Holotype** CC-1113

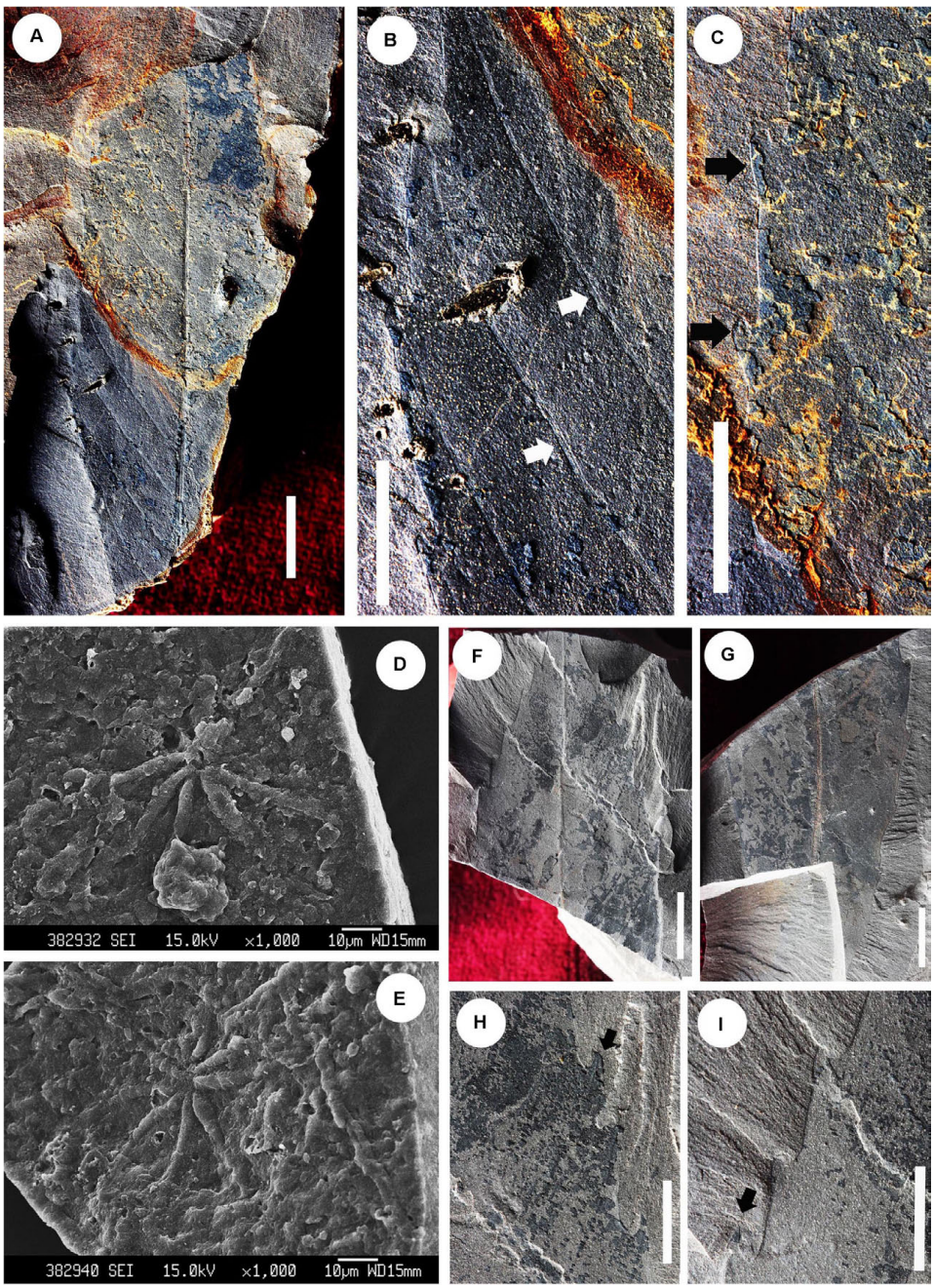


**FIGURE 8 |** Morphology of *Castanopsis* sp. **(A)** Specimen No. CC-1276, showing the leaf morphology; **(B)** enlargement of **(A)**, showing the secondary veins (white arrows) and tertiary veins; **(C)** enlargement of **(A)**, showing the teeth (black arrows); **(D,E)** SEM images showing the rugose outer surface and stellate trichomes. **(F)** Specimen No. CC-401, showing the leaf morphology; **(G)** specimen No. CC-343, showing the leaf morphology; **(H,I)** enlargement of **(F)**, showing the teeth (black arrows) and tertiary veins. Scale bars: 10 mm **(A,F,G)**; 5 mm **(B,C,H,I)**.

**Paratypes** CC-1126, CC-1237, CC-1238, CC-1281, CC-1284

**Etymology** The specific epithet "*changchangensis*" refers to the Changchang Formation from which the specimens were collected.

**Description** Leaf elliptic, preserved part 4.1–6.0 cm long, 1.2–1.8 cm wide (**Figure 9A**), base slightly asymmetry, cuneate with a short petiole, 4 mm long, 1 mm wide (**Figure 9B**). Margin serrate from 1/4 of the leaf to apex, teeth regularly spaced (**Figure 9A**), ST-ST or CV-CV with rounded sinus, respectively (**Figure 9C**). Midvein straight; secondary veins thin, secondary veins more than 8 pairs regularly spaced, pinnate, craspedodromous (**Figures 9A,C**). Tertiary veins opposite percurrent (**Figure 9C**); Quaternaries unclear. Leaf surface rugose with appressed parallel tufts (APT) trichomes with 2

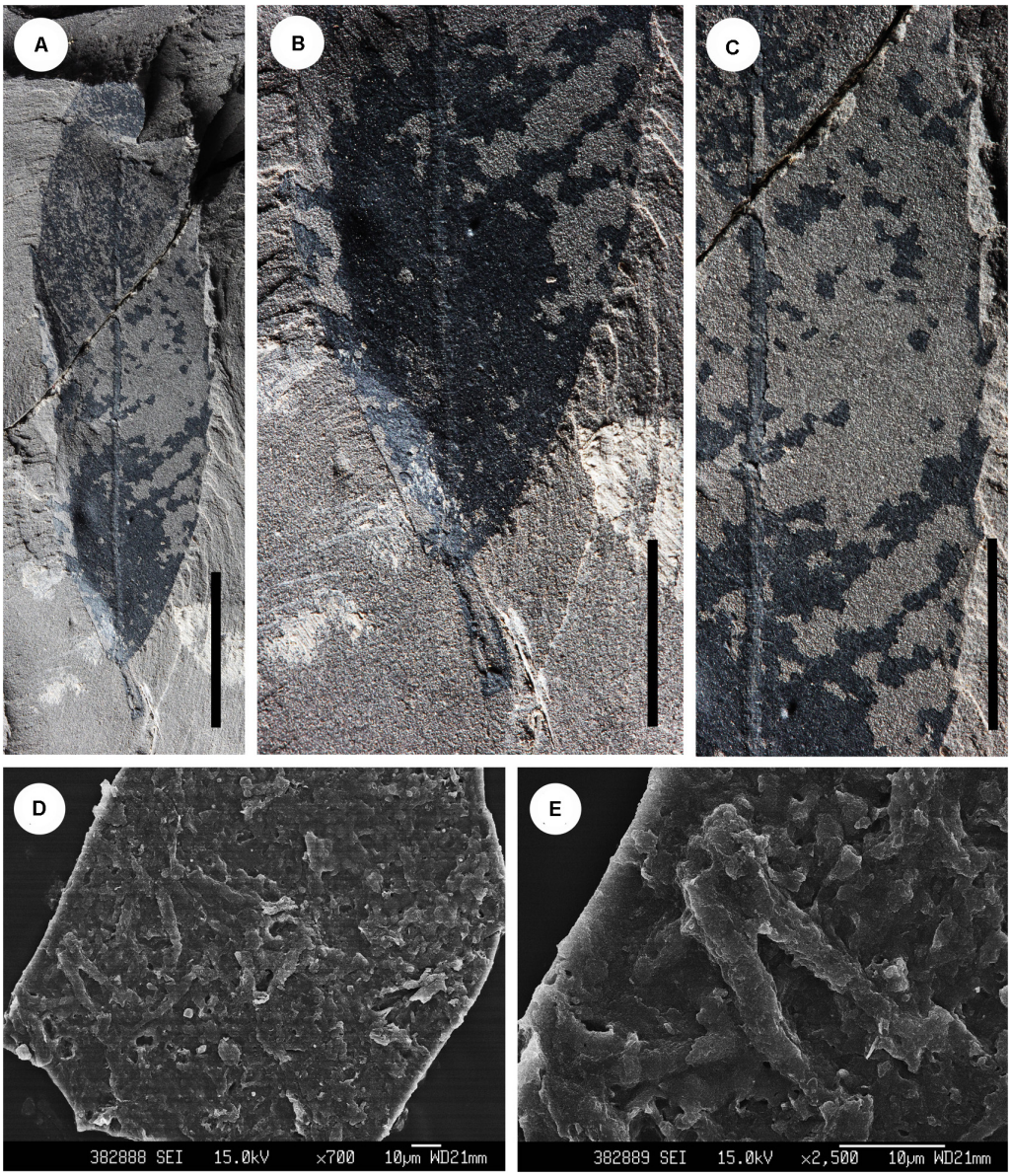


**FIGURE 9 |** Morphology of *Lithocarpus changchangensis* sp. nov. **(A)** Holotype. Specimen No. CC-1113, showing the leaf morphology; **(B)** enlargement of **(A)**, showing the base and petiole; **(C)** enlargement of **(A)**, showing the teeth and venation; **(D)** SEM image showing the rugose outer surface of leaf; **(E)** SEM image showing the appressed parallel tufts (APT) trichomes. Scale bars: 10 mm **(A)**; 5 mm **(B,C)**.

thick-walled, unicellular elements; Branches 3.7 μm long, 0.8 μm wide (**Figures 9D,E**).

**Comparison** Appressed parallel tufts (APT) trichome is unique trichome type in the genus *Lithocarpus*. The present fossils are confirmed to be *Lithocarpus* mainly based on leaf shape, venation and appressed parallel tufts (APT) trichomes with 2 thick-walled, unicellular elements (**Figure 9**). The tooth type and the secondary veins of the present fossils are similar to the extant *L. fordianus* (Hamsl.) Chun, but our fossils with the length of 4.1–6.0 cm are much smaller than *L. fordianus* with the length of 10–25 cm. The present fossils are different from all reported fossil records *Lithocarpus* leaves from the Cenozoic of China, Europe and North America. Therefore, our fossils are assigned to a new species *Lithocarpus changchangensis* sp. nov.

**Genus** *Quercus* L. 1753
**Subgenus** *Cerris* Oerst.
**Section** *Cyclobalanopsis* (Oerst.) Benth. et Hook.
**Species** *Quercus paleohypargyrea* X-Y Liu et J-H Jin sp. nov. (**Figure 10**)

**Diagnosis** Leaf elliptic, base cuneate with a petiole. Margin serrate from 1/5 of the leaf to apex, teeth regularly spaced, CC-CV to CC-CC with rounded sinus. Midvein slightly curved;

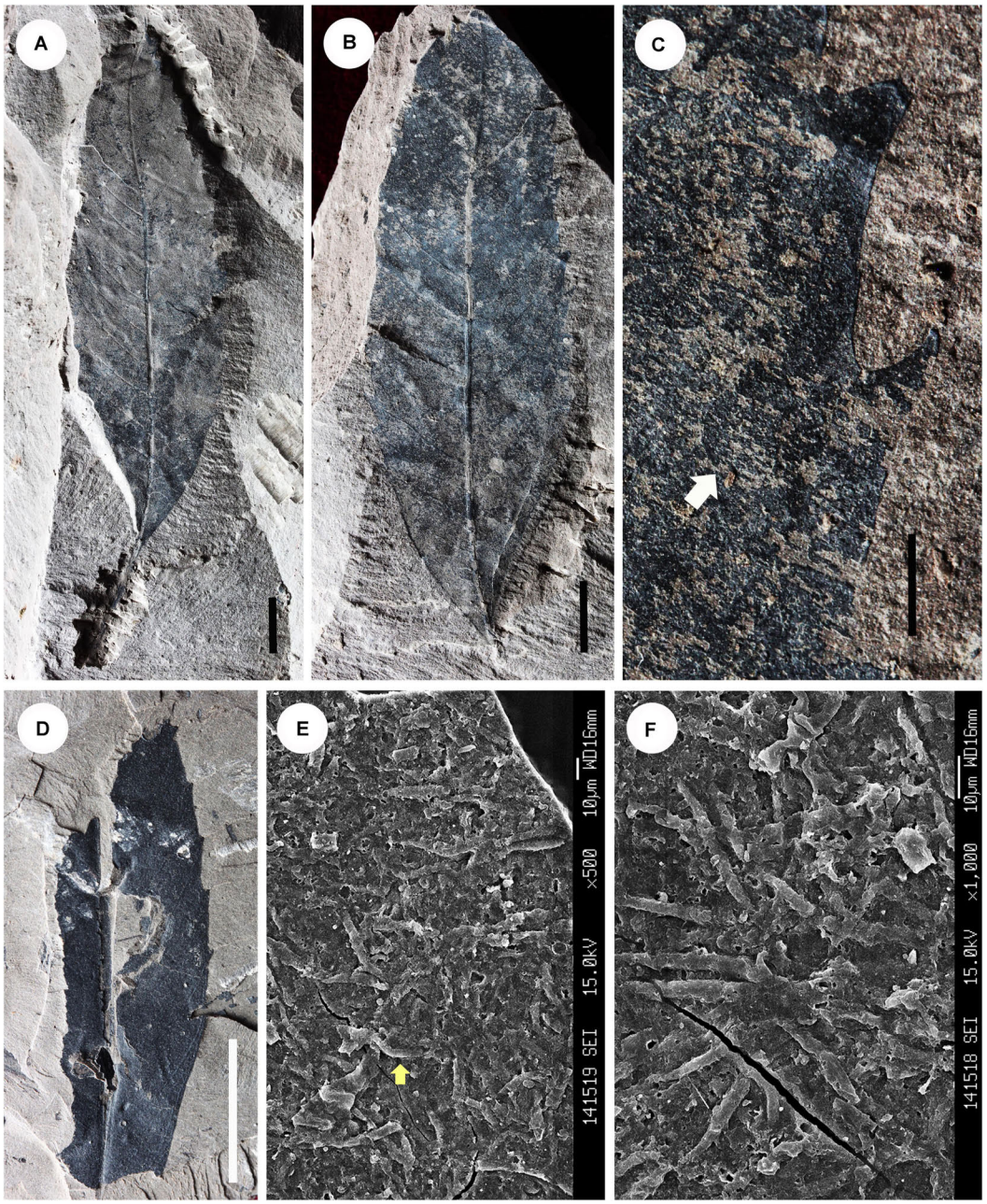


**FIGURE 10 |** Morphology of *Quercus paleohypargyrea* sp. nov. **(A)** Holotype. Specimen No. CC-1277a, showing the lanceolate leaf, more secondary vein; **(B)** counterpart of **(A)**, showing the median vein slightly bend; **(C)** Enlargement of **(A)**, showing the teeth and tertiary and quaternary veins (white arrow); **(D)** paratype Specimen No. CC-1108, showing the leaf morphology; **(E)** SEM image of **(D)**, showing the rugose outer surface and stellate trichomes (yellow arrow); **(F)** enlargement of E, showing the details of the stellate trichome. Scale bars: 10 mm **(A,B,D)**; 2 mm **(C)**.

secondary veins thin, 15–23 pairs regularly spaced, pinnate, craspedodromous, straight or slightly curved. Tertiary veins mixed percurrent; Quaternary veins regular, rectangular to polygonal reticulate. Leaf surface rugose with stellate trichomes with 4–8 solitary branches.

**Holotype** CC-1277 (a, b)

**Paratypes** CC-1108 (a, b), CC-1236, CC-1259

**Etymology** The specific epithet "*paleohypargyrea*" refers to its close affinity to the extant *Quercus hypargyrea* (Seemen ex Diels) C.C. Huang et Y.T. Chang.

**Description** Leaf elliptic, preserved part 3.8–8.9 cm long, 1.1–3.0 cm wide, base cuneate with the petiole 3.5–12 mm in length, 1–1.5 mm in width (**Figures 10A,B**). Margin serrate from 1/5 of the leaf to apex, teeth regularly spaced (**Figure 10B**),

CC-CV to CC-CC with rounded sinus (**Figure 10C**). Midvein slightly curved; secondary veins thin, 15–23 pairs regularly spaced, pinnate, craspedodromous, straight or slightly curved (**Figures 10A–D**). Tertiary veins mixed percurrent (**Figure 10C**); Quaternary veins regular, rectangular to polygonal reticulate (**Figure 10C**). Leaf surface rugose with stellate trichomes (some might be broken into separate ones) with 4–8 solitary branches; Branches 20.3–45.6 μm (mean = 32.3 μm) long, 2.6–6.7 μm (mean = 4.3 μm) wide (**Figures 10E,F**).

**Comparison** Our specimens are attributed to *Quercus* sect. *Cyclobalanopsis* by leaf shape, regularly spaced teeth and secondary veins as well as mixed percurrent tertiary veins (**Figures 10A–D**). The new species closest to *Q. hypargyrea* (Seemen ex Diels) C.C. Huang et Y.T. Chang, but they are significantly different: firstly, our fossils have cuneate base, while *Q. hypargyrea* is cuneate to subrounded; secondly, our specimens have15–23 pairs of secondary veins which is more than *Q. hypargyrea* (10–15); thirdly, the present fossils are longer and thinner than *Q. hypargyrea* (Huang et al., 1999). *Quercus paleohypargyrea* is distinctive by elliptic leaf shape, cuneate base, serrate margin with regularly spaced CC-CV to CC-CC teeth, multiple regularly spaced, pinnate, straight or slightly curved secondary veins, which is significantly different from the previously reported Cenozoic *Q.* sect. *Cyclobalanopsis* from China and North Amercia (MacGinitie, 1953; Axelrod, 1956, 1966b, 1992, 1995, 1998a,b, 2000; Writing Group of Cenozoic Plants of China [WGCPC], 1978; Tao et al., 2000). *Quercus paleohypargyrea* differs to the aforementioned *Castaneophyllum* cf. *moorii* and *Castanopsis* sp. which also have stellate trichomes by CC-CV to CC-CC teeth and pinnate secondary venation.

**Species** *Quercus paleolamellosa* X-Y Liu et J-H Jin sp. nov. (**Figure 11**).

**Diagnosis** Leaf elliptic, apex elongate acuminate, base cuneate, slightly asymmetric with the petiole. Margin serrate from 1/4 to 1/3 of the leaf to apex, teeth regularly spaced, CC-CV with rounded sinus. Midvein slightly curved; secondary veins thin, 15–23 pairs regularly spaced, pinnate, craspedodromous, straight or slightly curved. Tertiary veins mixed percurrent; Quaternary veins regular, rectangular to polygonal reticulate. Leaf surface rugose with stellate trichomes.

**Holotype** CC-1112 (a, b)

**Paratypes** CC-1110 (a, b), CC-1116, CC-1241(a, b), CC-1247, CC-1248, CC-1255, CC-1261, CC-1285

**Etymology** The specific epithet "*paleolamellosa*" refers to its close affinity to the extant *Quercus lamellosa* Smith.

**Description** Leaf elliptic, preserved part 4.5–8.3 cm long, 1.3–2.3 cm wide (**Figure 11A**), apex elongate acuminate (**Figure 11B**), base cuneate, slightly asymmetric with the petiole 9 mm in length, 0.8 mm in width (**Figure 11A**). Margin serrate from 1/4 to 1/3 of the leaf to apex, teeth regularly spaced (**Figures 11A,D**), CC-CV with rounded sinus (**Figure 11C**). Midvein slightly curved; secondary veins thin, 15–23 pairs regularly spaced, pinnate, craspedodromous, straight or slightly curved (**Figures 11A,C,D**). Tertiary veins mixed percurrent (**Figure 11C**); Quaternary veins regular, rectangular to polygonal reticulate (**Figure 11C**). Leaf surface rugose with stellate trichomes, branches 15.2–25.8 μm (mean = 20.5 μm) long, 2.4–3.0 μm (mean = 2.7 μm) wide (**Figures 11E,F**).

**Comparison** The present fossils are assigned to *Quercus* sect. *Cyclobalanopsis* base on the leaf morphological characteristics such as oval long elliptic leaf, regularly spaced teeth and secondary veins and the mixed percurrent tertiary veins (**Figures 11A–D**). The new species is most similar to the extant *Q. lamellosa* Smith on the elliptic leaf shape and stellate trichomes. However, the secondary veins of our fossils are curved close to the leaf margin, while those of *Q. lamellosa* are straight. In addition, the teeth of the present fossils are CC-CV in a uniform size, sometimes curved inward like a hook, while the teeth of *Q. lamellosa* are thin and long, sometimes spiny. Our specimens are distinguished from the previously described fossils of *Quercus* sect. *Cyclobalanopsis* from the Cenozoic of China and North American by the leaf characteristics of large size, ovate, obovate or oblong shape, and the number of secondary veins (Writing Group of Cenozoic Plants of China [WGCPC], 1978; Meyer and Manchester, 1997). This new species is distinct from *Q. paleohypargyrea*, known from the same site, by the shape and size of teeth and secondary veins.

**Species** *Quercus* cf. *myrsinifolia* Blume (**Figures 12A–D**)

**Specimen examined** CC-1272 (a, b), CC-1282, CC-1283

**Description** Leaf lanceolate, preserved part 4.2–5.9 cm long, 1.6–2.0 cm wide, apex acuminate (**Figure 12A**). Margin serrate, teeth regularly spaced (**Figure 12A**), CC-CC with rounded sinus (**Figure 12B**). Midvein thick, straight; secondary veins thin, at least 12 pairs regularly spaced, nearly opposite, craspedodromous, slightly curved with the angles 60–40° from base to apex (**Figure 12A**). Tertiary veins mixed percurrent (**Figure 12B**); Quaternary veins regular, rectangular to polygonal reticulate. Leaf surface rugose with stomata 16.2 μm long, 13.0 μm wide (**Figures 12C,D**).

**Comparison** The present fossils can be assigned to *Quercus* sect. *Cyclobalanopsis* base on the leaf shape, regularly spaced teeth and secondary veins as well as the mixed percurrent tertiary veins (**Figures 12A,B**). These specimens are similar to the extant *Q. myrsinifolia* Blume in the characteristics of gradually stronger midvein, nearly parallelled secondary veins, slender cuneate teeth and trichomes. However, the present specimens are different from *Q. myrsinifolia* by the lanceolate leaf shape and elongate acuminate apex. Our fossils are different with *Q. sinomiocenicum* Hu et Chaney from the Miocene of Lintong, Shandong Province in the leaf shape, teeth type and venation (Nanjing Institute of Geology and Mineral Resources [NIGMR], 1982). This species is distinguished from *Q. paleohypargyrea* and *Q. paleolamellosa* from the same locality by the lanceolate leaf shape and tooth size.

**Species** *Quercus paleoargyrotricha* X-Y Liu et J-H Jin sp. nov. (**Figures 12E–I**).

**Diagnosis** Leaf lanceolate, apex elongate acuminate. Margin serrate, teeth small, regularly spaced, CC-CV with rounded sinus. Midvein thick, straight; secondary veins thin, 12–15 pairs regularly spaced, opposite to pinnate from base to apex, craspedodromous, slightly curved. Tertiary veins mixed

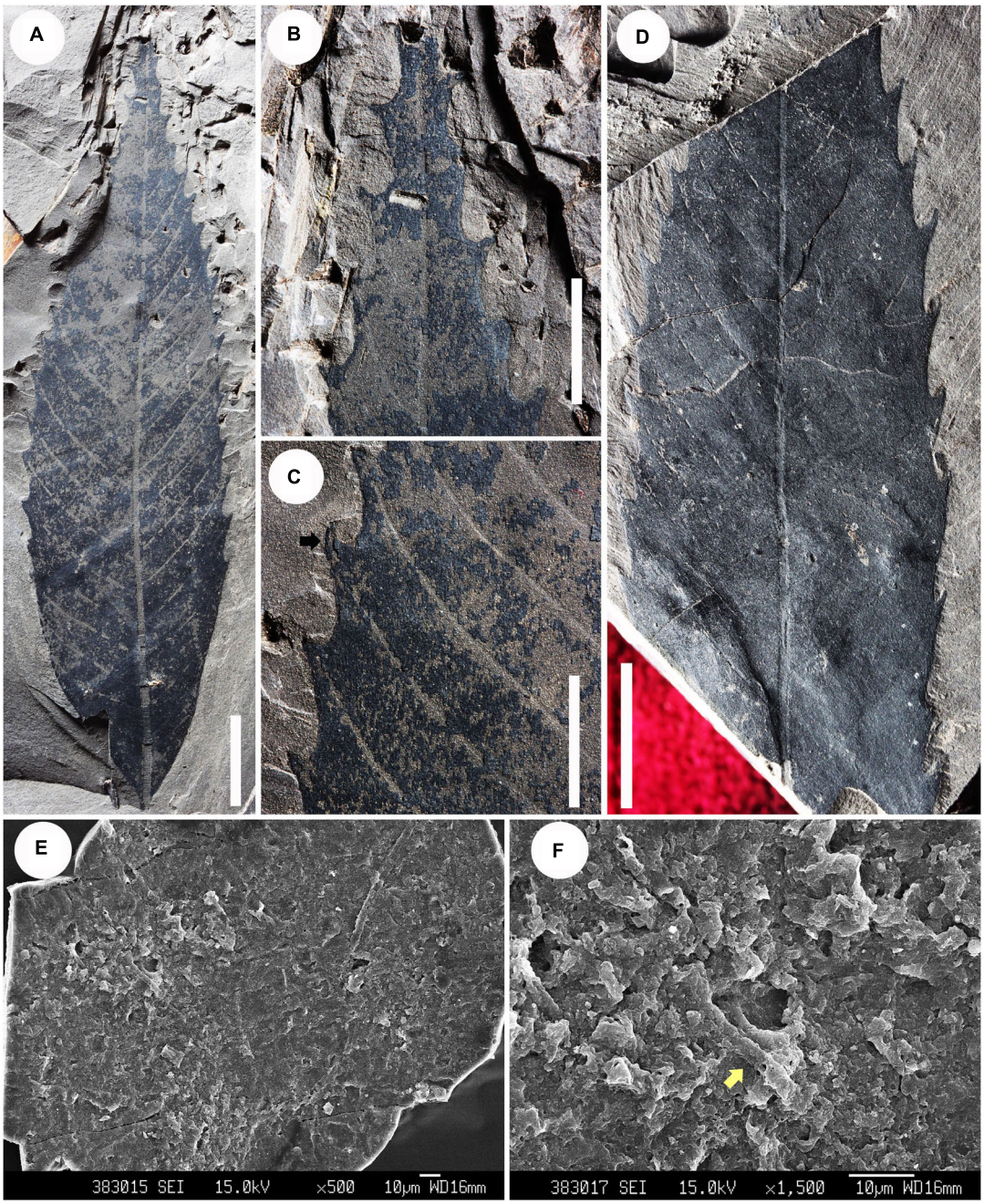


**FIGURE 11 |** Morphology of *Quercus paleolamellosa* sp. nov. **(A)** Holotype. Specimen No. CC-1112a, showing the lanceolate leaf and plenty of veins; **(B)** enlargement of **(A)**, showing the acuminate apex with teeth; **(C)** enlargement of **(A)**, showing the teeth (black arrow); **(D)** paratype. Specimen No. CC-1261, showing the teeth and venation. **(E)** SEM image of **(D)**, showing the rugose outer surface and solitary trichomes; **(F)** enlargement of **(E)**, showing the details of the solitary trichomes (yellow arrow). Scale: 10 mm **(A,D)**; 5 mm **(B,C)**.

percurrent; Quaternary veins regular, rectangular to polygonal reticulate. Leaf surface rugose with stellate trichomes and air hole of stomata.

**Holotype** CC-1287 (a, b)

**Paratype** CC-961

**Etymology** The specific epithet "*paleoargyrotricha*" refers to its close affinity to the extant *Quercus argyrotricha* A. Camus.

**Description** Leaf lanceolate, preserved part 5.5–7.7 cm long, 2.1–2.5 cm wide, apex elongate acuminate (**Figures 12E,F**). Margin serrate, teeth small, regularly spaced (**Figures 12E,F**), CC-CV with rounded sinus (**Figure 12G**). Midvein thick, straight; secondary veins thin, 12–15 pairs regularly spaced, opposite to pinnate from base to apex, craspedodromous, slightly curved (**Figures 12E–G**). Tertiary veins mixed percurrent

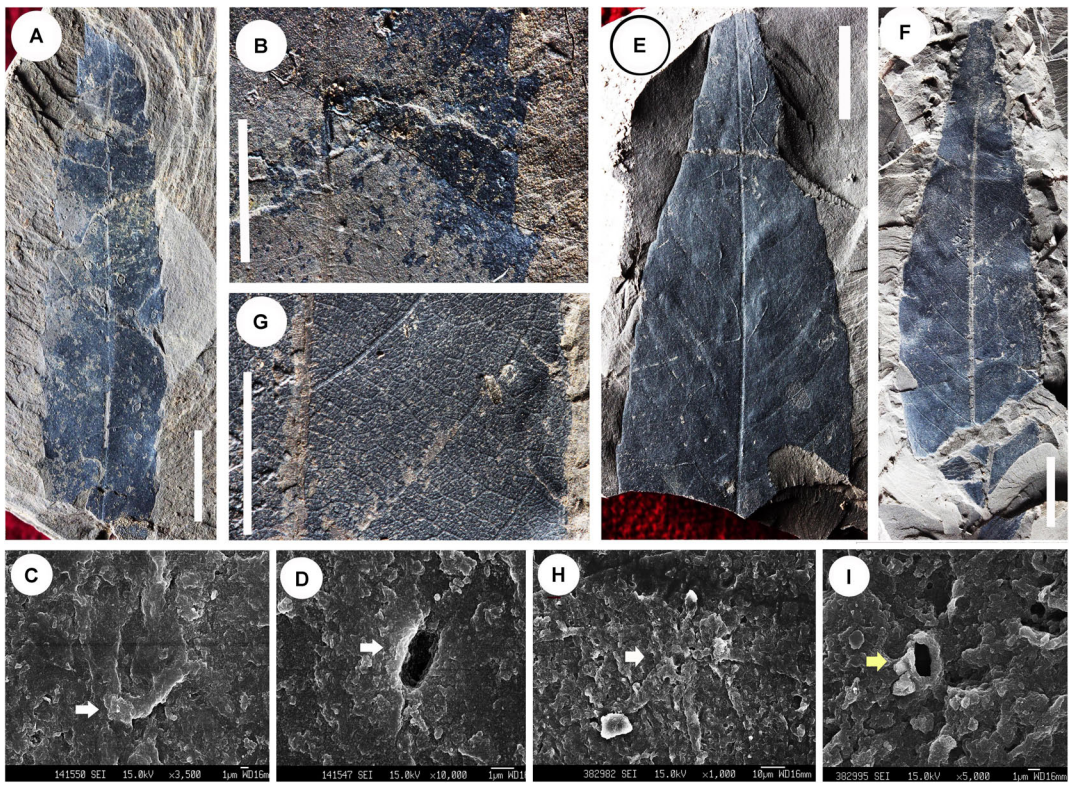


**FIGURE 12 |** Morphology of *Quercus* cf. *myrsinifolia* Blume **(A–D)** and *Q. paleoargyrotricha* sp. nov. **(E–I)**. **(A)** Specimen No. CC-1272a, showing the lanceolate leaf morphology; **(B)** enlargement of **(A)**, showing the teeth, secondary veins and mix percurrent tertiary veins; **(C)** SEM image showing the outer surface and a stoma (white arrow); **(D)** SEM image showing the air hole of a stoma (white arrow); **(E)** holotype. Specimen No. CC-1287a, showing the morphology of the leaf apex; **(F)** paratype. Specimen No. CC-961, showing the morphology of the leaf; **(G)** enlargement of **(F)**, showing the tooth, secondary veins and mix percurrent tertiary veins; **(H)** SEM image showing the stellate trichome (white arrow); **(I)** SEM image showing the air hole of a stoma (yellow arrow). Scale bars: 10 mm **(A,E,F)**; 5 mm **(B,G)**.

(**Figure 12G**); Quaternary veins regular, rectangular to polygonal reticulate (**Figure 12G**). Leaf surface rugose with stellate trichomes with 6–8 solitary branches, 16.2 μm long, 13.0 μm wide and air hole of stomata, rectangular, 2.8 μm long, 1.3 μm wide (**Figures 12H,I**).

**Comparison** The present specimens are assigned to *Quercus* sect. *Cyclobalanopsis* because the leaf shape, regularly spaced teeth and secondary veins, and mixed percurrent tertiary veins (**Figures 12E–G**). The new species is most similar to the extant *Q. argyrotricha* A. Camus in the characteristics of sparsely serrated margin, craspedodromous, slightly curved secondary veins, and stellate trichomes. However, the present specimens differ from *Q. argyrotricha* by the leaf shape, teeth details, and number of secondary veins. Our specimens have well-preserved trichomes (**Figure 12H**), while the previous reported fossil records from Cenozoic of east and west North America and southwest China lack trichome (Axelrod, 1956, 1992; Meyer and Manchester, 1997; Tao et al., 2000). The present specimens are different from *Q. paleohypargyrea* and *Q. paleolamellosa*, described above, in teeth shape and trichome branches.

**Species** *Quercus changchangensis* X-Y Liu et J-H Jin sp. nov. (**Figures 13A–C,E–H**).

**Diagnosis** Leaf lanceolate, apex elongate acuminate, base cuneate with petiole. Margin serrate from 1/3 of the leaf to apex, teeth regularly spaced, CC-RT with rounded sinus. Midvein thick to thin from base to apex, straight; secondary veins thin, 9 pairs regularly spaced, opposite to pinnate from base to apex, craspedodromous, with stable angles 50–60°, slightly curved near the margin. Tertiary veins mixed percurrent; Quaternary veins regular, polygonal reticulate. Leaf surface rugose with simple uniseriate trichomes and air hole of stomata.

**Holotype** CC-960

**Paratype** CC-1102

**Etymology** The specific epithet "*changchangensis*" refers to the Changchang Formation from which the specimens were collected.

**Description** Leaf lanceolate, 6.4–7.7 cm long, 1.5–1.8 cm wide, apex elongate acuminate (**Figure 13A**), base cuneate with petiole 10 mm long, 1 mm wide (**Figure 13C**). Margin serrate from 1/3 of the leaf to apex, teeth regularly spaced (**Figure 13A**), CC-RT with rounded sinus (**Figure 13B**). Midvein thick to thin from base to apex, straight; secondary veins thin, 9 pairs regularly spaced, opposite to pinnate from base to apex, craspedodromous, with stable angles 50–60°, slightly curved near the margin (**Figures 13A,B**). Tertiary veins mixed percurrent

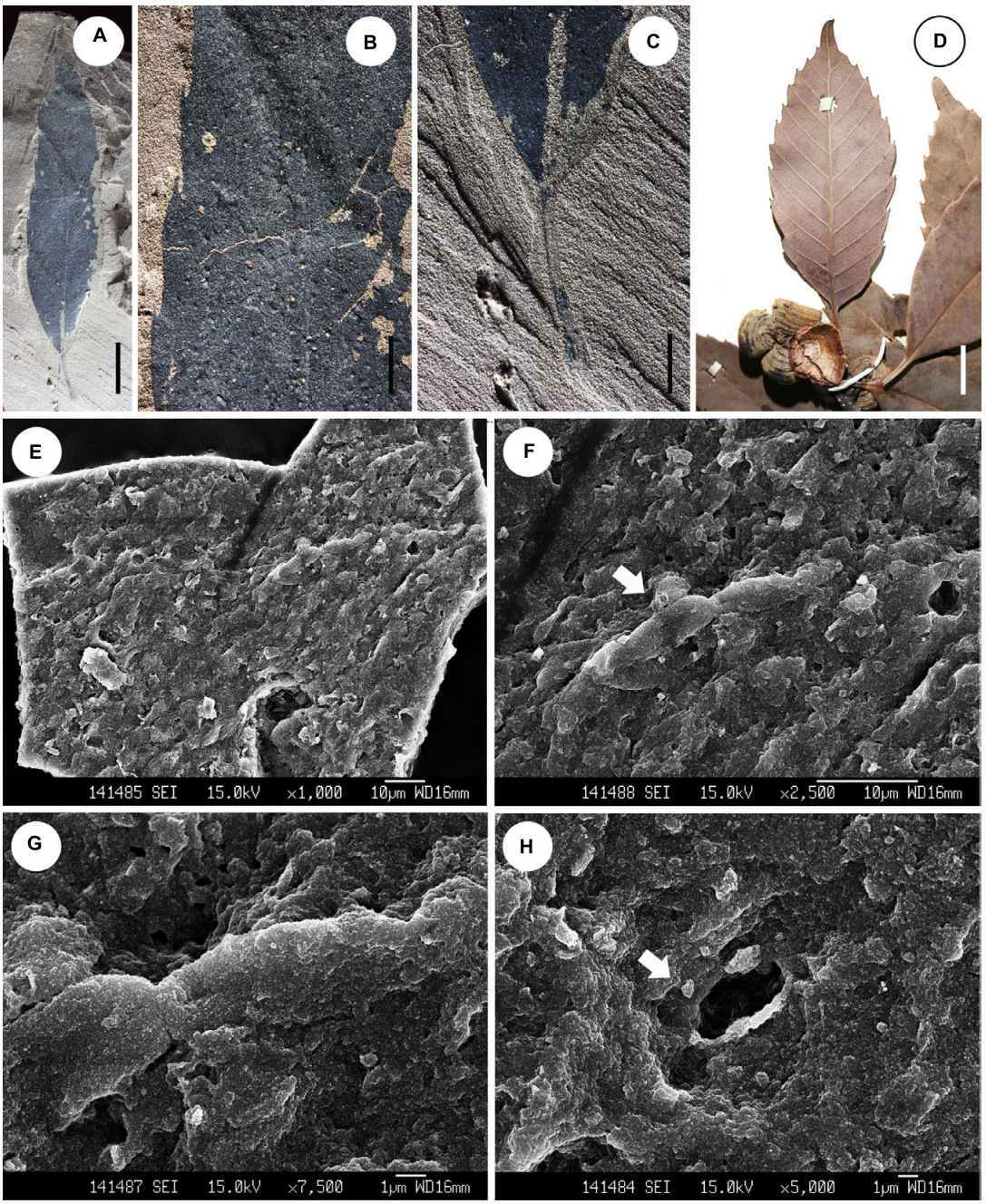


**FIGURE 13 |** Morphology of *Quercus changchangensis* sp. nov. **(A–C,E–H)** and the extant *Q. schottkyana* Rehd. et Wils. **(D)**. **(A)** Holotype. Specimen No. CC-960, showing the lanceolate leaf morphology; **(B)** enlargement of **(A)**, showing the teeth; **(C)** enlargement of **(A)**, showing the cuneate base and petiole; **(D)** elliptic leaf of *Q. schottkyana,* the Herbarium of the Sun Yat-sen University (SYS), No. 17306, collected by J. F. Rock; **(E)** SEM image showing the rugose outer surface of *Q. changchangensis*; **(F)** enlargement of **(E)**, white arrow indicates a uniseriate trichome; **(G)** enlargement of **(F)**, a cell of the uniseriate trichome; **(H)** outer face of *Q. changchangensis*, white arrow indicates the air hole of a stoma. Scale bars: 10 mm **(A,D)**; 5 mm **(B,C)**.

(**Figure 13B**); Quaternary veins regular, polygonal reticulate (**Figure 13B**). Leaf surface rugose with simple uniseriate trichomes composed of a single column of 3–4 thin-walled structures, apparently cells, 32.9 μm long, 3.9 μm wide and air hole of stomata, rectangular, 5.3 μm long, 2.8 μm wide (**Figures 13E–H**).

**Comparison** The present specimens are attributed to *Quercus* sect. *Cyclobalanopsis* because their leaf shape, regularly spaced teeth and secondary veins, and mixed percurrent tertiary veins (**Figures 13A–C**). This new species resembles the extant *Q. schottkyana* Rehd. et Wils. on the leaf shape and simple uniseriate trichomes (**Figures 13A,D**). This new species is

distinct from the extant *Q. schottkyana* Rehd. et Wils. and *Q. glauca* Thunb. which have simple uniseriate trichomes with the length of 160 and 265 μm in length, respectively (Luo and Zhou, 2001), by having much smaller simple uniseriate trichomes. Most of the previously described fossils reported fossil leaves of *Q.* sect. *Cyclobalanopsis* from the Cenozoic of China have no trichomes, except for *Q. praedelavayi* Y.W. Xing et Z.K. Zhou described from late Miocene of XundianXianfeng Basin with typical stellate trichomes including 16 branches (Xing et al., 2013). The present fossils are easily distinguished from *Q. praedelavayi* and above 4 species of *Quercus* described herein by the simple uniseriate trichome and lanceolate leaf with CC-RT teeth.

# DISCUSSION

## Phytogeographic Implications

Previously published fossil records indicate that *Berryophyllum* was widely distributed in strata from the Paleocene to the Eocene in Asia, North America, and Europe (**Figure 14A**; Writing Group of Cenozoic Plants of China [WGCPC], 1978; Takhtajan, 1982; Jones and Dilcher, 1988; Crepet and Nixon, 1989a; Mai, 1995; Zhou, 1996; Tao et al., 2000; Kvaček and Walther, 2010). The distribution range decreased since the Oligocene and finally disappeared from North America (**Figure 14A**; Tao et al., 2000; Kvaček and Walther, 2010). In China, this genus was present as early as Eocene in Fushun, Liaoning, and in Zhanhua, Shandong and become abundant in Yunnan after the Oligocene (**Figure 14A**; Tao et al., 2000). The present *Berryophyllum* fossils discovered on Hainan Island in South China indicates that the genus has been distributed in the low latitude tropical region at least since the Eocene.

*Castaneophyllum* has been in Asia and North America since the Paleocene (**Figure 14B**; Takhtajan, 1982; Jones and Dilcher, 1988). This genus not only appeared in Asia and North America but also spread to Europe in the Eocene (**Figure 14B**; Kvaček and Walther, 1989, 2010). However, fossil records of the genus only occurred in Europe and central Asia during the Oligocene (**Figure 14B**; Takhtajan, 1982; Kvaček and Walther, 1989, 2010). In China, the genus was only previously found in the Eocene in Fushun, Liaoning (**Figure 14B**; Tao et al., 2000). The *Castaneophyllum* fossils recovered here from Hainan Island are the lowest latitudinal distribution of the record for the genus.

*Castanopsis* fossils were widely distributed in Asia, North America, South America, and Europe during the Eocene, with the richest reproductive fossil records located in North America (**Figure 14C**; Wolfe, 1968; Huzioka and Takahasi, 1970; Takhtajan, 1982; Crepet and Nixon, 1989a; Manchester, 1994; Wilf et al., 2019). In China, however, *Castanopsis* fossils were mainly recovered from Yunnan, Sichuan, Zhejiang, and Guangxi during the Miocene to the Pliocene (**Figure 14C**; Tao and Du, 1982; Tao and Chen, 1983; Liu, 1993; Tao et al., 2000; Xia et al., 2009; Guo, 2011; Wu et al., 2014; Li et al., 2015). The *Castanopsis* fossils recovered here from the Eocene stratum on Hainan Island are both the earliest fossil records of the genus in China and also the lowest latitudinal distribution of the record in the world.

*Lithocarpus* was extensively distributed in North America and Europe in the Eocene, then extended into Asia during the Oligocene-Miocene, and finally almost disappeared from North America and Europe after the Miocene (**Figure 15A**; Andreansky and Kovaca, 1966; Axelrod, 1966a, 1998a; Takhtajan, 1982; Kvaček and Walther, 1989; Vikulin, 2011). In China, *Lithocarpus* fossils were mainly found from the Oligocene and Miocene strata of Yunnan, and diversified in the Miocene (**Figure 15A**; Writing Group of Cenozoic Plants of China [WGCPC], 1978; Tao et al., 2000; Guo, 2011; Mu et al., 2015). Additionally, they also occurred in the Pleistocene stratum of Guangxi (**Figure 15A**; Tao et al., 2000). The *Lithocarpus* fossils here from Hainan Island have similar implications compared to *Castanopsis* in that they have the earliest record in China and the lowest distribution latitudes in the world.

*Quercus*, including subgenus *Quercus* and subgenus *Cerris* (including *Q.* sect. *Cyclobalanopsis*, Denk et al., 2017), has the richest and widest distribution of both modern and fossil species. The fossil records suggest that *Q.* subg. *Quercus* has been widely distributed in East and South Asia, western North America, and southern Europe since the Eocene (**Figure 15B**; MacGinitie, 1941, 1953, 1969; Bones, 1979; Takhtajan, 1982; Daghlian and Crepet, 1983; Manchester, 1983, 1994; Mai and Walther, 1985; Kvaček and Walther, 1989; Vikulin, 2011; Tao et al., 2000). *Quercus* also occurred in the Eocene stratum in Fushun, Liaoning (**Figure 15B**; Tao et al., 2000). The fossil records of *Q.* sect. *Cyclobalanopsis* can be also dated back to the Eocene in western North America and eastern Germany (**Figure 15C**; Kvaček and Walther, 1989; Manchester, 1994). In China, the earliest reliable *Q.* sect. *Cyclobalanopsis* fossils were discovered from the Oligocene stratum in Yunnan and Guangdong provinces (**Figure 15C**; Writing Group of Cenozoic Plants of China [WGCPC], 1978; Liu et al., 2019). The *Quercus* fossils here from Hainan Island have a wide variety of species, including 5 species of *Q.* sect. *Cyclobalanopsis*, which are the lowest latitudinal distribution of the genus in the fossil record. Among these, the fossils assigned to *Q.* sect. *Cyclobalanopsis* are the earliest fossil records in China, as well as the earliest fossil records of the section in China. The above fossils suggest that the intragenus differentiation and the diversity evolution of the *Q.* sect. *Cyclobalanopsis* already started as early as the Eocene in South China.

Overall, as the earliest fossils of Fagaceae, such as *Berryophyllum* and *Castaneophyllum* were mainly distributed in high latitude regions, and the present occurrence of above five genera of Fagaceae from the middle Eocene Changchang Formation of Changchang Basin, Hainan Island of South China, a possible divergence pattern for the family is proposed that the family might be boreotropical origin and then migrated southward by the middle Eocene and highly differentiated at that time. The extinct genera, *Berryophyllum* and *Castaneophyllum* arrived at the low latitude of South China at least by the middle Eocene, and 7 fossils species in extant *Castanopsis, Lithocarpus,* and *Quercus* section *Cyclobalanopsis* show the diversity of the family in the middle Eocene of South China.

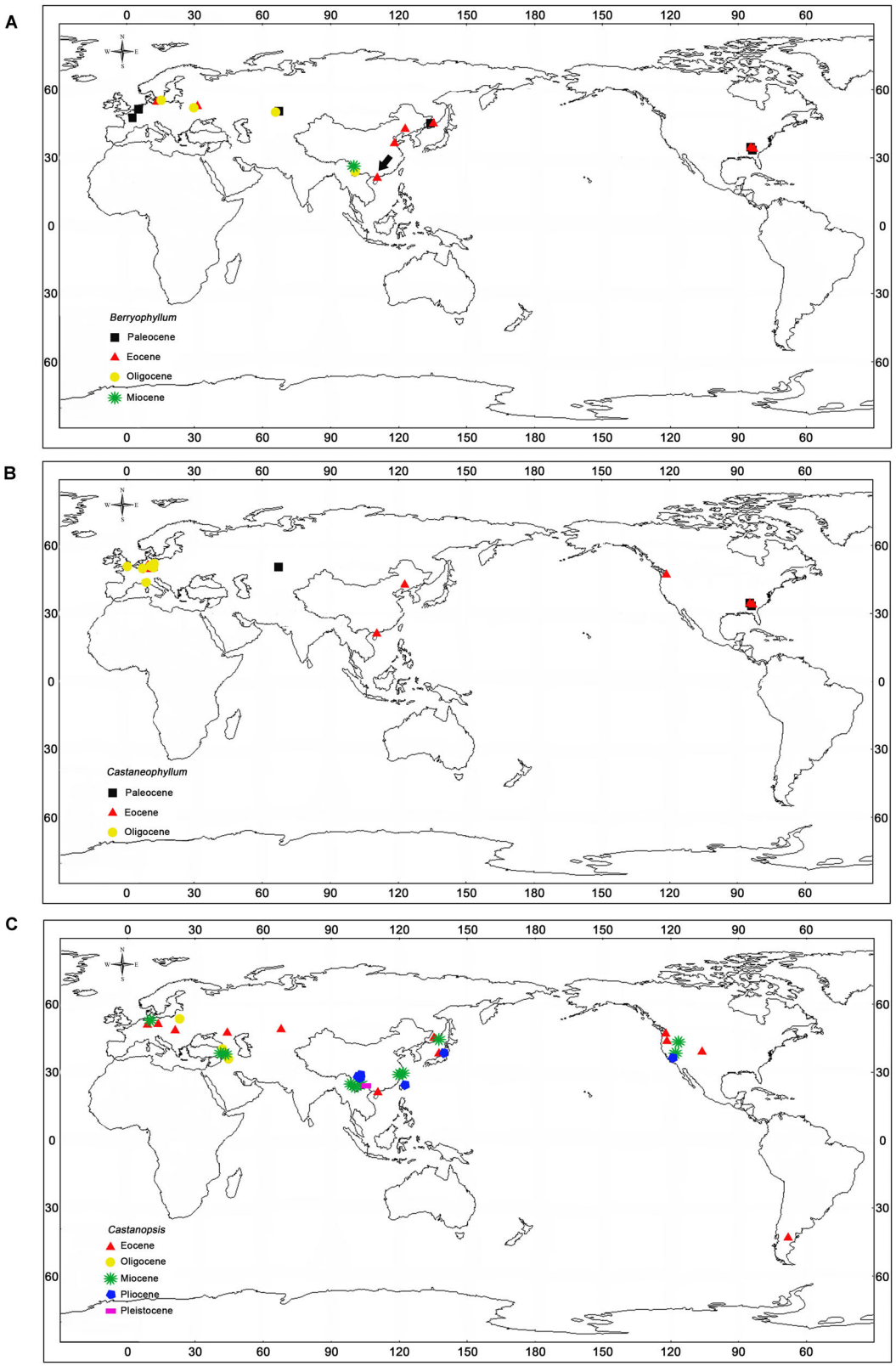


**FIGURE 14 |** Distribution of the fossil records for the genera *Berryophyllum*, *Castaneophyllum* and *Castanopsis*. **(A)** Distribution of the fossil records of *Berryophyllum*; **(B)** distribution of the fossil records of *Castaneophyllum*; **(C)** distribution of the fossil records of *Castanopsis*.

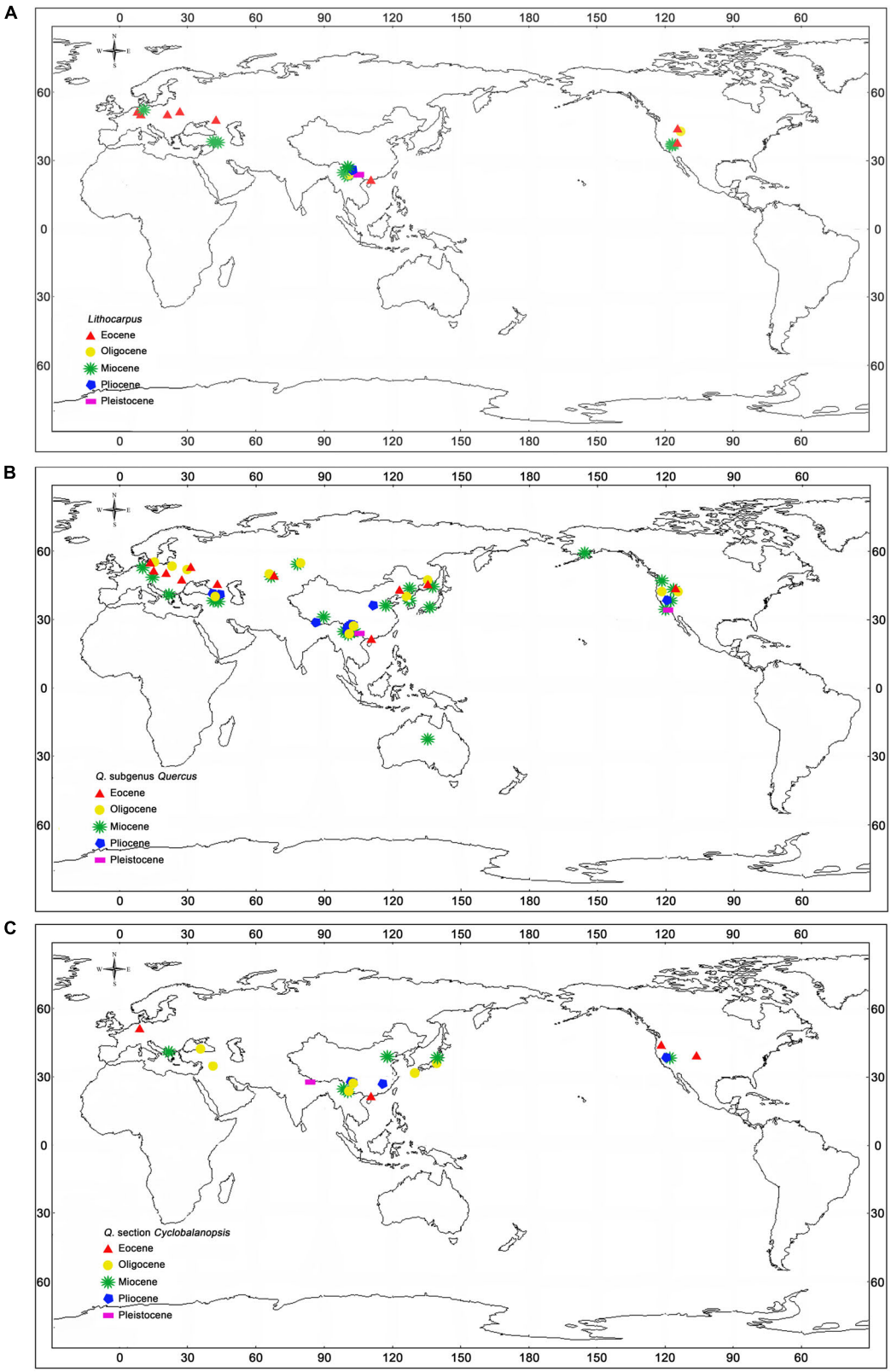


**FIGURE 15 |** Distribution of the fossil records for the *Lithocarpus*, *Quercus* subgenus *Quercus* and *Q.* section *Cyclobalanopsis*. **(A)** Distribution of the fossil records of *Lithocarpus*; **(B)** distribution of the fossil records of *Q.* subgenus *Quercus*; **(C)** distribution of the fossil records of *Q.* section *Cyclobalanopsis*.

## Paleoecological Implications

The five species described here are assigned to the extinct genera *Berryophyllum* and *Castaneophyllum* complexes. Both the *Berryophyllum* and *Castaneophyllum* complexes could likely thrive in these many environments due to their considerable variation in ecologically important parameters (e.g., leaf area and length to width ratios) and due to their interbreeding complex, similar to the extant *Quercus* (Jones and Dilcher, 1988). The interbreeding strategy, highly adaptive in the fluvial and near coastal environments (Jones and Dilcher, 1988), is supported by the reconstructed environment of our fossil locality; Changchang Basin is very close to the coastal areas. In the Eocene Hainan Island, the presence of *Berryophyllum* and *Castaneophyllum* complexes, as well as a great number of aquatic ferns, *Salvinia* (Wang et al., 2014), *Alseodaphne* (Li et al., 2009), palms (Zhou et al., 2013), and other angiosperms from the same layer, indicates a wet environment in the basin during that time.

The other 7 species presented in this study have been assigned to the extant evergreen genera *Castanopsis*, *Lithocarpus,* and *Quercus* section *Cyclobalanopsis*. They are the most diverse groups within the family Fagaceae, confined to East and Southeast Asia, and are important dominants in the evergreen broad-leaved forests (EBLF) in tropical and subtropical Asia (Tang, 2015). *Castanopsis* is generally distributed at lower altitudes, whereas *Lithocarpus* and *Quercus* section *Cyclobalanopsis* at higher altitudes, but sometimes they have been found to coexist in the same altitudinal range and be co-dominant in the same EBLF (Tang, 2015). Indochina, Southwest China, and South China have the highest species diversity of these three genera (Tang, 2015). The floristic composition of Hainan Island shows a strong tropical characteristics, with mostly tropical genera, e.g., *Lithocarpus* and some subtropical genera, e.g., *Castanopsis* and *Quercus* (Jiang et al., 2002). Many tropical genera, including *Sabalites* (Zhou et al., 2013), *Alseodaphne* (Li et al., 2009), *Palaeocarya* (Jin, 2009) closely related to extant *Engelhardtia* (Juglandaceae), and *Morinda* (Rubiaceae; Shi et al., 2012), have been recovered from the middle Eocene Changchang Formation of Changchang Basin, South China. *Castanopsis, Lithocarpus,* and *Q.* section *Cyclobalanopsis*, collected from the same layer with the above taxa, are the most abundant and diverse taxa (except for Lauraceae). This indicates that these three genera of Fagaceae dominated the evergreen tropical and subtropical forests in South China by at least the middle Eocene.

Palynological and Climate Leaf Analysis Multivariate Program (CLAMP) studies show the mean annual temperatures of 14.2–19.8°C and ∼22 ± 4.7°C, respectively, the mean annual precipitations of 784.7–1,113.3 mm, and growing season precipitation (GSP, effectively the mean annual precipitation) of 2020 ± 1220 mm, respectively for the middle Eocene Changchang Formation of Changchang Basin, South China (Yao et al., 2009; Spicer et al., 2014). Based on the above analysis of the living environment for the nearest living relatives of these fossils, we speculate that the climate of Hainan Island was warm and wet during the middle Eocene, which was suitable for the growth and differentiation of Fagaceae, especially for *Quercus* sect. *Cyclobalanopsis* which was well-developed and highly differentiated during the middle Eocene.

## DATA AVAILABILITY STATEMENT

All datasets presented in this study are included in the article/**Supplementary Material**.

## AUTHOR CONTRIBUTIONS

JJ and XL conceived and designed the study, conducted taxonomic treatments, phytogeographic, and paleoecological interpretations. JJ, HS, and XL photographed specimens and arranged the figures. XL carried out the cuticle experiments and data analyses and wrote the manuscript. HS formatted the references and figure captions. All authors read and approved the final manuscript.

## FUNDING

This study was supported by the National Natural Science Foundation of China (Nos. 31770241, 41820104002, and 41661134049), the Key Laboratory of Economic Stratigraphy and Palaeogeography, the Chinese Academy of Sciences (Nanjing Institute of Geology and Palaeontology) (No. 2016KF02), the Natural Science Foundation of Guangdong Province, China (No. 2017A030310411), the Fundamental Research Funds for the Central Universities (No. 17lgpy105), and the grant of the Natural Environment Research Council of Research Councils UK (No. NE/P013805/1).

## ACKNOWLEDGMENTS

We sincerely thank graduate students majoring in Botany at Sun Yat-sen University for participating in collecting the fossils in the field. We are grateful to the staff of the herbaria of the Harvard University, Florida Museum of Natural History, and South China Botanical Garden, and Sun Yat-sen University for the permission to examine and photograph the extant specimens of Fagaceae. We greatly thank Prof. Steven R. Manchester (Florida Museum of Natural History, University of Florida, United States) and Caitlyn R. Witkowski (University of Bristol) for their linguistic editing and comments.

## SUPPLEMENTARY MATERIAL

The Supplementary Material for this article can be found online at: https://www.frontiersin.org/articles/10.3389/fevo.2020.00255/full#supplementary-material

## REFERENCES


Andreansky, G., and Kovaca, E. (1966). Der verwandtschaftskreis der eichernfer unteroligozanen flora von kiseged bei Eger (Obcrungam): egri Muz Evk. *Am. J. Bot.* 2, 7–42.

Axelrod, D. I. (1956). *Mio-Pliocene Floras from West Central Nevada*. Berkeley, CA: University of California Publications in Geological Sciences.

Axelrod, D. I. (1962). *A Pliocene Sequoiadendron Forest from Western Nevada*. Berkeley, CA: University of California Publications in Geological Sciences.

Axelrod, D. I. (1966a). *The Eocene Copper Basin Flora of Northeastern Nevada*. Berkeley, CA: University of California Publications in Geological Sciences.

Axelrod, D. I. (1966b). *The Pleistocene Soboba Flora of Southern California*. Berkeley, CA: University of California Publications in Geological Sciences.

Axelrod, D. I. (1992). *The Middle Miocene Pyrimid Flora of Western Nevada*. Berkeley, CA: University of California Publications in Geological Sciences.

Axelrod, D. I. (1995). *The Miocene Purple Mountain Flora of Western Nevada*. Berkeley, CA: University of California Publications in Geological Sciences.

Axelrod, D. I. (1998a). *The Eocene Thunder Mountain Flora of Central Idaho*. Berkeley, CA: University of California Publications in Geological Sciences.

Axelrod, D. I. (1998b). *The Oligocene Haynes Creek Flora of Eastern Idaho*. Berkeley, CA: University of California Publications in Geological Sciences.

Axelrod, D. I. (2000). *A Miocene (10-12Ma) Evergreen Laurel-Oak Forest from Carmel Valley*. California: University of California Publications in Geological Sciences.

Berry, E. W. (1916). *The Lower Eocene Floras of Southeastern North America*. Reston, VA: United States Geological Survey.

Bhandari, S., Momohara, A., and Paudayal, K. N. (2009). Late Pleistocene plant macro-fossils from the Gokarna Formation of the Kathmandu Valley, Central Nepal. *Bull. Depart. Geol.* 12, 75–88. doi: 10.3126/bdg.v12i0.2252

Bones, T. J. (1979). Atlas of fossil fruit and seeds from North Central Oregon. *Oregon Mus. Sci. Ind. Occ. Pap. Nat. Sci.* 1, 1–23.

Borgardt, S. J., and Pigg, P. B. (1999). Anatomical and developmental study of petrified *Quercus* (Fagaceae) fruit from the middle Miocene, Yakima Canyon, Washington, USA. *Am. J. Bot.* 86, 307-325.

Chen, Y. Q. (2007). *The Phylogeny and Biogeography of Fagaceae*, Ph. D. thesis, Kunming Institute of Botany, Chinese Academy of Sciences, Kunming.

Colani, M. (1920). *Étude sur les Florès Tertiaires de Quelques Gisements de Lignite de l'Indochine et du Yunnan. Series: Bulletin du Service Geologique de l'Indochine, v. 8, Fasc. 1*. Hanoi: Imprimerie d'Extreme-Orient.

Crepet, W. L., and Daghlian, C. P. (1980). Castaneoid inflorescences from the middle Eocene of Tennessee and the diagnostic value of pollen (at the subfamily level) in the Fagaceae. *Am. J. Bot.* 67, 739–757. doi: 10.1002/j.1537-2197.1980.tb07704.x

Crepet, W. L., and Nixon, K. C. (1989a). Earliest megafossil evidence of Fagaceae: phylogenetic and biogeographic implications. *Am. J. Bot.* 76, 842–855. doi: 10.1002/j.1537-2197.1989.tb15062.x

Crepet, W. L., and Nixon, K. C. (1989b). Extinct transitional Fagaceae from the Oligocene and their phylogenetic implications. *Am. J. Bot.* 76, 1493–1505. doi: 10.1002/j.1537-2197.1989.tb15131.x

Daghlian, C. P., and Crepet, W. L. (1983). Oak catkins, leaves and fruits from the Oligocene Catahoula Formation and their evolutionary significance. *Am. J. Bot.* 70, 639–649. doi: 10.1002/j.1537-2197.1983.tb12444.x

Deng, M., Li, Q. S., Yang, S. T., Liu, Y. C., and Xu, J. (2013). Comparative morphology of leaf epidermis in the genus *Lithocarpus* and its implication in leaf epidermal feature evolution in Fagaceae. *Plant Syst. Evol.* 299, 659–681. doi: 10.1007/s00606-012-0751-0

Denk, T., Grimm, G. W., Manos, P. S., Deng, M., and Hipp, A. L. (2017). "An updated infrageneric classification of the oaks: review of previous taxonomic schemes and synthesis of evolutionary patterns," in *Oaks Physiological Ecology. Exploring the Functional Diversity of Genus Quercus L*, eds E. Gil-Pelegrín, J. J. Peguero-Pina, and D. Sancho-Knapik (Berlin: Springer), 13–38. doi: 10.1007/978-3-319-69099-5_2

Ellis, B., Daly, D. C., Hickey, L. J., Johnson, K. R., Mitchell, J. D., Wilf, P., et al. (2009). *Manual of Leaf Architecture*. Ithaca: Cornell University Press.

Guo, S. X. (1979). "Late Cretaceous and early Tertiary floras from the southern Guangdong and Guangxi with their stratigraphic significance," in *The Mesozoic and Cenozoic Red Beds of South China*, ed. Mesozoic and Cenozoic Red Beds of South China (Beijing: Science Press), 223–230.

Guo, S. X. (2011). The late Miocene Bangmai flora from Lincang county of Yunnan, southwestern China. *Acta Palaeontol. Sin.* 50, 353–408.

Hably, L. (2013). The late Miocene flora of Hungary. *Geol. Hungar. Ser. Palaeontol. Fasciculus* 59:175.

He, Y. L., Na, L., Wang, Z. X., Wang, H. F., Yang, G. L., Xiao, L., et al. (2014). *Quercus yangyiensis* sp. nov. from the late Pliocene of Baoshan, Yunnan and its paleoclimatic significance. *Acta Palaeontol. Sin.* 88, 738–747. doi: 10.1111/1755-6724.12234

Herendeen, P. S., Crane, P. R., and Drinnan, A. N. (1995). Fagaceous flowers, fruits, and cupules from the Campanian (Late Cretaceous) of central Georgia, USA. *ı Int. J. Plant Sci.* 156, 93–116. doi: 10.1086/297231

Hofmann, C. H., Kodrul, T. M., Liu, X. Y., and Jin, J. H. (2019). Scanning electron microscopy investigations of middle to late Eocene pollen from the Changchang Basin (Hainan Island, South China) – Insights into the paleobiogeography and fossil history of *Juglans*, *Fagus*, *Lagerstroemia*, *Mortoniodendron*, *Cornus*, *Nyssa*, *Symplocos* and some Icacinaceae in SE Asia. *Rev. Palaeobot. Palynol.* 265, 41–61. doi: 10.1016/j.revpalbo.2019.02.004

Huang, C. C., Zhang, Y. T., and Bartholomew, B. (1999). "Fagaceae," in *The Flora of China*, eds C. Y. Wu and P. H. Raven (Beijing: Science Press), 380–400.

Huzioka, K., and Takahasi, E. (1970). The Eocene flora of the ube coal-field, southwest Honshu, Japan. *J. Mining Coll. Akita Univ. Int. J. Min. Coll.* 4, 1–88.

Jia, H., Jin, P. H., Wu, J. Y., Wang, Z. X., and Sun, B. N. (2015). *Quercus* (subg. *Cyclobalanopsis*) leaf and cupule species in the late Miocene of eastern China and their paleoclimatic significance. *Rev. Palaeobot. Palynol.* 219, 132–146. doi: 10.1016/j.revpalbo.2015.01.011

Jiang, Y. X., Wang, B. S., Zang, R. G., Jin, J. H., and Liao, W. B. (2002). *Tropical Forest Biodiversity and Its Formation Mechanism in Hainan Island*. Beijing: Science Press.

Jin, J. H. (2009). Two Eocene fossil fruits from the Changchang Basin of Hainan Island, China. *Rev. Palaeobot. Palynol.* 153, 150–152. doi: 10.1016/j.revpalbo.2008.07.010

Jones, J. H. (1986). Evolution of the Fagaceae: the implications of foliar features. *Ann. Miss. Bot. Gar.* 73, 228–275.

Jones, J. H., and Dilcher, D. L. (1988). A study of the *Dryophyllum* leaf forms from the Paleogene of sontheastern North America. *Palaeontogr. Abt. B.* 208, 53–80.

Kvaćek, Z., and Walther, H. (1989). Paleobotanical studies in Fagaceae of the European Tertiary. *Plant Syst. Evol.* 162, 213–229. doi: 10.1007/978-3-7091-3972-1_11

Kvaćek, Z., and Walther, H. (2004). Oligocene flora of Bechlejovice at Děčín from the neovolcanic area of the České středohoří Mountains, Czech Republic. *Acta Mus. Nat. Pragae Ser. B Hist. Nat.* 60, 9–60.

Kvaćek, Z., and Walther, H. (2010). European Tertiary Fagaceae with chinquapin-like foliage and leaf epidermal characteristics. *Feddes Repert.* 121, 248–267. doi: 10.1002/fedr.201100005

Larson-Johnson, K. (2016). Phylogenetic investigation of the complex evolutionary history of dispersal mode and diversification rates across living and fossil Fagales. *New Phyto.* 209, 418–435. doi: 10.1111/nph.13570

Lei, Y. Z., Zhang, Q. R., He, W., and Cao, X. P. (1992). *Tertiary, Geology of Hainan Island*. Beijing: Geological Publishing House.

Li, H. M., and Guo, S. X. (1982). "Angiospermae," in *Paleontological Atlas of East China part 3, volume of Mesozoic and Cenozoic*, ed. Nanjing Institute of Geology and Mineral Resourses (Beijing: Geological Publishing House), 236–316.

Li, J. Q. (1996). On the phylogeny of the Fagaceae. *Acta Phytotaxon. Sin.* 34, 597–609.

Li, J. Z., Qiu, J., Liao, W. B., and Jin, J. H. (2009). Eocene fossil *Alseodaphne* from Hainan Island of China and its paleoclimatic implications. *Sci. China Ser. D Earth Sci.* 52, 1537–1542. doi: 10.1007/s11430-009-0120-1

Li, R. Y., Sun, B. N., Wang, Q. J., Ma, F. J., Xu, X. H., Wang, Y. F., et al. (2015). Two new *Castanopsis* (Fagaceae) species based on cupule and foliage from the upper Miocene of eastern Zhejiang, China. *Plant Syst. Evol.* 301, 25–39. doi: 10.1007/s00606-014-1051-7

Liu, M. Q., Deng, M., and Zhou, Z. K. (2009). Taxonomic and ecological implications of leaf cuticular morphology in *Castanopsis*, *Castanea*, and *Chrysolepis*. *Plant Syst. Evol.* 283, 111–123. doi: 10.1007/s00606-009-0220-6

Liu, X. Y., Xu, S. L., Han, M., and Jin, J. H. (2019). An early Oligocene fossil acorn, associated leaves and pollen of the ring-cupped oaks (*Quercus* subg. *Cyclobalanopsis*) from Maoming Basin, South China. *J. Syst. Evol.* 57, 153–168. doi: 10.1111/jse.12450

Liu, Y. S. (1993). A palaeoclimatic analysis on early Pleistocene flora of Changsheling Formation, Baise Basin, Guangxi. *Acta Palaeontol. Sin.* 32, 151–169.

Liu, Y. S., Momohara, A., and Mei, S. W. (1995). A revision on the Chinese megafossils of *Fagus* (Fagaceae). *Journ. Jap. Bot.* 71, 168–177.

Luo, Y., and Zhou, Z. K. (2001). Leaf epidermis of *Quercus* subgen. *Cyclobalanopsis* (Oerst.) Schneid (Fagaceae). *Acta Phytotaxo. Sin.* 39, 489–501.

MacGinitie, H. D. (1941). *A Middle Eocene Flora from the Central Sierra Nevada*. Washington, DC: Carnegie Institution of Washington publication.

MacGinitie, H. D. (1953). *Fossil Plants of the Florissant Beds, Colorado*. Washington, DC: Carnegie Institution of Washington Publication.

MacGinitie, H. D. (1969). *The Eocene Green River Flora of North Western Colorado and Northeastern Utah*. California: University of California.

Mai, D. H. (1995). *Tertiäre Vegetations Geschichte Europas*. Heidelberg: Spektrum Akademischer Verlag.

Mai, D. H., and Walther, H. (1985). Dieobereozänen floren des weisselster-beckens und seiner Randgebiete, Jahrb. *Staatl. Mus. Mineral. Dresden.* 33:220.

Manchester, S. R. (1983). Eocene fruits, wood and leaves of the Fagaceae from the Clarno Formation of Oregon. *Am. J. Bot.* 70:74.

Manchester, S. R. (1994). Fruits and seeds of the middle Eocene Nut Beds flora, Clarno Formation, Oregon. *Palaeontogr. Am.* 58:280.

Manchester, S. R., and Crane, P. R. (1983). Attached leaves, inflorescences and fruits of *Fagopsis*, an extinct genus of fagaceous affillity from the Oligocene florissant flora of Calorado, U.S.A. *Am. J. Bot.* 70, l147–l164.

Manchester, S. R., and Dillhoff, R. M. (2004). *Fagus* (Fagaceae) fruits, foliage, and pollen from the middle Eocene of Pacific Northwestern North America. *Can. J. Bot.* 82, 1509–1517. doi: 10.1139/b04-112

Meyer, H. W., and Manchester, S. R. (1997). *The Oligocene Bridge Creek Flora of the John Day Formation, Oregon*. Berkeley, CA: University of California Press.

Mindall, R. A., Stockey, R. A., and Beard, G. (2007). *Cascadiacarpa spinosa* gen. et sp. nov (Fagaceae): castaneoid fruits from the Eocene of Vancouver Island, Canada. *Am. J. Bot.* 94, 351–361. doi: 10.3732/ajb.94.3.351

Mindall, R. A., Stockey, R. A., and Beard, G. (2009). Permineralized *Fagus* nuts from the Eocene Vancouver Island. *Can. Int. J. Plant Sci.* 170, 551–560. doi: 10.1086/596335

Mu, X. Y., Li, J. X., Xia, X. F., and Zhao, L. C. (2015). Cupules and fruits of *Lithocarpus* (Fagaceae) from the Miocene of Yunnan, southwestern China. *Taxon* 64, 795–808. doi: 10.12705/644.10

Nanjing Institute of Geology and Mineral Resources [NIGMR] (1982). *Paleontological atlas of East China: Part 3. Volume of Mesozoic and Cenozoic*. Beijing: Geological publishing house.

Palamarev, E., and Tsenov, B. (2004). Genus *Quercus* in the late Miocene flora of Baldevo Formation (Southwest Bulgaria): taxonomical composition and palaeoecology. *Phytol. Balc.* 10, 147–156.

Shi, X. G., Jin, J. H., Ye, C. X., and Liu, W. Q. (2012). First fruit fossil record of *Morinda* (Rubiaceae) from China. *Rev. Palaeobot. Palynol.* 179, 13–16. doi: 10.1016/j.revpalbo.2012.04.001

Sims, H. J., Herendeen, P. S., and Crane, P. R. (1998). New genus of fossil Fagaceae from the Santonian (Late Cretaceous) of central Georgia, USA. *Int. J. Plant Sci.* 159, 391–404. doi: 10.1086/297559

Spicer, R. A., Herman, A. B., Liao, W. B., Spicer, T. E. V., Kodrul, T. M., Yang, J., et al. (2014). Cool tropics in the middle Eocene: evidence from the Changchang flora, Hainan Island, China. *Palaeogeogr. Palaeoclimatol. Palaeoecol.* 412, 1–16. doi: 10.1016/j.palaeo.2014.07.011

Takhtajan, A. (ed.) (1982). *Magnoliophyta Fossilia URSS, Ulmaceae-Betulaceae*. St. Petersburg: Russian Academy of Sciences.

Tang, C. Q. (2015). *The Subtropical Vegetation Of Southwestern China: Plant Distribution, Diversity And Ecology*. Berlin: Springer.

Tao, J. R., and Chen, M. H. (1983). "Cenozoic flora of Lincang in the southern Hengduan Mountains," in *Studies in Qinghai-Xizang (Tibet) Plateau—Special Issue of Hengduan Mountains Scientific Expedition (I)*, eds Team of Comprehensive Scientific Expedition to the Qinghai-Xizang (Tibet) Plateau and Chinese Academy of Sciences (Kunming: Yunanan People's Publishing House), 74–95.

Tao, J. R., and Du, N. Q. (1982). Neogene flora of Tengchong Basin in western Yunnan, China. *Acta Bot. Sin.* 24, 273–281.

Tao, J. R., Zhou, Z. K., and Liu, Y. S. (2000). *The Evolution of the Late Cretaceous—Cenozoic Floras in China*. Beijing: Science Press.

Vikulin, C. B. (2011). Thermophilic beech (Fagaceae): *Quercus*, *Lithocarpus*, *Castanopsis* from the late Eocene of the southern European Russia. *Read. Mem. A.N. Krishtofovich.* 7, 128–147.

Wang, L., Xu, Q. Q., and Jin, J. H. (2014). A reconstruction of the fossil *Salvinia* from the Eocene of Hainan Island, South China. *Rev. Palaeobot. Palynol.* 203, 12–21. doi: 10.1016/j.revpalbo.2013.12.005

Wilf, P., Nixon, K. C., Maria, A., and Gandolfo, C. N. R. (2019). Eocene Fagaceae from Patagonia and Gondwanan legacy in Asian rainforests. *Science* 364:972.

Wolfe, J. A. (1968). Paleogene biostratigraphy of nonmaine rocks in King County, Washington, U.S.A. *Geol. Surv. Prof. Pap.* 571, 1–33.

Wolfe, J. A., and Tanai, T. (1980). The Miocene Seldovia point flora from the Kenai group, Alaska, U.SA. *Geol. Surv. Prof. Pap.* 1105, 1–52.

Writing Group of Cenozoic Plants of China [WGCPC] (1978). *Cenozoic Plants from China: Fossil Plants of China*. Beijing: Science Press.

Wu, J. Y., Ding, S. T., Li, Q. J., Zhao, Z. R., Dong, C., and Sun, B. N. (2014). A new species of *Castanopsis* (Fagaceae) from the upper Pliocene of western Yunnan, China and its biogeographical implications. *Palaeoworld* 23, 370–382. doi: 10.1016/j.palwor.2014.10.005

Xia, K., Su, T., Liu, Y. S., Xing, Y. W., Frédéric, M. B., and Jacques Zhou, Z. K. (2009). Quantitative climate reconstructions of the late Miocene Xiaolongtan megaflora from Yunnan, southwest China. *Palaeogeogr. Palaeoclimatol. Palaeoecol.* 276, 80–86. doi: 10.1016/j.palaeo.2009.02.024

Xiao, L., Sun, B. N., Yan, D. F., Xie, S. P., and Wei, L. J. (2006). Cuticular structure of *Quercus pannosa* Hand.-Mazz. from the Pliocene in Baoshan, Yunnan Province and its palaeoenvironmental significance. *Acta Micropalaeontol. Sin.* 23, 23–30.

Xing, Y. W., Gandolfo, M. A., and Linder, H. P. (2015). The Cenozoic biogeographical evolution of woody angiosperms inferred from fossil distributions. *Global Ecol. Biogeogr.* 24, 1290–1301. doi: 10.1111/geb.12383

Xing, Y. W., Hu, J. J., Jacques, F. M. B., Wang, L., Su, T., Huang, Y. J., et al. (2013). A new *Quercus* species from the upper Miocene of southwestern China and its ecological significance. *Rev. Palaeobot. Palynol.* 193, 99–109. doi: 10.1016/j.revpalbo.2013.02.001

Xu, H., Su, T., Zhang, S. T., Deng, M., and Zhou, Z. K. (2016). The first fossil record of ring-cupped oak (*Quercus* L. subgenus *Cyclobalanopsis* (Oersted) Schneider) in Tibet and its paleoenvironmental implications. *Palaeogeogr. Palaeoclimatol. Palaeoecol.* 442, 61–71. doi: 10.1016/j.palaeo.2015.11.014

Xu, X., Dimitrov, D., Shrestha, N., Rahbek, C., and Wang, Z. (2019). A consistent species richness-climate relationship for oaks across the Northern Hemisphere. *Glob. Ecol. Biogeogr.* 28, 1051–1066.

Yao, Y. F., Bera, S., Ferguson, D. K., Mosbrugger, V., Paudayal, K. N., and Jin, J. H. (2009). Reconstruction of paleovegetation and paleoclimate in the early and middle Eocene, Hainan Island, China. *Clim. Chang.* 92, 169–189. doi: 10.1007/s10584-008-9457-2

Zhang, Q. R. (1980). *Stratigraphy and Palaeontology*. Yichang: Yichang Institute of Geology.

Zhou, W. J., Liu, X. Y., Xu, Q. Q., Huang, K. Y., and Jin, J. H. (2013). New coryphoid fossil palm leaves (Arecaceae: Coryphoideae) from the Eocene Changchang Basin of Hainan Island, South China. *Sci. China Earth Sci.* 56, 1493–1501. doi: 10.1007/s11430-013-4681-7

Zhou, Z. K. (1996). Studies on *Dryophyllum* complex from China and its geological and systematic implications. *Acta Bot. Sin.* 38, 666–671.

Zhou, Z. K. (1999). Fossils of the Fagaceae and their implications in systematics and biogeography. *Acta Phytotaxo. Sin.* 37, 369–385.

**Conflict of Interest:** The authors declare that the research was conducted in the absence of any commercial or financial relationships that could be construed as a potential conflict of interest.

frontiers in Ecology and Evolution

ORIGINAL RESEARCH
published: 22 September 2020
doi: 10.3389/fevo.2020.531947

# Modern Climate and Soil Properties Explain Functional Structure Better Than Phylogenetic Structure of Plant Communities in Northern China

*Yabo Shi, Chuang Su, Mingchen Wang, Xinliang Liu, Cunzhu Liang, Liqing Zhao, Xinyu Zhang, Hugjiltu Minggagud, Gang Feng* and Wenhong Ma**

*Ministry of Education Key Laboratory of Ecology and Resource Use of the Mongolian Plateau & Inner Mongolia Key Laboratory of Grassland Ecology, School of Ecology and Environment, Inner Mongolia University, Hohhot, China*

Examination of the mechanisms of the plant community assembly at a geographical scale is an interesting topic in ecology and biogeography, which are of great significance for the understanding of species coexistence and biodiversity conservation. But so far, only a few studies have simultaneously assessed the relative roles of multiple-scale factors in shaping the phylogenetic and functional structure of plant communities at a macroecological scale. In this study, we linked modern climate, glacial-interglacial climate change, and soil properties with the phylogenetic and functional structure of shrub and herbaceous plant communities in Inner Mongolia, China, an arid and semi-arid region. Our results showed that the functional structure of plant communities was more associated with modern climate and soil properties than the phylogenetic structure, especially for the soil properties. Modern precipitation was found in all the combinations of variables that were most closely related to the community structure in this arid and semi-arid region. These findings suggest that the phylogenetic and functional structure of biotic communities may be affected by processes at divergent spatial-temporal scales. That is, the functional structure is better linked with the modern and local factors while the phylogenetic structure is more associated with the historical and regional processes. This study highlights the importance of the associations between the different biodiversity dimensions and divergent drivers.

**Keywords: arid and semiarid region, community assembly, functional structure, modern precipitation, phylogenetic structure, soil properties**

OPEN ACCESS

***Edited by:***
*Zehao Shen,*
*Peking University, China*

***Reviewed by:***
*Dima Chen,*
*China Three Gorges University, China*
*Lingfeng Mao,*
*Nanjing Forestry University, China*

****Correspondence:***
*Gang Feng*
*qaufenggang@163.com*
*Wenhong Ma*
*whma@imu.edu.cn*

***Specialty section:***
*This article was submitted to Biogeography and Macroecology, a section of the journal Frontiers in Ecology and Evolution*

***Received:*** *02 February 2020*
***Accepted:*** *26 August 2020*
***Published:*** *22 September 2020*

***Citation:***
*Shi Y, Su C, Wang M, Liu X, Liang C, Zhao L, Zhang X, Minggagud H, Feng G and Ma W (2020) Modern Climate and Soil Properties Explain Functional Structure Better Than Phylogenetic Structure of Plant Communities in Northern China. Front. Ecol. Evol. 8:531947. doi: 10.3389/fevo.2020.531947*

## INTRODUCTION

How plant communities are assembled at a geographical scale is an important topic in ecology and biogeography because it could provide insight into the knowledge of species coexistence and biodiversity conservation (Webb et al., 2002; Freilich and Connolly, 2015; Daniel et al., 2019). Community assembly is codetermined by factors at divergent spatiotemporal scales (Feng et al., 2014; Blonder et al., 2018; Kubota et al., 2018). Specifically, historical processes, such as geological events and paleoclimate change, could affect the biodiversity and community structure through their effects on species speciation, migration, and extinction (Svenning et al., 2015). Modern factors,

such as modern climate and local habitat filtering, could also assemble local communities by limiting the species ranges, affecting the water availability, and providing niche diversity (Currie et al., 2004; Feng et al., 2014; Stein et al., 2014). Therefore, it is important to explore how these multiple-scale factors simultaneously contributed in assembling the local communities (Fine, 2015; Pärtel et al., 2016).

Stable paleoclimate could promote high species richness by both accelerating speciation and avoiding the extinction of relict species, resulting in a relatively over-dispersed phylogenetic structure, i.e., species are more distantly related (Feng et al., 2014, 2017; Kubota et al., 2018). In contrast, the cooling and drying during glacial periods may promote a relatively clustered phylogenetic structure by filtering on the phylogenetically conserved cold tolerance (Eiserhardt et al., 2015). For example, the phylogenetic structure of forest tree communities in China and the globe is more over-dispersed in regions with stable glacial-interglacial climate (Feng et al., 2014; Kubota et al., 2018). Except for the phylogenetic structure, paleoclimate change may also affect the functional structure of local communities by filtering the regional species pools based on climate-related traits (Ordonez and Svenning, 2015; Blonder et al., 2018). For example, the functional diversity deficits of plant assemblages in Europe are positively associated with the glacial-interglacial climate instability (Ordonez and Svenning, 2015).

Modern climate, including both temperature and precipitation, has also been widely linked with biodiversity and community structure at various spatial scales and regions, providing support for many climate–based hypotheses (Currie et al., 2004; Qian et al., 2015; Feng et al., 2019). For example, the water-energy dynamics hypothesis suggests that the geographic distribution of species was codetermined by water and energy (O'Brien, 1998; Field et al., 2005). The wet and warm tropics could also promote speciation and prevent extinction by supplying enough productivity, great ecological specialization, and diverse biotic interactions, resulting in high levels of taxonomic, phylogenetic, and functional diversity (Currie et al., 2004; Ordonez and Svenning, 2015; Qian et al., 2015). Besides these climate factors, other local environmental factors also play important roles in assembling local plant communities (Stock and Verboom, 2012; Zhou et al., 2019). For example, the dominance of low-nutrient adapted plant lineages in Western Australia and South African Cape is mainly driven by the filtering of low soil fertility (Stock and Verboom, 2012). Both the phylogenetic and functional structure of plant communities in Mount Kenya vary along the elevational gradient (Zhou et al., 2019).

Although previous studies have found that both the phylogenetic and functional structure of local communities could be affected by these different spatiotemporal factors, it is also suggested that the phylogenetic structure should be mainly driven by the historical and regional processes, while the functional structure is more associated with contemporary and local factors (Feng et al., 2014; Li et al., 2019). The explanation is that phylogenetic diversity reflects the evolutionary relationships among species, which is mainly linked with the biogeographic history; while functional diversity refers to the variation in species ecological traits, which is more plastic and mainly constrained by recent and local influence (Swenson, 2013; Feng et al., 2014; Li et al., 2019). For example, the phylogenetic structure of Chinese forest tree communities is strongly associated with the glacial-interglacial climate change, while the functional structure is significantly correlated with local disturbance (Feng et al., 2014).

The shrubland, which is inadequate studied compared with grassland, covers a wide climate gradient across Inner Mongolia, from the humid open mountain areas in the east to the dry desert regions in the west (Miao et al., 2018; Guo et al., 2019). Although water availability and soil nutrient availability are the most important limitations to the herbaceous plants in this region (Bai et al., 2008; Ma et al., 2010; Guo et al., 2019), woody plants (including semi-shrubs and shrubs) may show divergent patterns with water availability because of their different strategies to environmental constraints (Moro et al., 2015; Šímová et al., 2018; Massante et al., 2019). Moreover, although the current plant growth and ecological processes are severely limited by water and nutrient availability, these regions have experienced dramatic climatic fluctuations with alternating dry and wet conditions during the Late Quaternary, which may have significant legacy on the current plant diversity and community structure (Yang et al., 2011; Tian et al., 2017). However, so far, few studies have simultaneously linked these multiple-scale factors with the phylogenetic and functional structure of both herbaceous and woody plant communities in this arid and semi-arid region. In this study, we conducted field investigations including 114 shrubland sites along the large environmental gradients in this region, and aimed to test: (1) is the phylogenetic and functional structure of plant communities shaped by divergent factors?, (2) is precipitation the dominant factor for plant community structure in this arid and semi-arid region?, and (3) do shrub and herbaceous plant communities show divergent patterns?

# MATERIALS AND METHODS

## Study Area and Plant Investigation

We conducted surveys of the shrub communities in the Inner Mongolia Autonomous Region between June and August of 2015–2017 (**Figure 1**). The Inner Mongolia Autonomous Region is located in the arid and semi-arid areas of northern China. The mean annual precipitation (MAP) of study region ranges from 31 to 534 mm (from west to east) and the mean annual temperature ranges from -3.9 to 12.6°C (from east to west) (Wu et al., 2015; Miao et al., 2018).

One hundred fourteen (114) shrubland sites were investigated along a large geographic range (37°24′–53°23′N latitude, 97°12′–126°04′E longitude). At each site, we investigated shrub species in three plots of 5 m × 5 m and herbaceous species in three subplots (1 m × 1 m) at the diagonal of each plot. The distances between each plot within one site were 5–10 m (5 m in the mountain shrublands and 10 m in the desert sites due to the sparse distribution of shrubs). At each plot, we recorded all the species and measured the maximum height ($H_{max}$, the distance between the upper boundary of the photosynthetic tissues on a plant and the ground) of each shrub individuals and mean $H_{max}$

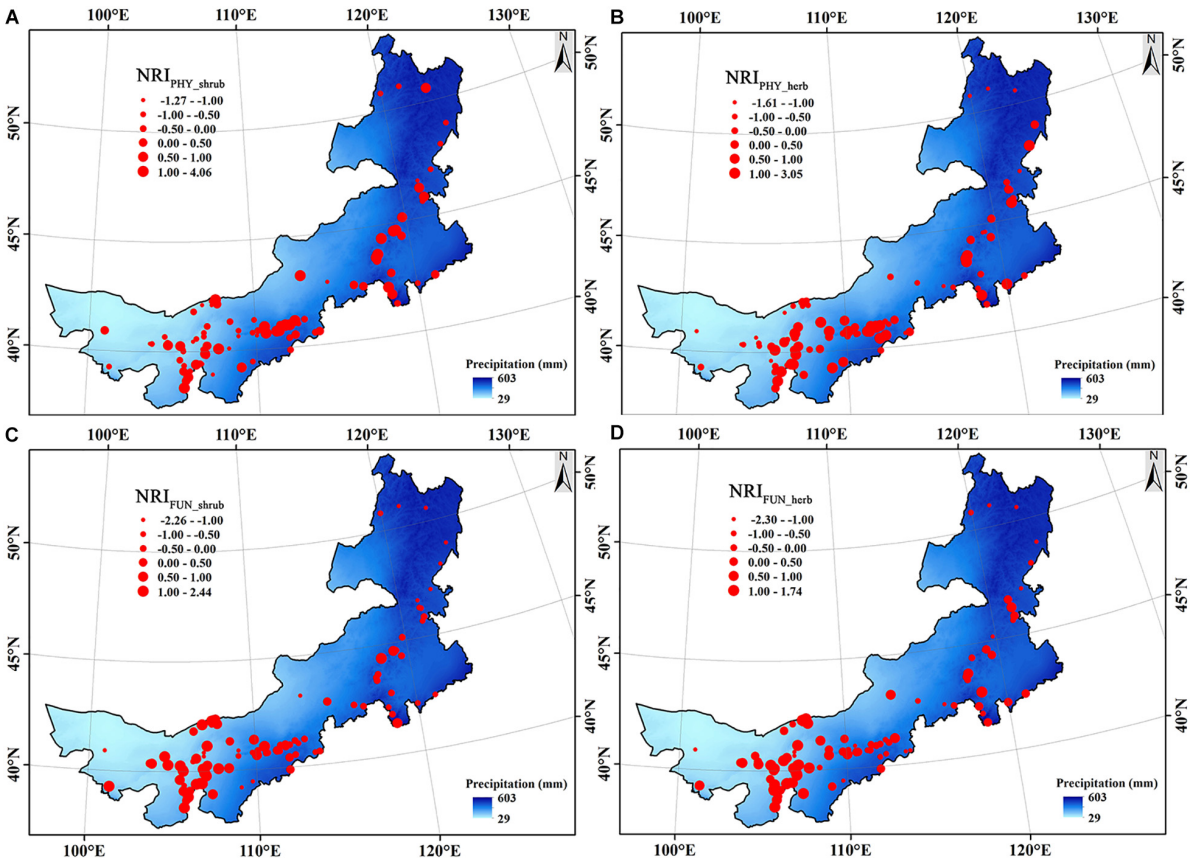


**FIGURE 1 |** The spatial distribution of the phylogenetic **(A,B)** and functional structure index **(C,D)** of each site along the modern precipitation gradient. All NRI values have been standardized in this figure. **(A)** the phylogenetic structure of shrubs ($NRI_{PHY\_shrub}$), **(B)** the phylogenetic structure of herbs ($NRI_{PHY\_herb}$), **(C)** the functional structure of shrubs ($NRI_{FUN\_shrub}$), and **(D)** the functional structure of herbs ($NRI_{FUN\_herb}$).

for each herb species. $H_{max}$, as a comprehensive and important trait, can reflect the ability of species to adapt to the environment, such as light competition and carbon storage capacity. And, it is also closely related to other functional traits such as leaf life, seed size, etc. (Moles et al., 2009; Long et al., 2015; Olson et al., 2018). Four hundred seventy-six (476) species were recorded (all are angiosperms), including 385 herbaceous species and 91 shrub or semi-shrub species. We used the mean value of the maximum height of a species among all the sites as the trait value of the species.

## Environmental Data

At each site, we used GPS to record the longitude and latitude. The mean annual temperature (MAT), MAP, and elevation (EL) were obtained from the WorldClim database (Hijmans et al., 2005). The mean of the Community Climate System Model version 3 (Collins et al., 2006) and Model for Interdisciplinary Research on Climate version 3.2 (Hasumi and Emori, 2004) were used to represent the values of the Last Glacial Maximum (LGM) MAT and LGM MAP. MAT anomaly and MAP anomaly (present-day values minus LGM values) are indicators of paleoclimate change (Sandel et al., 2011; Kissling et al., 2012).

Three soil samples at the upper 0–20 cm were sampled with a soil core along the diagonal of each plot and mixed together. Soil samples were transported to the laboratory and air dried, and then removed the roots and stones (>2 mm). After grounded to pass through a 100–mesh sieve, soil nitrogen content (SNC) was measured using an elemental analyzer (vario MACRO cube).

## Phylogenetic and Functional Structure

The relatedness index (NRI) is a measure to estimate the pairwise phylogenetic distances between co-occurring species and reflects the degree of clustering or over-dispersion of species in a community (Webb, 2000). The positive value of NRI indicates the clustering of community structure (species are more closely related/similar), while the negative value indicates over-dispersion (species are more distantly related/dissimilar).

The formula is:

$$NRI = -1 \times \frac{MPD_{obs} - meanMPD_{rnd}}{sdMPD_{rnd}}$$

where $MPD_{obs}$ is the observed mean phylogenetic distance (MPD) of a site, $meanMPD_{rnd}$ is the mean MPD of the 999 null models (null model = "taxa.labels"), and $sdMPD_{rnd}$ is the standard deviation of MPD of the 999 null models.

NRI index was used to calculate both the phylogenetic structure and functional structure. For the phylogenetic structure, a phylogenetic tree including 2,882 species recorded in the *Key to the vascular plants of Inner Mongolia* (Zhao and Zhao, 2014) was constructed in virtue of the mega-tree (Jin and Qian, 2019). To calculate the functional structure, the $H_{max}$ of the 385 herbaceous species and 91 shrub and semi-shrub species were used to build the herbaceous and shrub functional dendrograms, respectively. Euclidian distance was used to calculate the distance matrix for all species and the "complete linkage" was used for the cluster analyses. The phylogenetic tree and the functional dendrograms were then used for the following phylogenetic and functional NRI calculations for the species in each site.

## DATA ANALYSES

To unify the dimensions of all the independent and dependent variables, they were firstly standardized (mean = 0 and standard deviation = 1). The ordinary least squares models (OLS) were applied to fit the relationships between each structure index and explanatory variable.

To assess which combination of variables was most associated with each community structure, we also performed analyses with the Random Forest (RF) modeling, which could deal with the multiple correlation relationship and complex interaction between the independent variables (Cutler et al., 2007). We set up models, respectively, for all possible combinations of the six independent variables (63 combinations in total). For each model, we randomly split the data into 50% training and 50% evaluation data 1,000 times to avoid over-fitting the model. Six combinations of the variables with the highest explanatory power, which were indicated by the highest correlations between the environmental variables and phylogenetic or functional structure indices, were chosen in all the models.

The statistical analyses were performed in R 3.5.3 using the packages vegan (Oksanen et al., 2019), picante (Kembel et al., 2010), randomForest (Liaw and Wiener, 2002).

## RESULTS

Compared with the phylogenetic structure, the functional structure of both shrub and herbaceous communities showed clear patterns, i.e., functional clustering increased with decreasing precipitation from northeast to southwest (**Figure 1**). The ordinary least squares models showed that the MAP always occurred in the three variables most associated with the phylogenetic and functional structure of both shrub and herbaceous communities (**Figure 2** and **Supplementary Table S1**). In addition, the MAP was relatively weakly and positively associated with the phylogenetic structure of shrub, while relatively strongly and negatively associated with the functional structure, indicating that the regions with more precipitation tend to have a clustered phylogenetic structure but over-dispersed functional structure (**Figure 2**). Regions with a large precipitation anomaly also tend to have a clustered phylogenetic structure but over-dispersed functional structure (**Figure 2**). The soil nitrogen content was only negatively correlated with the functional structure, indicating an increasing over-dispersed functional structure with increasing soil nutrient availability (**Figure 2** and **Supplementary Table S1**).

The Random Forest modeling results showed that the functional structure of both shrub and herbaceous communities were better associated with explanatory variables than phylogenetic structure, especially for the soil nitrogen content (**Figure 3**). The soil nitrogen content, precipitation, and anomaly in precipitation were, again, the three variables that always occurred in the combinations of variables most associated with the phylogenetic and functional structure of plant communities (**Figure 3**).

## DISCUSSION

By linking the multiple-scale drivers with the plant community structure in this arid and semi-arid region, our results showed that modern precipitation was the main factor affecting the phylogenetic and functional structure of both shrub and herbaceous communities. Soil nitrogen content mainly affects the functional structure of the shrub and herbaceous communities. Notably, compared with the phylogenetic structure, the functional structure was more associated with these drivers.

### Modern Climate and Community Structure

As a major limiting factor in this arid and semi-arid region, modern precipitation was found to be the main driver of the phylogenetic and functional structure of both shrub and herbaceous communities. While previous studies showed that regions with high precipitation have an over-dispersed phylogenetic structure, e.g., vascular plant communities in Qinghai-Tibetan Plateau (Yan et al., 2013) and tree communities at global scale (Kubota et al., 2018), our results indicated that the sites with more precipitation tended to have a clustered phylogenetic structure, which is consistent with a study on woody plant communities distributed at a global scale (Massante et al., 2019). This discrepancy may be explained by the special relation between the temperature and precipitation in this region, i.e., the northeastern Inner Mongolia has a high precipitation but low temperature while the southwestern Inner Mongolia has a low precipitation but high temperature. This special climate distribution pattern makes it possible for harsh environments, featuring drought or cold, to become filters of the convergent phylogenetic structure (Kubota et al., 2018). The clustered phylogenetic structure of shrub communities with a lower temperature was consistent with previous studies (Yan et al., 2013; Feng et al., 2014). Notably, a recent study in the same region also found a weak relation between the phylogenetic structure of shrub communities and modern climate, suggesting a weak role of environmental filtering on the phylogenetic structure of plant communities in this region (Dong et al., 2019).

In contrast to the weak relations between the modern climate and phylogenetic structure, our results showed stronger

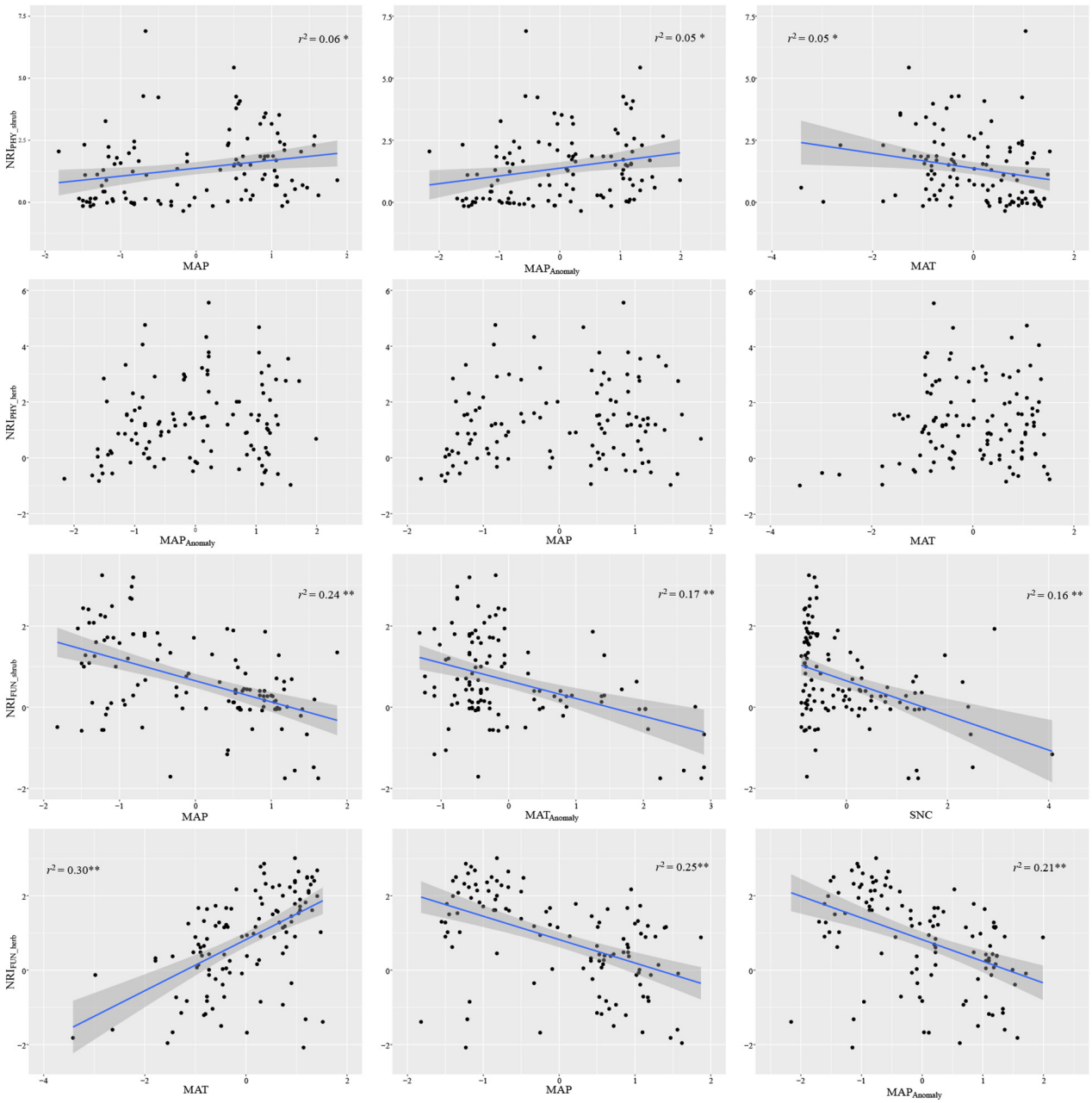


**FIGURE 2 |** Scatter plots of the three most associated variables against the different structure indices. $NRI_{PHY\_shrub}$, phylogenetic shructure of shrub; $NRI_{PHY\_herb}$, phylogenetic structure of herb; $NRI_{FUN\_shrub}$, functional structure of shrub; $NRI_{FUN\_herb}$, functional structure of herb. MAT, mean annual temperature; MAP, mean annual precipitation; SNC, soil nitrogen content; $MAT_{Anomaly}$, MAT anomaly; $MAP_{Anomaly}$, MAP anomaly.

and negative relations between the modern precipitation and functional structure, indicating that sites with good water conditions tended to have an over-dispersed functional structure. At the larger regional scale of China, the plant height also increases with modern temperature and precipitation (Mao et al., 2020). High precipitation in this arid and semi-arid region means high productivity, more resources, high soil nitrogen content, and soil moisture, which would promote the coexistence of more plant species and high functional diversity in height through an increased facilitation and competition for resources, such as light, soil moisture, and soil nutrition (Katabuchi et al., 2012; Spasojevic and Suding, 2012). Consistent with our findings, a study of alpine tundra in the Colorado Rocky Mountains also finds a positive relation between the functional diversity and resource availability (Spasojevic and Suding, 2012). In contrast, the increasing clustered functional structure with a less precipitation indicated a strong effect of environmental filtering on the functional structure in southwestern Inner Mongolia.

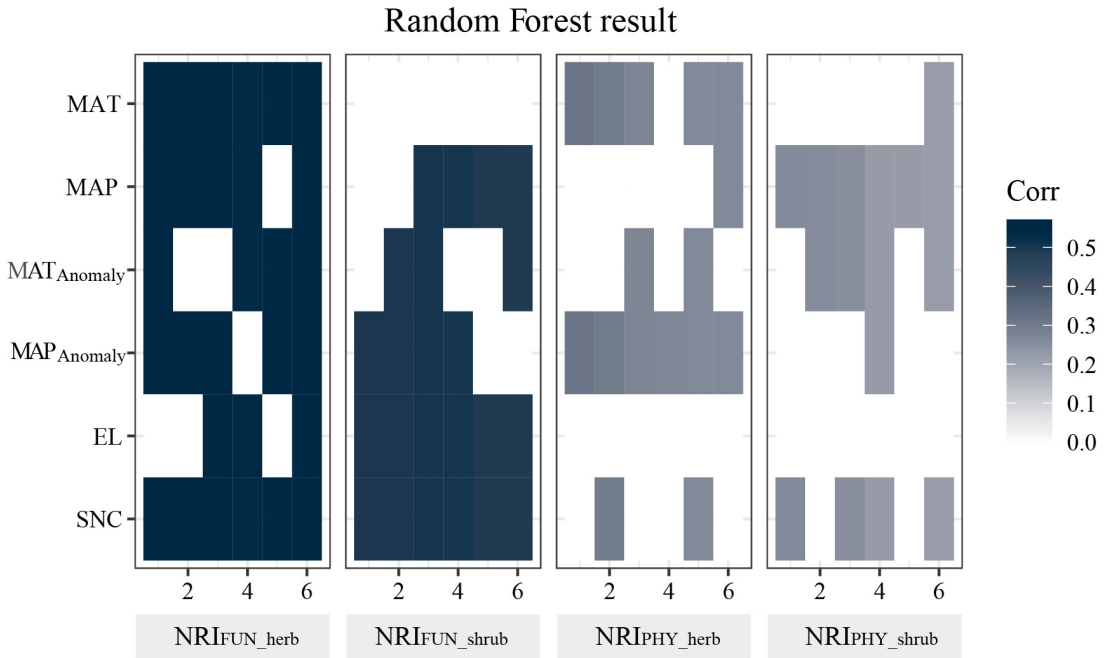


**FIGURE 3 |** Six combinations of the variables with the highest explanatory power for the community structure in the Random Forest modeling. Each row represents a variable. Blue plaque indicates the environmental factors that existed in the combinations. $NRI_{FUN\_herb}$, functional structure of herb; $NRI_{FUN\_shrub}$, functional structure of shrub; $NRI_{PHY\_herb}$, phylogenetic structure of herb; $NRI_{PHY\_shrub}$, phylogenetic structure of shrub. EL, elevation; MAT, mean annual temperature; $MAT_{Anomaly}$ means MAT anomaly; MAP, mean annual precipitation; $MAP_{Anomaly}$, MAP anomaly; SNC, soil nitrogen content.

## Soil Nitrogen Content and Community Structure

Being an important local driver of community structure, the soil nitrogen content at the site level was found to be only associated with the functional structure of shrub and herbaceous communities, and had no associations with the phylogenetic structure. This finding supports the idea that the functional structure should be better linked with local and contemporary drivers because the functional traits are more plastic compared with the phylogenetic relations, which are mainly shaped by historical and regional processes (Feng et al., 2014; Li et al., 2019). A recent study about shrub communities in this region also suggests that compared with the leaf width and leaf length, the height shows a low phylogenetic signal and high plasticity (Zheng et al., 2019).

The increasing over-dispersed functional structure in height with a high soil nitrogen content again suggests that high soil nutrient may promote a high functional diversity in height through the increased facilitation and competition for soil moisture and nutrition, which is essential for plants (Katabuchi et al., 2012; Spasojevic and Suding, 2012). Nitrogen and water promote the growth in twig size and number of dominant shrubs (She et al., 2016). The dominant species may occupy a wider ecological niche which results in an enhanced inter-species competition. In contrast, the increasing functional clustering with less soil nitrogen content indicates that low soil fertility may be a strong environmental filter and result in a clustered functional structure (Spasojevic and Suding, 2012; Miatto and Batalha, 2018). Our findings are consistent with previous studies on the prairie and seasonal forests in Brazil, Western Australia, and South Africa, where low soil factors limit the divergence of traits (Stock and Verboom, 2012; Miatto and Batalha, 2018). The direct effect of water and nitrogen on the functional structure may explain the high explanatory of functional structure than phylogenetic structure in our study.

## Glacial-Interglacial Climate Change and Community Structure

Climate turbulence during the past glacial-interglacial periods could affect biodiversity, community assembly, and ecosystem functioning through their effects on speciation, extinction, and migration (Svenning et al., 2015; Blonder et al., 2018). Previous studies have found that regions with a large glacial-interglacial climate instability would harbor biotic assemblages with clustered phylogenetic and functional structure because of the high extinction rate and lagged immigration (Feng et al., 2014; Ordonez and Svenning, 2017; Kubota et al., 2018). Consistent with these studies, our results indicated a trend of an increasing phylogenetic clustering with a large anomaly in precipitation. The significant relations between the anomaly in precipitation and functional structure may be resulted from the high correlation (0.80) between modern precipitation and anomaly in precipitation. Alternating dry and wet climate fluctuations may also mask the process of community assembly driven by climate anomaly.

## CONCLUSION

Being the first study simultaneously linking multiple-scale drivers with the phylogenetic and functional structure of both shrub and herbaceous communities in Inner Mongolia, China, we found that modern precipitation was the main driver of plant community structure in this arid and semiarid region. In addition, soil nutrient was only significantly associated with the plant functional structure. Notably, the plant functional structure was better explained by these drivers than the plant phylogenetic structure. Our findings highlight the importance of considering the multiple-scale drivers for the divergent dimensions of biodiversity.

## DATA AVAILABILITY STATEMENT

The datasets generated for this study are available on request to the corresponding author.

## AUTHOR CONTRIBUTIONS

GF and WM designed the research. CS, MW, XL, CL, LZ, XZ, HM, and WM performed the field investigation. YS and GF analyzed the data. YS, GF, and WM wrote the manuscript. All authors contributed to the article and approved the submitted version.

## FUNDING

This work was supported by the National Special Project of Basic Work of Science and Technology (2015FY110300) and the Inner Mongolia Autonomous Science and Technology Plan Project (No. 2019GG009).

## ACKNOWLEDGMENTS

We thank all the field investigators and Dr. Bailing Miao for his assistance in drawing the graph of the manuscript.

## SUPPLEMENTARY MATERIAL

The Supplementary Material for this article can be found online at: https://www.frontiersin.org/articles/10.3389/fevo.2020.531947/full#supplementary-material

## REFERENCES

Bai, Y., Wu, J., Xing, Q., Pan, Q., Huang, J., Yang, D., et al. (2008). Primary production and rain use efficiency across a precipitation gradient on the Mongolia Plateau. *Ecology* 89, 2140–2153. doi: 10.1890/07-0992.1

Blonder, B., Enquist, B. J., Graae, B. J., Kattge, J., Maitner, B. S., Morueta-Holme, N., et al. (2018). Late quaternary climate legacies in contemporary plant functional composition. *Glob. Chang. Biol.* 24, 4827–4840. doi: 10.1111/gcb.14375

Collins, W. D., Bitz, C. M., Blackmon, M. L., Bonan, G. B., Bretherton, C. S., Carton, J. A., et al. (2006). The community climate system model version 3 (CCSM3). *J. Clim.* 19, 2122–2143. doi: 10.1175/JCLI3761.1

Currie, D. J., Mittelbach, G. G., Cornell, H. V., Field, R., Guegan, J.-F., Hawkins, B. A., et al. (2004). Predictions and tests of climate-based hypotheses of broad-scale variation in taxonomic richness. *Ecol. Lett.* 7, 1121–1134. doi: 10.1111/j.1461-0248.2004.00671.x

Cutler, D. R., Edwards, T. C., Beard, K. H., Cutler, A., Hess, K. T., Gibson, J., et al. (2007). Random forests for classification in ecology. *Ecology* 88, 2783–2792. doi: 10.1890/07-0539.1

Daniel, J., Gleason, J. E., Cottenie, K., and Rooney, R. C. (2019). Stochastic and deterministic processes drive wetland community assembly across a gradient of environmental filtering. *Oikos* 128, 1158–1169. doi: 10.1111/oik.05987

Dong, L., Liang, C., Li, F. Y., Zhao, L., Ma, W., Wang, L., et al. (2019). Community phylogenetic structure of grasslands and its relationship with environmental factors on the Mongolian Plateau. *J. Arid Land* 11, 595–607. doi: 10.1007/s40333-019-0122-6

Eiserhardt, W. L., Borchsenius, F., Plum, C. M., Ordonez, A., and Svenning, J.-C. (2015). Climate-driven extinctions shape the phylogenetic structure of temperate tree floras. *Ecol. Lett.* 18, 263–272. doi: 10.1111/ele.12409

Feng, G., Ma, Z., Benito, B. M., Normand, S., Ordonez, A., Jin, Y., et al. (2017). Phylogenetic age differences in tree assemblages across the Northern Hemisphere increase with long-term climate stability in unstable regions. *Global. Ecol. Biogeogr.* 26, 1035–1042. doi: 10.1111/geb.12613

Feng, G., Mi, X. C., Bøcher, P. K., Mao, L. F., Sandel, B., Cao, M., et al. (2014). Relative roles of local disturbance, current climate and paleoclimate in determining phylogenetic and functional diversity in Chinese forests. *Biogeosciences* 11, 1361–1370. doi: 10.5194/bg-11-1361-2014

Feng, G., Yan, H., and Yang, X. (2019). Climate and food diversity as drivers of mammal diversity in Inner Mongolia. *Ecol. Evol.* 9, 2142–2148. doi: 10.1002/ece3.4908

Field, R., O'Brien, E. M., and Whittaker, R. J. (2005). Global models for predicting woody plant richness from climate: development and evaluation. *Ecology* 86, 2263–2277. doi: 10.1890/04-1910

Fine, P. V. A. (2015). Ecological and evolutionary drivers of geographic variation in species Diversity. *Annu. Rev. Ecol. Evol. Syst.* 46, 369–392. doi: 10.1146/annurev-ecolsys-112414-054102

Freilich, M. A., and Connolly, S. R. (2015). Phylogenetic community structure when competition and environmental filtering determine abundances: assessing phylogenetic community structure. *Global. Ecol. Biogeogr.* 24, 1390–1400. doi: 10.1111/geb.12367

Guo, Y., Schöb, C., Ma, W., Mohammat, A., Liu, H., Yu, S., et al. (2019). Increasing water availability and facilitation weaken biodiversity-biomass relationships in shrublands. *Ecology* 100:e02624. doi: 10.1002/ecy.2624

Hasumi, H., and Emori, S. (2004). K-1 coupled model (MIROC) description, K-1 Tech. Rep.1, 34 pp., Cent. for Clim. Syst. Res., Univ. of Tokyo, Tokyo.

Hijmans, R. J., Cameron, S. E., Parra, J. L., Jones, P. G., and Jarvis, A. (2005). Very high resolution interpolated climate surfaces for global land areas. *Int. J. Climatol.* 25, 1965–1978. doi: 10.1002/joc.1276

Jin, Y., and Qian, H. (2019). V.PhyloMaker: an R package that can generate very large phylogenies for vascular plants. *Ecography* 42, 1353–1359. doi: 10.1111/ecog.04434

Katabuchi, M., Kurokawa, H., Davies, S. J., Tan, S., and Nakashizuka, T. (2012). Soil resource availability shapes community trait structure in a species-rich dipterocarp forest: soil resources and community structure. *J. Ecol.* 100, 643–651. doi: 10.1111/j.1365-2745.2011.01937.x

Kembel, S. W., Cowan, P. D., Helmus, M. R., Cornwell, W. K., Morlon, H., Ackerly, D. D., et al. (2010). Picante: R tools for integrating phylogenies and ecology. *Bioinformatics* 26, 1463–1464. doi: 10.1093/bioinformatics/btq166

Kissling, W. D., Eiserhardt, W. L., Baker, W. J., Borchsenius, F., Couvreur, T. L. P., Balslev, H., et al. (2012). Cenozoic imprints on the phylogenetic structure of palm species assemblages worldwide. *Proc. Natl. Acad. Sci. U.S.A.* 109, 7379–7384. doi: 10.1073/pnas.1120467109

Kubota, Y., Kusumoto, B., Shiono, T., and Ulrich, W. (2018). Environmental filters shaping angiosperm tree assembly along climatic and geographic gradients. *J. Veg. Sci.* 29, 607–618. doi: 10.1111/jvs.12648

Li, Z., Jiang, X., Wang, J., Meng, X., Heino, J., and Xie, Z. (2019). Multiple facets of stream macroinvertebrate alpha diversity are driven by different ecological factors across an extensive altitudinal gradient. *Ecol. Evol.* 9, 1306–1322. doi: 10.1002/ece3.4841

Liaw, A., and Wiener, M. (2002). Classification and regression by randomForest. *R News* 2, 18–22.

Long, W., Schamp, B. S., Zang, R., Ding, Y., Huang, Y., and Xiang, Y. (2015). Community assembly in a tropical cloud forest related to specific leaf area and maximum species height. *J. Veg. Sci.* 26, 513–523. doi: 10.1111/jvs.12256

Ma, W., He, J.-S., Yang, Y., Wang, X., Liang, C., Anwar, M., et al. (2010). Environmental factors covary with plant diversity-productivity relationships among Chinese grassland sites: diversity-productivity relationships in Chinese grassland. *Global. Ecol. Biogeogr.* 19, 233–243. doi: 10.1111/j.1466-8238.2009.00508.x

Mao, L., Swenson, N. G., Sui, X., Zhang, J., Chen, S., Li, J., et al. (2020). The geographic and climatic distribution of plant height diversity for 19,000 angiosperms in China. *Biodivers. Conserv.* 29, 487–502. doi: 10.1007/s10531-019-01895-5

Massante, J. C., Götzenberger, L., Takkis, K., Hallikma, T., Kaasik, A., Laanisto, L., et al. (2019). Contrasting latitudinal patterns in phylogenetic diversity between woody and herbaceous communities. *Sci. Rep.* 9:6443. doi: 10.1038/s41598-019-42827-1

Miao, B., Li, Z., Liang, C., Wang, L., Jia, C., Bao, F., et al. (2018). Temporal and spatial heterogeneity of drought impact on vegetation growth on the Inner Mongolian Plateau. *Rangel. J.* 40, 113–128. doi: 10.1071/rj16097

Miatto, R. C., and Batalha, M. A. (2018). Are the cerrado and the seasonal forest woody floras assembled by different processes despite their spatial proximity? *J. Plant Ecol.* 11, 740–750. doi: 10.1093/jpe/rtx044

Moles, A. T., Warton, D. I., Warman, L., Swenson, N. G., Laffan, S. W., Zanne, A. E., et al. (2009). Global patterns in plant height. *J. Ecol.* 97, 923–932. doi: 10.1111/j.1365-2745.2009.01526.x

Moro, M. F., Silva, I. A., de Araújo, F. S., Nic Lughadha, E., Meagher, T. R., and Martins, F. R. (2015). The role of edaphic environment and climate in structuring phylogenetic pattern in seasonally dry tropical plant communities. *PLoS One* 10:e0119166. doi: 10.1371/journal.pone.0119166

O'Brien, E. (1998). Water-energy dynamics, climate, and prediction of woody plant species richness: an interim general model. *J. Biogeogr.* 25, 379–398. doi: 10.1046/j.1365-2699.1998.252166.x

Oksanen, J., Blanchet, F. G., Friendly, M., Kindt, R., Legendre, P., McGlinn, D., et al. (2019). *Vegan: Community Ecology Package*. Available online at: https://CRAN.R-project.org/package=vegan

Olson, M. E., Soriano, D., Rosell, J. A., Anfodillo, T., Donoghue, M. J., Edwards, E. J., et al. (2018). Plant height and hydraulic vulnerability to drought and cold. *Proc. Natl. Acad. Sci. U.S.A.* 115, 7551–7556. doi: 10.1073/pnas.1721728115

Ordonez, A., and Svenning, J.-C. (2015). Geographic patterns in functional diversity deficits are linked to glacial-interglacial climate stability and accessibility: glacial-interglacial legacies in functional diversity. *Global. Ecol. Biogeogr.* 24, 826–837. doi: 10.1111/geb.12324

Ordonez, A., and Svenning, J.-C. (2017). Consistent role of quaternary climate change in shaping current plant functional diversity patterns across European plant orders. *Sci. Rep.* 7:42988. doi: 10.1038/srep42988

Pärtel, M., Bennett, J. A., and Zobel, M. (2016). Macroecology of biodiversity: disentangling local and regional effects. *New Phytol.* 211, 404–410. doi: 10.1111/nph.13943

Qian, H., Wiens, J. J., Zhang, J., and Zhang, Y. (2015). Evolutionary and ecological causes of species richness patterns in North American angiosperm trees. *Ecography* 38, 241–250. doi: 10.1111/ecog.00952

Sandel, B., Arge, L., Dalsgaard, B., Davies, R. G., Gaston, K. J., Sutherland, W. J., et al. (2011). The influence of late quaternary climate-change velocity on species endemism. *Science* 334, 660–664. doi: 10.1126/science.1210173

She, W., Zhang, Y., Qin, S., Wu, B., and Bai, Y. (2016). Increased precipitation and nitrogen alter shrub architecture in a desert shrubland: implications for primary production. *Front. Plant Sci.* 7:1908. doi: 10.3389/fpls.2016.01908

Šímová, I., Violle, C., Svenning, J.-C., Kattge, J., Engemann, K., Sandel, B., et al. (2018). Spatial patterns and climate relationships of major plant traits in the New World differ between woody and herbaceous species. *J. Biogeogr.* 45, 895–916. doi: 10.1111/jbi.13171

Spasojevic, M. J., and Suding, K. N. (2012). Inferring community assembly mechanisms from functional diversity patterns: the importance of multiple assembly processes: functional diversity along gradients. *J. Ecol.* 100, 652–661. doi: 10.1111/j.1365-2745.2011.01945.x

Stein, A., Gerstner, K., and Kreft, H. (2014). Environmental heterogeneity as a universal driver of species richness across taxa, biomes and spatial scales. *Ecol. Lett.* 17, 866–880. doi: 10.1111/ele.12277

Stock, W. D., and Verboom, G. A. (2012). Phylogenetic ecology of foliar N and P concentrations and N:P ratios across mediterranean-type ecosystems. *Global. Ecol. Biogeogr.* 21, 1147–1156. doi: 10.1111/j.1466-8238.2011.00752.x

Svenning, J.-C., Eiserhardt, W. L., Normand, S., Ordonez, A., and Sandel, B. (2015). The Influence of paleoclimate on present-day patterns in biodiversity and ecosystems. *Annu. Rev. Ecol. Evol. Syst.* 46, 551–572. doi: 10.1146/annurev-ecolsys-112414-054314

Swenson, N. G. (2013). The assembly of tropical tree communities - the advances and shortcomings of phylogenetic and functional trait analyses. *Ecography* 36, 264–276. doi: 10.1111/j.1600-0587.2012.00121.x

Tian, F., Wang, Y., Chi, Z., Liu, J., Yang, H., Jiang, N., et al. (2017). Late quaternary vegetation and climate reconstruction based on pollen data from southeastern Inner Mongolia, China. *Rev. Palaeobot. Palyno.* 242, 33–42. doi: 10.1016/j.revpalbo.2017.03.003

Webb, C. O. (2000). Exploring the phylogenetic structure of ecological communities: an example for rain forest trees. *Am. Natur.* 156, 145–155. doi: 10.1086/303378

Webb, C. O., Ackerly, D. D., McPeek, M. A., and Donoghue, M. J. (2002). Phylogenies and community ecology. *Annu. Rev. Ecol. Syst.* 33, 475–505. doi: 10.1146/annurev.ecolsys.33.010802.150448

Wu, J., Zhang, Q., Li, A., and Liang, C. (2015). Historical landscape dynamics of inner mongolia: patterns, drivers, and impacts. *Landsc. Ecol.* 30, 1579–1598. doi: 10.1007/s10980-015-0209-201

Yan, Y., Yang, X., and Tang, Z. (2013). Patterns of species diversity and phylogenetic structure of vascular plants on the Qinghai-Tibetan Plateau. *Ecol. Evol.* 3, 4584–4595. doi: 10.1002/ece3.847

Yang, X., Scuderi, L., Paillou, P., Liu, Z., Li, H., and Ren, X. (2011). Quaternary environmental changes in the drylands of China - A critical review. *Q. Sci. Rev.* 30, 3219–3233. doi: 10.1016/j.quascirev.2011.08.009

Zhao, Y., and Zhao, L. (2014). *Key to the Vascular Plants of Inner Mongolia*. Beijing: Science Press.

Zheng, Y., Dong, L., Li, Z., Zhang, J., Li, Z., Miao, B., et al. (2019). Phylogenetic structure and formation mechanism of shrub communities in arid and semiarid areas of the Mongolian Plateau. *Ecol. Evol.* 3:5787. doi: 10.1002/ece3.5787

Zhou, Y., Wang, S., Njogu, A. W., Ochola, A. C., Boru, B. H., Mwachala, G., et al. (2019). Spatial congruence or mismatch between phylogenetic and functional structure of seed plants along a tropical elevational gradient: different traits have different patterns. *Front. Ecol. Evol.* 7:100. doi: 10.3389/fevo.2019.00100

**Conflict of Interest:** The authors declare that the research was conducted in the absence of any commercial or financial relationships that could be construed as a potential conflict of interest.

frontiers in Ecology and Evolution

ORIGINAL RESEARCH
published: 21 December 2020
doi: 10.3389/fevo.2020.544670

# Roles of Dispersal Limit and Environmental Filtering in Shaping the Spatiotemporal Patterns of Invasive Alien Plant Diversity in China

*Yiying Li and Zehao Shen**

*MOE Key Laboratory for Earth Surface Processes, College of Urban and Environmental Sciences, Institute of Ecology, Peking University, Beijing, China*

Biological invasion pose a severe threat to global biodiversity, and studies of bioinvasion patterns and the underlying mechanisms provide critical tests to ecological theories. China is a global hotspot of biodiversity and also biological invasions. The understanding of mechanisms for bioinvasion patterns has been limited by inadequacy of data spatial resolution, and lack of a historical perspective. This study compiled the first nation-scale distribution data with a sub-provincial spatial unit (prefecture) for 463 invasive alien plants species (IAPS) recorded in China, as well as their introduction times. The spatiotemporal patterns of species richness of invasive alien plants, including three life forms (annual-biennial, perennial, and woody) were explored, then related the species richness patterns with environmental, social-economic and historical factors. Statistical analyses included quantile regression, generalized linear model (GLM), and hierarchical variation partitioning. The results indicated that: (1) herbaceous species comprised 84% of the 463 IAPS in China; (2) plant introductions into China accelerated since 1800, reaching the maximum rate during 1900–1940. IAPS richness had a closer correlation with the time of newest introduction ($R^2$ = 0.155) than with that of the oldest introduction ($R^2$ = 0.472); (3) IAPS richness decreases with increasing latitude ($r = -0.32$, $P < 0.001$) and decreases from the coastal and southern terrestrial borders to inland regions, but doesn't increase with prefecture size. The three life forms of IAPS showed similar latitudinal patterns of species richness and divergent latitudinal patterns of species percentage. (4) IAPS richness showed significantly positive correlations with thermal climate and a negative relationship with climate seasonality. GLM explained up to 65% of the variation in spatial patterns of IAPS and three life forms; with much less variation explained in the species percentage patterns. The year of the most recent IAPS introduction and the low temperature limit jointly dominated spatial patterns of IAPS richness in China, whereas road density showed little effect. Therefore, global warming and economic globalization play a prominent role in promoting biological invasion in the last few decades, and will continue to drive the trend of plant invasion in China and probably elsewhere.

**Keywords: invasive alien plant, species richness, geographical patterns, introduction time, climate, sub-provincial unit**

OPEN ACCESS

***Edited by:***
*Hang Sun,*
*Kunming Institute of Botany, Chinese Academy of Sciences, China*

***Reviewed by:***
*Hao Wu,*
*Xinyang Normal University, China*
*Jianqing Ding,*
*Henan University, China*

***Correspondence:**
*Zehao Shen*
*shzh@urban.pku.edu.cn*

***Specialty section:***
*This article was submitted to Biogeography and Macroecology, a section of the journal Frontiers in Ecology and Evolution*

***Received:*** *21 March 2020*
***Accepted:*** *01 December 2020*
***Published:*** *21 December 2020*

***Citation:***
*Li Y and Shen Z (2020) Roles of Dispersal Limit and Environmental Filtering in Shaping the Spatiotemporal Patterns of Invasive Alien Plant Diversity in China. Front. Ecol. Evol. 8:544670. doi: 10.3389/fevo.2020.544670*

## INTRODUCTION

Along with globalization, anthropogenic species migration has accelerated (Seebens et al., 2018). An invasive alien species (IAS) is defined as a species of plant, animal, pathogen, or other organisms that are non-native to an ecosystem, where it may cause economic or environmental harm or adversely affect human health[1]. Biological invasions occur globally and they have become one of the primary threats to biodiversity, and cause huge losses to ecosystem functions and services, as well as public wealth (Pimentel et al., 2005; Pejchar and Mooney, 2009; Simberloff et al., 2013). It is estimated that the global loss caused by biological invasions is equivalent to 5% of gross domestic product (GDP) every year (Pimentel, 2002).

Since the pioneer work of Elton (1958), species invasiveness and habitat invasibility have been the central issues of biological invasion studies. Species related studies often focus on the effects of physiological characteristics, functional traits, and life history strategies of IAS (Davidson et al., 2011). Researches on invasive species diversity generally address the distribution patterns of invasive organisms and the habitat conditions affecting the dispersal and adaptation processes (Hierro et al., 2005; Denslow et al., 2009; Khuroo et al., 2012; Murray and Phillips, 2012) (e.g., environmental invulnerability), in order to predict potentially high-invasion risk areas (Zhu et al., 2007; Wolmarans et al., 2010), and to explore invasion mechanisms relating with environmental filters, dispersal pathways, and ecosystem resistance (Nentwig, 2007; Westphal et al., 2008; Pyšek et al., 2015; Dawson et al., 2017). Moreover, the study of invasive species diversity also seeks for novel understanding on the basic ecological problems of community assembly and species coexistence (Davis et al., 2005; Guisan et al., 2014).

Empirically, habitat disturbances erase standing vegetation and generate empty niches that facilitate biological invasions (Houseman et al., 2014; Jauni et al., 2015; Schrama and Bardgett, 2016). However, IAS richness is generally higher in habitats with high native biodiversity (Stohlgren et al., 1999; Pyšek et al., 2002; Bhattarai et al., 2014). These conflicting phenomena are induced by a set of scale dependent environmental filters that are critical for biological invasions (Milbau et al., 2009).

At regional to global scales, IAS diversity generally decrease with an increase in latitude, and low temperature normally acts as a primary limiting factor for the pattern, same as for the patterns of native species diversity (Sax, 2001; Pyšek et al., 2017). At the landscape scale, vegetation disturbances and land use changes (e.g., urbanization) commonly cause habitat fragmentation and degradation, intensify soil erosion, nutrient loss and water body eutrophication, and facilitate biological invasions in both terrestrial and aquatic habitats (Nentwig, 2007; Wang et al., 2011; Song et al., 2017; Wu et al., 2017). Because IAS generally has better dispersal capacity and wider environmental tolerance than native species, natural and anthropogenic landscape corridors also intensify bioinvasions (Minor et al., 2009; Resasco et al., 2014). At the local community scale, biotic and abiotic factors play a simultaneous role. Community structure show a prominent effect on resistance to bioinvasion (Houseman et al., 2014; Giorgis et al., 2016); the effects of soil fertility and soil microbes on plants also complicate the relationship between habitat invasibility and species invasiveness (Traveset and Richardson, 2014; Schrama and Bardgett, 2016).

Moreover, the positive correlation between introduction time and the distribution range of invasive species has been emphasized increasingly (Kowarik, 1995; Wu et al., 2004; Müllerová et al., 2005; Horvitz et al., 2017). The potential for species invasion generally increases with an increase of introduction time. A Hawaiian study found that only 1.8% of all alien species became invasive species, while 11% of those introduced more than 90 years ago became IAS (Schmidt and Drake, 2011). Introduction time is sometimes more important than species attributes in explaining the invasive nature of species (Pyšek and Jarošík, 2005; Pyšek et al., 2015). Therefore, when considering bioinvasion trends, the impact of introduction time or the time lag of the invasion should not be ignored.

The introduction of IAS into China has a long history and has caused great harm to the environment and economy of the country. For example, in Shanghai alone, the invasive species *Solidago canadensis* L. has eliminated more than 30 species of native plants in 20 years (Xu et al., 2006); *Eupatorium adenophorum* alone has caused a total of ¥119 million RMB per year of economic losses in Sichuan Province (Wan et al., 2009). Since Ding and Wang (1998) first listed invasive alien plant species and their provincial distribution in China, the list has been continuously updated to 188 species (Xu et al., 2004), 126 species (Liu et al., 2006), 270 species (Weber et al., 2008), 265 species (Xu et al., 2012), 515 species (Yan et al., 2014), and 404 species (Chen et al., 2017). In the last 20 years, a growing number of studies have addressed the geographical distribution and introduction mode (Chen et al., 2017), diffusion direction (Huang et al., 2012; Xu et al., 2012), origin (Weber et al., 2008; Yan et al., 2014), and influencing factors in plant invasions in China. Factors that are known to significantly affect IAS richness include annual mean temperature, annual precipitation, population density, GDP (Zhang et al., 2010), native species diversity (Weber et al., 2008; Wang et al., 2017), and the phylogenetic relationships between alien and native species (Zheng et al., 2018).

Although a body of evidence on the distribution of IAS in China is accumulating, the data resolution of national studies have all been at the provincial scale (e.g., Yan et al., 2014; Chen et al., 2017; Wang et al., 2017), and studies based on local data generally covered no larger than provincial regions (e.g., Feng et al., 2009). The unified real-time monitoring data at national scale is still lacking. By integrating the information of invasive alien plant species (IAPS) in the published literature, specimens, field surveys, and online database records, this research attempts to build the first database of IAPS distribution, origin, and introduction time in China below the provincial scale, and to quantify the impact of natural and social-economic factors on plant invasions.

Since speciation and extinction processes are ignorable in determining the geographical distribution of invasive species, we

[1]https://www.cbd.int/idb/2009/about/what/

hypothesized that, the geographical patterns of IAPS diversity in China should be primarily constrained by the current environmental filters and dispersal conditions, as well as vital ecological traits of species. Specifically, this study attempts to answer the following questions: (1) How are spatiotemporal patterns of IAPS diversity in China affected by different life-forms? (2) What are the differences in the roles of environmental filtering and diffusion restriction in the distribution of IAPS diversity? (3) Which factor, natural environmental or human habitat disturbance, plays the largest role in determining the distribution of invasive plants in China?

# MATERIALS AND METHODS

## List of Invasive Plants and Species Attributes Data

All known IAPS in China were included in the study, a total of 463 species. The list, biological attributes, and distribution data of these invasive plants were drawn from "The Survey Report of Invasive Plants in China" edited by Ma (2014). Ma integrated field investigation reports with specimen information and historical documents, recorded general and species specific information of invasive plants in eight regions comprising China, including Northeast China, North China, Northwest China, Central China, East China, South China, Central South China, and Southwest China. Information on invasive species compiled for each region included (but not limited to) species name, place of origin, introduction time, introduction mode, route of transmission, habitat, hazard level, county- or prefecture-level geographical distribution, as well as specimen information. Additional information about invasive plant distribution in China was obtained from the literature (Weber et al., 2008; Chen et al., 2017) and the Global Biodiversity Information Facility (GBIF) website (2018)[2]. The names of the species were integrated referring to the Plant List Database (The Plant List, 2013), with synonymous species removed from the list.

The objects of analyses in this paper were limited to those alien species explicitly identified in Ma (2014) as "invasive," rather than all alien or naturalized species. The following fields are uniformly compiled for each species and included in this study: taxonomy, life form, introduction time, county- or prefecture-level distribution.

## Time and Geographical Distribution Data of Species Introduction

We updated the species introduction time recorded in Ma (2014) by referring to GBIF records and recent literature (Weber et al., 2008; Chen et al., 2017). Plant introduction time, i.e., "minimum residence time" (MRT), which is common in invasion research, was obtained for 418 species. GBIF contributed approximately 10% of the total data, including the introduction times for 112 species not included in Ma (2014), and advanced the introduction time for 98 species (32%) of 306 species recorded in Ma (2014).

The geographical information data used in this study was from the Database of Global Administrative Areas (GADM, 2018). The confirmed distribution of each IAPS in counties and prefectures were systematically mapped to the shape file of China's county administrative regions. For some ambiguous records, such as "coastal counties in Fujian province," and "Southern Ganzhou Prefecture," the names of counties or prefectures were further confirmed manually. Finally, about 64,000 records of IAPS distribution were collected and allocated to 2,312 county-level areas (120 counties in China have not been invaded). However, not all IAPS had complete county-level distribution information so the accuracy of species distribution data was adjusted from the county to the prefecture level so as to avoid incompleteness and inconsistency in data. The final data comprised distribution information on 463 IAPS in 346 prefecture-level regions of China, and introduction time (i.e., years from present) for 418 of these species.

## Data of Natural and Social Environmental Factors

The climate data came from 19 bioclimatic variables with a resolution of 2.5′ arc (about 5 km) in database version 2.0[3]. Seven bioclimatic variables were selected, with reference to earlier studies: mean annual temperature (MAT), mean annual precipitation (MAP), annual temperature range (ATR), coefficient of variance of precipitation (CVP), mean temperature of the warmest month (MTWM), mean temperature of the coldest month (MTCM), and the annual biological temperature (ABT) (Fang, 1994). The administrative region was taken as the spatial unit to calculate the average value of these climate factors. The topographic information of the study area was derived from the Shuttle Radar Topography Mission data published by United States Geological Survey, with a spatial resolution of 30″.

The socio-economic data was obtained from the database of Circle-Asia Economic Information Co., Ltd. (CEIC, insights.ceicdata.com, 2018). With reference to earlier studies, the GDP, population, and road mileage were selected to comprehensively reflect the habitat empty caused by human activities and exposure to bioinvasions (McKinney, 2002; Richardson and Pyšek, 2006). Bioinvasion is a long-term process, thus difficult to correspond to the social-economic conditions of a particular year. Assuming that a recent data can more completely reflect the cumulative effects of social-economic drivers, data for 2010 was selected to represent current conditions and to match the time of IAPS distribution data. Population data was converted into population density (per $km^2$), road mileage into road density ($km/km^2$) to eliminate the effect of area, and GDP data was converted into per capita GDP to more reasonably reflect economic intensity. Alien species enter the country from land or sea boundaries, and distance to a land boundary is a significant predictor of invasive species richness (Huang et al., 2012). However, because China's population density and per capita GDP are significantly related to the distance to the coast

[2]https://www.gbif.org/

[3]http://www.worldclim.com

and ports, the distance variable was not included in the following analyses.

## Spatial Analysis and Statistics

We used the GIS software ArcGIS v 10.3 to establish the distribution range data of all IAPS and the environmental data of the study region. The Asia North Albers Equal Area Conic projection was applied to all data layer, uniformly taking the prefecture-level administrative region ("prefecture") as the geographical unit of the maps. Overlaying maps of all IAPS resulted in a species richness map. The digital terrain data were resampled into 100 m resolution. The .shp file of the administrative map of the study area was overlaid with a map of each explanatory variable in grid or vector format, to extract the corresponding values by each polygon.

This study analyzed the causal factors of IAPS diversity with regard to environmental filtering and invasion probability, which were related to area, climate, introduction time, and social-economic factors (**Table 1**). Chen et al. (2017) suggested that the distributions of annual and biennial invasive plants respond similarly to climate gradients, different from perennial herbs and woody species. The effect of plant life-form on bioinvasion was explored here by dividing IAPS into three categories: annual and biennial herbs (ABHs), perennial herbs, and woody plants. Both species number and percentage of species in the three life forms were considered in the analyses. Pearson correlation coefficient was used to detect the relationship between continuous environmental variables and invasive species richness. One-way ANCOVA was used to test the bioinvasion difference between plant life-forms after accounting for the effect of introduction time. Quantile regression efficiently describes the conditional distribution of response variables relative to explanatory variables (Huang et al., 2012). Quantile regression was used to predict the relationship between the introduction time and the distribution area, so as to reflect the influence of the variability of dispersal rate on the distribution area of IAPS over a given time. Since species richness and species percentage as responsive variables do not follow normal distribution, a generalized linear model (GLM) combining with the hierarchical variation partitioning algorithm was applied to quantify contributions of interpretative variables. According to earlier studies, collinearity was generally present among predicting variables, thus routine steps of variable selection were applied to optimize the model structure (Shen et al., 2012). To evaluate the contribution of different factors to the spatial variations of IAPS richness patterns, partial regression was also applied to partition the total variation in species richness into four parts (Borcard et al., 1992): (1) independent components, i.e., the proportions of variance explained exclusively by the included factors, respectively, (2) co-varying component, i.e., the overlapping part of the explained variance by every pair two factors, (3) joint component, i.e., the part of explained variance as overlapping of three factors, and (4) residual variation. Based on the GLM results, in the partial regressions, we took climate, time of introduction, and social-economic condition as three independent factors for IAPS diversity patterns.

All statistical analysis was completed in R (R Core Team, 2018). The R package used in the analysis includes hier.part, psych, quantreg, vegan.

# RESULTS

## Species Diversity of IAPS and Temporal Profile of Introduction

There are 463 IAPS recorded in China, belonging to 271 genera and 65 families. The dominant ten families are Compositae (76 species), Leguminosae (66 species), Poaceae (46 species), Amaranthaceae (34 species), Solanaceae (23 species), Euphorbiaceae (18 species), Convolvulaceae (16 species), Brassicaceae (15 species), Onagraceae (12 species), and Plantaginaceae (11 species) (**Supplementary Figure 1**). The first five families account for half of the total IAPS. At the genus level, *Amaranthus* (15 species), *Euphorbia* (15 species), *Solanum* (12 species), *Ipomoea* (10 species) and *Acacia* (8 species) constituted the top five genera for invasive species richness. There were 391 species of herbs, accounting for 84.4% of all IAPS in China, including 254 species of ABHs and 137 species of perennials; 72 species of woody plants account for 15.6% of all IAPS.

The records of alien plants introduction into China can be traced back to 2000 years ago (**Figure 1A**), with *Cannabis sativa* and *Coriander sativum* comprising some of the earliest records; however, 80% of alien plant introductions have occurred since 1840. The rate of alien plant introduction accelerated rapidly in the 19th century. A total of 266 species (63.6%) invaded after 1900, among which 182 species invaded between 1900 and 1940. Regarding the introduction mode, 287 species of plants were intentionally introduced, and other 140 species were unintentionally introduced (or naturally disturbed). With regard to the distribution of the IAPS, species with the widest invasion range include *Datura stramonium*, *Erigeron canadensis*, and *Hibiscus rustionum*, which have invaded 212, 203 and 187 prefecture level administrative areas in China, respectively. In contrast, 117 species were present in 1–10 prefectures, 200 species were recorded in 11–50 prefectures, 90 species were in 51–100 prefectures, and 56 species have occupied more than 100 prefectures.

The distribution area of invasive species increased with increasing introduction time ($r = 0.62$, $P < 0.001$), but there was an upper limit of about 2500 km for the square root of species range of all invasive species (**Figure 1A**). The relationship between the introduction time and distribution area showed significant variability. The quantile regression models showed that the rate of distribution area increased with the introduction time, varying from slope = $1.6^2 = 2.56$ km$^2$/year for the 5% quantile to slope = $9.5^2 = 90.25$ km$^2$/year for the 95% quantile. This reflects the variation of species expansion rate, while the intercept of quantile regression model as the initial introduction area remained comparable (**Figures 1B,C**).

There were no statistically significant differences in the introduction time among different life forms of invasive plants (**Figure 2A**). After the effect of introduction time was controlled by an one-way covariance analysis, the log-transformed area of

**TABLE 1 |** Factors and variables for measuring and explaining the geographical pattern of invasive plant species richness in China.

| Factors | Variables | Units | Description |
|---|---|---|---|
| Species diversity | Species richness | – | All IAPS in a prefecture, including three life-forms: annual-biennial, perennial, and woody |
| | Species percentage | % | The percentage of each life-form in species richness of all IAPS, calculated for each prefecture. |
| Climate | MAT | °C | Annual mean temperature of 1980–2010 |
| | MAP | mm | Mean annual precipitation of 1980–2010 |
| | ABT | °C | Annual biological temperature |
| | ATR | °C | Annual temperature range = MTWM–MTCM |
| | MTWM | °C | Mean temperature of the hottest month |
| | MTCM | °C | Mean temperature of the coldest month |
| | CVP | – | The standard deviation of month precipitation divided by the mean precipitation of 12 months |
| Social and economic | GDP per capita | RMB | Prefecture value of GDP per capita in 2010 |
| | Population density | Individual $km^{-2}$ | Population of a prefecture in 2010 divided by the prefecture area |
| | Road density | $km \cdot km^{-2}$ | Total length of highway, national road, provincial road and county road in a prefecture divided by the prefecture area, value in 2010 |
| Area | Area | $km^2$ | The prefecture area |
| Time | MRT | Year | Minimum residence time, based on earliest introduction report for an invasive species |

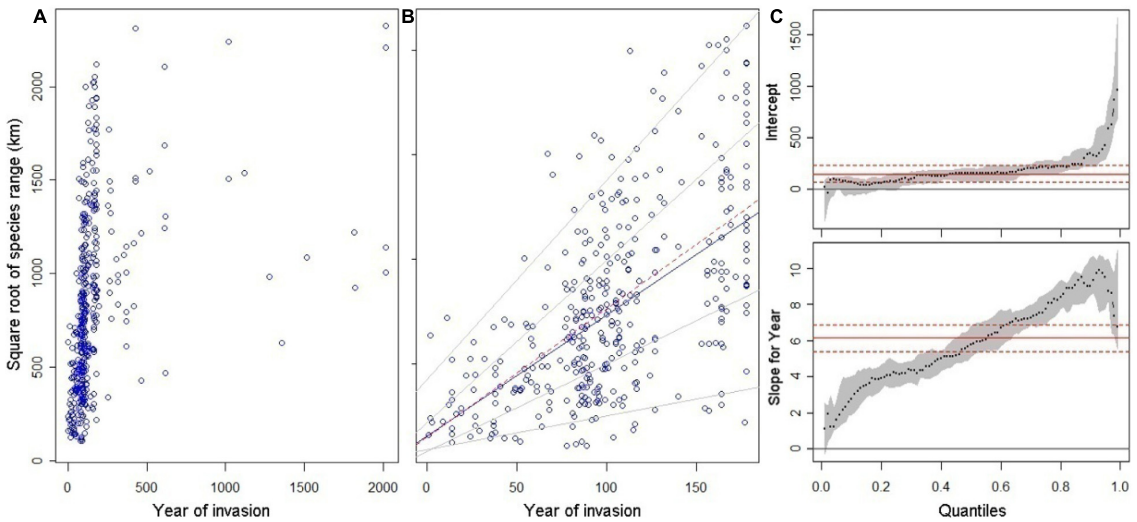


**FIGURE 1 |** Time accumulation of invasive alien plant species (IAPS) in China and its relationship with distribution area. **(A)** the relation between area (square root of species range) and the year of introduction for all IAPS tracing back to 2000 year ago; **(B)** the same relationship for IAPS introduced since 1840, and fitted lines with quantile (thin solid lines for 5, 25, 75, and 95% quantiles, thick solid line for median, from up to low) and linear (dash line) regression models; **(C)** the slopes and intercepts of the quantile regression models (dotted line and variation in gray) and the 95% confidence interval for random variation (solid and dotted horizontal lines in red).

ABH species was larger than that of perennial herb and woody species ($P = 0.004$ and $P = 0.005$, respectively), and there was no significant different between perennial herbs and woody species ($P = 0.76$) (**Figure 2B**).

## Geographical Patterns of Species Richness of Invasive Plants and Their Life-Forms

The IAPS richness in China decreased from south to north (**Figure 3**). Moreover, biological invasion was evidently more severe in the coastal areas and the land border areas adjacent to Southeast Asian countries, with more than 70 species per prefecture. The prefectures with high values belong to the provinces of Guangdong, Guangxi, Yunnan, Zhejiang, and Jiangsu. The IAPS diversity was seriously high in Taiwan Island and Hainan Island, to a less extent also in Northwest China prefectures adjacent to the central Asian countries, but very low in the areas adjacent to Mongolia, Russia, North Korea, and those neighboring the south border of the Qinghai-Tibet Plateau. In the interior of Central China and North China, the intensity of plant invasion in rural areas (∼30 species) was significantly lower

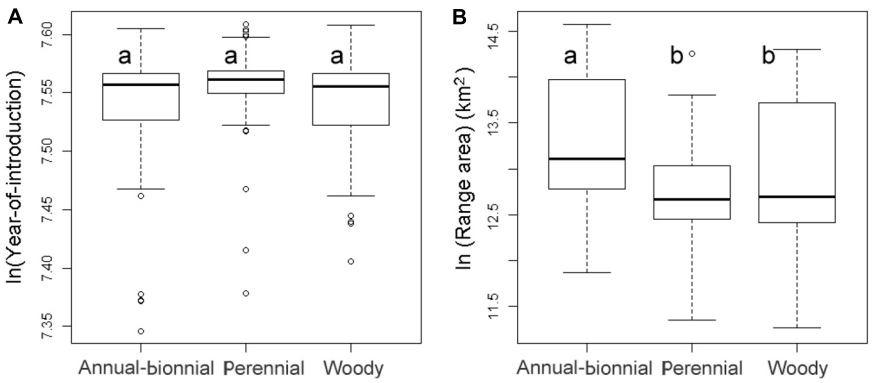


**FIGURE 2 |** Boxplots for the frequency distributions of **(A)** introduction time (log-transformed values) and **(B)** current species range area (log-transformed values) for IAPS of different growth forms. Labels a and b above boxes indicate significant difference between means of two categories.

than that in urban areas (>160 species). The top five cities of IAPS richness were all in the subtropical zone; namely, Guilin (227 species), Guangzhou (224 species), Shanghai (207 species), Hangzhou (203 species), and Xinbei city of Taiwan (202 species). The highest plant invasion intensity in North China was recorded as 127 species in Beijing, the capital of China.

With regard to different life forms, the richness pattern of ABHs was very similar to that of all IAPS. Subtropical coastal areas and Northwest China represented secondary invasion peak areas. In contrast, the percentage of ABHs to all IAPS showed an opposite latitudinal gradient, reaching the lowest values (30∼45%) in the tropical areas of Taiwan Island, Hainan Island, and Southern Yunnan. The highest values (up to 90%) appeared in the northwest of Qinghai-Tibet Plateau, Loess Plateau, Northeast China, and Shandong Peninsula, mainly temperate semi-arid regions. Invasive perennial species were mainly distributed in the southeast coastal areas, Taiwan Island, Hainan Island, Yunnan Province, and Chongqing city. Also, perennial species showed a peak value in the arid areas of Xinjiang and the central-western Inner Mongolia, reaching 20–40%. By contrast, low values of 5–20% were recorded in the vast area extending across the Qinghai-Tibet Plateau, Central China, North China, and most of Northeast China. Invasive woody species were mainly distributed in the south of subtropical region, with more than 30 species in some prefectures of Guangxi, Hainan, Yunnan, and Taiwan. However, in the regions north of 30°N, only 1–3 species were recorded in most areas. The percentage of invasive woody species had a similar pattern, with the highest value of 30% recorded in southern Yunnan and Guangxi, while absent in the vast northern regions (**Figure 4**).

## Determinants of Invasive Plant Species Richness Patterns

The relationship between IAPS richness in the three life forms (i.e., ABHs, perennial herbs, and woody plants) and the explanatory variables were estimated by linear models. IAPS richness had a positive correlation with energy indices of climate, including ABT, MAT, MTCM, and MTWM (**Figure 3** and **Supplementary Table 1**). The Pearson correlation coefficients reached a significant level ($P < 0.001$), with the correlation strongest with MTCM, and weakest with MTWM. IAPS richness was also positively correlated with MAP, but negatively correlated with CVP ($P < 0.001$). Regarding social-economic factors, IAPS richness increased significantly with an increase in GDP and population ($P < 0.001$), with ABHs showing the highest intensity of infestation, followed by perennial herbs and then woody species. The correlation between IAPS richness of road density was barely significant ($r = 0.10$, $P = 0.06$), in which there was only a significant but weak positive correlation with ABH species richness, and no correlation with the perennial herb and woody species richness. The correlation between the above factors and IAPS richness increased from woody to perennial to annual life forms, which suggests that the invasion processes and the drivers of these three types of plants were related rather than independent of each other (**Figure 5**).

There was an insignificant negative correlation between the log-transformed prefecture area and the log-transformed total invasive species richness (**Figure 6A**). However, the year of earliest records of invasive species were positively correlated with invasive species richness ($R^2 = 0.155$, $P < 0.001$), and the year of the most recent invasive species was negatively correlated with IAPS richness ($R^2 = 0.472$, $P < 0.001$).

## Variation Interpretation of the Invasive Species Richness Pattern

Based on the GLM and variance decomposition algorithm, a full model considering climate factors (seven variables), social-economic factors (three variables) and the most recent introduction time (Tmin) can explain 75.7% variance in the species richness pattern of all IAPS, and this value was 68.2, 78, and 78.5% for ABHs, perennial herbs, and woody plants, respectively. By contrast, with the same set of explaining variables, the variance of species percentage pattern was explained by 47.4, 22.8, and 35% for ABHs, perennial herbs and woody plants, correspondingly (**Figure 7**).

When breaking down the effects of Tmin, climate, and social-economic factors (as shown in **Table 1**) to the spatial patterns of invasive species richness (**Figure 7**), Tmin (19.6%), climate

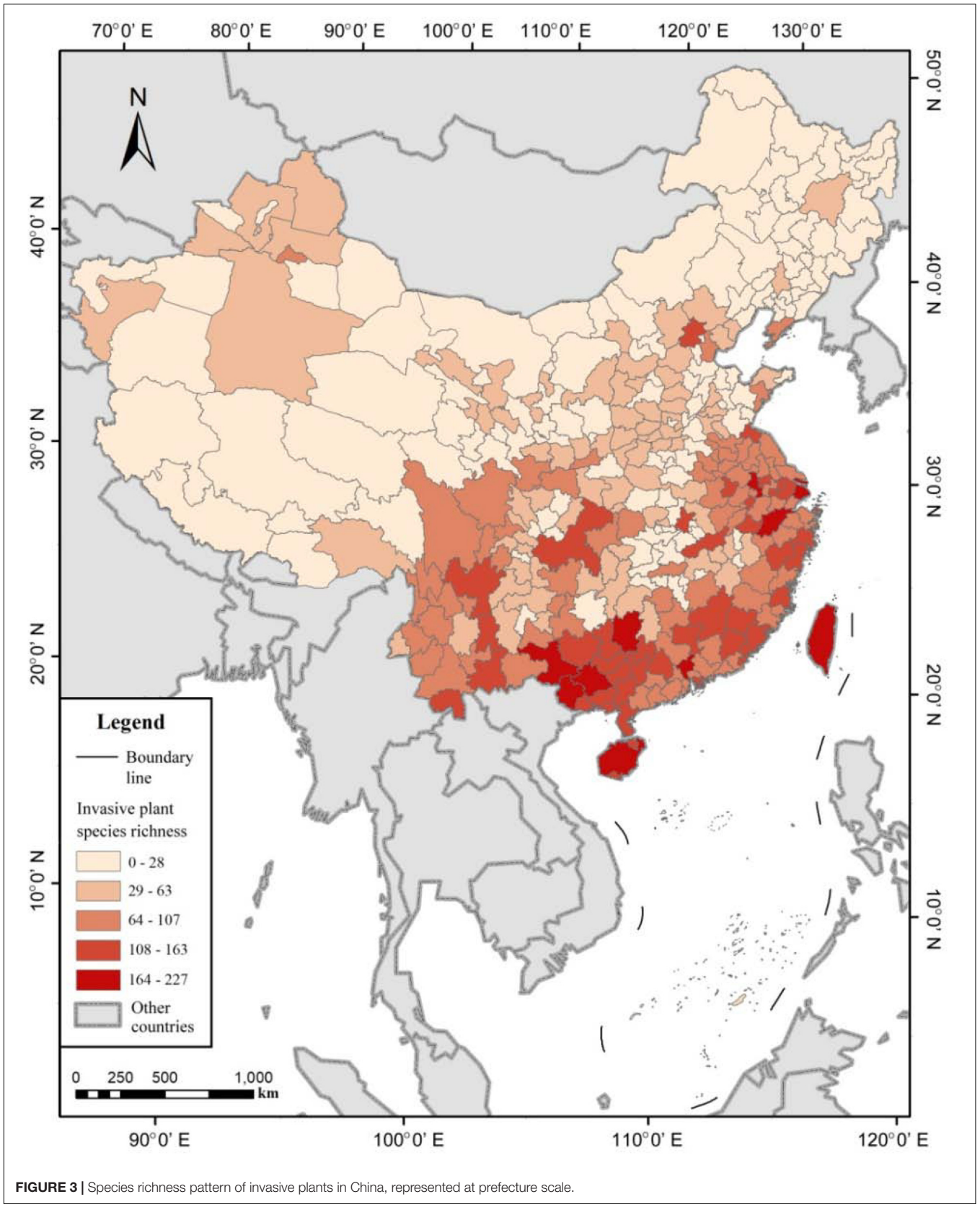


**FIGURE 3 |** Species richness pattern of invasive plants in China, represented at prefecture scale.

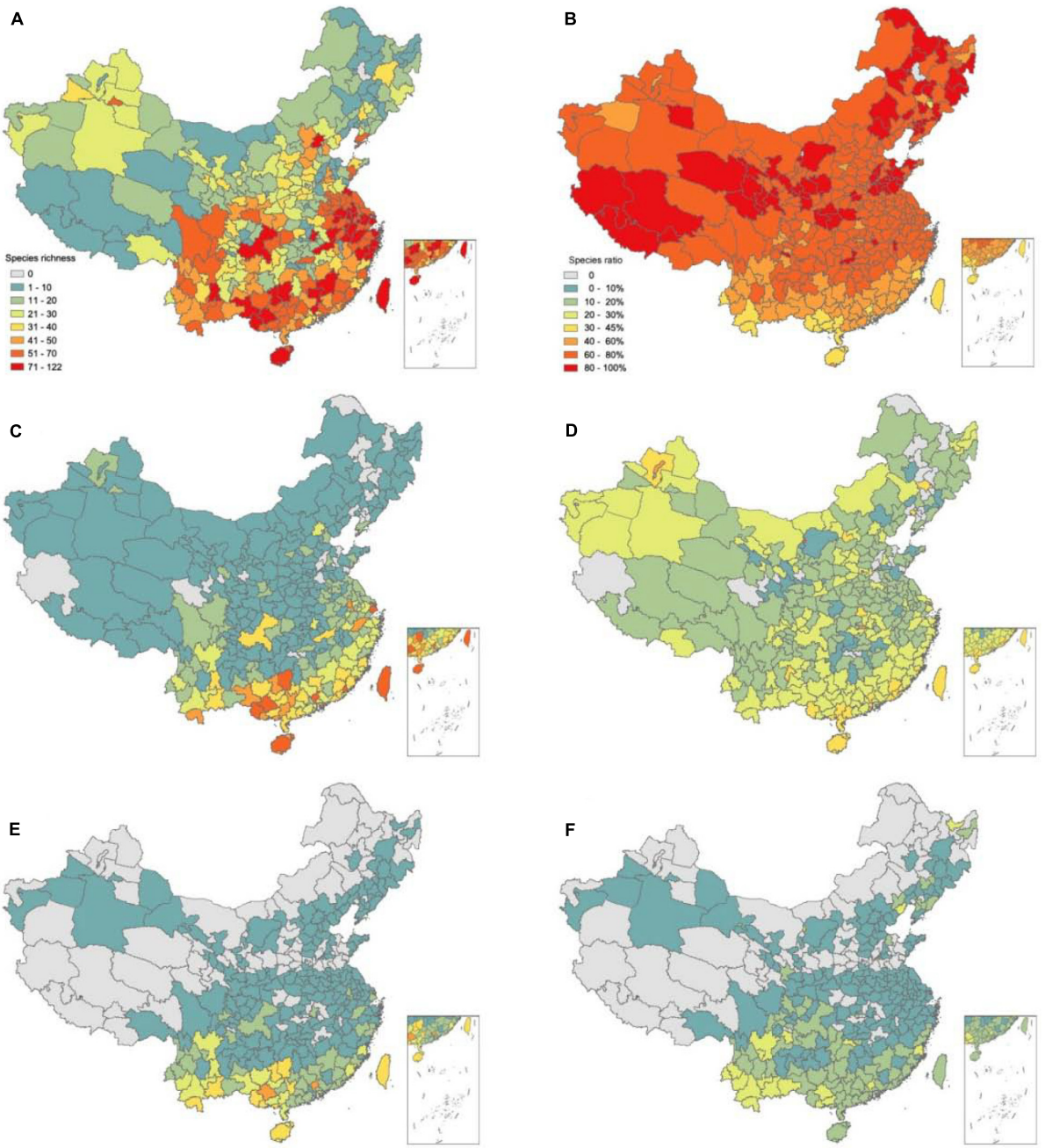


**FIGURE 4 |** Geographical patterns of species richness and percentage of invasive plants and three life-forms; panels **(A,C,E)** represent species richness of annual-biennial herbs, perennial herbs and woody species, respectively; panels **(B,D,F)** represent the species percentage of three corresponding life-forms.

(17.2%), and their interactions (28.5%), were shown to play major roles, while human activities had little influence (1.85%). These contributory levels were basically applicable for the three life forms of invasive plants. Moreover, from annuals to BPHs and then to woody plants, the independent contribution of Tmin gradually decreased from 23.1 to 7.8%, while the limiting effect of climate increased from 13.2 to 33.6%. On the other hand, climate factors played a primary role in the patterns of species percentages of the three life forms of invasive plants; human activities had a weak but independent contribution, and Tmin had little independent effect on these patterns.

The hier.part algorithm further ranked the importance of individual factors on the species richness pattern of IAPS (**Table 2**). For total invasive species richness, the importance of Tmin was the greatest (contributing 43.7% of $r^2$ of the full model), followed by temperature, especially MTCM (16.8%).

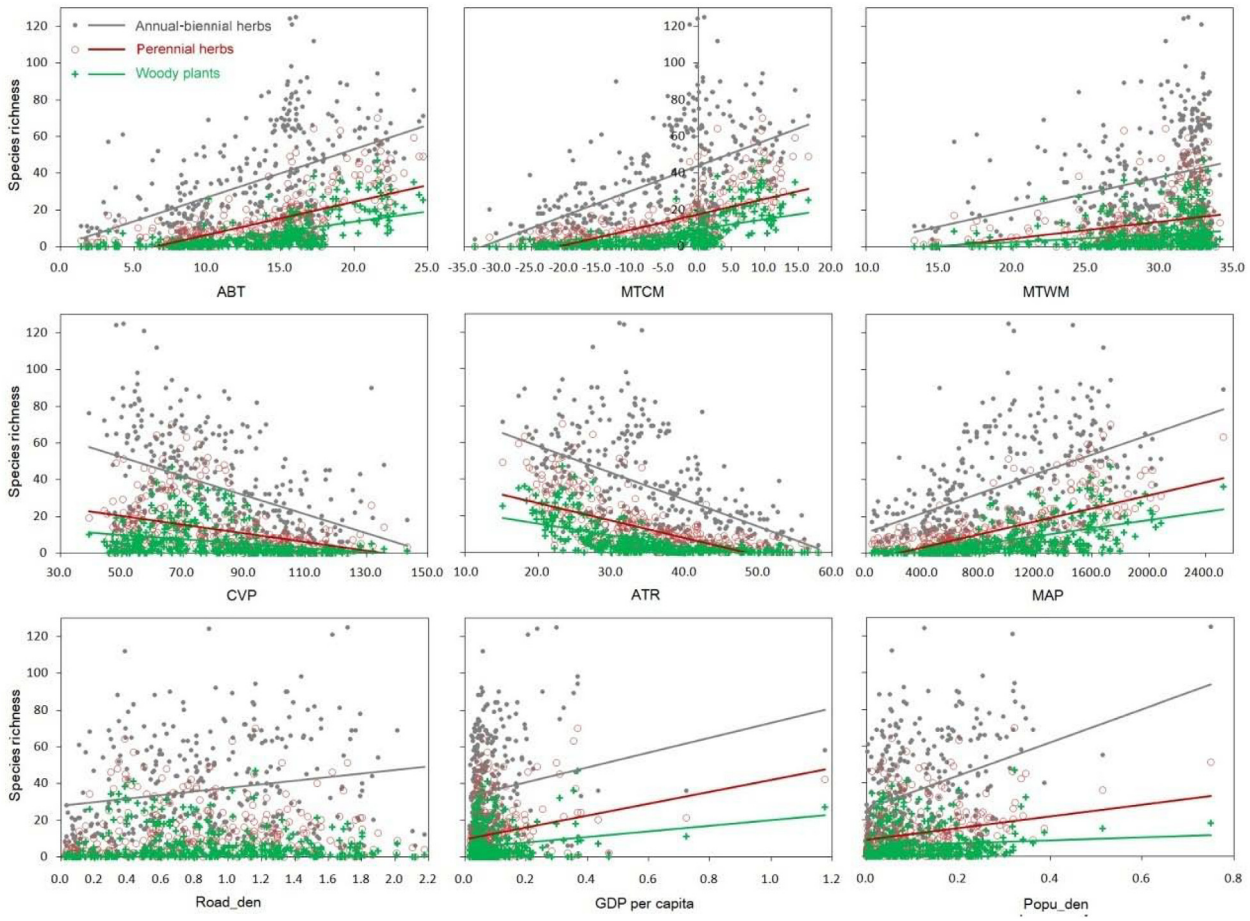


**FIGURE 5 |** Relationship between each environmental factor and invasive plant species richness (the fitting line was not added if the correlation was not significant).

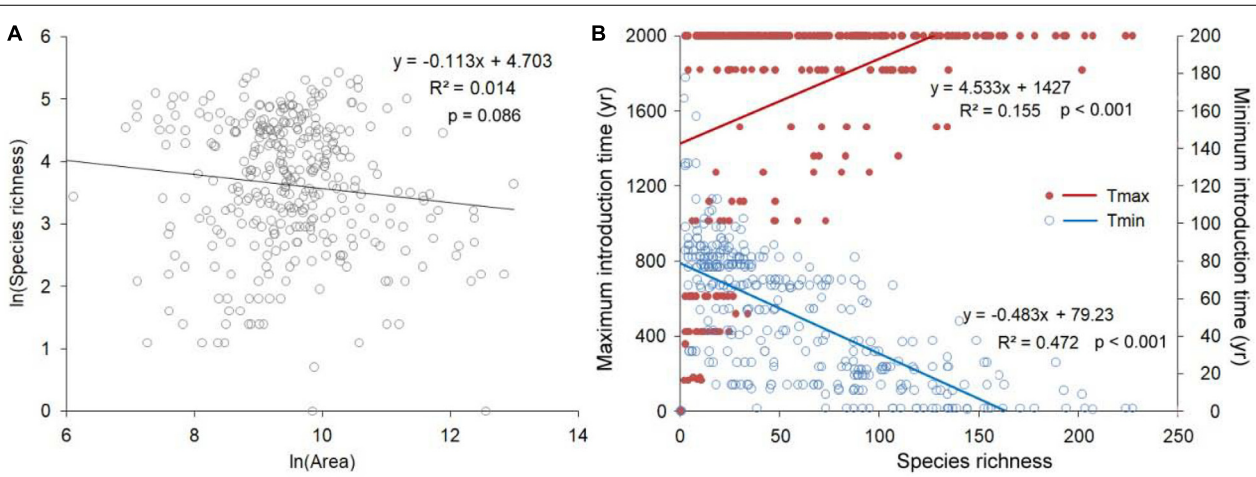


**FIGURE 6 |** Relationship between invasive species richness and **(A)** prefecture area, **(B)** the year of the earliest versus the most recent invasive species.

Tmin contributed the most (51.7%) for invasive ABH species, followed by MTCM and CVP; for the invasive perennial herb species, Tmin (35.9%) and MTCM (21.9%) played major roles, and ABT and MAP also contributed significantly. For invasive woody species richness, the influence of Tmin was weakened and the effect of temperature became stronger, especially ATR and

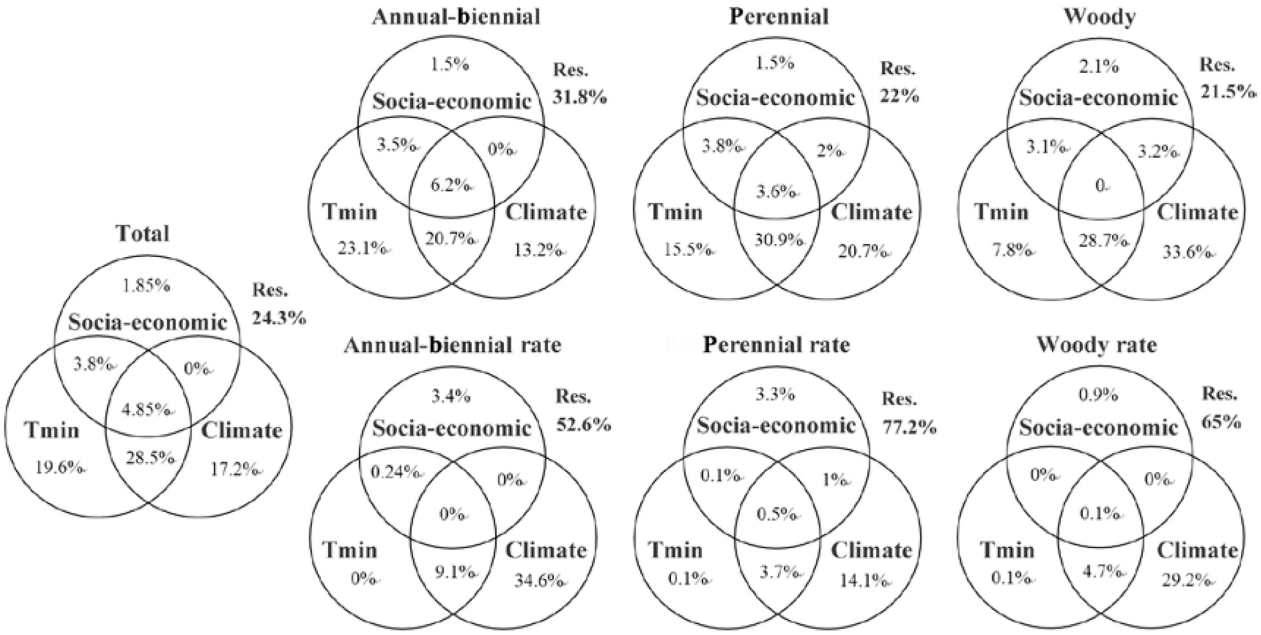


**FIGURE 7 |** Variation partitioning for species richness and species percentage of all IAPS and three subgroups of life form. Tmin, time of most recent introduction; Climate, seven climate indices in **Table 1**; Social-economic, three social-economic indices in **Table 1**.

MTCM. For the richness percentage of three life forms of invasive species, ABT and ATR were significant factors ($R^2$ = 0.263; $P$ = 0.01).

# DISCUSSION

## Species Composition and Geographical Pattern of Invasive Plants in China

Based on the most complete list of IAPS existing in China, this study produced the first data of invasive alien plants distribution in China at a sub-provincial (prefecture) scale, thus provided a more accurate description to the geographical pattern of invasive plant diversity than earlier studies. In accord with existing studies (Yan et al., 2014; Wang et al., 2017), the IAPS diversity in China decreased from south to north, with substantially higher values in subtropical and tropical areas than in temperate areas. There were prominent introductions of IAPS from the northwest border of China, and the intensity of plant invasion was significantly higher in coastal than in inland areas, and significantly higher in cities than in rural areas. It is noteworthy that there were intensive IAPS introductions in the southwest border areas with Vietnam, Laos, and Myanmar, as reported earlier (Lu et al., 2005; Li et al., 2019; Zhang et al., 2019). Given there is no physical barrier to the introduction of IAPS between this region and its neighboring countries, it would be expected that plant dispersal would have already reached saturated and stable condition, and there should be no significantly increased biological invasion. Thus the active IAPS introduction suggests that adjacent areas are also facing similar biological invasions from abroad.

By integrating multiple data sources, this study updated the time accumulation curve of invasive plant species in China (**Supplementary Figure 2**), which showed that 75 species of plants had been introduced to China before 1840, in contrast to 30 reported by Huang et al. (2010) and 39 by Chen et al. (2017). According to Chen et al. (2017), 82 and 83 species of alien plants were recorded in China during the first and second half of the 20th century, respectively. Our updated sequence time showed that the first half of the 20th century represented the outbreak period of alien plant introductions in China, and a total of 182 species invaded during the 1900–1940 period, while the introduction speed slowed down after 1950. This result is different from earlier studies that stressed the importance of the reform-and-opening policy and rapid economic growth since 1980's (Lin et al., 2007; Ding et al., 2008), for their contributions to species introduction and spread in China. However, recent studies with more complete historical data also showed the period of most rapid increase of invasive plant species, i.e., 1900–1950 (Huang et al., 2011). Nevertheless, this study provided the first estimate of the introduction rate of IAPS in China across the 20th century. As to the explanation for the outbreak of plant invasion during 1900–1940s, it is reasonable to think about the potential effects of wars, especially World War II that drove not only the rapid increase of commercial imports (of industrial goods including weapons), but also alien military invasions. The long period of wars caused unprecedented damage to everything across the country, including vegetation.

Seebens et al. (2017) pointed out that, globally, the spread of alien species has not slowed down, and the potential risk of bioinvasion is still accelerating. Their global patterns of temporal change in the records of alien plant introduction indicated a most

**TABLE 2 |** Rank of variable contributions to the variation of species richness and species percentage of all invasive plants and the three life-form subgroups.

| Variables | Total | ABH | Perennial | Woody | ABH% | perennial% | woody% |
|---|---|---|---|---|---|---|---|
| Tmin | 43.7% | 51.7% | 35.9% | 22.9% | 4.01% | | |
| Road | 1.0% | 0.9% | 1.9% | 6.4% | | | |
| GDP | 2.0% | 0.6% | 0.7% | | | | |
| People | 3.1% | 2.9% | 2.0% | 1.0% | | | |
| MAT | 10.4% | | | 13.1% | | | |
| MAP | 7.7% | 5.5% | 11.8% | 6.8% | | | |
| ATR | | 7.9% | | 19.1% | 17.9% | | 26.3% |
| CVP | 5.5% | 10.0% | 3.3% | 1.1% | | | |
| MTWM | | | 3.2% | | | | |
| MTCM | 16.8% | 11.8% | 21.9% | 17.2% | | | |
| ABT | 9.9% | 8.7% | 19.3% | 12.4% | 21.4% | 11.4% | |

*ABH%, perennial%, woody%, the richness percentages of the annual-biennial, perennial and woody invasive species, respectively.*

rapid increase in 1850–1900 and a level-off during 1900–1950, followed by a recovering increase in last half century. What was observed in China seemed not consistent with this global pattern, but had more similarity with their results for Asia as a part, which suggested a little increase during 1850–1900 and a peak value in the 1900–1950 period. Obviously, the spatial difference across continents at the temporal scale of decades revealed more influence from human activities than from climate changes.

## Similarity and Difference in Distribution of Different Life Forms of IAPS

Invasive alien plants species (IAPS) of different life-forms tend to responded distinctly to environmental drivers (Chen et al., 2017; Mehraj et al., 2018). The IAPS richness of three life forms in China revealed similar latitudinal patterns, but the latitudinal patterns of their percentages were different. The percentage of invasive ABHs decreased from north to south, but the highest value appeared in "the temperate semi-arid climate + grassland" region. This region is characterized by strong intra-annual and inter-annual fluctuations in precipitation, which causes severe degradation of perennial vegetation (Li et al., 2006), and forms large areas of bare habitat. This, in turn, facilitates the colonization of ABH plants. Invasive perennial herbs which are tolerant of more extreme climate, and are more competitive than annual herbs, so they can colonize more extensively than annuals in tropical and northern arid areas. Invasive woody species have a long generation cycle and lower dispersal rate, and adapt to habitats with relatively stable climate but more intensive competition; this means that invasive woody plants achieve a higher proportion in the south only. The spatial variations of the percentage composition of invasive species of different life forms reflect the differences in life history strategies and habitat selection (Liu et al., 2006; Huang et al., 2012).

## Spatial and Temporal Drivers for Plant Invasion as an Ongoing Process

The effect of spatial factors on invasive species richness did not follow the classic species-area relationship (Connor and McCoy, 1979; Powell et al., 2013), which confirms that, although China is rich in plant species, there are still empty habitats for plant invasion at the regional scale, and community niche spaces were not saturated, as also revealed at the global scale (Seebens et al., 2017). The dominant role of introduction time on the diversity of invasive species also indicated that the process of plant invasion is still active (Pyšek and Jarošík, 2005). Species dispersal is one of the leading factors for the present patterns of IAPS diversity in China.

In terms of the contributions of environmental and socio-economic factors on the patterns of IAPS diversity in China, our results are similar to earlier studies (Zhang et al., 2010; Chen et al., 2017; Wang et al., 2017). Natural factors such as climate play a dominant role. Among the climate indices, temperature exceeded the influence of precipitation, especially MTCM and ATR. The independent influence of social and economic activities reflected by per capita GDP and population density were also obvious, but road density showed a very weak effect. Although many studies have used road density as an important indicator of habitat fragmentation (Forman et al., 2002) and an important variable to predict biological invasion (McKinney, 2002; Resasco et al., 2014), it showed little impact on plant invasion in China in this study (**Figure 7**). There could be several reasons for this inconsistency. First, although roads are suggested to be good corridors for invasive species dispersal, the dispersal of plants by seeds, generally small and often with attachments facilitating dispersion, can make use of all types of empty or disturbed habitats such as farmlands, rivers and ditches and bare lands (Nentwig, 2007), therefore the correlation with road length could be non-linear; and the arrival of IAPS at China might be more important than the road length for alien plants dispersal. Second, there is generally a time lag between available roads and IAPS dispersal taking advantage of the roads, and this time lag will also revealed in the records (Murray and Phillips, 2012; Albano et al., 2018). In contrast, human activities including deforestation and land cultivation in China have changed habitats over substantial areas for thousands of years. This long existing available niche across China for IAPS may not be simply correlated with road density of a particular time. Third, the scale-related road effect on IAPS dispersal has been widely reported (Williamson, 1996; Milbau et al., 2009). Also in southwest mountainous areas of China, Liang et al. (2014) found the correlation between the

diversity of invasive plants and the density of low-grade rural roads is much higher than that of high-grade roads. Therefore, more research is needed to evaluate the multi-scale impacts of roads on biological invasions, the road density value of a particular time, as used in this study, seemed not to be an idea indicator for plant invasion.

Biological invasions are generally restricted by environmental filters and dispersal limitation (Vicente et al., 2014), and IAPS with different niche widths and dispersal capacities showed different distribution constraints (McDowell et al., 2014). Based on results of quantile regression, we divided the rate of the invasion range change with introduction year into four quartiles, which represented a sequence of species dispersal capacity from weak to strong. The primary explanatory factor for the diversity pattern of each quantile was different. In particular, for the IAPS groups corresponding to the quantile range of 26–100% and a spatial range of >10 prefectures (i.e., with a strong dispersal capacity), the diversity pattern was always dominated by MTCM, while for those IAPS located in the first quartile 0–25% and with a narrow distribution range (with a weak dispersal capacity), the diversity pattern was mainly limited by indicators of GDP and population. This result suggested that, IAPS of a weaker, rather than stronger, dispersal capacity benefit more from human induced habitat degradations, including soil erosion at terrestrial habitats and eutrophication in aquatic habitats (Scherer-Lorenzen et al., 2007; Albano et al., 2018).

The year of most recently introduction (Tmin) of IAPS in a prefecture is basically the year of most recent introduction into China. Tmin played the strongest role as a single variable in explaining IAPS diversity patterns of each life form or as a whole, this result has several important implications. First, the opportunity of arriving at China, from abroad by all means, is more important for a successful plant invasion than the dispersal condition and habitat availability within China, as also implied in a recent study on aquatic plant invasions (Wu and Ding, 2019). Second, the introductions of IAPS in recent decades is more important than the early introductions for the diversity pattern of IAPS, this is also supported by a larger $R^2$ for Tmin (0.472) than Tmax (0.155) in species richness ~ introduction year relationship (**Figure 6B**). Third, since prefectures on the national border generally have smaller Tmin values and more advanced economy and social bases, thus Tmin also indicated the effect of economic-social condition on plant invasion in China.

The past half century has seen the surge of rapid economic growth and globalization, particularly in the Asian-Pacific region. This has been accompanied by an unprecedented global warming since the 1970's (IPCC, 2014). If these two trends were to continue in the future, as most projections suggested, our results should predict an increasingly urgent threat of plant invasions, along with other invasive organisms.

## CONCLUSION

The current threat of plant invasion in China is represented by a total of 463 invasive alien plant species, comprising 84.4% herbaceous and 15.6% woody plants. With a long history of species introduction that traces back to 2000 years ago, plant introductions accelerated in the 19th century, reached a peak in the early half of the 20th century, and have kept a slower and more stable rate in the last 60 years; however, the spatial expansion of invasions have continued significantly over time. The latitudinal gradient, the coastal + southern border-inland gradient, and the urban-rural gradient characterized the prominent patterns of invasive plant species richness in China. This pattern is similar for the species richness of its three subgroups of life forms, but not for their diversity percentage patterns. Climatic thermal index, particularly low temperature, acted as a primary environmental filter to plant invasion, and the time of most recent introduction of IAPS in a prefecture showed the effect of dispersal limit on plant invasion, via either dispersal distance or dispersal capacity. These two factors jointly dominate the spatial pattern of IAPS richness, implying global warming and economy globalization as the main drivers of plant invasions in China, and probably elsewhere in general.

## DATA AVAILABILITY STATEMENT

The raw data supporting the conclusions of this article will be provided upon request to the corresponding author.

## AUTHOR CONTRIBUTIONS

YL compiled the data and prepared the first draft. ZS provided the idea and finalized the manuscript, tables, and figures. Both authors cooperated the data analyses.

## FUNDING

This work was funded by the Key Research and Development Plan of the Ministry of Science and Technology of China (2017YFC0505200) and the National Natural Science Foundation of China (Project Nos. 41971228 and 41371190).

## SUPPLEMENTARY MATERIAL

The Supplementary Material for this article can be found online at: https://www.frontiersin.org/articles/10.3389/fevo.2020.544670/full#supplementary-material

**Supplementary Figure 1 |** Species richness rank of the invasive alien plants of families in China.

**Supplementary Figure 2 |** The accumulative increase of alien invasive plant species (IAPS) richness in China since 1600 A.D.

**Supplementary Table 1 |** The Pearson coefficients between species richness of three life-forms of invasive plants and the environmental and social-economic variables of prefectures in China.

## REFERENCES


Albano, P. G., Gallmetzer, I., Haselmair, A., Tomašovıch, A., Stachowitsch, M., and Zuschin, M. (2018). Historical ecology of a biological invasion: the interplay of eutrophication and pollution determines time lags in establishment and detection. *Biol. Invasions* 20, 1417–1430. doi: 10.1007/s10530-017-1634-7

Bhattarai, K. R., Måren, I. E., and Subedi, S. C. (2014). Biodiversity and invasibility: distribution patterns of invasive plant species in the Himalayas, Nepal. *J. Mount. Sci.* 11, 688–696. doi: 10.1007/s11629-013-2821-3

Borcard, D., Legendre, P., and Drapeau, P. (1992). Partialling out the spatial component of ecological variation. *Ecology* 73, 1045–1055. doi: 10.2307/1940179

Chen, C., Wang, Q., Wu, J., Huang, D., Zhang, W., Zhao, N., et al. (2017). Historical introduction, geographical distribution, and biological characteristics of alien plants in China. *Biodivers. Conserv.* 26, 353–381. doi: 10.1007/s10531-016-1246-z

Connor, E. F., and McCoy, E. D. (1979). The statistics and biology of the species-area relationship. *Am. Nat.* 113, 791–833.

Davidson, A. M., Jennions, M., and Nicotra, A. B. (2011). Do invasive species show higher phenotypic plasticity than native species and, if so, is it adaptive? A meta-analysis. *Ecol. Lett.* 14, 419–431. doi: 10.1111/j.1461-0248.2011.01596.x

Davis, M. A., Thompson, K., and Grime, J. P. (2005). Invasibility: the local mechanism driving community assembly and species diversity. *Ecography* 28, 696–704. doi: 10.1111/j.2005.0906-7590.04205.x

Dawson, W., Moser, D., van Kleunen, M., Kreft, H., Pergl, J., Pyšek, P., et al. (2017). Global hotspots and correlates of alien species richness across taxonomic groups. *Nat. Ecol. Evol.* 1:0186. doi: 10.1038/s41559-017-0186

Denslow, J. S., Space, J. C., and Thomas, P. A. (2009). Invasive exotic plants in the tropical Pacific islands: patterns of diversity. *Biotropica* 41, 162–170. doi: 10.1111/j.1744-7429.2008.00469.x

Ding, J., and Wang, R. (1998). "The impacts of alien species on China's biodiversity," in *China's Biodiversity: a Country Study. China Environmental*, ed W. P. Zhang (Beijing: Science Press), 58–61.

Ding, J., Mack, R. N., Lu, P., Ren, M., and Huang, H. (2008). China's booming economy is sparking and accelerating biological invasions. *Bioscience* 58, 317–324. doi: 10.1641/b580407

Elton, C. (1958). *The Ecology of Invasions by Animals and Plants*. London: Chapman and Hall.

Fang, J. (1994). Arrangement of East-Asian vegetation-climate types on coordinates of temperature and precipitation. *Acta Ecol. Sin.* 14, 290–293.

Feng, J. M., Dong, X. D., and Xu, C. D. (2009). Spatial patterns of floristic composition of invasive alien plants in large scale and their climatic interpretation. *J. Wuhan Bot. Res.* 27, 159–164.

Forman, R. T. T., Sperling, D., Bissonette, J. A., Clevenger, A. P., Cutshall, C. D., and Dale, V. H. (2002). *Road Ecology - Science and Solutions*. London: Island Press.

GADM (2018). *Database of Global Administrative Areas[DB/OL]*. Available online at: https://gadm.org/ (accessed September 1, 2018).

Giorgis, M. A., Cingolani, A. M., Tecco, P. A., Cabido, M., Poca, M., and von Wehrden, H. (2016). Testing alien plant distribution and habitat invasibility in mountain ecosystems: growth form matters. *Biol. Invasions* 18, 2017–2028. doi: 10.1007/s10530-016-1148-8

Guisan, A., Petitpierre, B., Broennimann, O., Daehler, C., and Kueffer, C. (2014). Unifying niche shift studies: insights from biological invasions. *Trends Ecol. Evol.* 29, 260–269. doi: 10.1016/j.tree.2014.02.009

Hierro, J. L., Maron, J. L., and Callaway, R. M. (2005). A biogeographical approach to plant invasions: the importance of studying exotics in their introduced and native range. *J. Ecol.* 93, 5–15. doi: 10.1111/j.0022-0477.2004.00953.x

Horvitz, N., Wang, R., Wan, F., and Nathan, R. (2017). Pervasive human-mediated large-scale invasion: analysis of spread patterns and their underlying mechanisms in 17 of China's worst invasive plants. *J. Ecol.* 105, 85–94.

Houseman, G. R., Foster, B. L., and Brassil, C. E. (2014). Propagule pressure-invasibility relationships: testing the influence of soil fertility and disturbance with *Lespedeza cuneata*. *Oecologia* 174, 511–520. doi: 10.1007/s00442-013-2781-x

Huang, D., Zhang, R., Kim, K. C., and Suarez, A. (2012). Spatial pattern and determinants of the first detection locations of invasive alien species in mainland China. *PLoS One* 7:e31734. doi: 10.1371/journal.pone.0031734

Huang, Q. Q., Qian, C., Wang, Y., Jia, X., Dai, X. F., Zhang, H., et al. (2010). Determinants of the geographical extent of invasive plants in China: effects of biogeographical origin, life cycle and time since introduction. *Biodivers. Conserv.* 19, 1251–1259. doi: 10.1007/s10531-009-9751-y

Huang, Q., Wang, G., Hou, Y., and Peng, S. (2011). Distribution of invasive plants in China in relation to geographical origin and life cycle. *Weed Res.* 51, 534–542. doi: 10.1111/j.1365-3180.2011.00868.x

IPCC (2014). *Climate Change 2014: Synthesis Report. Contribution of Working Groups I, II and III to the Fifth Assessment Report of the Intergovernmental Panel on Climate Change*, eds Core Writing Team, R. K. Pachauri and L. A. Meyer. Geneva: IPCC, 151.

Jauni, M., Gripenberg, S., and Ramula, S. (2015). Non-native plant species benefit from disturbance: a meta-analysis. *Oikos* 124, 122–129. doi: 10.1111/oik.01416

Khuroo, A. A., Reshi, Z. A., Malik, A. H., Weber, E., Rashid, I., and Dar, G. H. (2012). Alien flora of India: taxonomic composition, invasion status and biogeographic affiliations. *Biol. Invasions* 14, 99–113. doi: 10.1007/s10530-011-9981-2

Kowarik, I. (1995). "Time lags in biological invasions with regard to the success and failure of alien species," in *Plant Invasions - General Aspects and Special Problems*, eds P. Pyšek, K. Prach, M. Rejmánek, and Wade, M (Hague: SPB Academic Publishing), 15–38.

Li, X. H., Jiang, D. M., Liu, Z. M., and Li, X. L. (2006). Seed germination characteristics of annual species in temperate semi-arid region. *Acta Ecol. Sin.* 26, 1194–1199.

Li, X., Tang, S., Wei, C., Pan, Y., and Wang, Y. (2019). Alien invasive plants in the Sino- Vietnamese border area, Guangxi. *J. Biosaf.* 28, 147–155.

Liang, J., Liu, Y., Ying, L., Li, P., Xu, Y., and Shen, Z. (2014). Do higher level roads have larger impacts on the mountain landscape? A case study of the three parallel rivers region. *Chin. Geogr. Sci.* 24, 15–27.

Lin, W., Zhou, G., Cheng, X., and Xu, R. (2007). Fast economic development accelerates biological invasions in China. *PLoS One* 11:e1208. doi: 10.1371/journal.pone.0001208

Liu, J., Dong, M., Miao, S. L., Li, Z. Y., Song, M. H., and Wang, R. Q. (2006). Invasive alien plants in China: role of clonality and geographical origin. *Biol. Invasions* 8, 1461–1470. doi: 10.1007/s10530-005-5838-x

Lu, P., Sang, W. G., and Ma, K. P. (2005). Progress and prospects in research of an exotic invasive species, *Eupatorium adenophorum*. *Chin. J. Plant Ecol.* 29, 1029–1037.

Ma, J. S. eds (2014). *The Survey Reports on Chinese Alien Invasive Plants (Part One, Part Two)*. Beijing: Higher Education Press.

McDowell, W. G., Benson, A. J., and Byers, J. E. (2014). Climate controls the distribution of a widespread invasive species: implications for future range expansion. *Freshw. Biol.* 59, 847–857. doi: 10.1111/fwb.12308

McKinney, M. L. (2002). Influence of settlement time, human population, park shape and age, visitation and roads on the number of alien plant species in protected areas in the USA. *Divers. Distrib.* 8, 311–318. doi: 10.1046/j.1472-4642.2002.00153.x

Mehraj, G., Khuroo, A. A., Qureshi, S., Muzafar, I., Friedman, C. R., and Rashid, I. (2018). Patterns of alien plant diversity in the urban landscapes of global biodiversity hotspots: a case study from the Himalayas. *Biodivers. Conserv.*¶ 27,¶ 1055–1072. doi: 10.1007/s10531-017-1478-6

Milbau, A., Stout, J. C., Graae, B. J., and Nijs, Y. (2009). A hierarchical framework for integrating invasibility experiments incorporating different factors and spatial scales. *Biol. Invasions* 11, 941–950. doi: 10.1007/s10530-008-9306-2

Minor, E. S., Tessel, S. M., Engelhardt, K. A. M., and Lookingbill, T. R. (2009). The role of landscape connectivity in assembling exotic plant communities: a network analysis. *Ecology* 90, 1802–1809. doi: 10.1890/08-1015.1

Müllerová, J., Pyšek, P., Jarošík, V., and Pergl, J. (2005). Aerial photographs as a tool for assessing the regional dynamics of the invasive plant species *Heracleum mantegazzianum*. *J. Appl. Ecol.* 42, 1042–1053. doi: 10.1111/j.1365-2664.2005.01092.x

Murray, B., and Phillips, M. L. (2012). Temporal introduction patterns of invasive alien plant species to Australia. *NeoBiota* 13, 1–14.

Nentwig, W. eds (2007). *Biological Invasion: Section III. Patterns of Invasion and Invasibility*. Berlin: Springer- Verlag, 145–214.

Pejchar, L., and Mooney, H. A. (2009). Invasive species, ecosystem services and human well-being. *Trends Ecol. Evol.* 24, 497–504. doi: 10.1016/j.tree.2009.03.016

Pimentel, D., Zuniga, R., and Morrison, D. (2005). Update on the environmental and economic costs associated with alien-invasive species in the United States. *Ecol. Econ.* 52, 273–288. doi: 10.1016/j.ecolecon.2004.10.002

Pimentel, D. (2002). *Biological Invasions: Economic and Environmental Costs of Alien Plant. Animal, and Microbe Species*. Boca Raton, FL: CRC Press.

Powell, K. I., Chase, J. M., and Knight, T. M. (2013). Invasive plants have scale-dependent effects on diversity by altering species-area relationships. *Science* 339, 316–318. doi: 10.1126/science.1226817

Pyšek, P., Manceur, A. M., Alba, C., Mcgregor, K. F., Pergl, J., Stajerova, K., et al. (2015). Naturalization of central European plants in North America: species traits, habitats, propagule pressure, residence time. *Ecology* 96, 762–774. doi: 10.1890/14-1005.1

Pyšek, P., Pergl, J., Essl, F., Lenzner, B., Dawson, W., and Kreft, H., et al. (2017). Naturalized alien flora of the world: species diversity, taxonomic and phylogenetic patterns, geographic distribution and global hotspots of plant invasion. *Preslia* 89, 203–274. doi: 10.23855/preslia.2017.203

Pyšek, P., and Jarošík, V. (2005). "Residence time determines the distribution of alien plants," in *Invasive Plants: Ecological and Agricultural Aspects*, ed S. Inderjit (Basel: Birkháuser Verlag).

Pyšek, P., Jarošìk, V., and Kučera, T. (2002). Patterns of invasion in temperate nature reserves. *Biol. Conserv*. 104, 13–24. doi: 10.1016/s0006-3207(01)00150-1

R Core Team (2018). *R: A Language and Environment for Statistical Computing*. Vienna: R Foundation for Statistical Computing.

Resasco, J., Haddad, N. M., Orrock, J. L., Shoemaker, D., Brudvig, L., Damschen, E., et al. (2014). Landscape corridors can increase invasion by an exotic species and reduce diversity of native species. *Ecology* 95, 2033–2039. doi: 10.1890/14-0169.1

Richardson, D. M., and Pyšek, P. (2006). Plant invasions: merging the concepts of species invasiveness and community invasibility. *Prog. Phys. Geog.* 30, 409–431. doi: 10.1191/0309133306pp490pr

Sax, D. (2001). Latitudinal gradients and geographic ranges of exotic species: implications for biogeography. *J. Biogeogr.* 28, 139–150. doi: 10.1046/j.1365-2699.2001.00536.x

Scherer-Lorenzen, M., Venterink, H. O., Buschmann, H. (2007). "Nitrogen enrichment and plant invasions: the importance of nitrogen-fixing plants and anthropogenic eutrophication," in *Biological Invasions. Ecological Studies 193*, ed W. Nentwig (Berlin: Springer), 163–180.

Schmidt, J. P., and Drake, J. M. (2011). Time since introduction, seed mass, and genome size predict successful invaders among the cultivated vascular plants of Hawaii. *PLoS One* 6:e17391. doi: 10.1371/journal.pone.0017391

Schrama, M., and Bardgett, R. D. (2016). Grassland invasibility varies with drought effects on soil functioning. *J. Ecol.* 104, 1250–1258. doi: 10.1111/1365-2745.12606

Seebens, H., Blackburn, T. M., Dyer, E. E., and Genovesi, P. (2017). No saturation in the accumulation of alien species worldwide. *Nat. Commun.* 8:14435.

Seebens, H., Blackburn, T. M., Dyer, E. E., Genovesi, P., Hulme, P., and Jeschke, J. M., et al. (2018). Global rise in emerging alien species results from increased accessibility of new source pools. *Proc. Natl. Acad. Sci.* 115, E2264–E2273.

Shen, Z., Fei, S., Feng, J., Liu, Y., Liu, Z., Tang, Z., et al. (2012). Geographical patterns of community-based tree species richness in Chinese mountain forests: the effects of contemporary climate and regional history. *Ecography* 35, 1134–1146. doi: 10.1111/j.1600-0587.2012.00049.x

Simberloff, D., Martin, J. -L., Genovesi, P., Maris, V., Wardle, D., Aronson, J., et al. (2013). Impacts of biological invasions: what's what and the way forward. *Trends Ecol. Evol.* 28, 58–66. doi: 10.1016/j.tree.2012.07.013

Song, X., Hogan, J. A., Brown, C., Cao, M., and Yang, J. (2017). Snow damage to the canopy facilitates alien weed invasion in a subtropical montane primary forest in southwestern China. *For. Ecol. Manag.* 391, 275–281. doi: 10.1016/j.foreco.2017.02.031

Stohlgren, T. J., Binkley, D., Chong, G. W., Kalkhan, M. A., Schell, L. D., Bull, K. A., et al. (1999). Exotic plant species invade hot spots of native plant diversity. *Ecol. Monogr.* 69, 25–46. doi: 10.1890/0012-9615(1999)069[0025:epsihs]2.0.co;2

The Plant List (2013). *Published on the Internet*. Available online at: http://www.theplantlist.org/ (accessed January 1, 2018).

Traveset, A., and Richardson, D. M. (2014). Mutualistic interactions and biological invasions. *Annu. Rev. Ecol. Evol. Sci.* 45, 89–113. doi: 10.1146/annurev-ecolsys-120213-091857

Vicente, J. R., Pereira, H. M., Randin, C. F., Gonçalves, J., Lomba, A., Alves, P., et al. (2014). Environment and dispersal paths override life strategies and residence time in determining regional patterns of invasion by alien plants. *Perspect. Plant Ecol.* 16, 1–10.

Wan, F. H., Guo, J. Y., and Zhang, F. ed. (2009). *Research on Biological Invasion in China*. Beijing: Science Press.

Wang, G. H., Bai, F., and Sang, W. G. (2017). Spatial distribution of invasive alien animal and plant species and its influencing factors in China *Plant Sci. J.* 35, 513–524.

Wang, H., López-Pujol, J., Meyerson, L. A., Qiu, J., Wang, X., and Ouyang, Z. (2011). Biological invasions in rapidly urbanizing areas: a case study of Beijing, China. *Biodivers. Conserv.* 20, 2483–2509.

Weber, E., Sun, S. G., and Li, B. (2008). Invasive alien plants in China: diversity and ecological insights. *Biol. Invasions* 10, 1411–1429. doi: 10.1007/s10530-008-9216-3

Westphal, M. I., Browne, M., MacKinnon, K., and Noble, I. (2008). The link between international trade and the global distribution of invasive alien species. *Biol. Invasions* 10, 391–398. doi: 10.1007/s10530-007-9138-5

Williamson, M. (eds). (1996). *Biological Invasions*. Berlin: Springer Science & Business Media.

Wolmarans, R., Robertson, M. P., and van Rensburg, B. J. (2010). Predicting invasive alien plant distributions: how geographical bias in occurrence records influences model performance. *J. Biogeogr.* 37, 1797–1810. doi: 10.1111/j.1365-2699.2010.02325.x

Wu, H., Carrillo, J., and Ding, J. (2017). Species diversity and environmental determinants of aquatic and terrestrial communities invaded by *Alternanthera philoxeroides*. *Sci. Total Environ.* 581–582, 666–675. doi: 10.1016/j.scitotenv.2016.12.177

Wu, H., and Ding, J. (2019). Global change sharpens the double-edged sword effect of aquatic alien plants in China and beyond. *Front. Plant Sci.* 10:787. doi: 10.3389/fpls.2019.00787

Wu, S. H., Hsieh, C. F., Chaw, S. M., and Rejmanek, M. (2004). Plant invasions in Taiwan: insights from the flora of casual and naturalized alien species. *Divers. Distrib.* 10, 349–362. doi: 10.1111/j.1366-9516.2004.00121.x

Xu, H., Ding, H., Li, M., Qiang, S., Guo, J., and Han, Z., et al. (2006). The distribution and economic losses of alien species invasion to China. *Biol. Invasions* 8, 1495–1500. doi: 10.1007/s10530-005-5841-2

Xu, H., Qiang, S., Genovesi, P., Ding, H., Wu, J., Meng, L., et al. (2012). An inventory of invasive alien species in China. *NeoBiota* 15, 1–26.

Xu, H., Qiang, S., Han, Z., Guo, J., Huang, Z., Sun, H., et al. (2004). The distribution and introduction pathway of alien invasive species in China. *Biodivers. Sci.* 12, 626–638.

Yan, X. L., Liu, Q. R., Shou, H. Y., Zeng, X. F., Zhang, Y., Chen, L., et al. (2014). The categorization and analysis on the geographic distribution patterns of Chinese alien invasive plants. *Biodivers. Sci.* 22, 667–676.

Zhang, L. Y., Li, Y. B., Huang, J. C., and Liu, X. F. (2019). Evaluation of the short-term and long-term performance of biological invasion management in the China-Myanmar border region. *J. Environ. Manage.* 240, 1–8.

Zhang, S., Guo, S. L., Guan, M., Yin, L. P., and Zhang, R. X. (2010). Diversity differentiation of invasive plants at a regional scale in China and its influencing factors: according to analyses on the data from 74 regions. *Acta Ecol. Sin.* 30, 4241–4256.

Zheng, S. S., Chen, X. B., Xu, W. N., Luo, Z. R., and Xia, G. S. (2018). Effects of exotic-native species relationship on naturalization and invasion of exotic plant species. *Chin. J. Plant Ecol.* 42, 990–999.

Zhu, L., Sun, O. J., Sang, W., Li, Z., and Ma, K. (2007). Predicting the spatial distribution of an invasive plant species (*Eupatorium adenophorum*) in China. *Landscape Ecol.* 22, 1143–1154. doi: 10.1007/s10980-007-9096-4

**Conflict of Interest:** The authors declare that the research was conducted in the absence of any commercial or financial relationships that could be construed as a potential conflict of interest.

frontiers in Ecology and Evolution

ORIGINAL RESEARCH
published: 14 January 2021
doi: 10.3389/fevo.2020.546433

# Soil Mesofauna Community Changes in Response to the Environmental Gradients of Urbanization in Guangzhou City

*Shiqin Yu[1,2,3], Junliang Qiu[1], Xiaohua Chen[1], Xiaofeng Luo[1], Xiankun Yang[1,2,3], Faming Wang[4] and Guoliang Xu[1,2,3]**

[1] School of Geography and Remote Sensing, Guangzhou University, Guangzhou, China, [2] Rural Non-point Source Pollution Comprehensive Management Technology Center of Guangdong Province, Guangzhou, China, [3] Centre for Climate and Environmental Changes, Guangzhou University, Guangzhou, China, [4] The CAS engineering Laboratory for Ecological Restoration of Island and Coastal Ecosystems, South China Botanical Garden, Chinese Academy of Sciences, Guangzhou, China

There has been a recent increase in interest on how urbanization affects soil fauna communities. However, previous studies primarily focused on some limited land use types or line transects of urban-rural gradients. At family and higher taxonomic levels, we investigated the changes of soil mesofauna communities (abundance, species richness, and community structure) with urbanization intensity along different disturbance features in 47 sites evenly located in downtown Guangzhou and adjacent regions. The 47 research sites were classified into four ecosystem types mainly according to the location (rural/urban), vegetation cover, and management intensity. In turn, the four types with increasing urbanization intensity were rural forest, urban forest, urban woodland, and urban park. Firstly, the role of urban soil property (soil physicochemical characteristic and soil heavy metal content) in regulating soil mesofauna community was investigated. The results showed that soil mesofauna abundance and diversity decreased with increasing soil pH, total nitrogen content (TN), and heavy metal comprehensive index (CPI). Soil Pb decreased soil mesofauna species richness (taxa number) and regulated soil mesofauna community structure. Secondly, we examined the effects of landscape changes on the soil mesofauna community. We found impervious surface (IS) ratio did not predict changes in soil mesofauna abundance, species richness, or community structure. Instead, IS ratio was positively correlated with soil pH, soil TN, and CPI. After excluding sites that belonged to rural forests and urban parks, site area was positively correlated with soil mesofauna abundance. Thirdly, our results revealed significant differences in soil property, landscape trait, and soil mesofauna community among the four ecosystem types. Interestingly, urban forest, the one lightly disturbed by urbanization, but not rural forest, had the highest soil mesofauna abundance. Soil mesofauna abundance in urban woodlands was similar to that in urban parks, which was about half of that in urban forests. Species richness in urban parks was 21% lower than that in rural forests. Our results also showed that urban woodland and urban parks had distinct mesofauna community structures compared to those in rural forests and urban forests. In conclusion, the present study suggested that (1) soil property changes due to urbanization, such as increased pH and heavy metal enrichment in urban soil, decreased

OPEN ACCESS

***Edited by:***
*Meng Yao,*
*Peking University, China*

***Reviewed by:***
*Rakesh Bhutiani,*
*Gurukula Kangri Vishwavidyalaya, India*
*Tibor Magura,*
*University of Debrecen, Hungary*

***Correspondence:**
*Guoliang Xu*
*xugl@gzhu.edu.cn*

***Specialty section:***
*This article was submitted to Biogeography and Macroecology, a section of the journal Frontiers in Ecology and Evolution*

***Received:*** *28 March 2020*
***Accepted:*** *08 December 2020*
***Published:*** *14 January 2021*

***Citation:***
*Yu S, Qiu J, Chen X, Luo X, Yang X, Wang F and Xu G (2021) Soil Mesofauna Community Changes in Response to the Environmental Gradients of Urbanization in Guangzhou City. Front. Ecol. Evol. 8:546433. doi: 10.3389/fevo.2020.546433*

soil mesofauna abundance and species richness, changed community structure, and mediated the effect of landscape change on soil mesofauna community; (2) however, soil and landscape changes could not explain the increase of abundance in urban forests, which supported the intermediate disturbance hypothesis.

**Keywords: urban biodiversity, soil diversity, land use change, soil invertebrate, soil heavy metal**

## INTRODUCTION

Urbanization has a tremendous effect on the economy and environment in the modern world. Habit loss and fragmentation, land use change, environmental pollution, and anthropogenic interruption during the urbanization process has caused biodiversity declines in mammals, birds, and amphibians (McKinney, 2006, 2008; Diego Ibanez-Alamo et al., 2017). Soil mesofauna, such as collembola and mite, can exert substantial effects on soil fundamental functions (Wolters, 2001; Bardgett and van der Putten, 2014). As a result, it is important to know how a soil mesofauna community would respond to the environmental changes induced by urbanization.

Urbanization always proceeds with enormous land use type change, which may be the strongest factor influencing soil fauna communities. Many previous studies investigated the urbanization effects on soil fauna by comparing communities among urban ecosystems of different land use types. In Phoenix, the soil arthropod community is significantly different among residential, industrial, agricultural, and desert remnants, especially when springtails, ants, and mites are excluded from the analysis (McIntyre et al., 2001). In a semi-arid city, Ge et al. (2019) showed that urban lawn soils have lower soil invertebrate evenness and diversity, but higher density than remnant patches of native coastal sage scrub. Joimel et al. (2018) investigated collembola communities in both extensive and productive green roofs, and found no differences in collembola taxonomic structures. However, it is not easy to know exactly which environmental factors shape a soil fauna community from such studies, because most environmental conditions vary dramatically and inconsistently among land use types.

More and more studies have begun to investigate the soil fauna response to a specific agent of urban environmental change. Soil in a city is sometime called "man-made soil," because it is someway re-created during city construction and residential daily lives (Gilbert, 1989). During the re-creation, man-made materials, such as broken bricks, glass and china, kitchen refuse, fertilizer, and so on, are mixed into urban soils, which result in a widely reported elevated soil pH (Jim, 1998; Pouyat et al., 2015; Asabere et al., 2018), increased soil nutrients (Pouyat et al., 2002; Trammell et al., 2020), and heavy metal accumulation (Wei and Yang, 2010). In urban green spaces under management, removal of aboveground litter, application of fertilizer and irrigation, and so on may also substantially change soil characteristics (Norton, 2011; Mao et al., 2014; Tresch et al., 2018, 2019).

Many efforts have been made to reveal the relationship between heavy metal and soil fauna. It is reasonable that soil fauna will be inhibited by heavy metal, which has been widely reported in ecotoxicological tests in lab incubations (Crommentuijn et al., 1993; Didden and Rombke, 2001; Herbert et al., 2004). However, there is no consensus in field studies. While some field studies found heavy metal in urban soils decrease soil fauna abundance and richness (Fiera, 2009; Santorufo et al., 2012), other studies showed contrary results (Fountain and Hopkin, 2004; Joimel et al., 2017; Milano et al., 2018; Sterzynska et al., 2018). In contrast, there are only a few studies exploring the relationships between soil fauna communities and other soil characteristics in urban ecosystems. In the city of Warsaw, Rzeszowski et al. (2017) found that factors contributing to significant collembola communities' variation are soil potassium and phosphorus concentrations and soil pH, whereas soil nitrogen and carbon do not have significant effects. In the Beijing Olympic Park, Song et al. (2015) also showed that there are significant correlations between soil physicochemical property and the soil mesofauna community. However, due to the limited number of studies, it is not clear that whether such relationships widely exist in different urban soils.

Most urban ecosystems are embedded within human construction and are of a small area with a large ratio of girth to area (Bradshaw, 2003; Hruska, 2006), which is typical of fragmented habitats. Such landscape characteristics could affect individual and gene exchanges, thus shaping the process of community construction (LaPoint et al., 2015; Lepczyk et al., 2017). Studies on aboveground organisms suggested that habitat area, connectivity, and landscape diversity are important in determining organism community composition and structure (Faeth et al., 2011; Braaker et al., 2014, 2017, Burrow, 2018). In contrast, studies on urban soil fauna seldom take landscape features into account (but see Bolger et al., 2000; Milano et al., 2018; Xie et al., 2018). A recent systematic review suggests that the underlying mechanisms regulating soil organisms may be inconsistent with those generated from studies on aboveground organisms (Thakur et al., 2019). As a result, it remains unclear whether landscape features could have significant effects on soil fauna community.

Some previous studies found species within a family or even a genus could have different capacities to resist environmental stress as a result of their different functions and physical traits (Magura et al., 2010; Santorufo et al., 2014). However, taxonomic analyses at a species level in soil fauna is expensive, both in terms of equipment and time. In recent years, many studies found it is realizable to indicate soil environmental changes at family or higher taxonomic levels (Parisi et al., 2005; Santorufo et al., 2012; Menta et al., 2018). These studies hypothesize that soil fauna within a higher taxonomic (family or order, etc.) level have similar capabilities to adapt to soil environmental changes, which was supported by many studies, especially in natural grassland

(Madej and Kozub, 2014), farmland (Rudisser et al., 2015), and degraded soils Madej and Kozub (2014).

In the present study, we made soil and soil mesofauna samples in 47 sites evenly located in the downtown of Guangzhou city and adjacent regions, representing urban soil ecosystems of different soil physicochemical properties, soil heavy metal pollution degree, and landscape trait. Our main objective was to advance the knowledge on the effect of specific urbanization agents on soil mesofauna abundance, diversity, and community structure at family and higher taxonomic levels.

## MATERIALS AND METHODS

### Study Area and Sample Design

The city of Guangzhou (22°26′ – 23°56′N and 112°57′ – 114°03′E) is the capital of Guangdong province in South China. The soil type in natural ecosystems in Guangzhou is latosolic red soil. The climate in Guangzhou is a subtropical, marine monsoon climate with an annual average temperature of 21.5–22.2°C and an annual average precipitation of 1,623.6–1,899.8 mm. Guangzhou has an annual average number of 149.2 rainy days, with most rainy days occurring during April to October. Typically, July is the hottest month with a mean temperature of 28.6°C, and January is the coldest with a mean temperature of 13.6°C.

To establish representative sites distributed evenly in the downtown of Guangzhou city and adjacent regions, we made preliminary selections of urban ecosystems in online satellite images along (but not closed to) the arterial roads across the study area. At first, 55 sites were chosen on the satellite images. After that, we went to each potential site to discriminate whether the site met our standards. In this procedure, sites that could not be reached or with newly translocated soils or newly planted plants were excluded. At last, 47 sites were established in the study area (**Figure 1**).

The 47 sites were classified into four ecosystem types according to the location, vegetation cover, amount of anthropogenic solid waste, dominant plant type, and management intensity (**Table 1**). The four typical ecosystem types with increasing urban disturbance intensity are rural forest (8 sites), urban forest (16 sites), urban woodland (13 sites), and urban park (10 sites). A rural forest site was always located in a consecutive forest and far from the city's infrastructure (such as roads and building), while an urban forest site was surrounded by human construction and isolated from other soil ecosystems. However, the urban forests were usually located on hills, thus only suffering mild human disturbances. Both the rural and urban forests were broadleaf evergreen forests and had high vegetation covers (>80%). The dominant plants in the rural forest and urban forest were native or/and alien trees. An urban woodland site was usually small and close to city construction. As a result, the soils in urban woodland were heavily polluted by solid anthropic wastes (such as plastic, wire, paper, brick, clothes, and so on), indicating a strong human disturbance. The dominant plants in urban woodlands were street trees or/and garden shrubs. There were only sparse and young plants in the urban woodlands, and thus with lower vegetation cover. The dominant plants in urban parks were similar to those in the urban woodlands. However, urban parks were managed ecosystems. The vegetation in the urban parks were pruned, watered and fertilized, and the aboveground plant litter was removed for sanitization. The soils may be turned over, and solid wastes polluted.

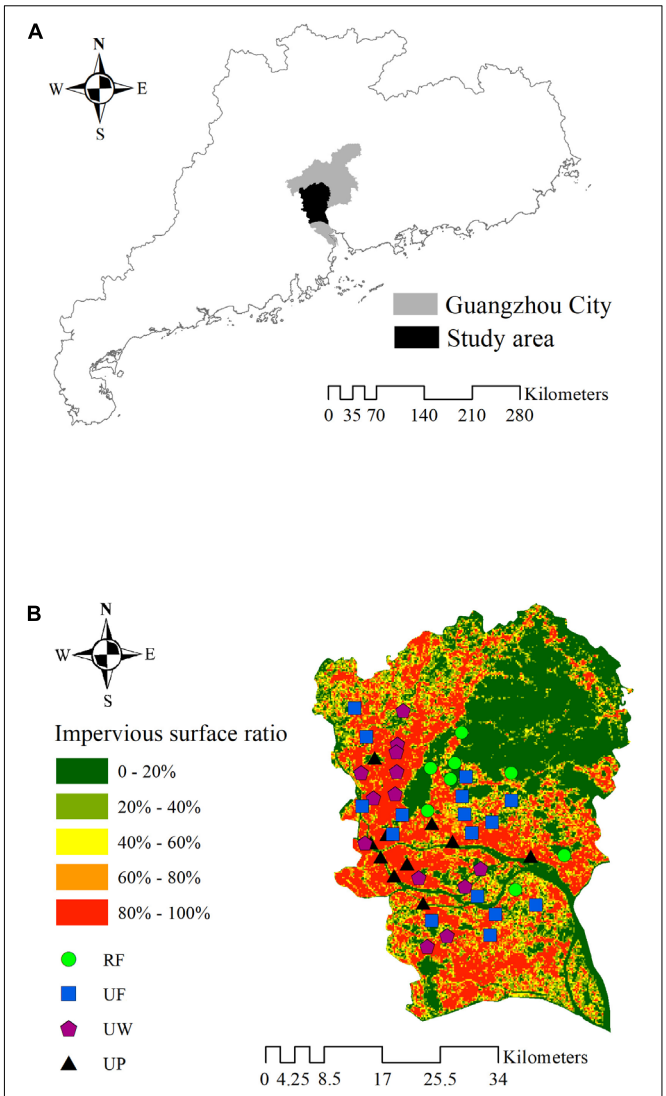


**FIGURE 1 | (A)** Locations of the study areas in Guangdong Province. **(B)** Impervious surface ratio of the study area and location of the 47 sites in downtown and the adjacent regions in Guangzhou City. RF, rural forest; UF, urban forest; UW, urban woodland; UP, urban park.

### Soil Mesofauna Collection and Identification

From October 2018 to December 2018, we sampled soil mesofauna in the study area once for each site. At each site, a transect including three 5 × 5 $m^2$ sub-plots separated by 10 m was established. In each sub-plot, three soil cores were randomly

**TABLE 1 |** Characteristics of rural forest (RF), urban forest (UF), urban woodland (UW), and urban park (UP).

| | Location | Vegetation cover | Anthropogenic wastes | Dominant plant type | Management |
|---|---|---|---|---|---|
| RF | Rural | >80% | No | Native or/and alien trees | No |
| UF | Urban | >80% | Little | Native or/and alien trees | No |
| UW | Urban | <50% | Much | Street trees or/and garden shrubs | No |
| UP | Urban | – | Little | Street trees or/and garden shrubs | Yes |

taken from surface soil (0–10 m) with a steel corer (5 cm inner diameter) to generate a soil sample for soil mesofauna extraction. Therefore, we collected three samples per site. Immediately after collection, the samples were transported to our laboratory, and soil collembola and mites were extracted using Tullgren dry funnels for 48 h. All specimens were sorted and counted and examined with an Olympus BX41 research microscope (Olympus, Tokyo, Japan). The mites were allocated to three groups, namely Mesostigmata, Oribatida, and Prostigmata, while the collembola were grouped according to family and others to order or class, mainly according to Yin (1998).

At each site, soil mesofauna abundance (number of soil mesofauna per $m^2$) and species richness (total number of taxa, *S*) were recorded and used to calculate Shannon diversity index as (Shannon, 1948):

$$H = -\Sigma P_i log_2 P_i$$

where $P_i$ is the ratio between the abundance of species i and the total soil mesofauna abundance. Evenness (*J*) was evaluated according to the Pielou index (Pielou, 1969):

$$J = H/log_2 S$$

## Soil Properties Analysis

At each transect, another three soil samples were taken using a steel corer (3 cm inner diameter) to generate a soil sample to test for soil physicochemical properties and heavy metal levels. Apart from five polluted samples, we assessed soil pH, soil organic matter (SOM), and soil total nitrogen (TN) for each site. Soil pH was measured using a 1: 2.5 soil: water suspension with the potentiometric method. SOM was determined using $H_2SO_4$-$K_2Cr_2O_7$ oxidation method. Soil TN was quantified by the Kjeldahl acid digestion method. Heavy metal concentration (Zn, Cu, Cd, and Pb) was analyzed after digestion in a mixture of nitric, perchloric acid, and hydrogen peroxide. Soil heavy metal comprehensive index (*CPI*) was calculated as (Li et al., 2008):

$$M_i = C_i/S_i$$

and,

$$CPI = \sqrt{\frac{\left(\frac{1}{n}\sum_{i=1}^{n} M_i\right)^2 + [\max(M_i)]^2}{2}}$$

where $M_i$ is the pollution index of heavy metal *i*; $C_i$ (mg $kg^{-1}$) is the measured heavy metal *i*; $S_i$ (mg $kg^{-1}$) is the environmental background value of Guangzhou City (Zhou et al., 2009); and *CPI* is the comprehensive pollution index.

## Assessments of Impervious Surface and Site Area

Land cover information was generated from a set of global 10-m resolution land cover map from Sentinel 2 images via the Google Earth Engine. Buildings and pavements were classified into impervious surface (IS). Circular buffers at radiuses of 200, 500, and 1000 m were established for each site with the site as circle center. After that, IS ratios of each circle buffer were calculated. The IS ratio at a radius of 500 m was chosen for the next analyses because it had higher correlation coefficients with soil property and soil mesofauna parameter in Pearson's correlation analysis (**Supplementary Table 1**). In addition, to show the overall view of the IS ratio of the study area, the original map of land cover was transformed to a map of geographic grid cells at 500 m. The IS ratio in each grid cell was calculated, respectively, and visualized in **Figure 1**. The area of each site was measured in the LocalSpaceViewer 4.0 using Google Earth Map. The area reported in this study did not include those of consecutive rural forest sites, because they were part of consecutive forests. In addition, the areas of urban park sites were not reported in the present study, because internal impervious pavements in urban parks could not be distinguished in the map.

## Statistical Analysis

For all analyses, values from three soil samples (sub-plots) in a site were averaged and treated as a single replicate per site ($N$ = 47 for soil mesofauna parameters, $N$ = 42 for soil properties). Data were square-rooted or log transformed to fulfill the hypothesis of normality and homogeneity. We plotted scatter plots and conducted Pearson's correlation to examine the relationship among landscape trait (IS ratio and site area), soil property (pH, SOM, TN and soil total Zn, Cu, Cd, Pb, CPI), and soil mesofauna community parameter (abundance, richness, Shannon's index, and Pielou's index). After that, according to the result of Pearson's correlation, linear regression was used to determine the variation of each soil mesofauna parameter along each soil property and landscape trait. We used one-way ANOVA to examine the differences in landscape trait, soil property, and soil mesofauna parameter among the four ecosystem types with different urbanization intensities. Least significance difference (LSD) was used after the ANOVA to test the differences between any two ecosystem types. Pearson's correlation, one-way ANOVA, and regression analysis were conducted in SPSS 19.0 (SPSS, Chicago, IL, United States).

To visualize the soil mesofauna community pattern, we performed ordination on community composition with non-metric multidimensional scaling (NMDS). Chao method was

chosen because of the unbalanced replicates among ecosystem types (Anderson and Millar, 2004). To this end, environmental variables were fitted on this NMDS space. A permutational multivariate analysis of variance (PERMANOVA) was conducted to test the significance of each environmental variable. We also used PERMANOVA to quantitatively examine the difference in soil mesofauna community among ecosystem types using a Chao dissimilarity matrix. The PERMANOVA and NMDS were conducted using Vegan in R 3.6.1. Significance level was set at $\alpha = 0.050$.

# RESULTS

## Effects of Urban Soil Property Changes on Soil Mesofauna Abundance and Diversity

There were significant negative relationships between soil properties and soil mesofauna abundance/diversity (**Figure 2**). Total soil mesofauna abundance was negatively correlated with soil pH ($R^2 = 0.218$, $p = 0.001$) and heavy metal CPI ($R^2 = 0.092$, $p = 0.028$) across the 42 sites. Species richness also responded negatively with soil pH ($R^2 = 0.104$, $p = 0.021$) and CPI ($R^2 = 0.115$, $p = 0.028$). In addition, we found Shannon's index decreased as soil TN ($R^2 = 0.099$, $p = 0.042$) and Soil Pb concentration ($R^2 = 0.145$, $p = 0.007$) increased.

## Effects of Urban Landscape Changes on Soil Mesofauna Abundance, Diversity, and Soil Property

Impervious surface ratio was not significantly correlated with any soil mesofauna parameters (**Supplementary Table 3**). In contrast, both soil pH ($R^2 = 0.255$, $p < 0.001$) and soil total nitrogen ($R^2 = 0.180$, $p = 0.005$) were positively correlated with IS ratio (**Figure 3**). Heavy metal CPI also increased with IS ratio ($R^2 = 0.119$, $p = 0.026$). In addition, as the Pearson's correlation analysis showed, soil total Zn, Cu, and Cd were significantly positively correlated with IS ratio (**Supplementary Table 3**).

After excluding the sites belonging to rural forests and urban parks, soil mesofauna abundance was positively correlated with site area ($R^2 = 0.259$, $p = 0.002$) (**Figure 4**). Both soil pH ($R^2 = 0.288$, $p = 0.005$) and heavy metal CPI ($R^2 = 0.358$, $p = 0.002$) were negatively correlated with site area (**Figure 4**). In addition, soil mite and collembola abundance significantly increased with site area, while total soil Zn, Cu, and Cd were significantly negatively correlated with site area (**Supplementary Table 3**). There were no significant correlations between soil mesofauna diversity and site area (**Supplementary Table 3**).

## Soil Property, Landscape Trait, and Soil Mesofauna Abundance and Diversity in Rural Forest, Urban Forest, Urban Woodland, and Urban Park

All measured landscape and soil property variables varied significantly among the four ecosystem types (all $p < 0.031$), except the SOM and total soil Pb. Impervious surface ratio, site area, soil pH, TN, total soil Zn, Cu, Cd, and CPI increased from rural forest, urban forest, urban woodland, to urban park (**Table 2**).

Soil mesofauna abundance in urban forests was the largest in the four ecosystem types (**Figure 5**). Rural forest had the second largest soil mesofauna abundance. Soil mesofauna abundance in urban woodland were similar to those in urban parks, which were only about half of that in urban forests. Specifically, total soil mesofauna abundance in the four ecosystem types were 76,076 ± 10,848, 98,156 ± 9,299, 51,341 ± 5,748, and 50,768 ± 4,985 ind. $m^{-2}$, respectively. The total soil mesofauna abundance in urban forests was significantly higher than those in urban woodland ($p < 0.001$) and urban parks ($p < 0.001$), and 20% higher than that in rural forests ($p = 0.080$).

## Effects of Urbanization on Soil Mesofauna Community Structure

Differences in mesofauna community structure among sampling sites were visualized with a non-metric multidimensional scaling (NMDS) (**Figure 6**). In addition, soil mesofauna community structure among the four ecosystem types were significantly different ($p = 0.036$) (**Table 3**). Except for the difference between rural forest and urban forest, differences between any two ecosystem types were significant (all $p \leq 0.033$). The results of permutational multivariate analysis of variance showed that only soil total Pb concentration was significant in explaining the variation of soil mesofauna community structure ($R^2 = 0.174$, $p = 0.036$) (**Supplementary Table 4**).

# DISCUSSION

## Soil Property Regulated Soil Mesofauna Abundance and Diversity in Urban Soils

Most soil pH values in the study area were higher than those of natural forests in this region (**Supplementary Table 2**; Liu et al., 2010). It is well known that soil alkalization can induce destruction in soil physical structure, which may decrease soil mesofauna abundance and diversity. Less clear is why soil mesofauna abundance and diversity decreased with increased soil pH at a lower range in urban soils as in the present study. In natural grassland, decrease in soil pH from 7.57 to 4.76 depresses soil nematode abundance by decreasing soil base cation availability and soil microbial biomass (Chen et al., 2015). In a study on mineral-poor dry heathlands, an increase in soil pH from 3.50 to 4.13 under liming treatments alleviates P limitation, thus increasing micro-arthropod abundance (mite and collembola) (Siepel et al., 2018). In the city of Warsaw, an increase in soil pH associated with lower concentrations of potassium and phosphorus depressed some collembola genus, thus changing soil collembola community structure (Rzeszowski et al., 2017). These studies may indicate that, besides physical structure, the effects of changed soil pH on an urban soil mesofauna community could be mediated by soil nutrient availability.

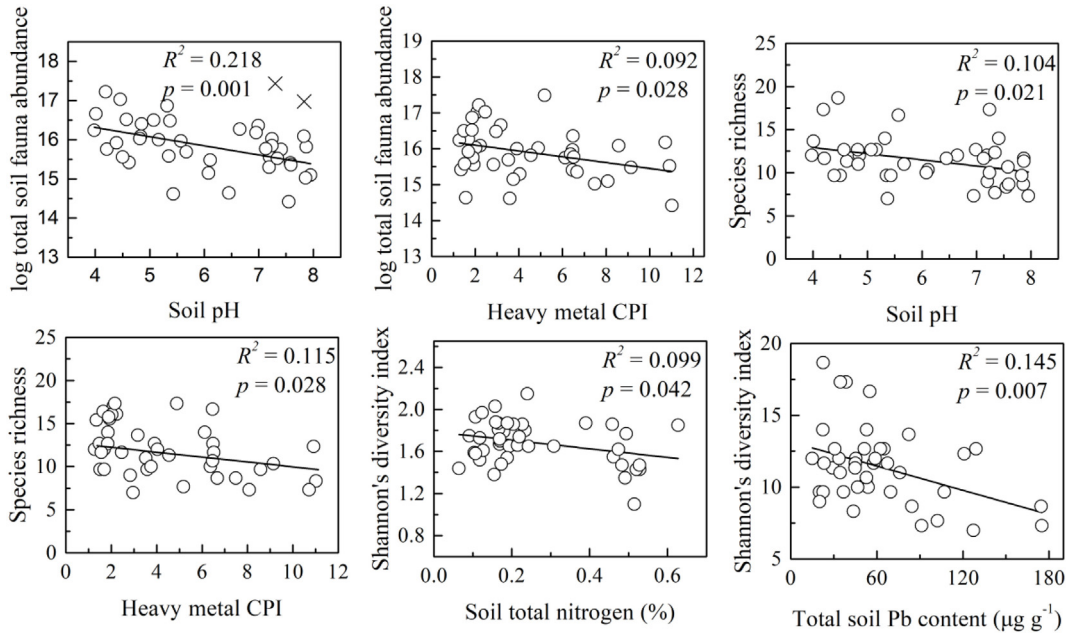


**FIGURE 2 |** Variations of soil mesofauna abundance and diversity with soil property. The cross-shape points are data points excluded in the linear regression. $R^2$ and $p$ were the fitness and significance of the linear regression models.

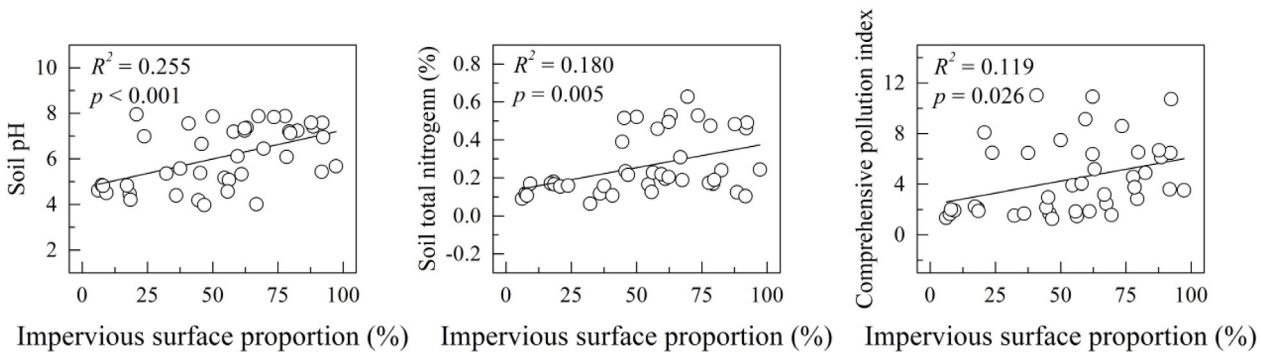


**FIGURE 3 |** Variations of soil property with impervious surface ratio. $R^2$ and $p$ were the fitness and significance of the linear regression models.

Compared to geogenic heavy metal concentrations in the city of Guangzhou (Zhou et al., 2009), most of the sampling sites had higher heavy metal contents (**Supplementary Table 2**). Toxicological evidence has been widely reported showing that high soil heavy metal concentration can induce soil fauna death in laboratory conditions, especially for collembola and enchytraeid (Crommentuijn et al., 1993; Didden and Rombke, 2001; Herbert et al., 2004). In urban field studies, there is still much controversy on whether accumulated heavy metal in soils could significantly inhibit soil mesofauna or change the community structure (Fountain and Hopkin, 2004; Fiera, 2009; Santorufo et al., 2012; Sterzynska et al., 2018). In ecosystems other than urban ecosystems, most of the controversy could result from the taxon-specific resistance to heavy metal toxicity. For example, in a grassland contaminated by Zn, while abundance of most soil fauna decreased, abundance of coleoptera and arachnida increased (Nahmani and Lavelle, 2002). In a shooting range with Pb and Sb 20 times higher than the surrounding soils, while total abundance and richness of soil mesofauna does not significantly change in the polluted soils, diplura and protura seem to benefit from heavy metal pollution, as they only occurred in soils of the shooting range (Migliorini et al., 2004). In the present field study, at family and higher taxonomic levels, our results suggested that heavy metals that accumulated in urban soils may be an important factor regulating soil mesofauna abundance, richness, diversity, and community structure. Moreover, our result indicated that comprehensive heavy metal pollution degree was more important in regulating soil mesofauna abundance and species richness than any single heavy metal, while soil Pb content seemed to be a key factor influencing soil mesofauna biodiversity

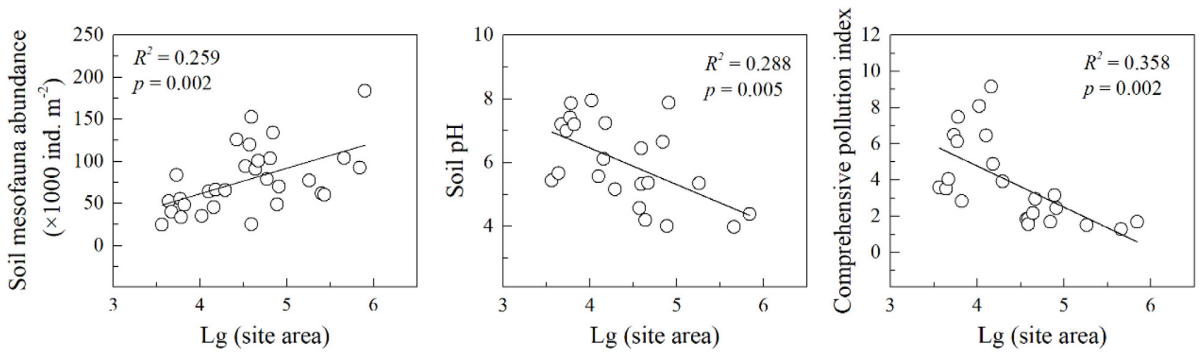


**FIGURE 4 |** Variations of soil mesofauna abundance and soil property with site area. $R^2$ and $p$ were the fitness and significance of the linear regression models. Note that sites that belonged to rural forest and urban park were excluded in the regressions. The "×" indicates the data point not included in the line regression analysis.

**TABLE 2 |** Mean values (SE) of landscape trait and soil property in rural forest (RF), urban forest (UF), urban woodland (UW), and urban park (UP).

| | RF | UF | UW | UP |
|---|---|---|---|---|
| IS ratio (%) | 14.3 (2.9)c | 55.8 (3.4)b | 61.8 (7.1)ab | 74.7 (5.0)a |
| Site area (ha) | – | 17.1 (5.9)a | 1.23 (0.4)b | – |
| pH | 4.61 (0.09)b | 5.33 (0.38)b | 6.65 (0.26)a | 7.32 (0.17)a |
| SOM (%) | 2.43 (0.34)a | 3.64 (0.93)a | 4.15 (0.69)a | 3.01 (0.78)a |
| TN (%) | 0.143 (0.014)c | 0.230 (0.037)bc | 0.284 (0.050)ab | 0.360 (0.053)a |
| Zn (μg/g) | 43.72 (7.91)c | 55.55 (9.79)c | 101.08 (13.88)b | 176.83 (22.01)a |
| Cu (μg/g) | 13.62 (2.42)b | 16.09 (2.49)b | 37.48 (6.36)a | 43.31 (7.21)a |
| Pb (μg/g) | 44.40 (6.81)a | 60.22 (8.98)a | 71.51 (14.55)a | 71.28 (8.84)a |
| Cd (μg/g) | 0.166 (0.044)c | 0.251 (0.051)bc | 0.362 (0.048)b | 0.542 (0.060)a |
| CPI | 2.45 (0.58)c | 3.62 (0.70)bc | 5.17 (0.64)b | 7.56 (0.83)a |

*The letters indicate significant differences at the level of α = 0.050 among different ecosystem types. IS ratio, impervious surface ratio; SOM, soil organic matter content; TN, soil total nitrogen content; Zn, Cu, Pb, Cd, soil total Zn, Cu, Pb and Cd concentration, respectively; CPI, heavy metal comprehensive index.*

and community structure. That is, soil mesofauna may respond differently to different soil heavy metal species/heavy metal index. Consistent with our result, Santorufo et al. (2012) found collembola abundance is negatively correlated with soil Pb and Zn concentration, but is not sensitive to Cu. A study on oribatida inhabiting leaf litter suggested that the oribatida community structure is regulated by litter Cd but not Zn, Pb, or Cu (Khalil et al., 2009).

## Landscape Change Effects on Soil Mesofauna Community Were Mostly Mediated by Soil Property

Impervious surface (IS) ratio is a direct and important index indicating urbanization intensity (Seress et al., 2014). In stream ecology studies, total impervious area is thought to be an excellent surrogate variable summarizing the effect of variables associated with urban stream syndrome (Walsh et al., 2005; King and Baker, 2010). However, the present study did not find a significant relationship between soil mesofauna community and IS in urban soils, as some previous studies did (Fogaca et al., 2013; Cordonnier et al., 2019). A study conducted in French cities showed that the dependence of ants on IS ratio varies with species identity and spatial scale studied (Fogaca et al., 2013). However, the relationships between soil mesofauna community and IS ratio at 200, 500, and 1000 m radiuses was not significant.

Decrease of habitat area is a consequence of habitat fragmentation due to urbanization. In this study, site area was positively correlated with soil mesofauna abundance. Contrasted to this result, soil collembola abundance in dry grassland does not show a significant relationship with site area (Querner et al., 2018). In a systematic literature review, Thakur et al. (2019) found only seven out of 12 studies on soil mesofauna provided support for the theory of island biogeography. Therefore, the question of whether the theory of island biogeography is applicable for soil mesofauna should be further investigated. Nevertheless, this study showed that higher site area could support higher soil mesofauna abundance in urban forests and urban woodland.

On the other hand, we found soil pH, TN, and CPI increased with IS ratio, indicating that IS ratio was a good indicator for these urban soil properties. Similar to IS ratio, site area was negatively correlated with soil pH and CPI. We concluded that habitat fragmentation due to urbanization may depress soil mesofauna abundance, however, to a larger extent, through influencing local soil property. This is in line with previous studies on aboveground arthropods in urban ecosystems (Smith and Schmitz, 2016; Kyro et al., 2018), which suggested local soil property is more important in regulating soil mesofauna communities than landscape trait.

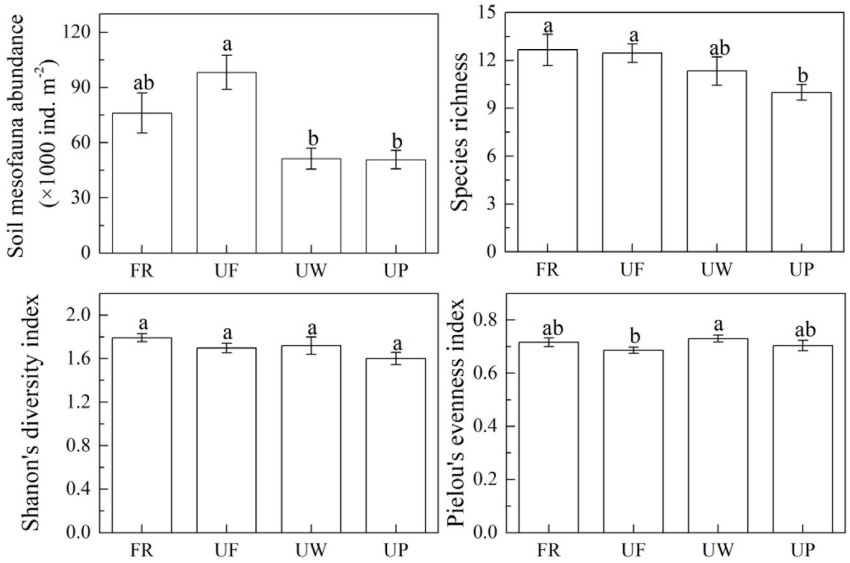


**FIGURE 5 |** Soil mesofauna community parameters in rural forest (RF), urban forest (UF), urban woodland (UW), and urban park (UP). Results are shown with means and standard errors. The letters indicate significant differences among the four ecosystem types at the level of $\alpha = 0.050$.

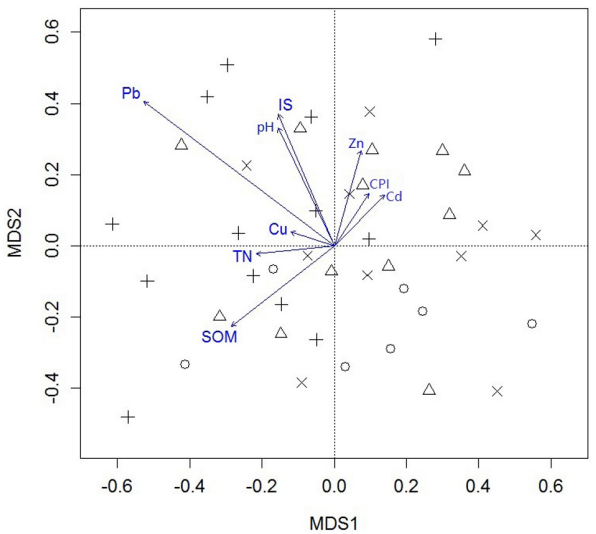


**FIGURE 6 |** Non-metric multidimensional scaling (NMDS) plot of soil mesofauna community structure (Stress = 0.250; method = Chao) and the environmental variables fitted on the NMDS spaces. IS ratio, impervious surface ratio; SOM, soil organic matter content; TN, soil total nitrogen content; Zn, Cu, Pb, Cd, soil total Zn, Cu, Pb, and Cd concentration, respectively; CPI, heavy metal comprehensive index. Circles: rural forests, triangles: urban forests, pluses: urban woodlands,corsses: urban parks.

**TABLE 3 |** Summary of permutational multivariate analysis of variance examining soil mesofauna community structure difference among rural forest (RF), urban forest (UF), urban woodland (UW), and urban park (UP).

| | RF | UF | UW | UP |
|---|---|---|---|---|
| FP | | $p = 0.588$ | $p = 0.018$ | $p = 0.015$ |
| | | $R^2 = 0.028$ | $R^2 = 0.175$ | $R^2 = 0.294$ |
| UF | | | $p = 0.006$ | $p = 0.033$ |
| | | | $R^2 = 0.191$ | $R^2 = 0.173$ |
| UW | | | | $p = 0.002$ |
| | | | | $R^2 = 0.265$ |
| UP | | | | |

## Soil Mesofauna Community Significantly Varied Among Rural Forest, Urban Forest, Urban Woodland, and Urban Park

Apart from the landscape and soil property changes, urbanization may affect soil mesofauna communities through species introduction, vegetation destruction, garden management practice, and so on (Bai et al., 2017). In the present study, 47 sites across Guangzhou City were classified into four ecosystem types with increasing urbanization intensity.

Located at hills, protected by laws, and far from urban buildings, the rural forest sites underwent the least anthropogenic disturbance. Consistent with the present study, many previous studies found a higher soil mesofauna richness in ecosystems with lower disturbance (Santorufo et al., 2012; Nagy et al., 2018; Lovei et al., 2019). Interestingly, urban forests had the highest soil mesofauna abundance. Urban forest sites were more isolated than rural forests, with an average IS ratio 290% higher. In addition, both soil pH and CPI, significantly and negatively correlated with soil mesofauna abundance, were higher in urban forests than those in rural forests. It seemed that we failed to define the specific disturbance features which overcame the negative effects of landscape and soil property changes and supported a more abundant soil mesofauna community. Nevertheless, consistent with some studies (e.g., Bogyo et al., 2015), our

study suggested that light urban disturbance could increase soil mesofauna abundance, which supported the intermediate disturbance hypothesis (IDH). However, some other studies found that soil fauna abundance and diversity decrease with increasing urbanization intensity (Gray, 1989; Nagy et al., 2018; Lovei et al., 2019), thus not supporting IDH. The contradiction could be attributed to taxa- or parameter-specified sensitivity to urban disturbance (Gonzalez et al., 2016; Yoccoz et al., 2018; Nielsen et al., 2019). As in the present study, the IDH predicted the soil mesofauna abundance but not the Shannon's diversity index or Pielou's evenness index in the four urban ecosystem types. In addition, most previous studies studied the urbanization effect on soil fauna by comparing several ecosystems along an urban - rural urbanization gradient (e.g., Santorufo et al., 2014; Nagy et al., 2018; Lovei et al., 2019), which might fail to capture a complete spectrum of environmental variation due to urbanization.

Typically, urban woodland and urban park sites were of small area (fragmented), adjacent to impervious pavements or buildings. As a result, they were subjected to serious anthropogenic disturbances. The stronger disturbances could cause substantial resource availability changes for soil mesofauna and, as the present study suggested, increases in soil pH and soil heavy metal concentration. These changes may account for the decrease of soil mesofauna abundance and change in soil mesofauna community structure in these two ecosystem types.

Besides abundance and community, soil mesofauna species richness substantially decreased in urban parks compared to rural forests. In addition, though urban woodland and urban parks had similar soil mesofauna abundance, they had distinct soil mesofauna community compositions, revealing that garden managements had significant and different effects on soil mesofauna from those in urban woodlands. Garden management practices, such as sanitation, tillage, and application of pesticide, can substantially alter resource availability and quality for soil mesofauna (Norton, 2011) and change soil physiochemical properties (Norton, 2011; Tresch et al., 2018, 2019), thus affecting soil mesofauna. In line with the present study, some previous studies found garden management decreased soil mesofauna abundance and diversity, thereby changing soil fauna community composition (Komarek et al., 2010; Dequiedt et al., 2011; Norton, 2011).

## DATA AVAILABILITY STATEMENT

The raw data supporting the conclusions of this manuscript will be made available by the authors, without undue reservation, to any qualified researcher.

## AUTHOR CONTRIBUTIONS

GX designed the experiments. SY and GX contributed to the field samples and data collection. XC and XL contributed to the soil mesofauna taxa identification. SY and XC analyzed the soil property. SY conducted the statistical analysis. JQ and XY conducted the GIS analysis. GX, FW, and SY wrote and revised the manuscript. All authors contributed to the article and approved the submitted version.

## FUNDING

This work was supported by the National Natural Science Foundation of China (42071061).

## SUPPLEMENTARY MATERIAL

The Supplementary Material for this article can be found online at: https://www.frontiersin.org/articles/10.3389/fevo.2020.546433/full#supplementary-material

## REFERENCES

Anderson, M. J., and Millar, R. B. (2004). Spatial variation and effects of habitat on temperate reef fish assemblages in northeastern New Zealand. *J. Exp. Mar. Biol. Ecol.* 305, 191–221. doi: 10.1016/j.jembe.2003.12.011

Asabere, S. B., Zeppenfeld, T., Nketia, K. A., and Sauer, D. (2018). Urbanization leads to increases in ph, carbonate, and soil organic matter stocks of arable soils of kumasi, ghana (West Africa). *Front. Environ. Sci.* 6:119. doi: 10.3389/fenvs.2018.00119

Bai, X., McPhearson, T., Cleugh, H., Nagendra, H., Tong, X., Zhu, T., et al. (2017). Linking urbanization and the environment: conceptual and empirical advances. *Ann. Rev. Environ. Resources* 42, 215–240. doi: 10.1146/annurev-environ-102016-061128

Bardgett, R. D., and van der Putten, W. H. (2014). Belowground biodiversity and ecosystem functioning. *Nature* 515, 505–511. doi: 10.1038/nature13855

Bogyo, D., Magura, T., Simon, E., and Tothmeresz, B. (2015). Millipede (Diplopoda) assemblages alter drastically by urbanisation. *Landscape Urban Plann.* 133, 118–126. doi: 10.1016/j.landurbplan.2014.09.014

Bolger, D. T., Suarez, A. V., Crooks, K. R., Morrison, S. A., and Case, T. J. (2000). Arthropods in urban habitat fragments in southern California: area, age, and edge effects. *Ecol. Appl.* 10, 1230–1248. doi: 10.1890/1051-0761(2000)010[1230:aiuhfi]2.0.co;2

Braaker, S., Ghazoul, J., Obrist, M. K., and Moretti, M. (2014). Habitat connectivity shapes urban arthropod communities: the key role of green roofs. *Ecology* 95, 1010–1021. doi: 10.1890/13-0705.1

Braaker, S., Obrist, M. K., Ghazoul, J., and Moretti, M. (2017). Habitat connectivity and local conditions shape taxonomic and functional diversity of arthropods on green roofs. *J. Animal Ecol.* 86, 521–531. doi: 10.1111/1365-2656.12648

Bradshaw, A. D. (2003). "Natural ecosystems in cities: a model for cities as ecosystems," in *Understanding Urban Ecosystems*, ed. A. R. Berkowitz (New York, NY: Springer), 76–94.

Burrow, C. (2018). Influence of connectivity & topsoil management practices of a constructed technosol on pedofauna colonization: a field study. *Appl. Soil Ecol.* 123, 416–419.

Chen, D., Lan, Z., Hu, S., and Bai, Y. (2015). Effects of nitrogen enrichment on belowground communities in grassland: relative role of soil nitrogen availability vs. *Soil acidification. Soil Biol. Biochem.* 89, 99–108. doi: 10.1016/j.soilbio.2015.06.028

Cordonnier, M., Gibert, C., Bellec, A., Kaufmann, B., and Escarguel, G. (2019). Multi-scale impacts of urbanization on species distribution within the genus

Tetramorium. *Landscape Ecol.* 34, 1937–1948. doi: 10.1007/s10980-019-00842-7

Crommentuijn, T., Brils, J., and Vanstraalen, N. M. (1993). Influence of cadmium on life-history characteristics of folsomia candida (Willem) in an artificial soil substrate. *Ecotoxicol. Environ. Saf.* 26, 216–227. doi: 10.1006/eesa.1993.1051

Dequiedt, S., Saby, N. P. A., Lelievre, M., Jolivet, C., Thioulouse, J., et al. (2011). Biogeographical patterns of soil molecular microbial biomass as influenced by soil characteristics and management. *Global Ecol. Biogeography* 20, 641–652. doi: 10.1111/j.1466-8238.2010.00628.x

Didden, W., and Rombke, J. (2001). Enchytraeids as indicator organisms for chemical stress in terrestrial ecosystems. *Ecotoxicol. Environ. Saf.* 50, 25–43. doi: 10.1006/eesa.2001.2075

Diego Ibanez-Alamo, J., Rubio, E., Benedetti, Y., and Morelli, F. (2017). Global loss of avian evolutionary uniqueness in urban areas. *Global Change Biol.* 23, 2990–2998. doi: 10.1111/gcb.13567

Faeth, S. H., Bang, C., and Saari, S. (2011). Urban biodiversity: patterns and mechanisms. *Ann. N. Y. Acad. Sci.* 1223, 69–81. doi: 10.1111/j.1749-6632.2010.05925.x

Fiera, C. (2009). Biodiversity of Collembola in urban soils and their use as bioindicators for pollution. *Pesquisa Agropecuaria Brasileira* 44, 868–873. doi: 10.1590/s0100-204x2009000800010

Fogaca, F. N. O., Gomes, L. C., and Higuti, J. (2013). Percentage of impervious surface soil as indicator of urbanization impacts in neotropical aquatic insects. *Neotropical Entomol.* 42, 483–491. doi: 10.1007/s13744-013-0155-z

Fountain, M. T., and Hopkin, S. P. (2004). Biodiversity of Collembola in urban soils and the use of Folsomia candida to assess soil 'quality'. *Ecotoxicology* 13, 555–572. doi: 10.1023/b:ectx.0000037192.70167.00

Ge, B., Mehring, A. S., and Levin, L. A. (2019). Urbanization alters belowground invertebrate community structure in semi-arid regions: a comparison of lawns, biofilters and sage scrub. *Landscape Urban Plann.* 192:103664. doi: 10.1016/j.landurbplan.2019.103664

Gilbert, O. L. (1989). *The Ecology of Urban Habitats*. London: Chapman & Hall.

Gonzalez, A., Cardinale, B. J., Allington, G. R. H., Byrnes, J., Endsley, K. A., et al. (2016). Estimating local biodiversity change: a critique of papers claiming no net loss of local diversity. *Ecology* 97, 1949–1960. doi: 10.1890/15-1759.1

Gray, J. S. (1989). Effects of environmental stress on species rich assemblages. *Biol. J. Linnean Soc.* 37, 19–32. doi: 10.1111/j.1095-8312.1989.tb02003.x

Herbert, I. N., Svendsen, C., Hankard, P. K., and Spurgeon, D. J. (2004). Comparison of instantaneous rate of population increase and critical-effect estimates in Folsomia candida exposed to four toxicants. *Ecotoxicol. Environ. Saf.* 57, 175–183. doi: 10.1016/s0147-6513(03)00033-2

Hruska, K. (2006). Notes on the evolution and organization of the urban ecosystem. *Urban Ecosystems* 9, 291–298. doi: 10.1007/s11252-006-0006-3

Jim, C. Y. (1998). Urban soil characteristics and limitations for landscape planting in Hong Kong. *Landscape Urban Plann.* 40, 235–249. doi: 10.1016/s0169-2046(97)00117-5

Joimel, S., Grard, B., Auclerc, A., Hedde, M., Le Doare, N., Salmon, S., et al. (2018). Are collembola "flying" onto green roofs? *Ecol. Eng.* 111, 117–124. doi: 10.1016/j.ecoleng.2017.12.002

Joimel, S., Schwartz, C., Hedde, M., Kiyota, S., Krogh, P. H., Nahmani, J., et al. (2017). Urban and industrial land uses have a higher soil biological quality than expected from physicochemical quality. *Sci. Total Environ.* 584, 614–621. doi: 10.1016/j.scitotenv.2017.01.086

Khalil, M. A., Janssens, T. K. S., Berg, M. P., and van Straalen, N. M. (2009). Identification of metal-responsive oribatid mites in a comparative survey of polluted soils. *Pedobiologia* 52, 207–221. doi: 10.1016/j.pedobi.2008.10.002

King, R. S., and Baker, M. E. (2010). Considerations for analyzing ecological community thresholds in response to anthropogenic environmental gradients. *J. North Am. Benthol. Soc.* 29, 998–1008. doi: 10.1899/09-144.1

Komarek, M., Cadkova, E., Chrastny, V., Bordas, F., and Bollinger, J. C. (2010). Contamination of vineyard soils with fungicides: a review of environmental and toxicological aspects. *Environ. Int.* 36, 138–151. doi: 10.1016/j.envint.2009.10.005

Kyro, K., Brenneisen, S., Kotze, D. J., Szallies, A., Gerner, M., and Lehvavirta, S. (2018). Local habitat characteristics have a stronger effect than the surrounding urban landscape on beetle communities on green roofs. *Urban Forestry Urban Greening* 29, 122–130. doi: 10.1016/j.ufug.2017.11.009

LaPoint, S., Balkenhol, N., Hale, J., Sadler, J., and van der Ree, R. (2015). Ecological connectivity research in urban areas. *Funct. Ecol.* 29, 868–878. doi: 10.1111/1365-2435.12489

Lepczyk, C. A., Aronson, M. F. J., Evans, K. L., Goddard, M. A., Lerman, S. B., et al. (2017). Biodiversity in the city: fundamental questions for understanding the ecology of urban green spaces for biodiversity conservation. *Bioscience* 67, 799–807. doi: 10.1093/biosci/bix079

Li, W.-X., Zhang, X.-X., Wu, B., Sun, S.-L., Chen, Y.-S., Pan, W.-Y., et al. (2008). A comparative analysis of environmental quality assessment methods for heavy metal-contaminated soils. *Pedosphere* 18, 344–352. doi: 10.1016/s1002-0160(08)60024-7

Liu, K.-H., Fang, Y.-T., Yu, F.-M., Liu, Q., Li, F.-R., and Peng, S.-L. (2010). Soil acidification in response to acid deposition in three subtropical forests of subtropical China. *Pedosphere* 20, 399–408. doi: 10.1016/s1002-0160(10)60029-x

Lovei, G. L., Horvath, R., Elek, Z., and Magura, T. (2019). Diversity and assemblage filtering in ground-dwelling spiders (Araneae) along an urbanisation gradient in Denmark. *Urban Ecosystems* 22, 345–353. doi: 10.1007/s11252-018-0819-x

Madej, G., and Kozub, M. (2014). Possibilities of using soil microarthropods, with emphasis on mites (Arachnida, Acari, Mesostigmata), in assessment of successional stages in a reclaimed coal mine dump (Pszów, S Poland). *Biol. Lett.* 51, 19–36. doi: 10.1515/biolet-2015-0003

Magura, T., Lövei, G. L., and Tóthmérész, B. (2010). Does urbanization decrease diversity in ground beetle (Carabidae) assemblages? *Global Ecol. Biogeography* 19, 16–26. doi: 10.1111/j.1466-8238.2009.00499.x

Mao, Q., Huang, G., Buyantuev, A., Wu, J., Luo, S., and Ma, K. (2014). Spatial heterogeneity of urban soils: the case of the Beijing metropolitan region. China. *Ecol. Process.* 3:23.

McIntyre, N. E., Rango, J., Fagan, W. F., and Faeth, S. H. (2001). Ground arthropod community structure in a heterogeneous urban environment. *Landscape Urban Plann.* 52, 257–274. doi: 10.1016/s0169-2046(00)00122-5

McKinney, M. L. (2006). Urbanization as a major cause of biotic homogenization. *Biol. Conserv.* 127, 247–260. doi: 10.1016/j.biocon.2005.09.005

McKinney, M. L. (2008). Effects of urbanization on species richness: a review of plants and animals. *Urban Ecosystems* 11, 161–176. doi: 10.1007/s11252-007-0045-4

Menta, C., Conti, F. D., Pinto, S., and Bodini, A. (2018). Soil biological quality index (QBS-ar): 15 years of application at global scale. *Ecol. Indicat.* 85, 773–780. doi: 10.1016/j.ecolind.2017.11.030

Migliorini, M., Pigino, G., Bianchi, N., Bernini, F., and Leonzio, C. (2004). The effects of heavy metal contamination on the soil arthropod community of a shooting range. *Environ. Pollut.* 129, 331–340. doi: 10.1016/j.envpol.2003.09.025

Milano, V., Maisto, G., Baldantoni, D., Bellino, A., Bernard, C., Croce, A., et al. (2018). The effect of urban park landscapes on soil Collembola diversity: a mediterranean case study. *Landscape Urban Plann.* 180, 135–147. doi: 10.1016/j.landurbplan.2018.08.008

Nagy, D. D., Magura, T., Horvath, R., Debnar, Z., and Tothmeresz, B. (2018). Arthropod assemblages and functional responses along an urbanization gradient: a trait-based multi-taxa approach. *Urban Forestry Urban Greening* 30, 157–168. doi: 10.1016/j.ufug.2018.01.002

Nahmani, J., and Lavelle, P. (2002). Effects of heavy metal pollution on soil macrofauna in a grassland of Northern France. *Eur. J. Soil Biol.* 38, 297–300. doi: 10.1016/s1164-5563(02)01169-x

Nielsen, T. F., Sand-Jensen, K., Dornelas, M., and Bruun, H. H. (2019). More is less: net gain in species richness, but biotic homogenization over 140 years. *Ecol. Lett.* 22, 1650–1657. doi: 10.1111/ele.13361

Norton, B. A. (2011). *The Sanitisation of Urban Ecosystems: Simplification of the Ground Layer in Eucalypt Woodlands and the Effects on Arthropod Communities*. Melbourne: University of Melbourne.

Parisi, V., Menta, C., Gardi, C., Jacomini, C., and Mozzanica, E. (2005). Microarthropod communities as a tool to assess soil quality and biodiversity: a new approach in Italy. *Agricult. Ecosystems Environ.* 105, 323–333. doi: 10.1016/j.agee.2004.02.002

Pielou, E. C. (1969). *An Introduction to Mathematical Ecology*. New York, NY: Wiley-Inter-science.

Pouyat, R., Groffman, P., Yesilonis, I., and Hernandez, L. (2002). Soil carbon pools and fluxes in urban ecosystems. *Environ. Pollut.* 116, S107–S118.

Pouyat, R. V., Yesilonis, I. D., Dombos, M., Szlavecz, K., Setala, H., Cilliers, S., et al. (2015). A global comparison of surface soil characteristics across five cities: a test of the urban ecosystem convergence hypothesis. *Soil Sci.* 180, 136–145. doi: 10.1097/ss.0000000000000125

Querner, P., Milasowszky, N., Zulka, K. P., Abensperg-Traun, M., Willner, W., Sauberer, N., et al. (2018). Habitat structure, quality and landscape predict species richness and communities of collembola in dry grasslands in Austria. *Insects* 9:81. doi: 10.3390/insects9030081

Rudisser, J., Tasser, E., Peham, T., Meyer, E., and Tappeiner, U. (2015). The dark side of biodiversity: spatial application of the biological soil quality indicator (BSQ). *Ecol. Indicat.* 53, 240–246. doi: 10.1016/j.ecolind.2015.02.006

Rzeszowski, K., Zadrozny, P., and Nicia, P. (2017). The effect of soil nutrient gradients on Collembola communities inhabiting typical urban green spaces. *Pedobiologia* 64, 15–24. doi: 10.1016/j.pedobi.2017.06.003

Santorufo, L., Cortet, J., Arena, C., Goudon, R., Rakoto, A., Morel, J. L., et al. (2014). An assessment of the influence of the urban environment on collembolan communities in soils using taxonomy- and trait-based approaches. *Appl. Soil Ecol.* 78, 48–56. doi: 10.1016/j.apsoil.2014.02.008

Santorufo, L., Van Gestel, C. A. M., Rocco, A., and Maisto, G. (2012). Soil invertebrates as bioindicators of urban soil quality. *Environ. Pollut.* 161, 57–63. doi: 10.1016/j.envpol.2011.09.042

Seress, G., Lipovits, A., Bokony, V., and Czuni, L. (2014). Quantifying the urban gradient: a practical method for broad measurements. *Landscape Urban Plann.* 131, 42–50. doi: 10.1016/j.landurbplan.2014.07.010

Shannon, C. E. (1948). A mathematical theory of communication. *Bell System Tech. J.* 27, 379–423.

Siepel, H., Vogels, J., Bobbink, R., Bijlsma, R. J., Jongejans, E., de Waal, R., et al. (2018). Continuous and cumulative acidification and N deposition induce P limitation of the micro-arthropod soil fauna of mineral-poor dry heathlands. *Soil Biol. Biochem.* 119, 128–134. doi: 10.1016/j.soilbio.2018.01.025

Smith, J. R., and Schmitz, O. J. (2016). Cascading ecological effects of landscape moderated arthropod diversity. *Oikos* 125, 1261–1272. doi: 10.1111/oik.02887

Song, Y.-S., Li, X.-W., Li, F., and Li, H.-M. (2015). Influence of different types of surface on the diversity of soil fauna in Beijing Olympic Park. *J. Appl. Ecol.* 26, 1130–1136.

Sterzynska, M., Nicia, P., Zadrozny, P., Fiera, C., Shrubovych, J., and Ulrich, W. (2018). Urban springtail species richness decreases with increasing air pollution. *Ecol. Indicat.* 94, 328–335. doi: 10.1016/j.ecolind.2018.06.063

Thakur, M. P., Phillips, H. R. P., Brose, U., De Vries, F. T., Lavelle, P., et al. (2019). Towards an integrative understanding of soil biodiversity. *Biol. Rev.* 95, 350–364.

Trammell, T. L. E., Pataki, D. E., Pouyat, R. V., Groffman, P. M., Rosier, C., Bettez, N., et al. (2020). Urban soil carbon and nitrogen converge at a continental scale. *Ecol. Monographs.* 90:e01401.

Tresch, S., Frey, D., Bayon, R.-C. L., Mäder, P., Stehle, B., Fliessbach, A., et al. (2019). Direct and indirect effects of urban gardening on aboveground and belowground diversity influencing soil multifunctionality. *Sci. Rep.* 9:9769.

Tresch, S., Moretti, M., Le Bayon, R. C., Mader, P., Zanetta, A., Frey, D., et al. (2018). A gardener's influence on urban soil quality. *Front. Environ. Sci.* 6:25. doi: 10.3389/fenvs.2018.00025

Walsh, C. J., Roy, A. H., Feminella, J. W., Cottingham, P. D., Groffman, P. M., and Morgan, R. P. (2005). The urban stream syndrome: current knowledge and the search for a cure. *J. North Am. Benthol. Soc.* 24, 706–723. doi: 10.1899/04-028.1

Wei, B., and Yang, L. (2010). A review of heavy metal contaminations in urban soils, urban road dusts and agricultural soils from China. *Microchem. J.* 94, 99–107. doi: 10.1016/j.microc.2009.09.014

Wolters, V. (2001). Biodiversity of soil animals and its function. *Eur. J. Soil Biol.* 37, 221–227. doi: 10.1016/s1164-5563(01)01088-3

Xie, T., Wang, M., Chen, W., and Uwizeyimana, H. (2018). Impacts of urbanization and landscape patterns on the earthworm communities in residential areas in Beijing. *Sci. Total Environ.* 626, 1261–1269. doi: 10.1016/j.scitotenv.2018.01.187

Yin, W. (1998). *Llustrated Handbook of Soil Animals in China*. Beijing: Science Press.

Yoccoz, N. G., Ellingsen, K. E., and Tveraa, T. (2018). Biodiversity may wax or wane depending on metrics or taxa. *Proc. Natl. Acad. Sci. U S A.* 115, 1681–1683. doi: 10.1073/pnas.1722626115

Zhou, W., Tang, J., and Guan, D. (2009). The distributive character and pollution assessment of heavy metals in urban soil of guangzhou. *ACta Scientiarum Naturalium Universitatis Sunyatseni* 48, 47–51.

**Conflict of Interest:** The authors declare that the research was conducted in the absence of any commercial or financial relationships that could be construed as a potential conflict of interest.

frontiers in Ecology and Evolution

ORIGINAL RESEARCH
published: 09 February 2021
doi: 10.3389/fevo.2020.540948

# The Effects of Multi-Scale Climate Variability on Biodiversity Patterns of Chinese Evergreen Broad-Leaved Woody Plants: Growth Form Matters

*Yue Xu[1,2†], Zehao Shen[2*†], Jinlong Zhang[3], Runguo Zang[1] and Youxu Jiang[1]*

*[1] Research Institute of Forest Ecology, Environment and Protection, Key Laboratory of Forest Ecology and Environment of National Forestry and Grassland Administration, Chinese Academy of Forestry, Beijing, China, [2] Institute of Ecology, the Key MOE Laboratory for Earth Surface Processes, Peking University, Beijing, China, [3] Flora Conservation Department, Kadoorie Farm and Botanic Garden, Hong Kong, China*

Large-scale patterns of species diversity are thought to be linked to contemporary climate variability and Quaternary glacial–interglacial climate change. For plants, growth forms integrate traits related to competition or migration capacity, which determine their abilities to deal with the climate variability they face. Evergreen broad-leaved woody plants (EBWPs) are major components of numerous biomes in the subtropical and tropical regions. Hence, incorporating phylogenetic (temporal) and biogeographic (spatial) approaches, we assessed the relative importance of short- and long-term climate variability for biodiversity patterns of different growth forms (i.e., tree, shrub, liana, and bamboo) in EBWPs. We used a dated phylogeny and the distribution records for 6,265 EBWP species which are naturally occurred in China, and computed the corrected weighted endemism, standardized phylogenetic diversity and net relatedness index for the four growth forms, respectively. Ordinary least squares linear regressions, spatial error simultaneous autoregressive models, partial regression and hierarchical variation partitioning were employed to estimate the explanatory power of contemporary climate variability and climate-change velocity from the Last Glacial Maximum to the present. Our results showed that short- and long-term climate variability play complementary role in the biogeographic patterns of Chinese EBWPs. The former had larger effects, but the legacy effects of past climate changes were also remarkable. There were also differences in the effects of historical and current climate among the four growth forms, which support growth forms as a critical plant trait in predicting vegetation response to climate change. Compared to the glacial-interglacial climate fluctuation, seasonality as a unique feature of mid-latitude monsoon climate played a dominant role in the diversification and distribution of EBWP species at the macroscale. The results indicated that the relative importance of climate variability at different temporal scales may relate to distinct mechanisms. To understand effects of future climate change on species distribution more thoroughly, climate conditions in different time scales should be incorporated.

**Keywords: biodiversity patterns, climate variability, evergreen broadleaved woody plants, multi-scale, temporal**

OPEN ACCESS

***Edited by:***
*Luciano Bosso, Università degli Studi di Napoli Federico II, Italy*

***Reviewed by:***
*Liy Mingyang, Nanjing Forestry University, China*
*Shunzhong Wang, Chinese Academy of Sciences, China*

****Correspondence:***
*Zehao Shen*
*shzh@urban.pku.edu.cn*

*† These authors have contributed equally to this work*

***Specialty section:***
*This article was submitted to Biogeography and Macroecology, a section of the journal Frontiers in Ecology and Evolution*

***Received:*** *06 March 2020*
***Accepted:*** *20 August 2020*
***Published:*** *09 February 2021*

***Citation:***
*Xu Y, Shen Z, Zhang J, Zang R and Jiang Y (2021) The Effects of Multi-Scale Climate Variability on Biodiversity Patterns of Chinese Evergreen Broad-Leaved Woody Plants: Growth Form Matters. Front. Ecol. Evol. 8:540948. doi: 10.3389/fevo.2020.540948*

## INTRODUCTION

The striking uneven distribution of global biodiversity across space and time has caused wide concerns of ecologists for two centuries (von Humboldt and Bonpland, 1807; Sandel et al., 2020). Despite a long history of studies, the underlying mechanisms of large−scale biodiversity patterns are not fully understood (Gaston, 2000; Lu et al., 2018). Specifically, a number of hypotheses relating to ecological, evolutionary and biogeographic processes have been proposed to explain the patterns along latitudinal gradient (Fine, 2015). While the overwhelming emphasis has been on diversity responses to average or extreme values of climate variables, increasing evidences indicate that climate variability may also play a deterministic or stochastic role in species persistence and biodiversity maintenance (Letten et al., 2013; Mohammadi et al., 2019; Zhang et al., 2019). It is widely detected that climate change causes major shifts in species distributions, reshuffling regional species composition (Parmesan and Yohe, 2003). Moreover, increasing extreme weather events arose from the altered climatic variability regimes, is urging ecologists to expand their purview beyond mean climate conditions (White et al., 2010). In this context, studying the influence of climate variability on biodiversity patterns is invaluable for insight into biodiversity conservation.

Biodiversity encompasses many aspects of biological complexity (Stevens and Tello, 2018). Comparison of taxonomic, ecological and phylogenetic diversity patterns clearly showed the multifaceted nature of biodiversity and incongruence across biodiversity dimensions (Smiley et al., 2020). Besides, climatic factors have different relationships with each dimension of biodiversity, and the variation provides opportunities to explore the mechanisms that underlie biodiversity patterns (Oliveira et al., 2016). Species endemism can reveal the limitation of a biological taxon to a specific geographical area, which is critical for understanding the distribution and evolution of regional flora (Myers et al., 2000; Feng et al., 2019). Phylogenetic diversity metrics reflect variation in species evolutionary history and may be better indicators of species vulnerability to climate change than is species richness (Cardinale et al., 2012; Srivastava et al., 2012). As a result, incorporating information of taxonomic, endemic and phylogenetic diversity distribution patterns may help to predict the change of biodiversity facing future climate scenarios, and to develop more effective approaches for long-term conservation (Burgio et al., 2019).

Different hypotheses have been proposed to relate climate variability with patterns of biodiversity. For example, climate stability hypothesis stipulates that areas subjected to more stable climate might accumulate more species over time (Fine, 2015). According to the Rapoport's rule, organisms in high latitudes need to form a broader physiological tolerance to cope with the stronger climate seasonality, and species were able to widen their climatic niches and become more widespread (Stevens, 1989). It is also recognized that high environmental variability can be harmful to species persistence because of reduced population growth rates and increased vulnerability to stochastic extinction (Boyce et al., 2006). In contrast, tropical regions with less change in climate conditions could promote speciation and buffer extinction (Kozak and Wiens, 2010). Despite the quantification and application of climate variability in ecology and biogeography studies, the ecological implications of existing metrics and related temporal scales have not been fully understood so far (Garcia et al., 2014). For example, climatic seasonality is a frequent environmental variability compared to the life span of perennial plant species that physiological and phenological adaptation are generally required to ensure species survival (Preston and Sandve, 2013). In contrast, the glacial-interglacial climate fluctuations occur in such a long temporal scale that plant species respond mainly by population migration and species range shifting (Svenning et al., 2015; Ma et al., 2016). It was reported that instability of short-term variables such as temperature annual range and seasonality were the most important environmental variables associated with plant endemism in Borneo (Raes et al., 2009). Recent studies have also identified long−term climate variability as an important factor shaping plant species diversity and phylogenetic structure (Feng et al., 2016; Ma et al., 2016; Sandel et al., 2020). Although the multi-scale temporal variability of climate are presumed to convey complementary information, representing different threats and opportunities for biodiversity (Garcia et al., 2014), there is no consensus whether historical climate fluctuation or current climate seasonality will be more important for explaining modern biodiversity patterns.

Related studies have rarely examined the different responses of biodiversity to climate variability among growth forms of plants. Plant growth-form is characterized by morphological and physiological attributes of plant species that enable them to respond to environmental (e.g., climatic) stresses (Shmida and Burgess, 1988). Empirical studies indicate that there is no consistent pattern in the diversity distribution for different life-form categories (Sánchez-González and López-Mata, 2005; Desalegn and Beierkuhnlein, 2010). Plant species of different growth forms generally differ in life span, dispersal capacities, nutrient cycling, and physiological regulation, evolution rate, and environmental tolerance (Smith and Donoghue, 2008; Way and Oren, 2010; Chen et al., 2013; Kubota et al., 2017; Beckman et al., 2018). These differences of ecological strategies among growth forms may have in turn distinctly constrained plant species in their capacities of responding to climate changes (Valladares et al., 2000). For example, climate variability has been found to exert stronger effects on groups with poorer dispersal abilities (Feng et al., 2016). Thus, growth-form provides critical information for exploring plant diversity patterns and understanding their relationship with climate variability.

Evergreen broad-leaved woody plants (EBWPs) widely distribute all over the world, supporting the persistence of other biodiversity components in forest, shrubland and savanna ecosystems (DeFries et al., 2000; Xu et al., 2017). EBWPs are of great importance for biodiversity conservation. Most of the 35 global hotspots of biodiversity are located in tropical and subtropical regions dominated by EBWPs (Mittermeier et al., 2011). As one of the most important vegetation types, subtropical evergreen broadleaved forests represent the natural vegetation in approximately 25% of terrestrial area in China (Shen et al., 2012).

Subjected to severe human disturbance, most of the primary subtropical evergreen broadleaved forests have degraded to secondary forests and shrubs (Song et al., 2013). Understanding the factors shaping species distributions of EBWPs in China could shed light on predicting possible future changes in plant species distributions and assist in generating more efficient conservation and management strategies.

In the present study, we addressed the question of how short- and long-term climate variabilities shape biogeographic patterns of Chinese EBWPs. In particular, we assessed how the present distribution of species endemism and phylogenetic structure are affected by (a) contemporary climate seasonality and, (b) climate fluctuation between the Last Glacial Maximum and present. According to their morphological features, we classified 6,265 EBWP species into four growth forms: trees, shrubs, lianas and bamboos, regarding their differences in regeneration, competition or migration capacity. Specifically, we tested the following three hypotheses: (1) The relative importance of climate variability on EBWPs' biodiversity patterns may vary between time scales. (2) Endemism as an integrative metrics of species range should be more responsive to historical climate change, while the environmental filtering effect of climate seasonality would dominate the phylogenetic diversity and phylogenetic structure of plant assemblages. (3) The extent that biodiversity patterns of different growth forms influenced by climate variability metrics should be affected by their life-history strategies.

# MATERIALS AND METHODS

## Data Set

The county-level species distribution data of EBWPs were collected from the "Atlas of woody plants in China: Distribution and climate" (Fang et al., 2011), which contains 11,405 woody species and is the most complete atlas of native woody plants in China until present. To eliminate the potential bias of unequal area on subsequent analyses, we converted the county distribution of each species into a grid map at a resolution of 50 km × 50 km. Grid cells with more than 50% of land area located within China's border were included in this study. We further supplemented the species distribution data using field records of 1,494 forest plots on 63 mountains across China (Shen et al., 2012). The Plant List[1] was used to standardize the botanical nomenclature of the species in this database. Growth form information (tree, shrub, liana or bamboo) of each species were gathered from Flora of China,[2] and resulted in a total of 1,925 trees, 3,320 shrubs, 550 lianas, and 470 bamboos (the species list and growth form of each species is available in **Supplementary Materials** of this manuscript).

Comparative studies showed that values of phylogenetic diversity calculated based on phylogenies derived from common synthesis trees are correlated significantly with those of purpose-built phylogenies (Li et al., 2019). Therefore, we did not build phylogenetic trees specifically based on gene sequence data. Instead, we used a recently published, the currently largest dated mega phylogeny for seed plants, constructed using 79,881 taxa in GenBank with a backbone tree provided by Open Tree of Life version 9.1 (GBOTB), as a backbone to generate a phylogeny for the Chinese EBWPs. We used the R package V. PhyloMaker (Jin and Qian, 2019) to generate species-level phylogenetic trees of different growth forms in EBWPs.

## Biogeographic Indices

Here we adopted three common biodiversity metrics—corrected weighted endemism (CWE), standardized phylogenetic diversity (SPD) and net relatedness index (NRI) — to quantify the multi-facetted biodiversity patterns.

In order to avoid high correlations between species richness and endemism due to the sampling effect caused by species numbers, we used CWE to measure species endemism. CWE emphasizes areas incorporating a high proportion of range-restricted species, where are not necessarily species-rich. CWE is calculated with the following formula (Crisp et al., 2001):

$$CWE = \sum_{j=1}^{S} \frac{1}{R_j} / S_i \times 100$$

where $S_i$ is the number of taxa in the $i$th grid cell, $R_j$ is the total grid cell number of the $j$th species.

To quantify the relationship between phylogenetic diversity (PD) and species richness, we used a randomization-adjusted method to calculate SPD. Specifically, we calculated PD for each grid cell using a randomly selected sample of EBWPs of identical species number, from the species pool of China, and this step was repeated for 1,000 times to estimate a mean of the randomized PD values, and then calculated SPD with the following formula (Kembel et al., 2010):

$$SPD = (\mathrm{PD}_{\mathrm{observed}} - \mathrm{meanPD}_{\mathrm{randomized}} / \mathrm{sdPD}_{\mathrm{randomized}}$$

where, $\mathrm{PD}_{\mathrm{observed}}$ refers to the observed PD, mean $\mathrm{PD}_{\mathrm{randomized}}$ refers to the expected PD of the randomized sample assemblages of EWBPs ($n$ = 1000), and $\mathrm{sdPD}_{\mathrm{randomized}}$ refers to the standard deviation of the PD for the randomized assemblages.

NRI estimates the mean pairwise phylogenetic relatedness in an assemblage. We calculated NRI based on the mean phylogenetic distance (MPD) for each grid cell using the following formula (Webb et al., 2002):

$$NRI = (\mathrm{MPD}_{\mathrm{randomized}} - \mathrm{meanMPD}_{\mathrm{observed}} / \mathrm{sdMPD}_{\mathrm{randomized}}$$

where, $\mathrm{MPD}_{\mathrm{observed}}$ refers to the observed MPD, $\mathrm{MPD}_{\mathrm{randomized}}$ refers to the expected MPD of randomly generated assemblages, and $\mathrm{sdMPD}_{\mathrm{randomized}}$ refers to the standard deviation of 1000 iterations of $\mathrm{MPD}_{\mathrm{randomized}}$. A positive NRI value indicates that species are more closely related than expected in a random sample, and thus corresponds to phylogenetic clustering. By contrary, a negative NRI corresponds to phylogenetic evenness or overdispersion.

The value frequency distributions were calculated to detect the normality of the three biogeographic indices (**Figure 1**). Since

[1] www.theplantlist.org

[2] http://www.efloras.org/

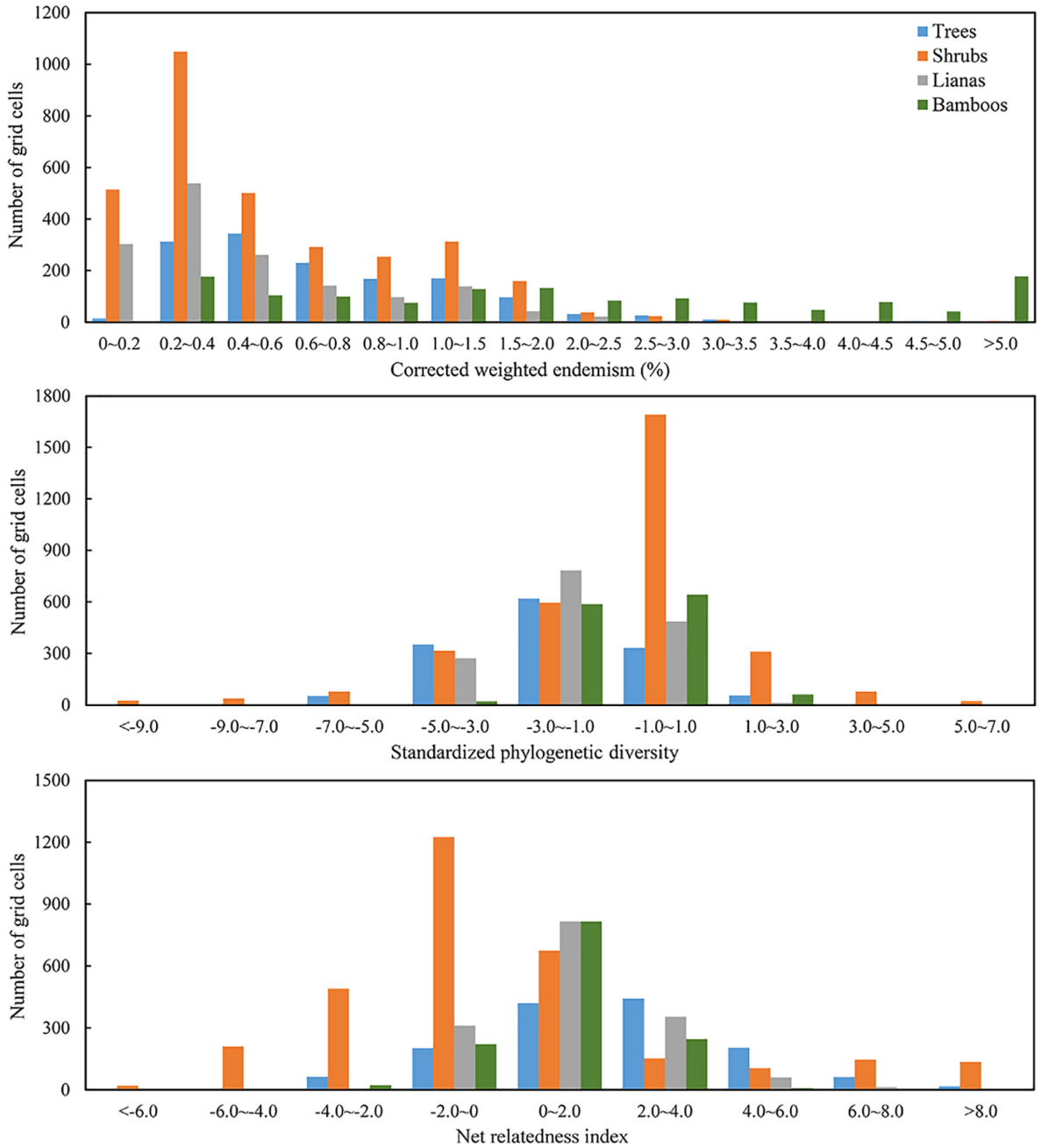


**FIGURE 1 |** Frequency distribution histogram of corrected weighted endemism (CWE), standardized phylogenetic diversity (SPD), and net relatedness index (NRI) for trees, shrubs, lianas and bamboos of evergreen broad-leaved woody plant species (EBWPs) within the grids of 50 km × 50 km resolution in China.

CWE for EWBPs in four growth-forms were prominently left-skewed, it was log-transformed in the following statistics. SPD and NRI were calculated using the R package "picante." The calculation of SPD and NRI for distinct growth forms (tree, shrub, liana and bamboo) followed the above procedure.

## Climate Change Variables

Variability in climate conditions was initially considered at two time-scales: short-term (contemporary seasonality) and long-term (glacial-interglacial fluctuation). To estimate the effects of contemporary climate variability on the biogeographic pattern of EBWP species, we chose two variables to represent the short-term climate variability, i.e., annual temperature range (ATR); and precipitation seasonality (PSN).

To test the effects of long-term climate variability, we applied the climate-change velocity for mean annual temperature (MATV) and mean annual precipitation (MAPV) from the Last Glacial Maximum (LGM, c. 21 ka) to the present

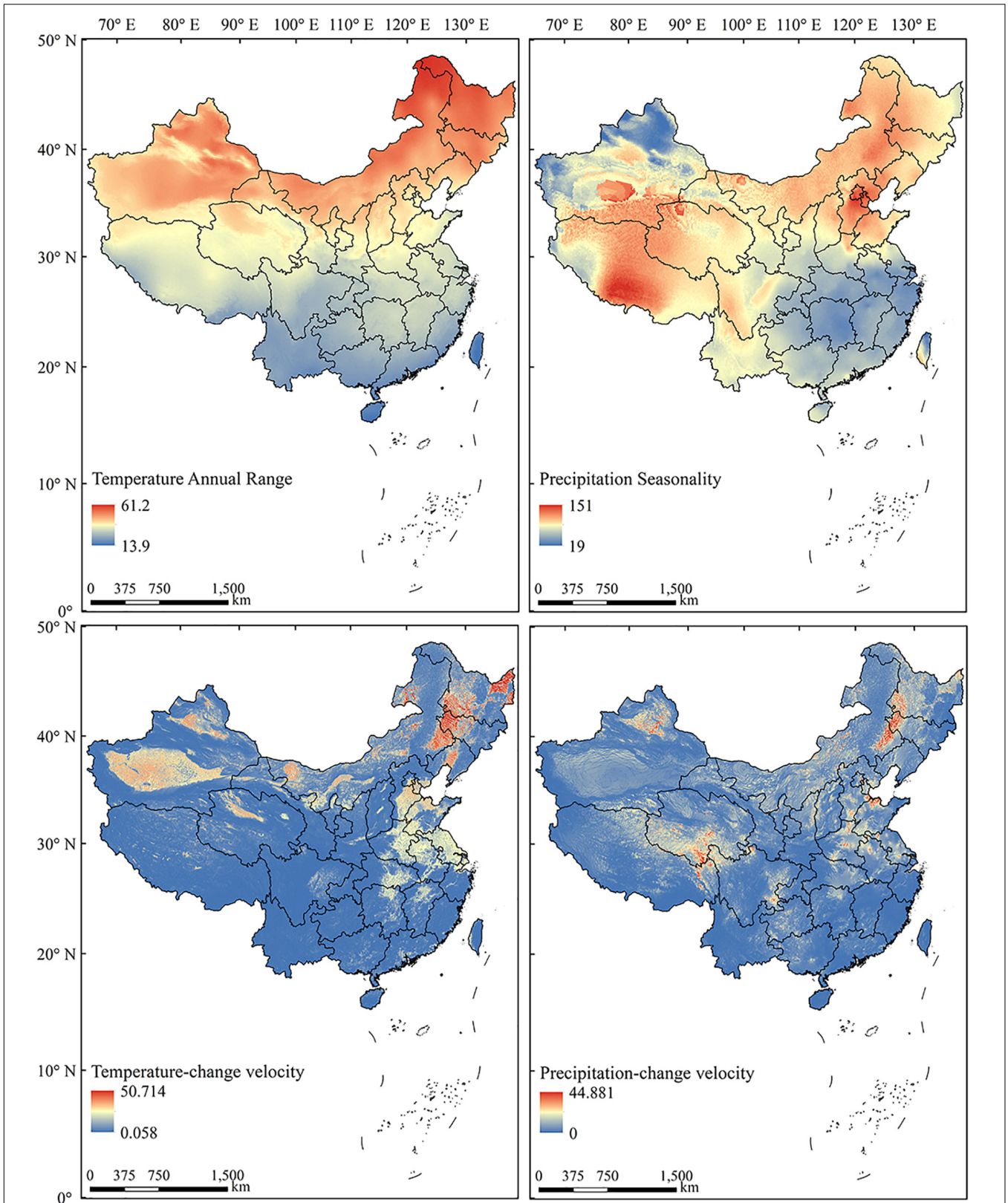


**FIGURE 2 |** The spatial patterns of current (1970–2000) annual temperature range, precipitation seasonality, and historical (LGM to present) temperature-change velocity and precipitation-change velocity in China.

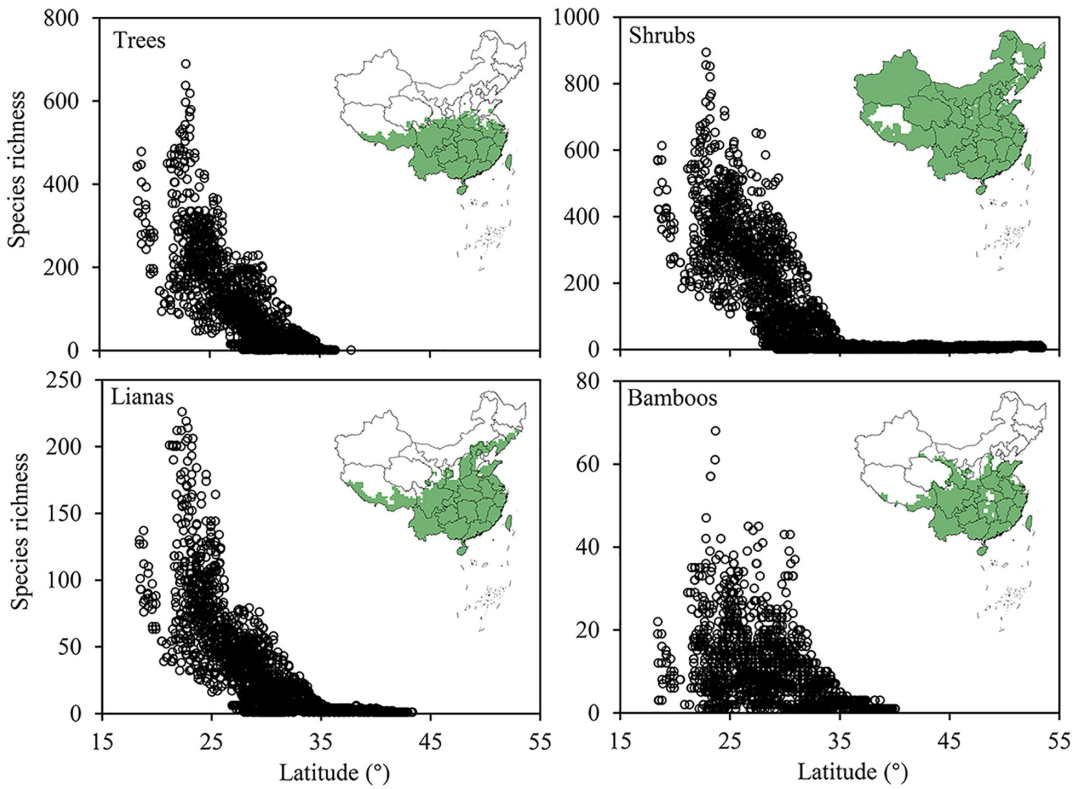


**FIGURE 3 |** The spatial patterns of species richness of the four growth forms (i.e., tree, shrub, liana, and bamboo) of evergreen broad-leaved woody plants (EBWPs) in China. Empty areas indicate the absence of EBWPs.

(Sandel et al., 2011). Climate-change velocity represents the local rate of displacement of climate conditions along Earth's surface, and is defined as the ratio of temporal vs spatial gradients of climate (Loarie et al., 2009). Implementation of the four climate variability metrics nationwide revealed that each characterized a distinct pattern (**Figure 2**).

Current (1970–2000) and LGM climate data were downloaded on October 25, 2019 from the WorldClim v2.0 database[3] at a spatial resolution of 1 km × 1 km (Fick and Hijmans, 2017). Because of the uncertainty of past climatic models, we used the average value of three available LGM simulations based on the CCSM4 (Community Climate System Model version 4) models, MPI-ESM−P (Max-Planck-Institute Earth System Model) and MIROC-ESM (The Earth system model, Model for Interdisciplinary Research on Climate-Earth system model) (Xu et al., 2019).

## Data Analysis

NRI cannot be calculated with less than two species in each grid cell. Therefore, after deleting grids with a land area smaller than half of the grid cell (i.e., 1250 km$^2$), grid cells containing fewer than two EBWP species were also excluded from the statistical analyses. Based on the value frequency distribution, MATV and MAPV were log-transformed to improve the normality of model residuals. Afterward, we standardized all variables to make the regression coefficients comparable.

Firstly, we performed ordinary least squares (OLS) linear regressions to explore the bivariate relationships between CWE, SPD, NRI and each explanatory variable. To account for spatial autocorrelation in the residuals of OLS models which may bias parameter estimation, we also used spatial error simultaneous autoregression (SAR) models for single variable analyses. We used a partial regression method (Legendre and Legendre, 1998) to partition the contributions of contemporary climate variability and Quaternary glacial–interglacial climate change to the spatial variation of CWE, SPD, and NRI for each growth form, respectively. Moreover, we used a Hierarchical Partitioning (HP) method to compare the independent contributions of each environmental variable to the variation in the spatial distributions of CWE, SPD, and NRI of the four growth forms, respectively. The method resolves the collinearity problems among variables through comparing all possible models fitted with all subsets of explanatory variables to estimate the independent effect of each variable (Olea et al., 2010). SAR modeling and related OLS modeling were implemented using the open macroecological software "SAM 4.0" ([4], Rangel et al., 2010). Partial regressions were conducted in R 3.6.2 with the "vegan"

[3]http://www.worldclim.org

[4]http://www.ecoevol.ufg.br/sam/

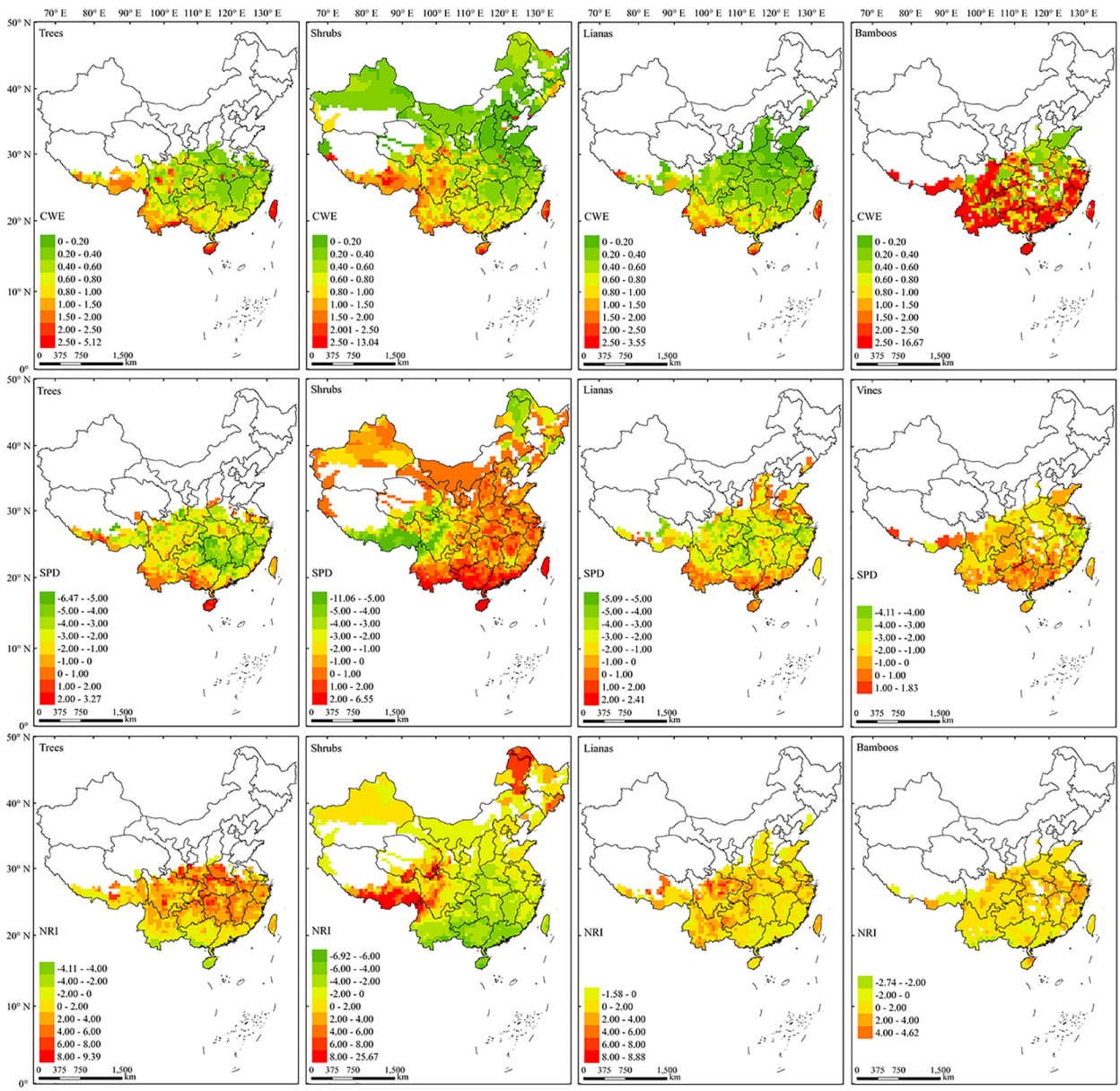


**FIGURE 4 |** The spatial patterns of CWE (up), SPD (middle), and NRI (low) of the four growth forms of EBWPs in China. Empty areas are those with less than two species of EBWP recorded in one grid cell.

package (Oksanen et al., 2010), and HP was performed with the "hier.part" package (Walsh and Mac Nally, 2008).

# RESULTS

## Geographic Patterns of CWE, SPD, and NRI for EBWPs

The evergreen broadleaved tree, shrub, liana and bamboo species distributed in 33.7, 86.6, 40.5, and 36.7% of all grid cells, respectively. Shrub species in all have a much broader distribution range, covering most area across China, while trees, lianas and bamboos showed comparable distribution ranges, mostly restricted to the tropic and subtropic regions south of 30°N. Within the subtropic-tropic region, the latitudinal gradient of species richness is prominent for trees, shrubs and liana, but not for bamboos (**Figure 3**).

There was no clear latitudinal gradient for the CWE of EBWPs (**Figure 4**, up). Generally, the regions with high endemism value distributed more to the southwestern than the eastern part of China for three growth-forms other than bamboo. Several endemism centers of EBWPs for trees, shrubs and lianas emerged, most in the Eastern Himalaya and the Hengduan Mountain Ranges (EHHMRs), southwest border regions, Hainan Island and

Taiwan Island. Bamboos extended to the mountains of North China with low CWE values. While in the south of 30°N, CWE of bamboos was generally high except for the plain regions along the Yangtze River in the northern part.

For each growth form, the high SPD values generally concentrated in the tropical area of South and Southwest China (**Figure 4**, middle). For trees, SPD was lower in the eastern part than that in the western part of subtropical region. For shrubs, there were two regions with obvious low SPD values, i.e., the Greater Hing'an Mountains (GHMs) in Northeast China, and the EHHMRs in Southwest China. Lianas generally had much lower SPD value in subtropical than in tropical areas. Meanwhile, the SPD value of bamboos was more homogeneous across the range of bamboos, although higher values located more to the southern subtropical region and the eastern Himalaya.

With respect to NRI (**Figure 4**, bottom), evergreen broad-leaved trees exhibited strong phylogenetic overdispersion in the tropics, while tended to be clustering in the extratropical region and reached the highest clustering in the northern boundary of their distribution. Shrubs revealed distinct NRI pattern, with overdispersion in the broad tropic-subtropic area while strongly clustered in the EHHMRs and GHMs. Lianas and bamboos were mostly phylogenetic clustering across their distribution ranges, with phylogenetic random or overdispersion patches scattered mainly in the southern tropic regions.

## Influence of Climate Variability on Biodiversity Patterns

Corrected weighted endemism of all EBWPs had a negative power associated with ATR, MATV, and MATP, but the relationship with PSN appeared much weaker and showed a rough triangle shape, with highest CWE corresponding to middle values of PSN. These relationships similarly applied to all four growth forms of EWBPs (**Supplementary Figure S1a**), indicating that a lower endemism of EWBPs can resulted from either larger current temperature seasonality or faster climate velocities.

Non-linear relationships were generally shown between climate variability indices and SPD of EBWPs (**Supplementary Figure S1b**). Specifically, along the gradient of ATR, a negative trend of SPD (when ATR < 30) was followed by a random pattern generally applicable for four growth-forms. The relationships between SPD and PSN were all complex and unclear. Whereas, both MATV and MAPV had a generally triangle relationship with SPD, i.e., largest and lest SPD values occurred at the lowest climate velocity, and high climate velocities corresponded to SPD values around zero.

Likewise, the effect of climate variability on NRI varied substantially across climate indices and growth forms (**Supplementary Figure S1c**). A triangle pattern generally applied to the relationship between NRI and climate velocity (MATV and MAPV) for four growth forms of EBWPs. NRI increased with ATR (when ATR < 30) and then roughly fluctuated around zero, while the variability of NRI on the gradient of PSN were less clear for different growth forms.

The climate variability factors considered here accounted for 0∼52.2, and 5.4∼68.3% of variance in geographical patterns of CWE by OLS and SAR models, respectively (**Table 1**). The $R^2$ values were mostly lower for moisture than temperature index. ATR generally explained the most variations in CWE, while PSN accounted for the least variance in CWE of shrubs, lianas and bamboos.

The variability of SPD and NRI were accounted for by single climate variables at much lower percentages in general, i.e., 0∼14.2 and 2.3∼27.5% by OLS and SAR models for SPD, and 0∼23.5 and 4.7∼71.0% by OLS and SAR models for NRI (**Table 1**). ATR was negatively associated with SPD and positively associated with NRI across growth forms. PSN had inconsistent relationship with SPD and NRI across growth forms. For MATV and MAPV, OLS models were mostly insignificant, while SAR models provided some explanatory powers.

## Contributions of Current vs Historical, Temperature vs Moisture Variability

The total climate variability could account for considerable percentages of variance in the spatial patterns of CWE, i.e., 51.5, 48.0, 62.0, and 37.2% for trees, shrubs, lianas and bamboos, respectively (**Figure 5**). However, the explanatory power of climate variability for SPD (6.6∼32.9%) and NRI (9.3∼33.8%) were much lower. The effect of climate variability on biogeographic patterns of EBWPs varied substantially across growth forms. Climate variability had the highest explanatory power on CWE for lianas, and the highest explanatory power on SPD and NRI for trees.

Contemporary climate seasonality overwhelmed historical climate velocities in affecting biogeographic variables for trees of EBWPs. For shrubs and bamboos, the two aspects showed comparable effects on CWE and SPD, but stronger effects of current climate variability revealed for NRI. For lianas, climate seasonality dominated CWE, while climate variability at two temporal scales were comparable for SPD and NRI. Moreover, the current climate seasonality and historical climate velocity had consistently strong joint effects on the geographic pattern of CWE for all growth types. Whereas, the effect of contemporary climate seasonality and that of long-term glacial-interglacial cycle were almost independent of each other for SPD and NRI.

On the other hand, the effects of temperature variability at different temporal scales (i.e., ATR and MATV) were generally stronger than those of moisture variability (i.e., PSN and MAPV) for CWE of four growth forms (**Table 1** and **Supplementary Figure S2**). In contrast, the contemporary precipitation seasonality was more important than temperature range for SPD and NRI, while temperature-change velocity was more important than precipitation-change velocity.

# DISCUSSION

## Importance of Climate Variability for Biogeographic Patterns

Temporal climatic variability is increasingly recognized as a critical determinant of biogeographic patterns (Guo and Werger,

**TABLE 1 |** R-squares of single climate variable of the ordinary least squares linear regressions model (OLS) and simultaneously autoregressive model (SAR) for predicting spatial patterns of corrected weighted endemism (CWE), standardized phylogenetic diversity (SPD) and net relatedness index (NRI) of tree, shrub, liana and bamboo EBWPs.

| Index | Climatechange | Trees ($n$ = 1283) | | Shrubs ($n$ = 2870) | | Lianas ($n$ = 1410) | | Bamboos ($n$ = 1209) | |
|---|---|---|---|---|---|---|---|---|---|
| | | $R^2_{OLS}$ | $R^2_{SAR}$ | $R^2_{OLS}$ | $R^2_{SAR}$ | $R^2_{OLS}$ | $R^2_{SAR}$ | $R^2_{OLS}$ | $R^2_{SAR}$ |
| CWE | ATR | (–)0.387*** | 0.499 | (–)0.341*** | 0.419 | (–)0.522*** | 0.458 | (–)0.303*** | 0.323 |
| | PSN | 0.180*** | 0.247 | (–)0.015*** | 0.118 | 0.005* | 0.461 | – | 0.054 |
| | MATV | (–)0.221*** | 0.312 | (–)0.375*** | 0.429 | (–)0.282*** | 0.683 | (–)0.230*** | 0.275 |
| | MAPV | (–)0.076*** | 0.222 | (–)0.160*** | 0.174 | (–)0.186*** | 0.596 | (–)0.179*** | 0.202 |
| SPD | ATR | (–)0.128*** | 0.245 | (–)0.014*** | 0.045 | – | 0.275 | (–)0.026*** | 0.039 |
| | PSN | 0.142*** | 0.206 | (–)0.077*** | 0.085 | 0.030*** | 0.226 | 0.030*** | 0.033 |
| | MATV | – | 0.195 | 0.054*** | 0.082 | 0.034*** | 0.215 | (–)0.008** | 0.027 |
| | MAPV | – | 0.192 | – | 0.034 | – | 0.226 | – | 0.023 |
| NRI | ATR | 0.235*** | 0.710 | 0.049*** | 0.076 | (–)0.004* | 0.071 | 0.051*** | 0.093 |
| | PSN | (–)0.076*** | 0.154 | 0.145*** | 0.141 | 0.036*** | 0.068 | (–)0.109*** | 0.117 |
| | MATV | – | 0.153 | (–)0.009*** | 0.151 | (–)0.056*** | 0.059 | 0.012*** | 0.053 |
| | MAPV | 0.009*** | 0.144 | 0.003* | 0.056 | – | 0.047 | – | 0.048 |

*ATR, annual temperature range; PSN, precipitation seasonality; MATV, temperature–change velocity since Last Glacial Maximum; MAPV, precipitation-change velocity since Last Glacial Maximum; slash indicate insignificant relationship; (–), negative relationship; star indicates level of significance, *p < 0.05; **p < 0.01; ***p < 0.001.*

2010; Letten et al., 2013; Irl et al., 2015; Ma et al., 2016). Seasonal and interannual climate variability were frequently selected among the predictors in explaining variation of relative dominance of a particular biological assemblage (Gray et al., 2006; Engemann et al., 2016). Species richness or endemism at different scales were also found to be strongly affected by paleoclimate changes (Jansson, 2003; Feng et al., 2016; Xu et al., 2019). In the meantime, species in unstable environments tend to be more phylogenetically clustered, as Patrick and Stevens (2016) argued, because species with narrow ranges were generally limited by dispersal capacity and more easily whipped out by interannual climate variability, indicating an interdependent relationship among different mechanisms. However, which of the biogeographic patterns, i.e., diversity, endemism and phylogenetic structure, were more suspect to climate variability, and how do different mechanisms contribute to the patterns, remain unresolved.

This study simultaneously assessed the importance of climate variability on patterns of three biogeographic diversity indices for EBWPs. The results revealed that the influence of temporal climate variability is more important for species endemism than for phylogenetic diversity and structure of EBWPs in China. And the current climate seasonality had a greater or at least equivalent impact than the Quaternary glacial-interglacial climate changes. Meanwhile, energy dominated the effect of climate variability on endemism while moisture variability was generally more important for SPD and NRI patterns.

Although this study focused on climate variability for biogeographic patterns, additional abiotic factors such as mean resource availability and biotic interactions such as competition most probably play important roles as well. As shown by our results, there is no reason to claim that either short- or long-term climate variability or a combination of them adequately account for geographic variations of EBWPs biodiversity. The geographical variance explained is relatively low especially for the phylogenetic structure, in spite of the statistically significant relationships. In other words, those models do not explain biodiversity patterns well enough, which most likely caused by omission of key variables driving biodiversity.

## Stronger Effects of Climate Variability on Endemism Than on Phylogenetic Diversity and Structure

A higher percentage of variations in CWE than those in SPD and NRI patterns of EBWPs were accounted for by climate variability of different temporal scales (**Figure 5**). In other words, climate variability had much stronger effects on species distribution process than on species assembling for EBWPs.

The constraint effects of climate variability on species ranges is straightforward and has been commonly reported (Jansson, 2003; Feng et al., 2019), and this effect also linked the latitudinal patterns of species richness with the Rapoport's role (Stevens, 1989). On the other hand, the phylogenetic diversity and structure patterns of biological assemblage are outcomes of deterministic and stochastic assembly processes acting at multi-scales across space and time (Kozak and Wiens, 2010; Feng et al., 2014; Eiserhardt et al., 2015). With regard to SPD and NRI patterns of EBWPs in China, the very complex patterns and a generally lack of latitudinal trend (**Supplementary Figures S1b,c**) indicated that the patterns were dominated by regional rather than global or hemispheric scale process. Indeed, the difference between tropic and out-of-tropic were prominent in the NRI patterns, supportive to the tropic niche conservatism theory (Kubota et al., 2017). Moreover, the longitudinal variations and topography related anomaly highlighted the role of mechanisms such as dispersal barriers, disturbance and vegetation degradation, other than climate variability.

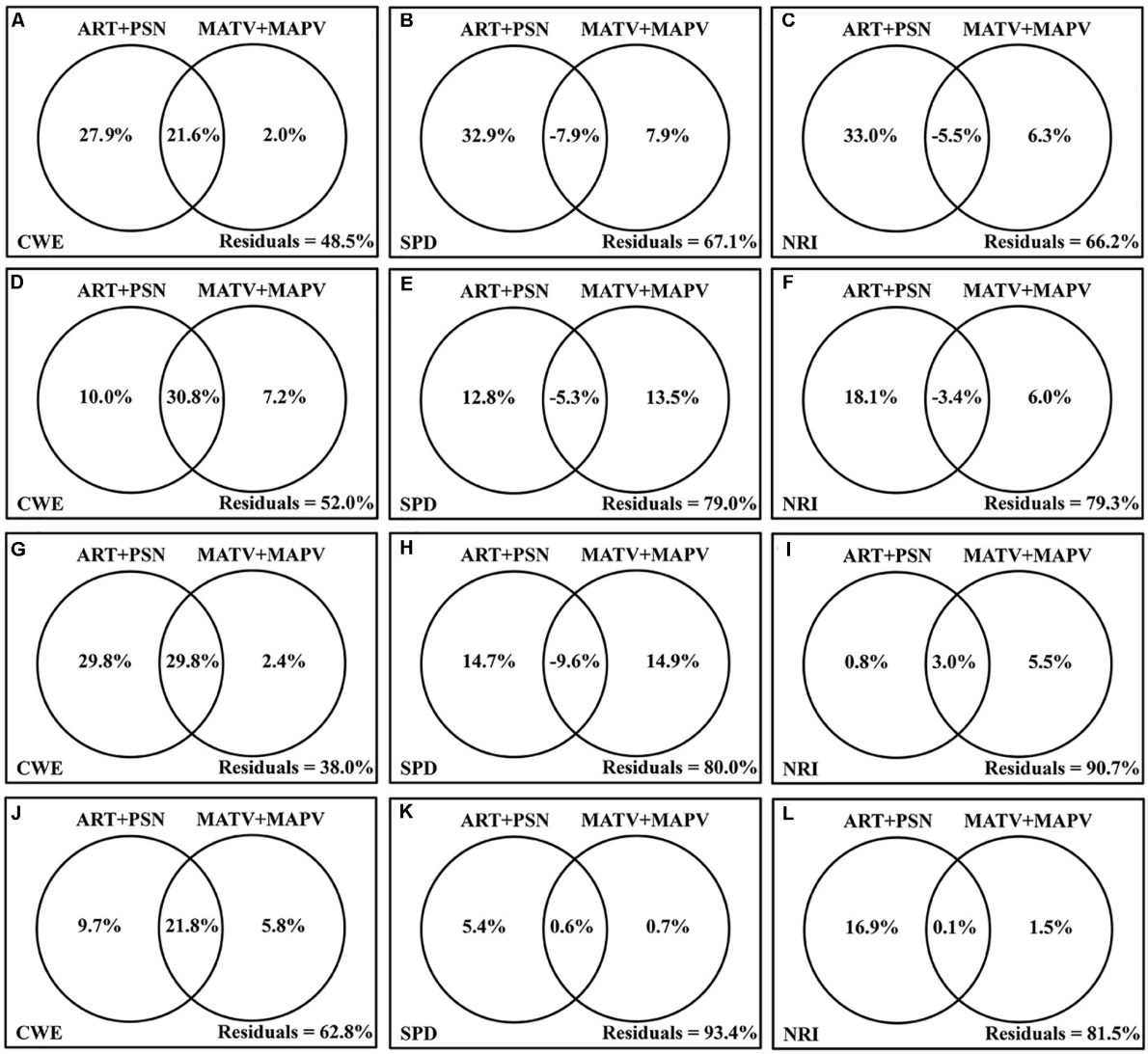


**FIGURE 5 |** The partitioning of the variance ($R^2$,%) in CWE, SPD, and NRI of trees **(A–C)**, shrubs **(D–F)**, lianas **(G–I)**, bamboos **(J–L)** of EBWPs, accounted for by contemporary climate seasonality (ART + PSN) and Quaternary glacial–interglacial climate change (MATV + MAPV) using partial regression model of OLS.

## The Relationship Between Effects of Short- and Long-Term Climate Variability

Overall, the current climate seasonality showed a greater or equivalent influence on the biogeographic patterns of EBWPs in China compared with the glacial-interglacial climate velocities, supporting our first hypothesis. Contemporary climate seasonality showed stronger or comparable effects than historical climate velocities on all three biogeographic variables for EBWPs, which is inconsistent with our second hypothesis. And the effects of climate variability at two temporal scales were more interdependent on endemism, but less (or even offset) on phylogenetic structure, indicating potentially distinct underlying mechanisms.

The existence of ecliptic obliquity determines climate seasonality as a fundamental feature of climate out of tropics. Precipitation seasonality in China is also intensified by Asian monsoons (Murakami and Matsumoto, 1994; Ji et al., 2005). The existence of climate seasonality is much longer (i.e., ∼140 million year) than the glacial-interglacial climate fluctuations in Quaternary (GICFQ) (Preston and Sandve, 2013). Therefore, it should be imprinted deeper within the evolutionary and biogeographic processes of plant species. This may help to explain the more prominent effect of seasonality than GICFQ on the biogeographic patterns. Plants respond to seasonality mainly through physiological and phenological adaptations, such as the time of flowering, fruiting and seed dispersal, resulting in life history traits evolution (Peng et al., 2008; Post, 2013) and deterministic community assembly (Che et al., 2019). Meanwhile, climate seasonality influences the location of species range margins by driving episodes of population colonization and local extinction (Guo and Werger, 2010; Bennie et al., 2013).

It is showed that areas with higher climate velocities tend to show neutral NRI and SPD value, while very low (phylogenetic overdispersaion) and high (clustering) NRI values both corresponded to low climate velocities (**Figure 4** and **Supplementary Figures S1b,c**). Regions with low climate velocities corresponded to high mountains, where environmental filtering is intensive and lead to a clustered phylogenetic structure; while regions with low climate velocities and very low NRI (and high SPD) mainly located in or near tropics, where biological competition dominates and phylogenetic structure is overdispersed. Long−term climate variability may contribute to current endemism and phylogenetic diversity gradients in three ways. Firstly, areas with high climatic variability may favor species with broader range sizes and high dispersal abilities that enable them to cope with rapid climate displacement (Sandel et al., 2011). Secondly, climatic variability may reduce speciation rates by lowering the likelihood of clade specialization on a narrow array of climate conditions (Jansson and Dynesius, 2002). Thirdly, small-ranged species face greater extinction risks in areas with unstable climates because of the challenges of persistence and diversification under strong climate variability (Zuloaga et al., 2019). Extinction risk studies on phylogenetic trees suggest that extinction is often selective and concentrated in certain lineages (Eiserhardt et al., 2015), which was in line with the decrease of SPD and increase of NRI with increasing temperature-change velocity in this study.

It is noteworthy that, climatic variability indicators act not in an isolation way, but interact constantly. Long-term changes that drive shifts in species ranges can cover up the influences of short-term climatic variability (Gray et al., 2006). In this study, the effect of GICFQ on CWE patterns was mostly nested within the effect of the current climate variability. Moreover, the historical climate velocities had much weaker and even negative joint effects with climate seasonality on the SPD and NRI patterns. In other words, the legacy of GICFQ may be offset by seasonal climate variability, or *vice versa*. Therefore, examining multiple metrics simultaneously can show how different dimensions of climate change interact to intensify or lighten species' exposure to climate change (Garcia et al., 2014).

## Effects of Temperature vs Precipitation Variability

The effects of temperature variability, in short or long-term, was consistently stronger on EBWPs endemism than that of precipitation. The results indicated that temperature variability has a generally more crucial role in affecting biodiversity than precipitation, that's why latitudinal pattern is a primary biodiversity pattern (Fine, 2015). In fact, the fluctuations of temperature in both short- and long-term presented a more predictable latitudinal gradient, making migration a worthy and successful strategy. While precipitation and its seasonal variation are both influenced by ground features such as topographic heterogeneity, and thus less predictable and more difficult for plants to track (White et al., 2010).

On the other hand, precipitation seasonality was more important than temperature range for phylogenetic diversity and structure, indicating that the Asia monsoons are critical for the generation and assemblage of EBWPs. It is also noteworthy that while the CWE of EBWPs in China consistently decreased with increasing ATR, it reached the maximum value at medium PSN (**Supplementary Figure S1a**). It may suggest that, while temperature seasonal range primarily limits the distribution of EBWPs endemic to China, this floristic component has more or less adapted to precipitation seasonality, which is a fundamental feature of summer monsoon of East Asia (Yao et al., 2010).

## Growth Form Effects on EBWPs Responses to Climate Variability

Linking multiple temporal scales of climate variability to threats for species is just the first step. To ultimately understand the influences of climate variability on biodiversity, the abilities of plants to deal with, or adapt to challenges they face must be taken in consideration (Chevin et al., 2010). Previous studies on the response of plants to climate variability across growth forms have pointed to mixed results. For the vascular plants in Europe, there are no significant differences between the importance of postglacial migration limitations between shrubs and trees in determining species ranges (Normand et al., 2011). However, the relationship between range size of vascular plants in China and velocity was more significant for shrubs than for trees and lianas (Xu et al., 2018). Consistent with our third hypothesis, the effect of climate variability metrics differs considerably among the four growth forms of EBWPs (**Table 1** and **Figure 5**). In general, the constraints of climate variability in short- or long-term, and in temperature or precipitation were relatively consistent and more significant for trees, while the responses of other growth patterns to climate variability were weaker and less consistent.

Shrubs exhibited larger responses than other growth forms to paleoclimate change (**Supplementary Figure S2**). The climate-change velocity in temperature and precipitation was high in temperate regions in China, which is in accordance with global patterns (Garcia et al., 2014). The evergreen broadleaved trees, lianas and bamboos were mostly limited to the tropical and subtropical regions, whereas evergreen shrubs were distributed throughout the whole country. The stronger effects of climate-change velocity for distribution patterns of shrubs may be attributed to their extension into the high-latitude regions. As for species with specialized climatic conditions in the tropical and subtropical regions like evergreen trees and lianas, they are likely threatened more by short-term variability, because of reduced phenotypic plasticity and physiological adaptation in such circumstances (Araújo et al., 2013).

With nearly 1,500 species, bamboos are grouped into three tribes: Arundinarieae (temperate woody), Bambuseae (tropical woody), and Olyreae (herbaceous) (Bamboo Phylogeny Group, 2012). All bamboos distributed in China are woody species, which have a tree-like habit and highly lignified culms. The influences of both short-term and long-term climate variability in bamboos were less important than that of other growth forms (**Table 1** and **Figure 5**). This should mainly relate to their unique life history. As a group of typical clonal

plants, bamboo ordinarily rely on asexual reproduction from below ground, spread horizontally within their habitat by plagiotropic stems, and establish localized and patched ramets with differences in resource supply (Evans and Turkington, 1988). This life history strategy can thus effectively buffer against small scale environmental variability in both spatial and temporal dimensions (Stuefer et al., 1994; Zhuang et al., 2011).

The differential links between biodiversity patterns of four growth forms and climate variability indicate that vulnerability to climate change of EBWPs is non-randomly distributed across growth forms. Growth form is associated with functional traits, which determine the ability to survive in the changing climate of a species (Engemann et al., 2016). It has been reported that particular functional groups were removed by glaciation from a given area depending on their traits with respect to cold and drought tolerance (Svenning, 2003). Furthermore, due to the significant phylogenetic signal in growth forms across phylogeny (Qian and Zhang, 2014), differential responses of growth forms to climate variability may also result in phylogenetically selective extinction and cause significantly greater losses of phylogenetic diversity (Feng et al., 2014; Eiserhardt et al., 2015). Therefore, this study supports the prediction that future climate change could result in shifted trait compositions, altered patterns of plant functional groups and changed ecosystem functioning (Engemann et al., 2016).

## CONCLUSION

We used EBWP species in China to quantify biogeographic patterns for four growth forms separately. We found that areas with high species endemism and phylogenetic diversity of EBWPs corresponded well with the tropical and subtropical mountains. Our results showed that both current and historical environmental variability is influential to the maintenance of biodiversity, and the relative importance of climate variability on diversity varied along with the change of ecological and evolutionary time scales. Our study suggested differential effects of short- and long-term climate variability on growth forms, highlighting the need for scientists to integrate the different responses of growth forms to future climate change. To understand effects of future climate change on biodiversity more thoroughly, climate conditions in different time scales should be incorporated.

## DATA AVAILABILITY STATEMENT

The datasets generated for this study are available on request to the corresponding author.

## AUTHOR CONTRIBUTIONS

ZS and YX designed the study and compiled the data. YX and JZ conducted the phylogenetic analyses. YX conducted the statistical analyses and wrote the first version of the manuscript. ZS, JZ, RZ, and YJ contributed to manuscript revisions. All authors contributed to the article and approved the submitted version.

## FUNDING

This work was supported by the projects of the National Natural Science Foundation of China [grant numbers 41701055 and 41971228] and the National Key Research and Development Program of China [grant number 2017YFC0505200].

## SUPPLEMENTARY MATERIAL

The Supplementary Material for this article can be found online at: https://www.frontiersin.org/articles/10.3389/fevo.2020.540948/full#supplementary-material

**FIGURE S1 |** The point patterns of biogeographical metrics [**(a)** CWE, **(b)** SPD, and **(c)** NRI] and four climate change variables for four growth-forms of EWBPs. Four columns from left to right were trees, shrubs, lianas, and bamboos. ATR, annual temperature range; PSN, precipitation seasonality; MATV, temperature-change velocity since Last Glacial Maximum; MAPV, precipitation-change velocity since Last Glacial Maximum.

**FIGURE S2 |** Independent contributions of environmental variables accounting for the variation in the spatial patterns of CWE, SPD, and NRI of tree, shrub, liana and bamboo EBWPs. ATR, annual temperature range; PSN, precipitation seasonality; MATV, temperature-change velocity since Last Glacial Maximum; MAPV, precipitation-change velocity since Last Glacial Maximum.

## REFERENCES

Araújo, M. B., Ferri-Yáñez, F., Bozinovic, F., Marquet, P. A., Valladares, F., and Chown, S. L. (2013). Heat freezes niche evolution. *Ecol. Lett.* 16, 1206–1219. doi: 10.1111/ele.12155

Bamboo Phylogeny Group (2012). An updated tribal and subtribal classification of the bamboos (Poaceae: Bambusoideae). *J. Am. Bamboo Soc.* 1, 3–27.

Beckman, N. G., Bullock, J. M., and Salguero-Gómez, R. (2018). High dispersal ability is related to fast life-history strategies. *J. Ecol.* 106, 1349–1362. doi: 10.1111/1365-2745.12989

Bennie, J., Hodgson, J. A., Lawson, C. R., Holloway, C. T., Roy, D. B., Brereton, T., et al. (2013). Range expansion through fragmented landscapes under a variable climate. *Ecol. Lett.* 16, 921–929. doi: 10.1111/ele.12129

Boyce, M. S., Haridas, C. V., Lee, C. T., and Group, N. S. D. W. (2006). Demography in an increasingly variable world. *Trends Ecol. Evol.* 21, 141–148. doi: 10.1016/j.tree.2005.11.018

Burgio, K. R., Presley, S. J., Cisneros, L. M., Davis, K. E., Dreiss, L. M., Klingbeil, B. T., et al. (2019). Dimensions of passerine biodiversity along an elevational gradient: a nexus for historical biogeography and contemporary ecology. *bioRxiv* doi: 10.1101/842138 [Preprint].

Cardinale, B. J., Duffy, J. E., Gonzalez, A., Hooper, D. U., Perrings, C., Venail, P., et al. (2012). Biodiversity loss and its impact on humanity. *Nature* 486, 59–67. doi: 10.1038/nature11148

Che, X., Chen, D., Zhang, M., Quan, Q., Møller, A. P., and Zou, F. (2019). Seasonal dynamics of waterbird assembly mechanisms revealed by patterns in phylogenetic and functional diversity in a subtropical wetland. *Biotropica* 51, 421–431. doi: 10.1111/btp.12648

Chen, Y., Han, W., Tang, L., Tang, Z., and Fang, J. (2013). Leaf nitrogen and phosphorus concentrations of woody plants differ in responses to climate, soil and plant growth form. *Ecography* 36, 178–184. doi: 10.1111/j.1600-0587.2011.06833.x

Chevin, L. M., Lande, R., and Mace, G. M. (2010). Adaptation, plasticity, and extinction in a changing environment: towards a predictive theory. *PLoS Biol.* 8:e1000357. doi: 10.1371/journal.pbio.1000357

Crisp, M. D., Laffan, S., Linder, H. P., and Monro, A. N. N. A. (2001). Endemism in the Australian flora. *J. Biogeogr.* 28, 183–198. doi: 10.1046/j.1365-2699.2001.00524.x

DeFries, R. S., Hansen, M. C., Townshend, J. R., Janetos, A., and Loveland, T. R. (2000). A new global 1-km dataset of percentage tree cover derived from remote sensing. *Global Change Biol.* 6, 247–254. doi: 10.1046/j.1365-2486.2000.00296.x

Desalegn, W., and Beierkuhnlein, C. (2010). Plant species and growth form richness along altitudinal gradients in the southwest Ethiopian highlands. *J. Veg. Sci.* 21, 617–626.

Eiserhardt, W. L., Borchsenius, F., Plum, C. M., Ordonez, A., and Svenning, J. C. (2015). Climate-driven extinctions shape the phylogenetic structure of temperate tree floras. *Ecol. Lett.* 18, 263–272. doi: 10.1111/ele.12409

Engemann, K., Sandel, B., Enquist, B. J., Jørgensen, P. M., Kraft, N., Marcuse-Kubitza, A., et al. (2016). Patterns and drivers of plant functional group dominance across the Western Hemisphere: a macroecological re-assessment based on a massive botanical dataset. *Bot. J. Linn. Soc.* 180, 141–160. doi: 10.1111/boj.12362

Evans, R. C., and Turkington, R. (1988). Maintenance of morphological variation in a biotically patchy environment. *New Phytol.* 109, 369–376. doi: 10.1111/j.1469-8137.1988.tb04207.x

Fang, J., Wang, Z., and Tang, Z. (2011). *Atlas of Woody Plants in China: Distribution and Climate*. Beijing: Springer Science and Business Media Press.

Feng, G., Ma, Z., Sandel, B., Mao, L., Normand, S., Ordonez, A., et al. (2019). Species and phylogenetic endemism in angiosperm trees across the Northern Hemisphere are jointly shaped by modern climate and glacial–interglacial climate change. *Global Ecol. Biogeogr.* 28, 1393–1402. doi: 10.1111/geb.12961

Feng, G., Mao, L., Sandel, B., Swenson, N. G., and Svenning, J. C. (2016). High plant endemism in China is partially linked to reduced glacial-interglacial climate change. *J. Biogeogr.* 43, 145–154. doi: 10.1111/jbi.12613

Feng, G., Mi, X., Bøcher, P. K., Mao, L., Sandel, B., Cao, M., et al. (2014). Relative roles of local disturbance, current climate and paleoclimate in determining phylogenetic and functional diversity in Chinese forests. *Biogeosciences* 11, 1361–1370. doi: 10.5194/bg-11-1361-2014

Fick, S. E., and Hijmans, R. J. (2017). WorldClim 2: new 1-km spatial resolution climate surfaces for global land areas. *Int. J. Climatol.* 37, 4302–4315. doi: 10.1002/joc.5086

Fine, P. V. (2015). Ecological and evolutionary drivers of geographic variation in species diversity. *Annu. Rev. Ecol. Evol. S.* 46, 369–392. doi: 10.1146/annurev-ecolsys-112414-054102

Garcia, R. A., Cabeza, M., Rahbek, C., and Araújo, M. B. (2014). Multiple dimensions of climate change and their implications for biodiversity. *Science* 344:1247579. doi: 10.1126/science.1247579

Gaston, K. J. (2000). Global patterns in biodiversity. *Nature* 405, 220–227.

Gray, S. T., Betancourt, J. L., Jackson, S. T., and Eddy, R. G. (2006). Role of multidecadal climate variability in a range extension of pinyon pine. *Ecology* 87, 1124–1130. doi: 10.1890/0012-9658(2006)87[1124:romcvi]2.0.co;2

Guo, K., and Werger, M. J. (2010). Effect of prevailing monsoons on the distribution of beeches in continental East Asia. *For. Ecol. Manage.* 259, 2197–2203. doi: 10.1016/j.foreco.2009.11.034

Irl, S. D. H., Harter, D. E. V., Steinbauer, M. J., Puyol, D. G., Fernández-Palacios, J. M., Jentsch, A., et al. (2015). Climate vs. topography – spatial patterns of plant species diversity and endemism on a high-elevation island. *J. Ecol.* 103, 1621–1633. doi: 10.1111/1365-2745.12463

Jansson, R. (2003). Global patterns in endemism explained by past climatic change. *P. Roy. Soc. B-Biol. Sci.* 270, 583–590. doi: 10.1098/rspb.2002.2283

Jansson, R., and Dynesius, M. (2002). The fate of clades in a world of recurrent climatic change: milankovitch oscillations and evolution. *Annu. Rev. Ecol. S.* 33, 741–777. doi: 10.1146/annurev.ecolsys.33.010802.150520

Ji, J., Shen, J., Balsam, W., Chen, J., Liu, L., and Liu, X. (2005). Asian monsoon oscillations in the northeastern Qinghai–Tibet Plateau since the late glacial as interpreted from visible reflectance of Qinghai Lake sediments. *Earth Planet. Sci. Lett.* 233, 61–70. doi: 10.1016/j.epsl.2005.02.025

Jin, Y., and Qian, H. (2019). V. PhyloMaker: an R package that can generate very large phylogenies for vascular plants. *Ecography* 42, 1353–1359. doi: 10.1111/ecog.04434

Kembel, S. W., Cowan, P. D., Helmus, M. R., Cornwell, W. K., Morlon, H., Ackerly, D. D., et al. (2010). Picante: r tools for integrating phylogenies and ecology. *Bioinformatics* 26, 1463–1464. doi: 10.1093/bioinformatics/btq166

Kozak, K. H., and Wiens, J. J. (2010). Accelerated rates of climatic-niche evolution underlie rapid species diversification. *Ecol. Lett.* 13, 1378–1389. doi: 10.1111/j.1461-0248.2010.01530.x

Kubota, Y., Kusumoto, B., Shiono, T., and Tanaka, T. (2017). Phylogenetic properties of Tertiary relict flora in the East Asian continental islands: imprint of climatic niche conservatism and in situ diversification. *Ecography* 40, 436–447. doi: 10.1111/ecog.02033

Legendre, P., and Legendre, L. F. (1998). *Numerical Ecology*. Oxford: Elsevier.

Letten, A. D., Ashcroft, M. B., Keith, D. A., Gollan, J. R., and Ramp, D. (2013). The importance of temporal climate variability for spatial patterns in plant diversity. *Ecography* 36, 1341–1349. doi: 10.1111/j.1600-0587.2013.00346.x

Li, D., Trotta, L., Marx, H. E., Allen, J. M., Sun, M., Soltis, D. E., et al. (2019). For common community phylogenetic analyses, go ahead and use synthesis phylogenies. *Ecology* 100:e02788. doi: 10.1002/ecy.2788

Loarie, S. R., Duffy, P. B., Hamilton, H., Asner, G. P., Field, C. B., and Ackerly, D. D. (2009). The velocity of climate change. *Nature* 462, 1052–1055.

Lu, L. M., Mao, L. F., Yang, T., Ye, J. F., Liu, B., Li, H. L., et al. (2018). Evolutionary history of the angiosperm flora of China. *Nature* 554, 234–238.

Ma, Z., Sandel, B., and Svenning, J. C. (2016). Phylogenetic assemblage structure of North American trees is more strongly shaped by glacial–interglacial climate variability in gymnosperms than in angiosperms. *Ecol. Evol.* 6, 3092–3106. doi: 10.1002/ece3.2100

Mittermeier, R. A., Turner, W. R., Larsen, F. W., Brooks, T. M., and Gascon, C. (2011). "Global biodiversity conservation: the critical role of hotspots," in *Biodiversity Hotspots*, ed. J. C. Habel (Springer), 3–22. doi: 10.1007/978-3-642-20992-5_1

Mohammadi, S., Ebrahimi, E., Moghadam, M. S., and Bosso, L. (2019). Modelling current and future potential distributions of two desert jerboas under climate change in Iran. *Ecol. Inform.* 52, 7–13. doi: 10.1016/j.ecoinf.2019.04.003

Murakami, T., and Matsumoto, J. (1994). Summer Monsoon over the Asian Continent and Western Northern Pacific. *J. Meteoro. Soc. Jap.* 72, 719–745. doi: 10.2151/jmsj1965.72.5_719

Myers, N., Mittermeier, R. A., Mittermeier, C. G., Da Fonseca, G. A., and Kent, J. (2000). Biodiversity hotspots for conservation priorities. *Nature* 403, 853–858. doi: 10.1038/35002501

Normand, S., Ricklefs, R. E., Skov, F., Bladt, J., Tackenberg, O., and Svenning, J.-C. (2011). Postglacial migration supplements climate in determining plant species ranges in Europe. *P. Roy. Soc. B.* 278, 3644–3653. doi: 10.1098/rspb.2010.2769

Oksanen, J., Blanchet, F. G., Kindt, R., Legendre, P., O'hara, R., Simpson, G. L., et al. (2010). *Vegan: Community Ecology Package. R Package Version 1.17-4*.

Olea, P. P., Mateo-Tomas, P., and De Frutos, Á (2010). Estimating and modelling bias of the hierarchical partitioning public-domain software: implications in environmental management and conservation. *PLoS One* 5:e11698. doi: 10.1371/journal.pone.0 011698

Oliveira, B. F., Machac, A., Costa, G. C., Brooks, T. M., Davidson, A. D., Rondinini, C., et al. (2016). Species and functional diversity accumulate differently in mammals. *Global Ecol. Biogeogr.* 25, 1119–1130. doi: 10.1111/geb.12471

Parmesan, C., and Yohe, G. (2003). A globally coherent fingerprint of climate change impacts across natural systems. *Nature* 421, 37–42. doi: 10.1038/nature01286

Patrick, L. E., and Stevens, R. D. (2016). Phylogenetic community structure of North American desert bats: influence of environment at multiple spatial and taxonomic scales. *J. Anim. Ecol.* 85, 1118–1130. doi: 10.1111/1365-2656.12529

Peng, Y., Lin, W., Wei, H., Krebs, S. L., and Arora, R. (2008). Phylogenetic analysis and seasonal cold acclimation associated expression of early light-induced protein genes of Rhododendron catawbiense. *Physiol. Plant.* 132, 44–52.

Post, E. (2013). *Ecology of Climate Change: the Importance of Biotic Interactions*. Princeton, NJ: Princeton University Press.

Preston, J. C., and Sandve, S. R. (2013). Adaptation to seasonality and the winter freeze. *Front. Plant Sci.* 4:167. doi: 10.3389/fpls.2013.00167

Qian, H., and Zhang, J. (2014). Using an updated time-calibrated family-level phylogeny of seed plants to test for non-random patterns of life forms across the phylogeny. *J. Syst. Evol.* 52, 423–430. doi: 10.1111/jse.12086

Raes, N., Roos, M. C., Slik, J. F., Van Loon, E. E., and Steege, H. T. (2009) Botanical richness and endemicity patterns of Borneo derived from species distribution models. *Ecography* 32, 180–192. doi: 10.1111/j.1600-0587.2009.05800.x

Rangel, T. F., Diniz-Filho, J. A. F., and Bini, L. M. (2010). SAM: a comprehensive application for spatial analysis in macroecology. *Ecography* 33, 46–50. doi: 10.1111/j.1600-0587.2009.06299.x

Sánchez-González, A., and López-Mata, L. (2005). Plant species richness and diversity along an altitudinal gradient in the Sierra Nevada, Mexico. *Divers. Distrib.* 11, 567–575. doi: 10.1111/j.1366-9516.2005.00186.x

Sandel, B., Arge, L., Dalsgaard, B., Davies, R. G., Gaston, K. J., Sutherland, W. J., et al. (2011). The influence of Late Quaternary climate-change velocity on species endemism. *Science* 334, 660–664. doi: 10.1126/science.1210173

Sandel, B., Weigelt, P., Kreft, H., Keppel, G., van der Sande, M. T., Levin, S., et al. (2020). Current climate, isolation and history drive global patterns of tree phylogenetic endemism. *Global Ecol. Biogeogr.* 29, 4–15. doi: 10.1111/geb.13001

Shen, Z., Fei, S., Feng, J., Liu, Y., Liu, Z., Tang, Z., et al. (2012). Geographical patterns of community-based tree species richness in Chinese mountain forests: the effects of contemporary climate and regional history. *Ecography* 35, 1134–1146. doi: 10.1111/j.1600-0587.2012.00049.x

Shmida, A., and Burgess, T. L. (1988). "Plant growth form strategies and vegetation types in arid environments," in *Plant Form and Vegetation Structure*, eds M. J. A. Werger, P. J. M. van der. Aart, H. J. During, and J. T. A. Verhoeven (Hague: SPB Academic Publishing), 211–241.

Smiley, T. M., Title, P. O., Zelditch, M. L., and Terry, R. C. (2020). Multi-dimensional biodiversity hotspots and the future of taxonomic, ecological and phylogenetic diversity: a case study of North American rodents. *Global Ecol. Biogeogr.* 29, 516–533. doi: 10.1111/geb.13050

Smith, S. A., and Donoghue, M. J. (2008). Rates of molecular evolution are linked to life history in flowering plants. *Science* 322, 86–89. doi: 10.1126/science.1163197

Song, Y., Wang, X., and Yan, E. (2013). *Evergreen Broad-leaved Forests in China: Classification, Ecology, Conservation*. Beijing: Science Press.

Srivastava, D. S., Cadotte, M. W., MacDonald, A. A. M., Marushia, R. G., and Mirotchnick, N. (2012). Phylogenetic diversity and the functioning of ecosystems. *Ecol. Lett.* 15, 637–648. doi: 10.1111/j.1461-0248.2012.01795.x

Stevens, G. C. (1989). The latitudinal gradient in geographical range: how so many species coexist in the tropics. *Am. Nat.* 133, 240–256. doi: 10.1086/284913

Stevens, R. D., and Tello, J. S. (2018). A latitudinal gradient in dimensionality of biodiversity. *Ecography* 41, 2016–2026. doi: 10.1111/ecog.03654

Stuefer, J. F., During, H. J., and de Kroon, H. (1994). High benefits of clonal integration in two stoloniferous species, in response to heterogeneous light environments. *J. Ecol.* 82, 511–518. doi: 10.2307/2261260

Svenning, J. C. (2003). Deterministic Plio-Pleistocene extinctions in the European cool-temperate tree flora. *Ecol. Lett.* 6, 646–653. doi: 10.1046/j.1461-0248.2003.00477.x

Svenning, J. C., Eiserhardt, W. L., Normand, S., Ordonez, A., and Sandel, B. (2015). The influence of paleoclimate on present-day patterns in biodiversity and ecosystems. *Annu. Rev. Ecol. Syst.* 46, 551–572. doi: 10.1146/annurev-ecolsys-112414-054314

Valladares, F., Martinez-Ferri, E., Balaguer, L., Perez-Corona, E., and Manrique, E. (2000). Low leaf-level response to light and nutrients in Mediterranean evergreen oaks: a conservative resource-use strategy? *New Phytol.* 148, 79–91. doi: 10.1046/j.1469-8137.2000.00737.x

von Humboldt, A., and Bonpland, A. (1807). *Essai sur la Géographie des Plantes*. Paris: Levrault, Schell and Co Press.

Walsh, C., and Mac Nally, R. (2008). *Package Hier. Part Version 1.0–3. R Statistics Project, University of Bristol*.

Way, D. A., and Oren, R. (2010). Differential responses to changes in growth temperature between trees from different functional groups and biomes: a review and synthesis of data. *Tree physiol.* 30, 669–688. doi: 10.1093/treephys/tpq015

Webb, C. O., Ackerly, D. D., McPeek, M. A., and Donoghue, M. J. (2002). Phylogenies and community ecology. *Annu. Rev. Ecol. Syst.* 33, 475–505. doi: 10.1146/annurev.ecolsys.33.010802.150448

White, E. P., Ernest, S. M., Adler, P. B., Hurlbert, A. H., and Lyons, S. K. (2010). Integrating spatial and temporal approaches to understanding species richness. *Phil. T. Roy. Soc. B* 365, 3633–3643. doi: 10.1098/rstb.2010.0280

Xu, W., Svenning, J. C., Chen, G., Chen, B., Huang, J., and Ma, K. (2018). Plant geographical range size and climate stability in China: growth form matters. *Global Ecol. Biogeogr.* 27, 506–517. doi: 10.1111/geb.12710

Xu, Y., Shen, Z., Ying, L., Wang, Z., Huang, J., Zang, R., et al. (2017). Hotspot analyses indicate significant conservation gaps for evergreen broadleaved woody plants in China. *Sci. Rep.* 7, 1–10.

Xu, Y., Shen, Z., Ying, L., Zang, R., and Jiang, Y. (2019). Effects of current climate, paleo-climate, and habitat heterogeneity in determining biogeographical patterns of evergreen broad-leaved woody plants in China. *J. Geogr. Sci.* 29, 1142–1158. doi: 10.1007/s11442-019-1650-x

Yao, C., Qian, W., Yang, S., and Lin, Z. (2010). Regional features of precipitation over Asia and summer extreme precipitation over Southeast Asia and their associations with atmospheric–oceanic conditions. *Meteorol. Atmos. Phys.* 106, 57–73. doi: 10.1007/s00703-009-0052-5

Zhang, Y., Clauzel, C., Li, J., Xue, Y., Zhang, Y., Wu, G., et al. (2019). Identifying refugia and corridors under climate change conditions for the Sichuan snub-nosed monkey (Rhinopithecus roxellana) in Hubei Province. *China. Ecol. Evol.* 9, 1680–1690. doi: 10.1002/ece3.4815

Zhuang, M., Li, Y., and Chen, S. (2011). Advances in the researches of bamboo physiological integration and its ecological significance. *J. Bamb. Res.* 30, 5–9.

Zuloaga, J., Currie, D. J., and Kerr, J. T. (2019). The origins and maintenance of global species endemism. *Global Ecol. Biogeogr.* 28, 170–183. doi: 10.1111/geb.12834

**Conflict of Interest:** The authors declare that the research was conducted in the absence of any commercial or financial relationships that could be construed as a potential conflict of interest.

# Advantages of publishing in Frontiers

**OPEN ACCESS**
Articles are free to read for greatest visibility and readership

**FAST PUBLICATION**
Around 90 days from submission to decision

**HIGH QUALITY PEER-REVIEW**
Rigorous, collaborative, and constructive peer-review

**TRANSPARENT PEER-REVIEW**
Editors and reviewers acknowledged by name on published articles

**Frontiers**
Avenue du Tribunal-Fédéral 34
1005 Lausanne | Switzerland

**Visit us:** www.frontiersin.org
**Contact us:** frontiersin.org/about/contact

**REPRODUCIBILITY OF RESEARCH**
Support open data and methods to enhance research reproducibility

**DIGITAL PUBLISHING**
Articles designed for optimal readership across devices

**FOLLOW US**
@frontiersin

**IMPACT METRICS**
Advanced article metrics track visibility across digital media

**EXTENSIVE PROMOTION**
Marketing and promotion of impactful research

**LOOP RESEARCH NETWORK**
Our network increases your article's readership